CONTRACT NO. 950137

RANGER TV SUBSYSTEM FLIGHT EVALUATION REPORT FOR FLIGHT MODEL III-2 (RA-7)

FACILITY FORM 602

N65 16739 (ACCESSION NUMBER)

316 (PAGES)

CR-60656 (NASA CR OR TMX OR AD NUMBER)

(THRU)

1 (CODE)

07 (CATEGORY)

Prepared for

JET PROPULSION LABORATORY
CALIFORNIA INSTITUTE OF TECHNOLOGY
PASADENA, CALIFORNIA

GPO PRICE $ _____

OTS PRICE(S) $ _____

Hard copy (HC) $7.00

Microfiche (MF) $1.00

By the

ASTRO-ELECTRONICS DIVISION
DEFENSE ELECTRONIC PRODUCTS
RADIO CORPORATION OF AMERICA
PRINCETON, NEW JERSEY

AED R-2473

Issued: October 30, 1964

CONTRACT NO. 950137

RANGER TV SUBSYSTEM FLIGHT EVALUATION REPORT FOR FLIGHT MODEL III-2 (RA-7)

Prepared for

JET PROPULSION LABORATORY
CALIFORNIA INSTITUTE OF TECHNOLOGY
PASADENA, CALIFORNIA
NAS 7-100

By the

ASTRO-ELECTRONICS DIVISION
DEFENSE ELECTRONIC PRODUCTS
RADIO CORPORATION OF AMERICA
PRINCETON, NEW JERSEY

AED R-2473

Issued: October 30, 1964

Table of Contents

Section		Page
	PREFACE	iii
I.	INTRODUCTION	1-1
II.	TV SUBSYSTEM DESIGN	2-1
	A. Introduction	2-1
	B. Camera Group	2-2
	C. Telecommunications Group	2-9
	D. Controls Group	2-14
	E. Power Group	2-22
	F. Thermal Design and Structure	2-25
III.	RANGER-7 MISSION AND REAL-TIME DATA	3-1
	A. Spacecraft Data Analysis Team	3-1
	B. Ground Support Equipment	3-31
IV.	FLIGHT MODEL III-2 (RA-7) EQUIPMENT PERFORMANCE	4-1
	A. General	4-1
	B. Camera Group	4-1
	C. Thermal Control	4-23
V.	CONCLUSIONS AND RECOMMENDATIONS	5-1
	A. Conclusions	5-1
	B. Recommendations	5-1

Appendices

A.	TESTING OF RANGER FLIGHT MODEL III-2 TV SUBSYSTEM AT JPL	A-1
B.	PRELAUNCH TESTING OF FLIGHT MODEL III-2 AT EASTERN TEST RANGE (ETR)	B-1

Table of Contents (Continued)

Appendices		Page
C.	EXPOSURE TIME SEQUENCE FOR PARTIAL-SCAN CAMERAS . . .	C-1
D.	LEAST SQUARES FIT OF SPACECRAFT TEMPERATURES	D-1
E.	RANGER CALCULATION - FLIGHT DISCREPANCY (Ratio Factors from RA-6)	E-1

List of Illustrations

Figure		Page
2-1	Ranger TV Subsystem, Logic block diagram	2-3/4
2-2	Video Output to communications equipment	2-8
2-3	Power Amplifier output power profile	2-11
2-4	Four-Port Hybrid output power profile	2-12
2-5	F-Channel turn-off circuitry	2-15
2-6	Clock-Start command circuitry	2-16
2-7	Cruise-mode command circuitry	2-17
2-8	TV Subsystem turn-on circuitry contained in the DCU	2-20
2-9	Electronic Clock Assembly, block diagram	2-21
2-10	Current-drain profile during a typical Ranger mission	2-23
2-11	Voltage-profile during a typical Ranger mission	2-24
3-1	Sample frame of cruise-mode telemetry data from 15-point commutator	3-9
3-2	Actual F_a-Camera Lens Housing temperature during cruise mode	3-12
3-3	Predicted F_a-Camera Lens Housing temperature during cruise mode	3-12
3-4	Actual P-Battery internal temperature during cruise mode	3-13
3-5	Predicted P-Battery internal temperature during cruise mode	3-13
3-6	Actual Top Hat temperature (-Y) during cruise mode	3-14
3-7	Predicted Top Hat temperature envelope during cruise mode	3-14

List of Illustrations (Continued)

Figure		Page
3-8	Actual Lower-Shroud temperature during cruise mode	3-15
3-9	Predicted Lower-Shroud temperature during cruise mode	3-15
3-10	Actual F_b-Camera Electronics temperature during cruise mode	3-16
3-11	Predicted F_b-Camera Electronics temperature during cruise mode	3-16
3-12	Actual Top Hat (Shroud) temperature during terminal mode	3-17
3-13	Actual Lower Shroud temperature during terminal mode	3-17
3-14	Actual F_b-Camera Electronics temperature during terminal mode	3-18
3-15	Actual F-Battery Case temperature during terminal mode	3-18
3-16	Actual P-Battery Case temperature during terminal mode	3-19
3-17	Actual Lower Shroud temperature during terminal mode	3-19
3-18	Actual Bottom Deck temperature during terminal mode	3-20
3-19	Actual Second Deck temperature during terminal mode	3-20
3-20	Actual P-Transmitter Power-Amplifier Heat-Sink temperature during terminal mode	3-21
3-21	Actual F-Battery internal temperature during terminal mode	3-21
3-22	Actual F-Transmitter Power-Amplifier Heat-Sink temperature during terminal mode	3-22
3-23	Actual F_a-Camera Lens Housing temperature during terminal mode	3-22
3-24	Actual Camera Bracket temperature during terminal mode	3-24
3-25	F- and P-Channel budgeted and actual battery capacities	3-24

List of Illustrations (Continued)

Figure		Page
3-26	F-Channel Battery voltage during cruise mode	3-25
3-27	P-Channel Battery voltage during cruise mode	3-25
3-28	Low-Current Voltage Regulator output during cruise mode	3-26
3-29	F-Channel Battery voltage and current during terminal mode	3-26
3-30	P-Channel Battery voltage and current during terminal mode	3-27
3-31	Low-Current Voltage Regulator output during terminal mode	3-27
3-32	F- and P-Channel High-Current Voltage Regulators outputs during terminal mode	3-30
3-33	F-Channel Video Combiner output during terminal mode	3-30
3-34	Mission configuration curves	3-33
3-35	Grid Drive as a function of film density after the mission	3-36
3-36	Scene Brightness as a function of film density curves	3-37
3-37	Typical displays on typical display	3-41
4-1	Northwest Lobe of Maru Nubium F_a-Camera Image with overlays indicating Nesting	4-5
4-2	Wrinkle Ridges of Northwest Mare Nubium taken by F_a-Camera	4-6
4-3	Last of Known Craters; Image taken by F_a-Camera	4-7
4-4	Crater rays; Picture taken by F_a-Camera	4-8
4-5	Light transfer characteristic curves for Ranger-7 Full-Scan Cameras	4-10
4-6	Light transfer characteristic curves for Ranger-7 Partial-Scan Cameras	4-11

List of Illustrations (Continued)

Figure		Page
4-7	Calibration set-up for Ranger-7 Cameras	4-12
4-8	Partial-Scan Video for alternate exposures	4-13
4-9	Full-Scan Video for alternate exposures	4-14
4-10	Final F_a-and P3-Camera Frames taken by Ranger-7	4-16
4-11	Lines 1070, 1072, 1073 and 1074 of last F_a-Frame	4-17
4-12	Readout sequence, full-scan cameras	4-18
4-13	F_b-Camera Video output (Frame No. 380)	4-19
4-14	F_a-Camera Video output (Frame No. 379)	4-20
4-15	Noise pulses induced by end of stroke of shutter in Camera P1. Pulse Populations due to Ten overlapping exposures of P1	4-22
4-16	Thermal configuration of the TV Subsystem	4-24
4-17	Reflected solar radiation and moonshine $\theta_s = 40°$, 11° S. Lat. 21° W. Longitude	4-35
A-1	Video output of F_a-Camera showing poor horizontal sync level in GSE	A-5
A-2	Matchmate Test set-up	A-7
A-3	RF meter calibration for System Test	A-11
A-4	RF test set-up	A-11
A-5	RF losses for vibration test arrangement at JPL	A-18
A-6	P2- and P4-Cameras read out in P2 position (35-mm Frame No. 252)	A-25
A-7	Test setup for Subsystem Verification Test	A-27

List of Illustrations (Continued)

Figure		Page
A-8	Single Video lines of P-Camera outputs lost during Subsystem Verification Test	A-29
A-9	Sync tearing observed on F-Camera video output during Subsystem Verification Test	A-31
A-10	Power measurement test set-up for the Pre-Thermal-Vacuum verification test	A-34
A-11	P2 Camera video output showing noise spikes (35-mm frame No. 90)	A-36
A-12	Power-measurement test setup for special subsystem test	A-45
A-13	Spacecraft test configuration	A-49
A-14	Radio frequency test connections for ESA test No. 1	A-54
B-1	RF Setup for the Post-Shipment Electrical Test	B-4
B-2	P1-Camera video output during Back-up Functions Test	B-8
B-3	Typical frames of P-Camera video output during Back-up Functions Test	B-10
B-4	Typical frames of F_a-Camera video output during Back-up Functions Test	B-11
B-5	Typical frames of F_b-Camera video output during Back-up Functions Test	B-12
B-6	RF Connection for Back-up Functions Test	B-13
B-7	F_a-Camera video output during System Test No. 10	B-17
B-8	F_b-Camera video output during System Test No. 10	B-17
B-9	Effect of noise spike in mask portion of signal	B-21
B-10	Noise transient observed in one P4-Camera frame during r-f Link Test	B-22

List of Illustrations (Continued)

Figure		Page
B-11	Operational checkout, RF Link Test configuration	B-24
B-12	Test configuration for ESA High-Power Test	B-27
B-13	RFI in P3-Cameras video output during ESA Low-Power Test	B-30
B-14	RFI in F_a-Camera video during ESA Low-Power Test	B-31
B-15	RFI in F_b-Camera video output during ESA Low-Power Test	B-31
B-16	Test configuration for ESA Low-Power Test	B-33
B-17	P3-Camera video output with interference during the Special RFI Test	B-38
B-18	F_a-Camera video output during the Special RFI Test	B-40
B-19	F_b-Camera video output during Special RFI Test	B-41
B-20	Test configuration for ESA Television Reduced Power test	B-42
B-21	Video Interference during Precountdown Dummy Run	B-47
B-22	RF Test configuration for Precountdown Dummy Run	B-49
B-23	Video signal near antenna null during Combined Radiation Test	B-53
B-24	Video signal after null during Combined Radiation Test	B-54
B-25	P-Camera video during Combined Radiation Test	B-55
B-26	Video signals before the gantry antenna is disconnected during J-Fact Test	B-60
B-27	Video signal after the gantry antenna is disconnected during J-Fact Test	B-61
B-28	P-Camera video at beacon minimum during J-Fact Test	B-62

List of Illustrations (Continued)

Figure		Page
B-29	P-Camera video before the gantry antenna is disconnected during J-Fact Test	B-62
B-30	P-Camera video after the gantry antenna is disconnected during J-Fact Test	B-63
B-31	J-Fact power profiles as measured with Spectrum Analyzer at OSE	B-63
B-32	Comparison of F_a-Camera RETMA pattern during the Pre-Flight System Test	B-72
B-33	Comparison of F_b-Camera RETMA pattern during the Pre-Flight System Test	B-73
B-34	Pre-Flight System Test RF Configuration	B-74
B-35	Comparison of P-Camera video before and after switchover of the JPL beacon during the ESA High-Power Test	B-80
B-36	Comparison of F_a-Camera video before and after switchover of the JPL beacon during the ESA High-Power Test	B-81
B-37	Comparison of F_b-Camera video before and after switchover of the JPL beacon during the ESA High-Power Test	B-82
B-38	ESA Full-Power test r-f test configuration	B-83
B-39	Comparison of P-Camera video before, during, and after switchover of the JPL beacon signal during the ESA Low-Power Test	B-86
B-40	Comparison of F_a-Camera video before and after beacon signal reached nominal power output during the ESA Low-Power Test	B-88
B-41	Comparison of F_b-Camera video during and after switchover of beacon signal during the ESA Low-Power Test	B-89
B-42	P-Camera video at null during simulated launch	B-97
B-43	P-Camera video at null during Countdown on First Day	B-99

List of Illustrations (Continued)

Figure		Page
B-44	F-Camera video at null during Countdown on First Day.	B-100
B-45	P-Camera video at null during Countdown on Second Day	B-102
B-46	F-Camera video output at null during Countdown on Second Day	B-104
C-1	Last Lines (166 and 167) of video P3-Camera	C-4
C-2	Line of Video from F_a-Camera at Impact	C-5
C-3	Line Video from Camera F_a Two frames Prior to Impact	C-6

List of Tables

Table		Page
2-1	Summary of Camera Characteristics	2-5
2-2	Outputs of each F- and P-Camera Electronics Assembly	2-7
2-3	Outputs from the Sequencer Power Supply Assembly	2-10
2-4	Power Distribution for the Ranger TV Split System	2-18
3-1	RA-7 Mission Events List	3-3
3-2	TV Subsystem Parameters Monitored during Terminal Mode by 90-Point Telemetry Commutator	3-28
3-3	CRT and HVPS Status	3-32
3-4	Black and White Densities from Film Recorders Nos. 1 and 2	3-35
4-1	Light Levels 8 minutes before Impact	4-9
4-2	Variation in Alternate Frame Exposure Attributable to Variation in Shutter Speed	4-12
4-3	Cruise Mode Equilibrium Temperature Predictions for Subsystem Locations Monitored by Cruise-Mode Telemetry	4-28
4-4	Cruise-Mode Equilibrium Temperature Predictions for Flight Model III-2	4-30
4-5	Spectral-Measurement History	4-31
4-6	Values of Solar Absorptivity of the RA-7 Fins	4-31
4-7	Comparison of Predicted to Actual Flight Temperatures	4-34
A-1	TV Subsystem Tests at JPL	A-1
A-2	Post-Shipment Electrical Test Sequence	A-3
A-3	System Test No. 8 Test Sequence	A-12

List of Tables (Continued)

Table		Page
A-4	RF Link Test Sequence	A-14
A-5	X-Axis Vibration Test Sequence	A-18
A-6	Post-Vibration Functional Verification Test Sequence	A-19
A-7	Battery-Cell Voltages Prior to Start of Pre-Thermal-Vacuum Verification Test	A-33
A-8	Battery-Cell Voltages at Conclusion of Pre-Thermal-Vacuum Verification Test	A-35
A-9	Mission Verification Test No. 4 Test Sequence	A-37
A-10	RF Power Output Profile for Mission Verification Test No. 4	A-40
A-11	Battery-Cell Voltages at Conclusion of Mission Verification Test No. 4	A-41
A-12	Mission Verification Test No. 5 Test Sequence	A-42
A-13	RF Power Output Profile During Mission Verification Test No. 5	A-43
A-14	Special TV Subsystem Test Sequence	A-46
A-15	Cell Voltage of Batteries Measured After Special Subsystem Test	A-47
A-16	Test Sequence for Terminal-Mode Portion of Pre-Countdown Phase of Space Simulator Operational Checkout	A-51
A-17	ESA Test No. 1 Test Sequence	A-55
A-18	Relative Amplitude of RF Signals Recorded During ESA Test No. 2	A-57
A-19	Backup Functions Test No. 3 Test Sequence	A-60

List of Tables (Continued)

Table		Page
B-1	Tests Performed at ETR	B-2
B-2	Post-Shipment Electrical Test Sequence	B-3
B-3	Power Profile Taken During Post-Shipment Electrical Test	B-4
B-4	Commands Tested During Back-Up Functions Test	B-6
B-5	Backup Functions Test Sequence	B-6
B-6	Power Profile Taken During Backup Functions Test	B-13
B-7	Sequence of Events During System Test No. 10	B-15
B-8	Power Profile Taken During System Test No. 10	B-18
B-9	Sequence of Events for the Operational Checkout	B-20
B-9A	RF Power During Terminal Maneuver	B-23
B-10	ESA High-Power Test Sequence	B-26
B-11	Power Profile Taken During the ESA High-Power Test	B-26
B-12	Power Profile Obtained from Telemetry During ESA High-Power Test	B-28
B-13	Low-Power Test Sequence	B-29
B-14	Power Profile Taken During the ESA Low-Power Test	B-32
B-15	Battery Profile for ESA Low-Power Test	B-34
B-16	Power Profile Taken During Low-Power Test No. 2	B-35
B-17	Battery Profile During ESA Low-Power Test No. 2	B-36
B-18	Power Profile Taken During the Special RFI Test	B-39
B-19	Battery Profile for Special RFI Test	B-43

List of Tables (Continued)

Table		Page
B-20	Sequence of Events During Pre-Countdown Dummy Run	B-45
B-21	Input Voltage Profile During Pre-Countdown Dummy Run	B-50
B-22	Sequence of Events During the Combined Radiation Test	B-51
B-23	Input Profile During the Combined Radiation Test	B-56
B-24	Sequence of Events During J-Fact Test	B-58
B-25	Input Voltage Profile During the Joint Flight Acceptance Composite Test	B-64
B-26	90-Point Telemetry Results of Run No. 3 on Points Nos. 75 and 80	B-67
B-27	Results of Camera Calibration Run No. 4 on Telemetry Points Nos. 75 and 80	B-68
B-28	Camera Calibration Test Results	B-69
B-29	Sequence of Events for the 3.5-Minute Terminal Mode Test	B-71
B-30	Power Profile During Pre-Flight System Test using External Power	B-75
B-31	Power Profile Taken During Pre-Flight System Test using Battery Power	B-75
B-32	Input Voltage Profile During Test using Battery Power	B-76
B-33	Cell Voltages Taken During Test using Battery Power	B-77
B-34	Test Sequence for the ESA High-Power Test	B-78
B-35	Power Profile for ESA High-Power Test	B-79
B-36	Input Voltage Profile During ESA High-Power Test	B-84
B-37	Power Profile During ESA Low-Power Test	B-90

List of Tables (Continued)

Table		Page
B-38	Input Voltage Profile During ESA Low-Power Test	B-90
B-39	Sequence of Events During Pre-Countdown Test	B-92
B-40	Pre-Countdown Test Battery Voltages	B-94
B-41	Sequence of Events for TV Subsystem During Simulated Launch	B-96
B-42	Simulated Launch Battery Voltages	B-97
B-43	Battery Voltages Obtained During Countdown on First Day	B-101
B-44	Launch Battery Voltages	B-103
C-1	Exposure Occurrence After Start of Drive Pulse	C-1
C-2	Shutter Speeds	C-1
C-3	Final Partial Scan Camera Sequence	C-3
C-4	Partial-Scan Camera Angular Coverage	C-3
D-1	Different Constraints for Least-Squares Fit	D-7
E-1	TV Subsystem Temperatures	E-1

Section I

Introduction

Section I

Introduction

On July 28, 1964, at 16:50:08 GMT, the Ranger-7 Spacecraft was launched from Cape Kennedy, Florida. Approximately 68-1/2 hours later, RA-7 impacted on the lunar surface after returning 4316 pictures of the surface of the moon. This collection of data satisfied the requirements of the Block III Ranger mission as stated in EPD 156. In summary, all aspects of the performance of the TV Subsystem during the flight of RA-7 met or surpassed all mission requirements.

This report continues the documentation of the history of Flight Model III-2 of the Ranger TV Subsystem begun with the Test Report for Modified Flight Model III-2 (AED R-2407, issued July 17, 1964). The period of time covered by the report starts with the shipment to JPL and continues through the flight of Ranger 7. It also documents the performance of the TV Subsystem during the RA-7 mission and presents an evaluation of the performance of the various equipment that comprised Flight Model III-2. Appendix A of this report describes the testing at JPL, and Appendix B presents the testing at ETR.

Section II of this report describes the configuration of the TV Subsystem that was Flight Model III-2. Section III is devoted to the period of time that comprised the Ranger-7 mission and the real-time data collected and evaluated during the mission. Section IV presents an evaluation of the performance of the TV Subsystem in relation to the collected information. Section V presents the conclusions that were reached on the basis of the collected information and summarizes the RCA recommendations for the next Ranger missions.

Section II

TV Subsystem Design

A. Introduction

B. Camera Group

C. Telecommunications Group

D. Controls Group

E. Power Group

F. Thermal Design and Structure

Section II

TV Subsystem Design

A. Introduction

The TV Subsystem of the Ranger 7 Spacecraft was basically composed of six vidicon cameras (2 full-scan, 4 partial-scan); the electronic equipment to control these cameras; the communications chains to transmit the acquired video information back to earth; telemetry components to monitor the operation of the functional components; a completely independent power source (batteries) for the entire TV Subsystem; a structure to house and support all electronic gear; and passive-thermal-control components.

The components that make up the various functional groups within the Subsystem were arranged in two completely redundant, electrically separated channels of operation: the F-Channel and P-Channel. Channel separation is characterized by the basic differences that exist between the full-scan and partial-scan cameras. The two camera types differ in the area of the scanned image and, consequently, in the scanning time and frame rate. For this reason, each channel, in addition to the cameras, consists of video-combiner, sequencer, transmitter, control, and power-distribution circuits. This arrangement results in two channels which are capable of operating either independently or simultaneously. The block diagram shown in Figure 2-1 describes the electronic components that make up the 381-pound TV Subsystem.

Besides the two-Channel separation, the electronic components of the TV Subsystem are arranged into major functional groups. These groups include:

- Camera Group;
- Telecommunications Group;
- Controls Group;
- Power Group; and
- Thermal Design and Structure Group.

B. Camera Group

1. General

The Camera Group consists of the Cameras (2 full-scan, and 4 partial-scan) and associated Camera Electronics Assemblies; Video Combiner; Control Programmer and Camera Sequencer; Sequencer Power Supply; and 15-kc Filter Assembly. The Camera Group provides video signals to the RF Transmitters in the Telecommunications Group via the Video Combiners. Sync and control signals are provided to the Cameras by the Control Programmer and Camera Sequencers. The control signals provide for sequential Camera operation in the P-Channel, and alternate Camera operation in the F-Channel. That is, while one P-Camera is being read out, the remaining three P-Cameras are in the process of being erased and prepared for subsequent operation. The procedure is the same in the case of the F-Cameras, with one Camera being read out while the other is being erased and prepared for exposure. In general, the lunar image viewed is focused on the vidicon faceplate by the Camera lens and converted to a video signal. The video signals derived by readout of the six cameras are amplified by the associated Camera Electronics Assembly and sent to the F- and P-Channel Video Combiners to be summed into composite F- and P-video signals suitable for transmission to earth.

2. Cameras

There are three wide-angle cameras and three narrow-angle cameras in the Camera Group. A summary of the characteristics of these cameras is presented in Table 2-1. One F-Camera is equipped with a 25-mm, f/0.95 lens and the other with a 75-mm, f/2 lens, thus providing fields of view of 25 and 8.4 degrees, respectively. Of the four P-Cameras, two are equipped with the 76-mm, f/2 lenses with 2.1-degree fields of view, and two are equipped with the 25-mm, f/0.95 lenses with 6.3-degree fields of view. Both the wide- and narrow-angle cameras have a fixed focus, but are capable of taking pictures from high altitudes down to less than 2000 feet above the moon's surface.

The vidicon used in the TV Cameras is a ruggedized, one-inch, slow-scan RCA tube, type C74072C. Each vidicon uses electrostatic deflection and focusing techniques and has an aspect ratio of one to one. The photoconductive surface of the vidicons has excellent sensitivity, retentivity, and erasure characteristics. The active area of the photoconductive surface that is scanned is a 0.44-inch square for the F-Cameras, and a 0.11-inch square for the P-Cameras. The gamma (slope of the light-transfer characteristic curve) is approximately 0.75. Each vidicon is capable of supplying a signal current greater than 10 nanoamperes at a light level of 0.3 foot-candle-second and has a dynamic

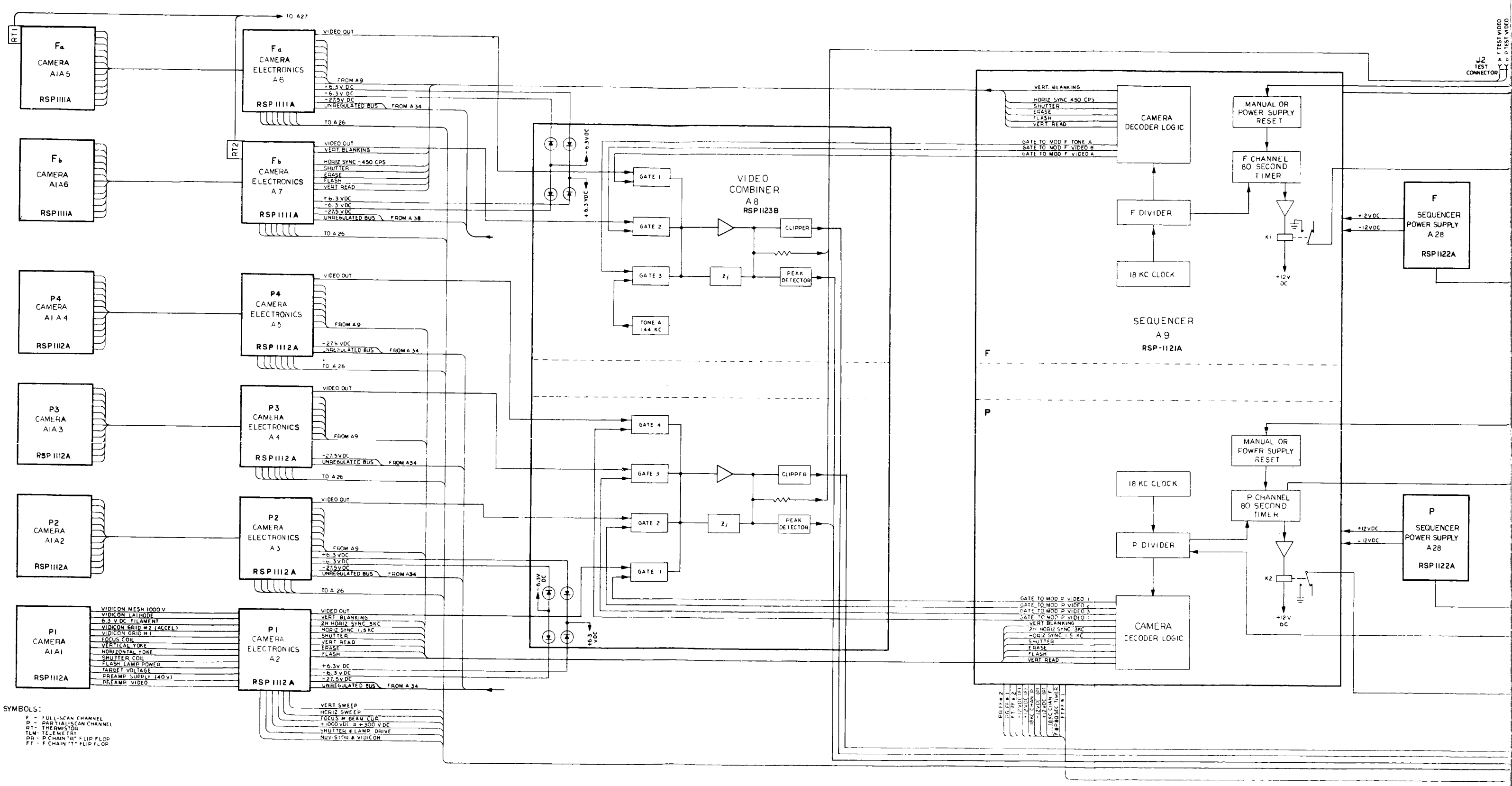
Fa CAMERA A1A5 RSP1111A
Fb CAMERA A1A6 RSP1111A
P4 CAMERA A1A4 RSP1112A
P3 CAMERA A1A3 RSP1112A
P2 CAMERA A1A2 RSP1112A
P1 CAMERA A1A1 RSP1112A
Fa CAMERA ELECTRONICS A6 RSP1111A
Fb CAMERA ELECTRONICS A7 RSP1111A
P4 CAMERA ELECTRONICS A5 RSP1112A
P3 CAMERA ELECTRONICS A4 RSP1112A
P2 CAMERA ELECTRONICS A3 RSP1112A
P1 CAMERA ELECTRONICS A2 RSP1112A
RT1
RT2
TO A27
VIDEO OUT
FROM A9
+6.3 V DC
-6.3 V DC
-27.5V DC
UNREGULATED BUS
FROM A34
TO A26
VERT. BLANKING
HORIZ SYNC ~450 CPS
SHUTTER
ERASE
FLASH
VERT READ
+6.3 VDC
-6.3 VDC
-27.5 VDC
VIDICON MESH 1000 V
VIDICON CATHODE
6.3 V DC FILAMENT
VIDICON GRID #2 (ACCEL)
VIDICON GRID #1
FOCUS COIL
VERTICAL YOKE
HORIZONTAL YOKE
SHUTTER COIL
FLASH LAMP POWER
TARGET VOLTAGE
PREAMP SUPPLY (40 V)
PREAMP VIDEO
2H HORIZ SYNC 3KC
HORIZ SYNC 1.5KC
VERT SWEEP
HORIZ SWEEP
FOCUS & BEAM CUR
+1000 VDC & +300 V DC
SHUTTER & LAMP DRIVE
NUVISTOR & VIDICON
+6.3 VDC
-6.3 VDC
VIDEO COMBINER A8 RSP1123B
GATE 1
GATE 2
GATE 3
GATE 4
TONE A 1.44 KC
CLIPPER
PEAK DETECTOR
SEQUENCER A9 RSP-1121A
F
P
CAMERA DECODER LOGIC
MANUAL OR POWER SUPPLY RESET
F CHANNEL 80 SECOND TIMER
P CHANNEL 80 SECOND TIMER
F DIVIDER
P DIVIDER
18 KC CLOCK
K1
K2
+12V DC
GATE TO MOD F TONE A
GATE TO MOD F VIDEO B
GATE TO MOD F VIDEO A
GATE TO MOD P VIDEO 1
GATE TO MOD P VIDEO 2
GATE TO MOD P VIDEO 3
GATE TO MOD P VIDEO 4
+12VDC
-12VDC
F SEQUENCER POWER SUPPLY A28 RSP1122A
P SEQUENCER POWER SUPPLY A28 RSP1122A
J2 TEST CONNECTOR
F TEST VIDEO
P TEST VIDEO
SYMBOLS:
F - FULL-SCAN CHANNEL
P - PARTIAL-SCAN CHANNEL
RT- THERMISTOR
TLM- TELEMETRY
PR - P CHAIN "R" FLIP FLOP
FT - F CHAIN "T" FLIP FLOP

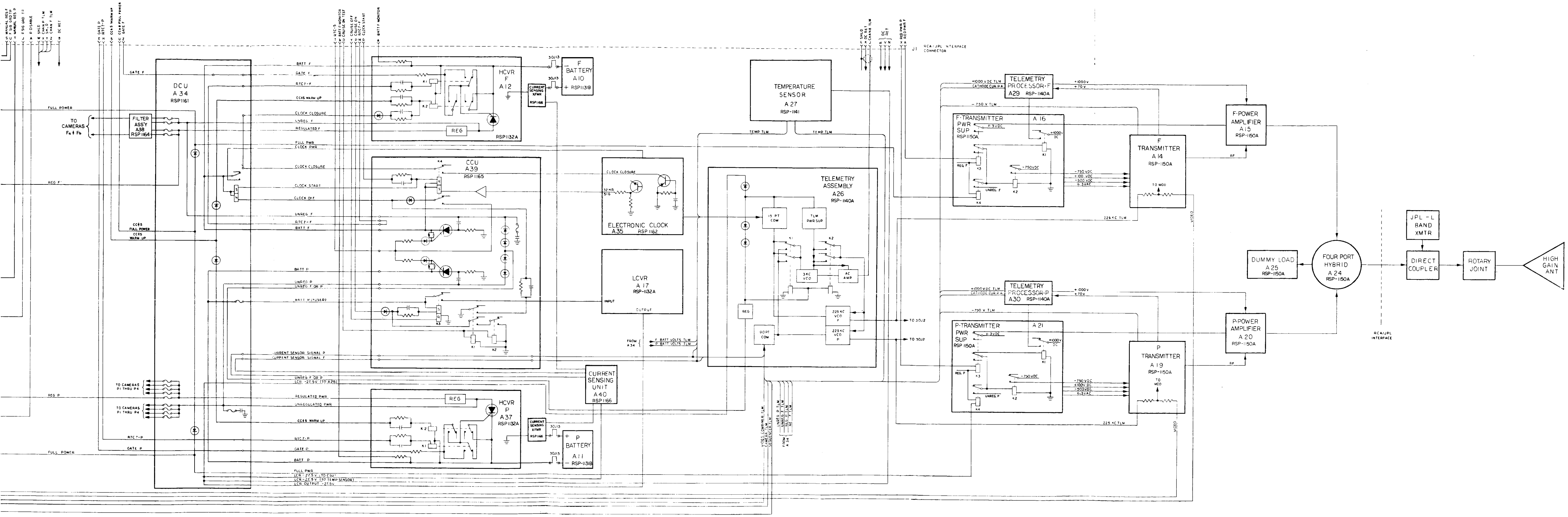

Figure 2-1. Ranger TV Subsystem, Logic block diagram

TABLE 2-1 SUMMARY OF CAMERA CHARACTERISTICS				
Characteristics	Cameras			
	F_a and F_b		P1, P2, P3, and P4	
Scan Area	0.44 x 0.44 inch		0.11 x 0.11 inch	
Real Resolution Lines	800 lines		200 lines	
Line Rate	450 cps		1500 cps	
Horizontal Scanning Lines	1150 lines		300 lines	
Horizontal Line Time	2.22 milliseconds		666.6 microseconds	
Horizontal Blanking	0.22 milliseconds		111.1 microseconds	
Frame Rate	0.39 cps		5 cps	
Frame Time	2.56 seconds		0.2 seconds	
Vertical Blanking	46.6 milliseconds		6.6 milliseconds	
Group Vertical Blanking	-		40 milliseconds	
Video Bandwidth	200 kc		200 kc	
Erase Time	2.24 seconds		360 milliseconds	
Exposure Time (Shutter Speed)	5 milliseconds		2 milliseconds	
Optics	F_a	F_b	P1 and P2	P3 and P4
	25mm, f/0.95	76mm, f/2.0	76mm, f/2.0	25mm, f/0.95

range of greater than 30 to 1. The readout time for one frame is 2.56 seconds for the F-Cameras and 0.2 second for the P-Cameras.

Each F- and P-Camera is provided with a metallic focal-plane, slit-type shutter and an erase lamp. The shutters are a solenoid-operated, sliding-aperture type that travels from one side of the lens to the other each time a picture is taken. Shutter speed is 5 milliseconds for the F-Cameras, and 2 milliseconds for the P-Cameras. The erase lamp uniformly floods the target area of the associated vidicon for 80 milliseconds prior to electron-beam scanning. The horizontal erase scan rate for the F-Cameras is 25 cps and the amplitude level of the residual video attributable to the previous exposure is less than 5 percent. For the P-Cameras, the horizontal erase scan rate is 2500 cps, with a residual video amplitude level of less than 10 percent.

3. *Camera Electronics Assembly*

Each F- and P-Camera Assembly contains the necessary circuitry to amplify the Camera video signals and supply them serially to the Video Combiner Assembly. Each Camera Electronics Assembly also supplies the necessary operating voltages, sweep signals, and focus signals for the vidicon and yoke assembly of the associated Camera Subassemblies. In addition, the P1-Camera Electronics contains the circuitry to provide a free-running capability to the P1-Camera, that is, the P1-Camera is capable of operating without the external timing signals normally supplied by the Camera Sequencer. The various circuits that comprise the Camera Electronics Assembly are as follows:

- Converter Power Supply - Converts regulated minus 27.5-volt d-c supply to square waves of required operating voltages at a pulse repetition frequency of 1500 to 2000 cps;

- High- and Low-Current Voltage Regulators - Converts regulated minus 27.5-volt d-c supply to required nominal d-c voltages;

- G1 and Focus Regulators and Telemetry - Regulates potential of the G1 grid with respect to the potential of the G2 grid, and provides telemetry voltages of 0 to -5.0 volts d-c as a function of G1 and focus current;

- Deflection Amplifier and Programmers - Supplies the deflection yoke of the vidicon with sweep-drive signals from waveforms provided by the Control Programmer and Camera Sequencer;

- Preamplifier and Video Amplifier - The preamplifier matches the vidicon output impedance to the input of the video amplifier. The video amplifier provides an output signal with a nominal amplitude of 0.9 volt peak-to-peak; this output signal consists of sync tip, black video, and white video;

- Shutter and Lamp Drive - Provides the current pulses required to operate the shutter and flash the erase lamp;

- Free-Running Circuitry (P1-Camera Electronics only) - Provides internally generated timing signals for operation of P1-Camera in the absence of external timing signals from the Control Programmer and Camera Sequencer Assembly; and

- Horizontal- and Vertical-Sync Generators (P1-Camera Electronics only) - The horizontal-sync generator provides time-base-related horizontal-read-rate and horizontal-erase-rate sync pulses to the P1-Camera. The vertical-sync generator provides time-base-related vertical-read, lamp-drive, vertical-erase, dark-current-sample, and shutter-drive sync pulses to the P1-Camera.

A summary of the outputs provided by each Camera Electronics Assembly is given in Table 2-2.

TABLE 2-2
OUTPUTS OF EACH F- AND P-CAMERA ELECTRONICS ASSEMBLY

Output	Characteristics	Destination
Video (Composite)	0 to 0.9 volt, peak-to-peak max.	Video Combiner Assembly
Telemetry:		
Vertical Sweep	0 to -5 volts dc	Telemetry Equipment
Horizontal Sweep	0 to -5 volts dc	Telemetry Equipment
G1 and Focus	0 to -5 volts dc	Telemetry Equipment
1000V and +300V	0 to -5 volts dc	Telemetry Equipment
Shutter and Lamp Drive	0 to -5 volts dc	Telemetry Equipment
Vidicon Filament	0 to -5 volts dc	Telemetry Equipment
Video Combiner Assembly Voltages	DC Ground	Video Combiner
	+6.3 volts dc	Video Combiner
	-6.3 volts dc	Video Combiner
	-27.5 volts dc	Video Combiner

4. *Video Combiner Assembly*

The Video Combiner Assembly is separated into two similar, but independent channels of operation. One channel processes the video signals from the F-Cameras, and the other channel processes the video from the P-Cameras. Two summing amplifiers, two amplitude limiters (clippers), and a camera black-strip control provide the circuitry necessary to amplify, pre-emphasize, clip, and send the composite video signal to the communications equipment for transmission. A tone oscillator in the F-Channel generates a 144-kc signal that is used to identify the full-scan camera in use. The output of the tone oscillator is applied to the F-summing amplifier.

Summing amplifiers are provided for both the F- and P-television cameras. The F-summing amplifier contains a summing network consisting of three video gates and a feedback summing amplifier. In addition to summing the F-Channel video signals, this amplifier combines the tone signal for the F_b-Camera during the vertical blanking period. The P-summing amplifier is made up of four video gates and a feedback summing amplifier. The composite video signal for each channel is amplified and pre-emphasized by these networks. The output of each summing amplifier is amplitude limited by clipper circuits to prevent excessive modulator deviation.

The output provided by the F- and P-Channel of the Video Combiner is illustrated in Figure 2-2.

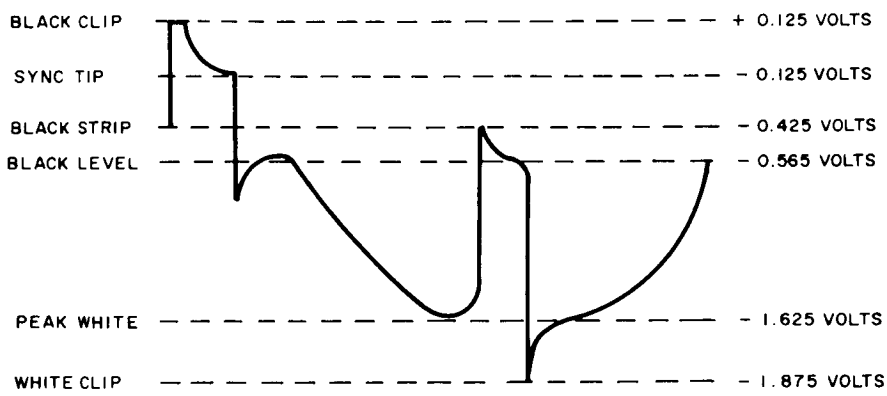

Figure 2-2. Video Output to communications equipment

5. *Control Programmer and Camera Sequencer Assembly*

The Control Programmer and Camera Sequencer consists of two similar signal channels (F and P), which provide synchronizing and sequencing signals for the F- and

P-Cameras and gating signals for the Video Combiner. The Assembly also generates a command that energizes the power amplifier of the Transmitter Assembly in the Telecommunications Group. The circuits that comprise each channel of the Control Programmer and Camera Sequencer Assembly are a timing oscillator (18-kc clock), a time-division chain, logic decoder, video-combiner logic, 80-second timer, and power-amplifier turn-on logic.

In the camera-sequencer portion of the Control Programmer and Camera Sequencer Assembly, the crystal-controlled timing oscillator generates the basic timing signal for the channel (an 18-kc pulse). This frequency output is divided in the division chain to provide timing pulses for the 80-second-timer circuit and gating commands for the logic-decoder and video-combiner-logic circuits. The logic-decoder circuit employs the gating commands from the division chain to generate synchronizing and control signals for the associated cameras. The video-combiner-logic circuit uses the gating-command output of the division chain and the video-control signal output of the logic decoder circuit to provide video and tone gates to the Video-Combiner Assembly.

In the control-programmer portion, the power-amplifier turn-on logic circuits receives the output signals from the associated 80-second timer circuit and applies them to gates to provide an output signal in the form of a contact closure that permits application of plate potential to the power amplifier of the Telecommunications Group.

6. Sequencer Power Supply

The F- and P-Channel Sequencer Power Supplies are dc-to-dc converter units that provide the positive and negative voltages required in the Control Programmer and Camera Sequencer Assembly. The Sequencer Power Supplies derive their -27.5 vdc input from their respective High-Current Voltage Regulator Assemblies. The outputs provided by the Sequencer Power-Supply Assembly are presented in Table 2-3.

C. Telecommunications Group

1. General

The Telecommunications Group of the Ranger RA-7 TV Subsystem consists of two similar transmitting channels, an r-f combining section, and telemetry components. The major function of the Telecommunications Group is to receive the composite-video outputs from the Video Combiner Assembly, convert these signals to the proper

TABLE 2-3 OUTPUTS FROM THE SEQUENCER POWER SUPPLY ASSEMBLY		
Line		Destination
1	Six Redundant F-Channel Outputs, +12 ±0.25 vdc, 500 ma. to 1.2 amp.	Control Programmer and Camera Sequencer
2	Six Redundant F-Channel Lines, Signal Reference Ground	
3	Six Redundant F-Channel Outputs, -12 ±0.25 vdc, zero to 250 ma.	
4	Six Redundant P-Channel Outputs, +12 ±0.25 vdc, 600 ma. to 1.2 amp.	
5	Six Redundant P-Channel Lines, Signal Reference Ground	
6	Six Redundant P-Channel Outputs, -12 ±0.25 vdc, zero to 280 ma.	
7	Six Redundant Outputs, Chassis Ground	

frequency and amplitude, combine them in the r-f combining section, and apply the resultant video information to the JPL high-gain antenna system for transmission to earth. A number of telemetry components are also included in the Telecommunications Group. These units receive the telemetry signals from various equipments of the TV Subsystem and process them for transmission to earth. The two similar transmitting channels consist of an L-band FM transmitter, a 60-watt power amplifier, a transmitter power supply, and a transmitter-telemetry processor. The r-f section is made up of the Four-Port Hybrid Ring and a Dummy Load. The telemetry equipment in the Telecommunications Group includes the Telemetry Assembly, Temperature Sensor, Current Sensing Unit, and F- and P-Channel Current Sensing Transformers.

2. *Communications Equipment*

The communications equipment of the Telecommunications Group comprises:

- Two L-Band FM Transmitters, each consisting of:
  - An FM Modulator,
  - An X12 and an X4 Frequency Multiplier, and
  - An Intermediate Power Amplifier;
- Two 60-watt Power Amplifiers;
- Two Telemetry Processors; and
- Two Transmitter Power Supplies.

The L-band transmitters receive signal inputs from the Video Combiner Assembly and Telemetry Assembly and apply an r-f output to the Power Amplifier which in turn applies the r-f signals to the Four-Port Hybrid Assembly for combining. The input from the Video Combiner is a composite video signal with a 187-kc base bandwidth. The terminal-mode telemetry from the voltage-controlled oscillators in the Telemetry Assembly is a 225-kc subcarrier with a peak-to-peak deviation of 10 kc and a peak-to-peak amplitude of 1.5 volts. The output power profile of the power amplifier is presented in Figure 2-3.

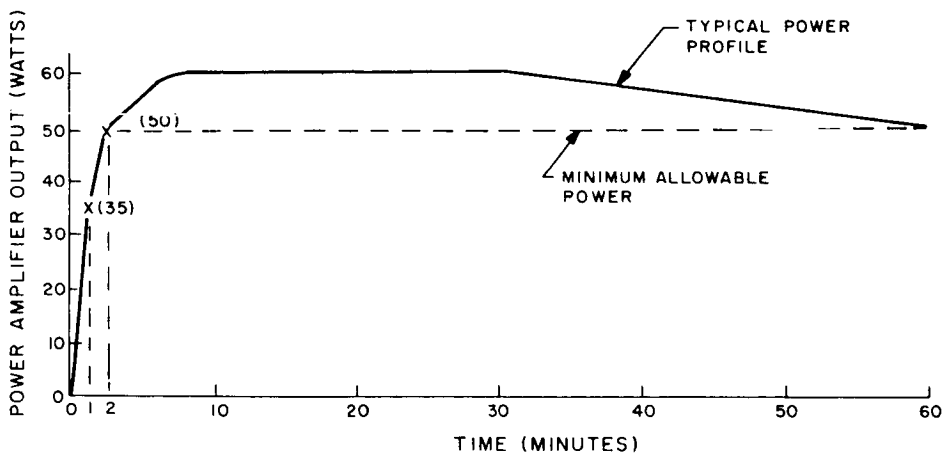

Figure 2-3. Power Amplifier output power profile

The transmitter power supplies provide the necessary operating voltages to the transmitter for reduced-power, warmup-mode, and full-power operation of the communications equipment. When provided with an unregulated dc input, the Transmitter Power Supply provides outputs of +1000 vdc at 130 ma; -750 vdc at 70 ma; +250 vdc at 20 ma; +100 vdc at 300 ma; and 6.1 vac at 1 amp.

The telemetry processor properly scales the telemetry signals from the communications equipment and applies them to the Telemetry Assembly. The telemetry information provided includes:

- +1000 volts dc (Power-Amplifier High Voltage)
- Power Amplifier Cathode Voltage
- -75 volts dc (Intermediate Power Amplifier High Voltage)

3. *RF Combining Section*

The RF combining section of the Telecommunications Group is made up of the Four-Port Hybrid Ring and the Dummy Load. The Four-Port Hybrid combines the power outputs of The F- and P-Channel power amplifiers, and provides a minimum isolation of 26 db between the two outputs. The output power profile of the Four-Port Hybrid is presented in Figure 2-4.

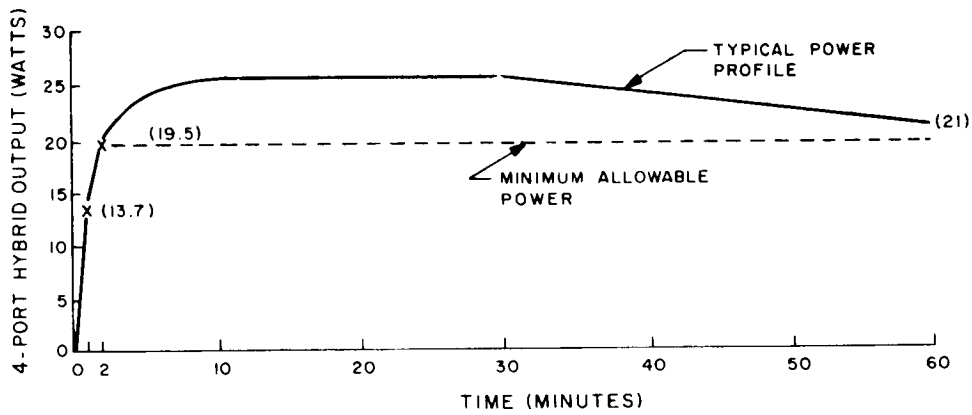

Figure 2-4. Four-Port Hybrid output power profile

A Dummy Load is included in the r-f equipment to dissipate the combining loss. The Dummy Load provides a termination with a voltage standing wave ratio of less than 1.3 for the Four-Port Hybrid and is capable of dissipating 60 watts.

4. *Telemetry Equipment*

The telemetry equipment of the Telecommunications Group consists of the Telemetry Assembly, Temperature Sensor, Current Sensing Unit, and Current Sensing Transformers. The purpose of these circuits is to obtain and process signals that will enable ground-station personnel to monitor the operation of critical components throughout the TV Subsystem.

The Temperatur Sensor Assembly employs 15 associated thermistors to detect the temperature at 15 pre-selected locations within the TV Subsystem. These temperatures are then translated into representative voltages by the circuitry of the Temperature Sensor Assembly and sent to the Telemetry Assembly for transmission to earth.

The Current Sensing Transformers sample the d-c currents of the F- and P-Batteries. These currents are sent to the Current Sensing Unit and converted to linearly related d-c voltages suitable for application to the Telemetry Assembly.

The Telemetry Assembly of the Telecommunications Group converts 15 bits (channels) of parallel-input telemetry information into a serial, scaled-frequency-deviation telemetry output during cruise-mode and terminal-mode operation of the TV Subsystem. In addition, a 90-point telemetry input is processed during terminal-mode operations. To accomplish the required telemetry-data conversion and transmittal to the transmitters, the Telemetry Assembly employs the following circuits:

- 15- and 90-point Telemetry Commutators;
- Power Supply;
- Channel-8 Voltage Controlled Oscillator (VCO);
- F- and P-Channel 225-kc Voltage Controlled Oscillators;
- A-C Amplifier;
- Reference Voltage Circuits;
- VCO Turn-on Circuits; and
- Voltage Regulator Circuit.

During cruise-mode operation, a 15-point sampling switch (commutator) in the Telemetry Assembly operates at a rate of one point per second to sample critical temperatures and voltages. The output of this commutator drives a Channel-8 IRIG subcarrier oscillator. An a-c amplifier and transformer couple the oscillator output across the spacecraft interface where it is mixed with other telemetry signals for transmission via the JPL transponder.

During terminal-mode operation, a 90-point sampling switch (commutator) operates at a rate of 3 points per second to sample critical TV Subsystem parameters. The output of the 90-point commutator is fed continuously into the P-Channel 225-kc voltage controlled oscillator and is also applied to the Channel-8 VCO at Subsystem warmup. The output of the 15-point commutator is then fed continuously to the F-Channel 225-kc VCO, and discontinued from the Channel-8 VCO. The outputs of the F- and P-Channel VCO's are then sent to the L-band transmitter for transmission to earth, while the output of the Channel-8 VCO is coupled to the JPL transponder for transmission.

D. Controls Group

1. General

The Controls Group of the Ranger TV Subsystem receives the commands issued by the JPL Spacecraft and processes these commands to perform the required operations. The circuits of the Controls Group are designed so that there is complete separation of the F- and P-Channels. This method ensures that a failure in one channel cannot affect the operation of the other channel. The components that make up the Controls Group are the Command Control Unit (CCU), Distribution Control Unit (DCU), and the Electronic Clock.

2. Command Control Unit (CCU)

The Command Control Unit (CCU) is designed so that it contains the circuitry to perform the following functions:

- Turn-off F- and P-Channel power when desired;
- Transfer the Clock-start command to the Distribution Control Unit (DCU);
- Enable F-Channel turn-on via the Electronic Clock and prime the Clock for turn-off after the 32-hour signal from the Clock is received;
- Process Cruise-Mode Commands; and
- Provide unregulated power to the Telemetry Assembly at warmup of F- or P-Channel.

a. F-Channel and P-Channel Turn-off.

Turn-off circuitry is the same for the F- and P-Channels. During normal operation, power is applied to the F-Channel (or P-Channel) by turning on the Silicon Controlled Rectifier (SCR) in the F-Channel (or P-Channel) High-Current Voltage Regulator (HCVR). A nominal voltage (approximately 31 volts) is impressed across capacitor C1 and the TV Subsystem channel load (see Figure 2-5). The F-Channel turn-off capacitor, C1, also charges to this potential (negative on the channel load side and zero on the anode side of SCR CR2).

When an RTC-5 command is received by the TV Subsystem, the gate of SCR CR2 is grounded through diode CR2 and resistor R5. This causes the SCR CR2 to conduct. The anode voltage of SCR CR2 immediately decreases to a negative value approximately

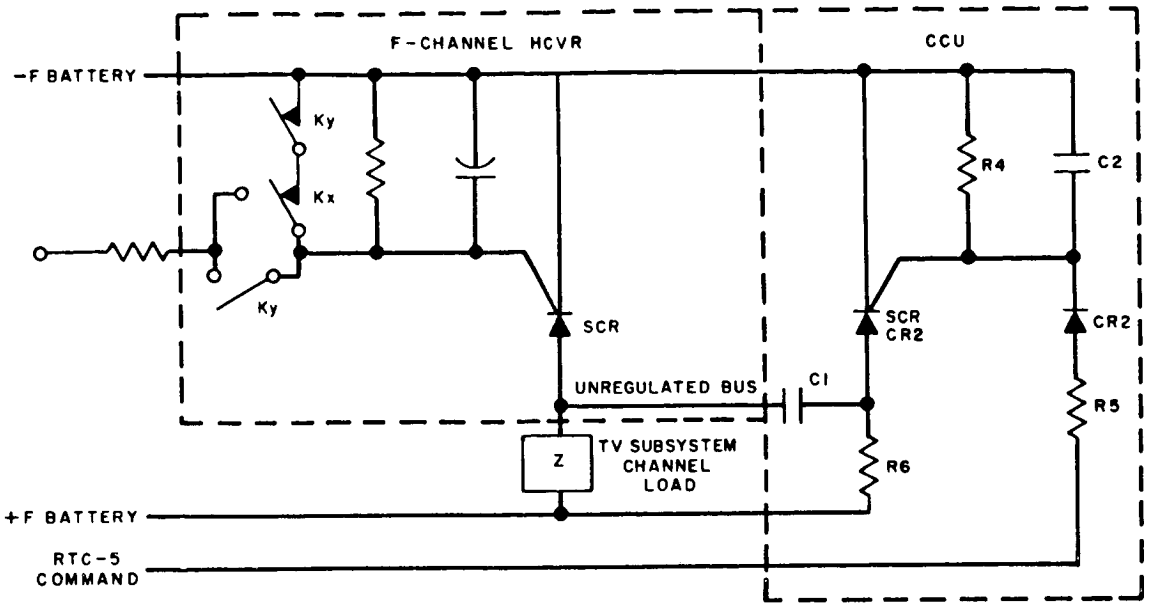

Figure 2-5. F-Channel turn-off circuitry

1.0 volt less than battery voltage. Capacitor C1, which was previously charged to a nominal value (zero on the anode side of the SCR CR2), couples this negative pulse to the anode of the SCR in the HCVR sufficiently to turn the TV Subsystem off (40μ sec is the minimum time necessary to back bias this SCR to turn it off). The SCR CR2 also turns off because its cathode current is limited below the holding current of the SCR by R6.

b. Clock Start Command.

At S + O, the Clock Start command is initiated by a separation switch closure on the JPL Bus. This command is capacitor coupled to relay K4 reset coil in the CCU and to relay K1 set coil in the DCU (see Figure 2-6). When the set coil is energized, F-Battery voltage is applied to the Clock, which starts its operation. The energizing of relay K4 reset coil opens the Clock relay K1 reset coil line to an RTC-5 command and disables the F-Channel warmup command.

Thirty-two hours after the Clock is turned on, an output from the Clock (minus 13 volts d-c) turns on transistor Q1. The transistor output energizes the set coil of relay K4, which enables the F-Channel warmup command from the Clock to turn on the F-Channel, and enables an RTC-5 command to turn off the Clock.

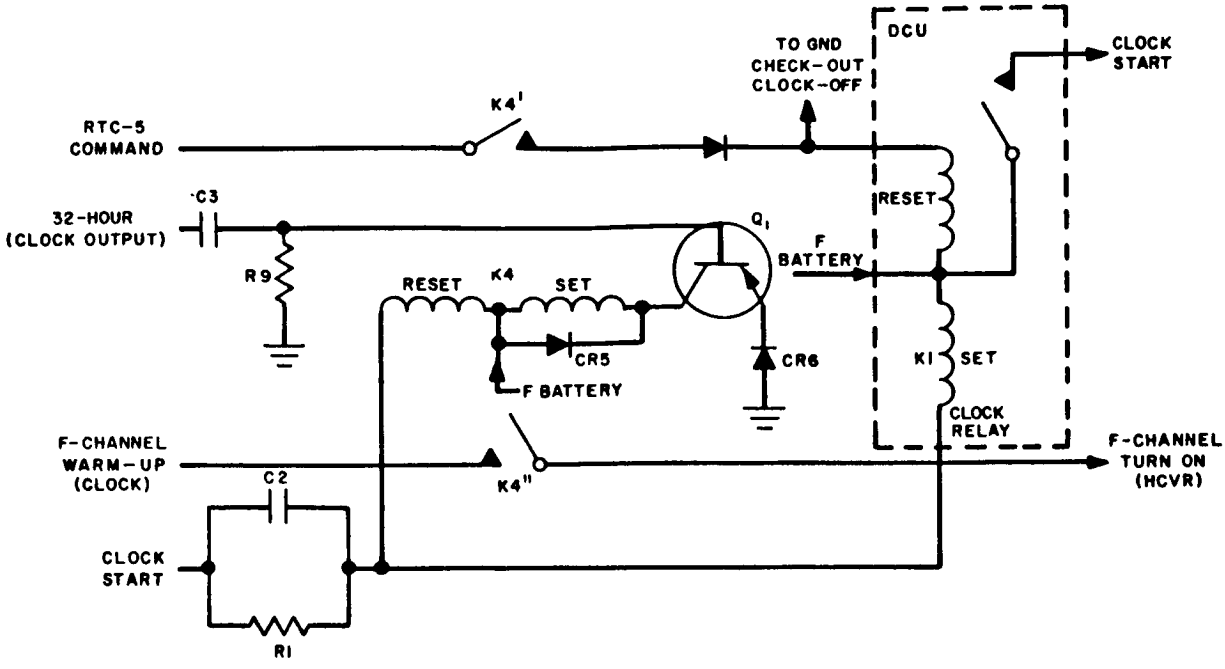

Figure 2-6. Clock-Start command circuitry

c. Cruise Mode Commands.

Figure 2-7 shows the relay logic requirements for the various cruise-mode commands. The Cruise On command is initiated at S + 17, L + 60, and S + 45 in the Range Bus as a backup command to the Cruise On Test command, which is initiated prior to launch. This command is capacitor coupled to relay K3 set coil in the CCU. The set coil of relay K3 is energized, and P-Battery voltage is applied to the LCVR, which drives the Temperature Sensors and the cruise mode telemetry circuits.

The Cruise On Test command initiates cruise-mode at launch. When this command is initiated, 28 volts d-c is supplied by an external power supply to energize relays K1 and K2. The set coil of relay K3 is in turn energized and P-Battery voltage is applied to the LCVR, which drives the Temperature Sensors and the cruise-mode telemetry circuits.

When K1 in the CCU is energized, it also provides a capacitive coupled signal to the reset coil of the Clock relay K1 in the DCU.

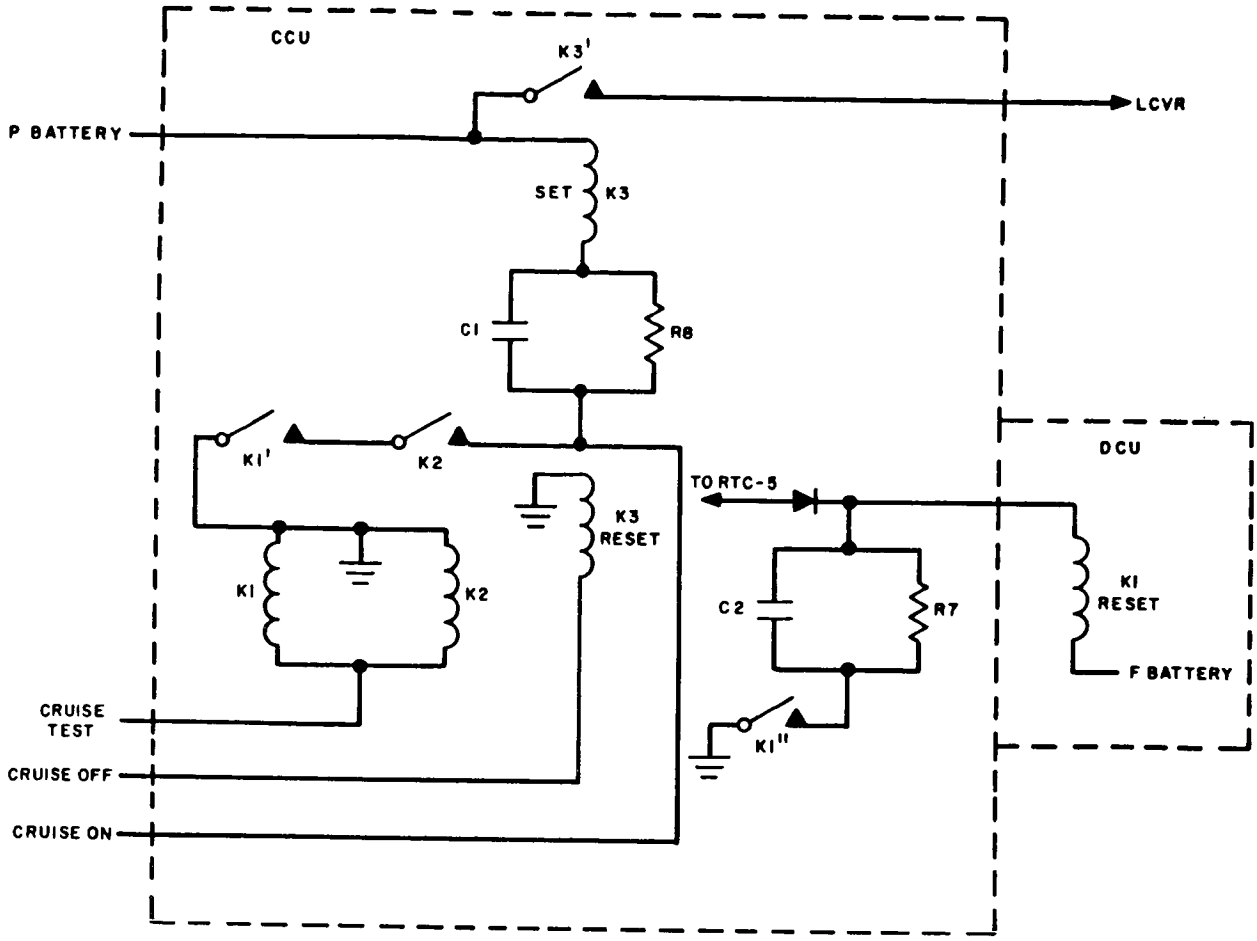

Figure 2-7. Cruise-mode command circuitry

The Cruise Off command is used for launch-pad checkout only. When the command is initiated, external power of -28 volts d-c is applied to the CCU. This voltage energizes the reset coil of the cruise-mode relay K3, which in turn removes P-Battery voltage from the Low-Current Voltage Regulator input.

d. Telemetry Power.

The Command Control Unit has a circuit consisting of four isolation diodes. When either F- or P-Channel goes into warmup, this circuit applies unregulated d-c power to the telemetry regulator of the Telemetry Assembly.

3. *Distribution Control Unit (DCU)*

The primary purpose of the Distribution Control Unit (DCU) is to function as a distribution and isolation point for regulated and unregulated voltages in the split configuration of the Ranger TV Subsystem. In addition, the DCU provides protection of each power source from failure of an individual unit by means of fuses, and isolation of full-power commands by means of isolation diodes.

The F-Channel Battery and HCVR supply voltage through the DCU to the F-Channel components and the Electronic Clock Assembly. The P-Channel Battery and HCVR supply voltage to the P-Channel components and Low-Current Voltage Regulator (LCVR) also through the DCU. Table 2-4 gives the voltage and anticipated current distribution to the F- and P-Channels.

TABLE 2-4
POWER DISTRIBUTION FOR THE RANGER TV SPLIT SYSTEM

Assembly	Type of Voltage	Approximate Current (Amperes)	Remarks
F-Channel Distribution			
Camera Electronics F_a	Unregulated Regulated	2.5 0.7	Fused Fused
Camera Electronics F_b	Unregulated Regulated	2.5 0.7	Fused Fused
Transmitter Power Supply	Unregulated	3.0	Four Wires, Not Fused
DCU	Battery	0.1	Not Fused
Clock	Battery	0.1	Not Fused
Command Control Unit	Battery Regulated	--- 0.3	Not Fused Not Fused
Terminal Mode Telemetry	Unregulated	0.8	Not Fused
Sequencer Power Supply	Regulated	1.4	Not Fused

TABLE 2-4 POWER DISTRIBUTION FOR THE RANGER TV SPLIT SYSTEM (Continued)			
Assembly	Type of Voltage	Approximate Current (Amperes)	Remarks
P-Channel Distribution			
Camera Electronics P1	Unregulated Regulated Unregulated	2.5 0.6 2.5	Fused Fused Fused
Camera Electronics P2	Regulated Unregulated	0.6 2.5	Fused Fused
Camera Electronics P3	Regulated Unregulated	0.6 2.5	Fused Fused
Camera Electronics P4	Regulated	0.6	Fused
Transmitter Power Supply	Unregulated	3.0	Four Wires, Not Fused
Command Control Unit	Battery Regulated	--- 0.3	Not Fused Not Fused
Sequencer Power Supply	Regulated	1.4	Fused
Low-Current Voltage Regulator	Battery	0.7	Fused
Current Sensing Unit	Regulated	0.03	Not Fused
Cruise Telemetry	Regulated	0.25	Not Fused
Terminal Mode Telemetry	Unregulated	0.8	Not Fused

Certain power lines supplying individual units within the TV Subsystem are fused in the DCU to prevent failure of an entire channel due to an individual unit failure. Units which do not have fused power lines are unique to a particular channel. Failure of these units would cause the entire channel to fail. The fused power lines are indicated in Table 2-4.

TV Subsystem turn-on is also accomplished through circuitry located in the DCU (see Figure 2-8). Upon initiation of the CC&S warmup command at terminal-mode operation, ground potential is applied to the anodes of CR1 and CR2. This enables the K2 relays of the HCVR's, supplying warmup power to both channels of the TV Subsystem. At the actuation of a separation switch in the JPL Bus, latching relay K1 in the DCU (shown in Figure 2-8) is energized, providing F-Battery power to the Clock. A clock-reset signal (RTC-5) can be used to de-energize the clock during flight after 32 hours of clock operation.

One command (CC&S Full Power) from the JPL Bus initiates full-power turn-on of both channels. Separate-channel full-power turn-on signals initiate from the Sequencer Assembly. The CC&S full-power command is divided and isolated by diodes CR3 and CR7 in the DCU. The output of diode CR3 is "or" gated with the P-Channel full-power signal from the Sequencer, and the output of diode CR7 is "or" gated with the F-Channel full-power signal from the Sequencer. In the event that the CC&S full-power command is sent, both the F- and P-Channel Transmitters would be turned on; however, the full-power signals from the Sequencer accomplish individual channel turn-on.

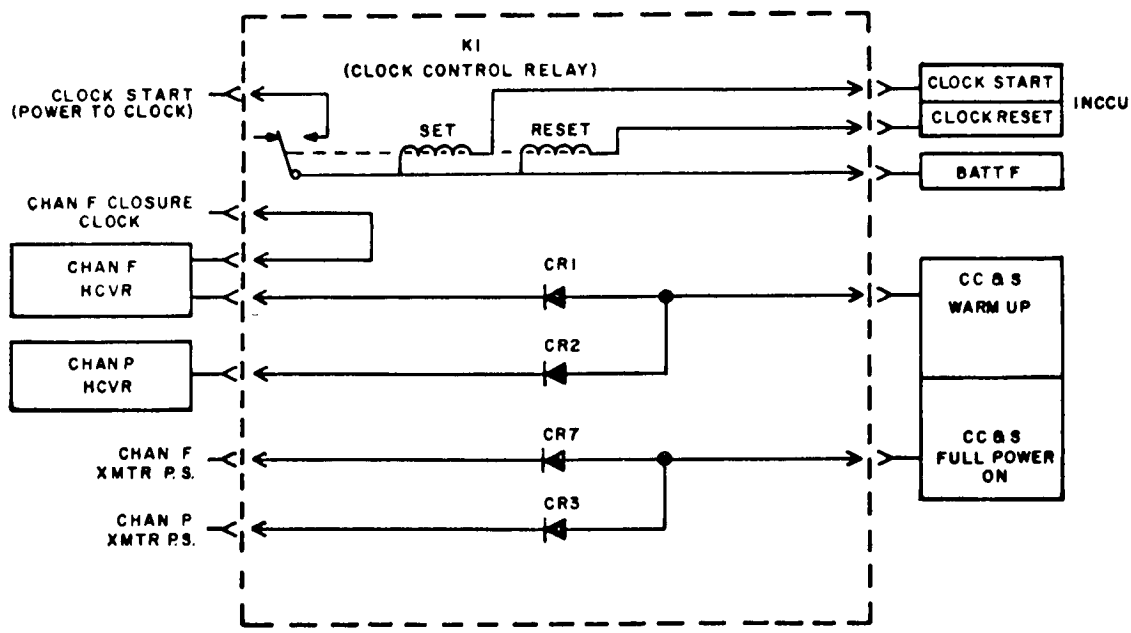

Figure 2-8. TV Subsystem turn-on circuitry contained in the DCU

4. *Electronic Clock*

The Controls Group of the Ranger TV Subsystem contains an accurate solid-state timer to provide an emergency source for the energization of the F-Channel portion of the TV Subsystem in the event that both the CC&S and RTC-7 commands fail to accomplish the turn-on function. The Electronic Clock Assembly, shown in Figure 2-9, commences operation at Agena separation (S + O) when unregulated power is applied through the K1 "Clock Start" relay in the DCU.

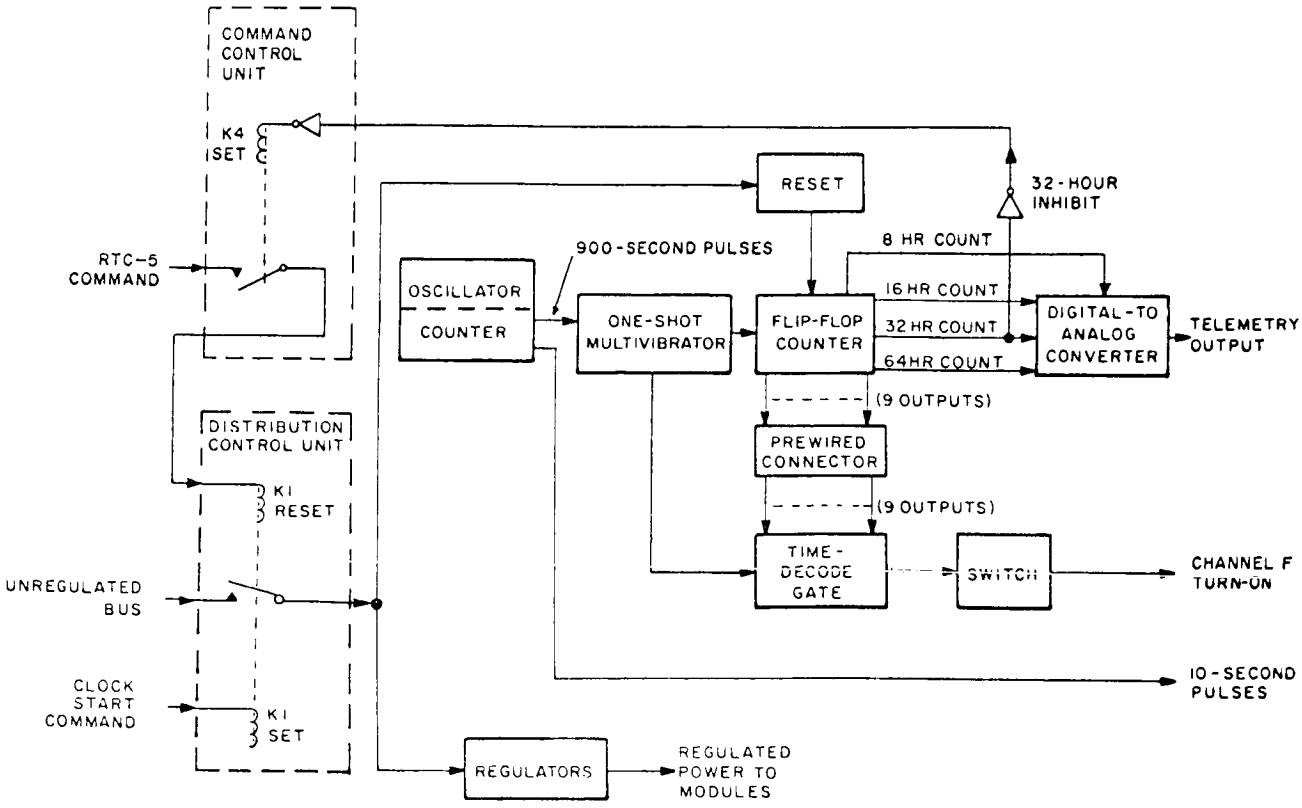

Figure 2-9. Electronic Clock Assembly, block diagram

The oscillator portion of the oscillator-counter generates 100-cps pulses which are divided in the counter portion to provide a pulse at 10-second intervals and are then further divided to provide pulses at 15-minute intervals. The 10-second pulses are used for checkout of clock operation. The 15-minute pulses are used to trigger a one-shot multivibrator, whose output in turn triggers a flip-flop counter.

When the counted time equals the preset time of the connector, the time-decode gate generates a signal that triggers an electronic switch. The output of this switch is applied to the F-Channel HCVR, through the K4 "Clock Enable" relay in the CCU, to effect F-Channel turn-on.

Should the Clock function not be required, the assembly can be disabled after 32 hours of operation by the initiation of an RTC-5 command which will remove power from the Clock.

E. Power Group

1. General

The Power Group consists of two Batteries, two High-Current Voltage Regulators (HCVR), and one Low-Current Voltage Regulator (LCVR). The TV Subsystem has completely self-contained power sources and has no connection with the power system for the remainder of the Spacecraft.

2. Batteries

The F- and P-Batteries provide all the necessary power to operate the electrical components of the Ranger TV Subsystem for a lunar mission of approximately 66 hours duration. Each battery consists of 22 series-connected cells and two temperature transducers. They are hermetically sealed, silver-zinc composition, wet-electrolyte, ruggedized units capable of providing 40 ampere-hours at 34 volts. A current profile of a typical mission of 30-minutes full-power operation on the F-Channel and 10-minutes full-power operation on the P-Channel, including final pre-launch checkout, is shown in Figure 2-10. Figure 2-11 shows the corresponding voltage profile for this mission.

3. Voltage Regulators

Two High-Current Voltage Regulators (F-Channel and P-Channel) supply regulated -27.5 volts dc to the equipment of the Ranger TV Subsystem. These regulators control application of regulated and unregulated power in response to external "on" and "off" commands. This control is provided by silicon controlled rectifiers (SCR) that act as switches to turn the current on and off in response to the external commands. An input module is contained in the HCVR to keep the gate circuit of the SCR clamped to a negative voltage until the output of the HCVR is required. At that time, a pair of relays in the module are operated, releasing the negative clamp and applying positive voltage to the gate circuit of the SCR. SCR turn-on is accomplished in the F-Channel HCVR by means of RTC-7, CC&S, or Clock commands. P-Channel HCVR turn-on is accomplished by RTC-7 or CC&S commands.

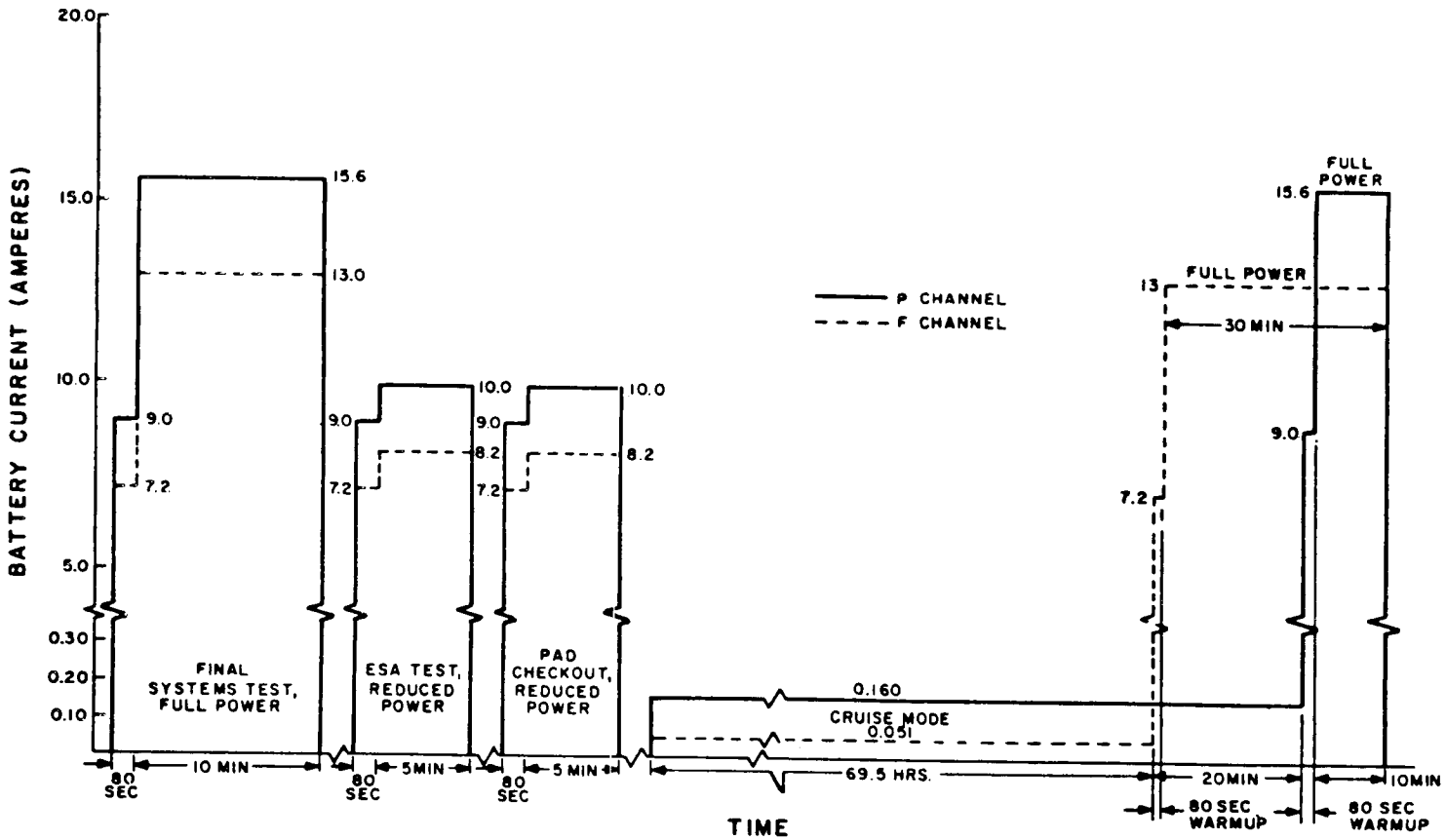

Figure 2-10. Current-drain profile during a typical Ranger mission

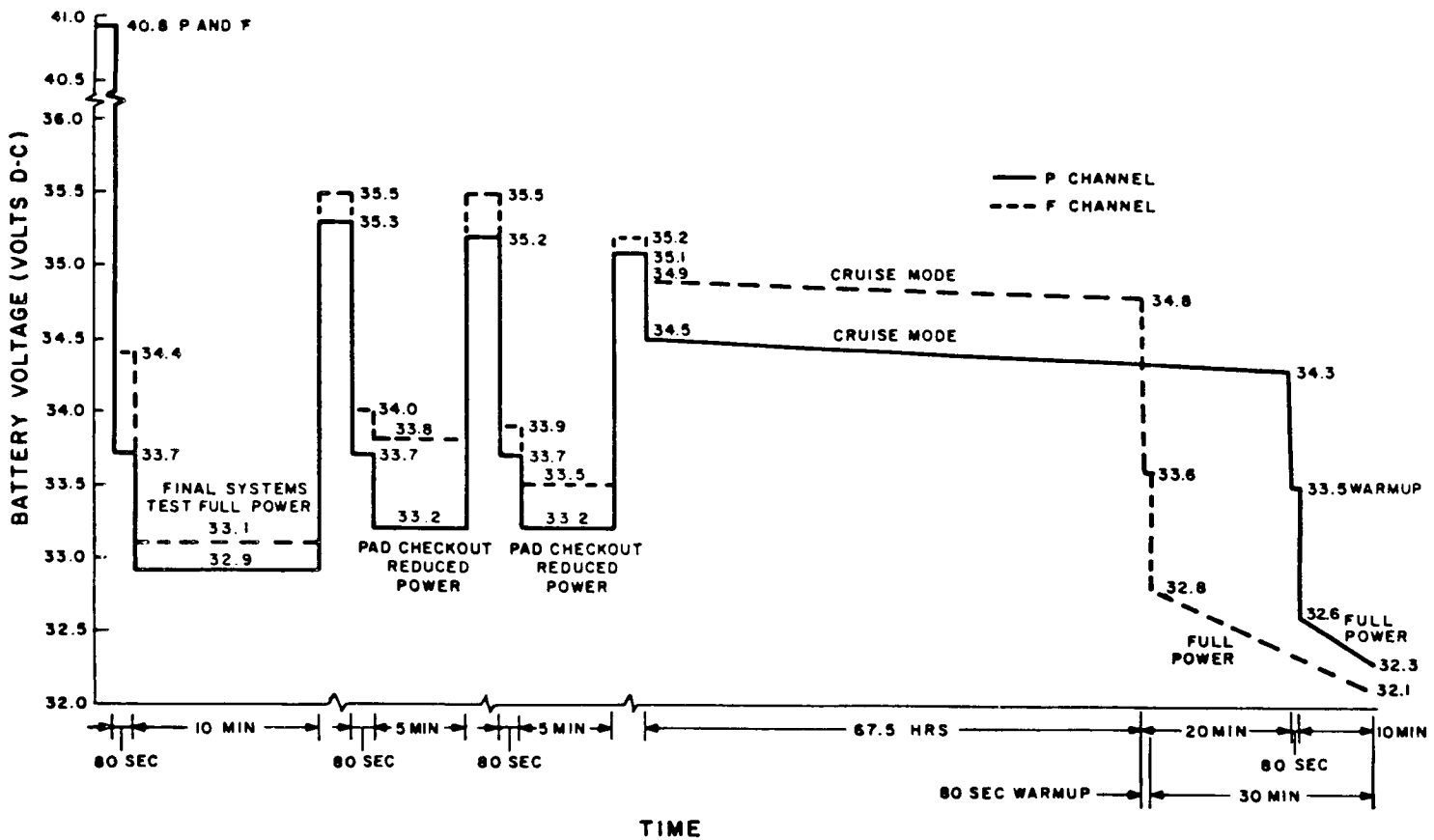

Figure 2-11. Voltage-profile during a typical Ranger mission

The Low-Current Voltage Regulator also provides regulated -27.5 volts d-c. However, it does not employ an SCR turn-on circuit or an input-module circuit as the HCVR. Also, the load requirements of the LCVR are less than that of the HCVR. The LCVR is connected to the P-Channel Battery only and is primarily used to provide a regulated power source for the operation of the cruise-mode telemetry functions.

F. Thermal Design and Structure

The Thermal Group is comprised of the thermal shroud (polished aluminum vehicle skin), thermal fins, and thermal shields. The method of temperature control used on the TV Subsystem is entirely passive. The thermal shield and fins, with appropriate surfaces and finishes, control the radiative exchange of energy between the TV Subsystem and other sources (or skins) of thermal energy. Solar energy striking the spacecraft parallel to its axis illuminates only the top surfaces of the fins. No direct sunlight is incident upon the thermal shroud proper. The solar energy is dissipated through reflection, and absorbtion and radiation. The thermal mass of the basic structure acts as the primary heat sink for the energy dissipated by the operating equipment of the TV Subsystem.

The basic structure of the TV Subsystem consists of the load carrying members joined to the appropriate mounting locations on the JPL Spacecraft. Mounting locations and attachment points are provided on the structure for the flight equipment assemblies and for the JPL omnidirectional antenna. The structure itself comprises an upper structural assembly, lower structural assembly, and a shroud assembly. The appearance of the structure is that of the frustrum of a right cone topped by a cylindrical section. The primary strength of the structure is provided by an interior box spar consisting of stiffened panel sections supported by four longerons. The external thermal shroud provides secondary structural stiffness, increasing the bending stiffness as well as providing a torsional structural member.

Section III

Ranger-7 Mission and Real-Time Data

A. Spacecraft Data Analysis Team

B. Ground Support Equipment

Section III

Ranger-7 Mission and Real-Time Data

A. Spacecraft Data Analysis Team

1. General

The function of the Spacecraft Data Analysis Team (SDAT) was to establish the pre-flight procedures and guidelines for control of the RA-7 Television Subsystem both for standard and nonstandard modes of operation during the RA-7 Mission, and to analyze the TV Subsystem telemetry data being transmitted by the Spacecraft in order to establish the best possible flight plan for the TV Subsystem.

The deep-space tracking network, with stations at Woomera, Australia; Johannesburg, South Africa; and Goldstone, California, received the transmitted signals from the Spacecraft and relayed the data, in real time, to the Flight Operations Facility at Jet Propulsion Laboratory in Pasadena, California. The TV Subsystem SDAT analyzed this data, determined the status of the TV Subsystem, and established the flight procedure for the remainder of the mission. It was the responsibility of the TV Subsystem SDAT to inform the SDAT and Flight Operations Director (FOD) of any changes to the flight plan required to obtain optimum TV Subsystem performance. The SDAT also assisted in the pre-launch test evaluation as telemetry data was transmitted, in real time, from the Eastern Test Range (ETR). Thus, from launch minus approximately 3 hours to impact, the TV Subsystem SDAT continuously monitored and analyzed the data from the TV Subsystem. Based on this data, the TV Subsystem SDAT continuously updated the TV Subsystem flight procedure to ensure the RA-7 mission requirement would be fulfilled; that is, high-resolution television pictures of the lunar surface obtained.

2. Ranger 7 Mission Profile

a. Pre-launch

Approximately 3 hours before launch, the Television Subsystem was turned on in the reduced-power mode for a final system check. Telemetry and video

indications were normal at this time. The countdown continued, and at launch minus 25 minutes, cruise-mode telemetry was turned on. The telemetry data, evaluated by both the ETR launch team and SDAT, indicated that all assemblies of the Television Subsystem were functioning normally.

b. Launch

The Ranger 7 Spacecraft was successfully launched from the Eastern Test Range (ETR) at 16:50:08 GMT on July 28, 1964. The launch was accomplished by an Atlas-Agena launch vehicle. The complete RA-7 Mission Events List is presented in Table 3-1. At launch, the umbilical cable was disconnected from the launch vehicle, removing the full-power-inhibit circuit, which permitted only a reduced-power output of approximately 50 milliwatts from the Television Subsystem. Television Subsystem telemetry data was received by SDAT from the ETR during the first few minutes of launch. It was approximately 24 hours after lift off before the ETR down-range data was available and evaluated. This data confirmed that the TV Subsystem parameters were normal during the entire launch phase.

The tracking station at Johannesburg, South Africa, acquired the Spacecraft approximately 31 minutes after launch and started sending telemetry data to SDAT. The Spacecraft entered the earth's shadow at approximately the time of Johannesburg acquisition, where it remained for 39 minutes. The temperature sensors located on the external shrouds of the TV Subsystem indicated the resulting decrease in temperature during this time.

c. Cruise Mode

Agena-booster separation occurred at L+32.5 minutes and generated a command to the TV Subsystem Clock to start its 67-3/4 hour count. Clock turn-on was verified four seconds later on cruise-mode telemetry. Agena-booster separation also provided a backup for the removal of the full-power-inhibit circuit, and started a mechanical timer which provided backup functions for the Spacecraft. One of these functions was to provide a backup circuit which would enable the SCR gates in the TV Subsystem High-Current Voltage Regulators at separation plus 30 minutes. Approximately 43 seconds prior to start of the mechanical timer, the Spacecraft solar panels were deployed and activated a microswitch which provided the initial arming of the SCR gates. At L+75 minutes, Spacecraft acquisition of the sun was accomplished, and 2 hours and 39 minutes later, the earth acquisition occurred. Thus, the Spacecraft was oriented in its normal cruise-mode position, with the Z-axis pointing toward the sun and high-gain antenna pointing toward the earth. The 15-point telemetry continued to indicate

TABLE 3-1
RA-7 MISSION EVENTS LIST

Mission Event	Event Time (GMT)		Nominal Mission Time
	Actual	Predicted	
Day 210			
1. Cruise Mode On	13:44:00		L-116'
2. Reduced Power On	13:52:18		L-109'
3. TV Subsystem Off	13:54:26		L-106'
4. Cruise Mode On (special test during hold)	15:11:22		L-60'
5. Cruise Mode Off	15:15:23		L-60'
6. Cruise Mode On (final turn-on before launch)	16:25:25		L-15'
7. Launch (L)	16:50:08	16:50:00	L + 0
8. Shroud Ejection	16:55:13		
9. ETR-DSIF-71 Lost Lock (Spacecraft over horizon)	16:57:49		
10. Spacecraft Entered Earth's Shadow	*17:21	17:21:00	
11. DSIF-59 Acquired Spacecraft	17:21:01		
12. DSIF-51 Acquired Spacecraft	17:21:38		
13. Spacecraft/Agena Separation(S) (Mark-12)	17:22:36		S + 0
14. TV Back-Up Clock-Start Indication	**17:22:40	17:22:36	S + 0
15. DSIF 51 & 59 Lost Lock (over horizon)	17:32:00		
16. DSIF-41 Acquired (one-way lock)	17:35:24		

TABLE 3-1
RA-7 MISSION EVENTS LIST (Continued)

Mission Event	Event Time (GMT)		Nominal Mission Time
	Actual	Predicted	
Day 210 (Cont.)			
17. DSIF-41 Acquired (two-way lock)	17:38:48		
18. TV Subsystem SCR Gates Armed (Solar-Panel Microswitch)	*17:51:17		L + 61'
19. TV Subsystem SCR Gates Armed (Hydraulic Timer Backup)	*17:52:00		S + 30'
20. Spacecraft Exited Earth's Shadow	*18:00:00		
21. Spacecraft Acquired Sun	18:05:00		L + 100'
22. Spacecraft Acquired Earth	20:44:00		L + 241'
23. End of DSIF-41 Track Period and Start of DSIF-51 Track Period	21:57:00		
Day 211			
24. TV Backup Clock 8-Hour Pulse	**01:22:40	01:22:40	S + 8 Hr.
25. End of DSIF-51 Track Period and Start of DSIF-12 Track Period	06:55:00		
26. TV Backup Clock 16-Hour Pulse	**09:22:40	09:22:40	S + 16 Hr
27. Start Midcourse Maneuver	10:00:39		M + 0
28. Mode II Telemetry on Channel 8	10:16:42	10:16:43	
29. Mode III Telemetry on Channel 8	10:30:40	10:30:39	M + 30'

TABLE 3-1

RA-7 MISSION EVENTS LIST (Continued)

Mission Event	Event Time (GMT)		Nominal Mission Time
	Actual	Predicted	
Day 211 (Cont.)			
30. Spacecraft Reacquired Sun	10:36:00		M + 60'
31. Spacecraft Reacquired Earth	10:58:39		M + 88'
32. TV Backup Clock 24-Hour Pulse	**17:22:40	17:22:40	S + 24 Hr.
33. End of DSIF-12 Track Period and Start of DSIF-41 Track Period	18:37:00		
Day 212			
34. TV Backup Clock 32-Hour Pulse	**01:22:37	01:22:40	S + 32 Hr
35. End of DSIF-41 Track Period and Start of DSIF-51 Track Period	01:46:00		
36. End of DSIF-51 Track Period and Start of DSIF-12 Track Period	07:18:00		
37. TV Backup Clock 48-Hour Pulse	**17:22:31	17:22:40	S + 48 Hr
38. End of DSIF-12 Track Period and Start of DSIF-41 Track Period	17:55:00		
39. End of DSIF-41 Track Period and Start of DSIF-51 Track Period	22:39:00		

TABLE 3-1

RA-7 MISSION EVENTS LISTS (Continued)

Mission Event	Event Time (GMT)		Nominal Mission Time
	Actual	Predicted	
Day 213			
40. End of DSIF-51 Track Period and Start of DSIF-12 Track Period	07:36:00		
41. TV Backup Clock 64-Hour Pulse	**09:22:23	09:22:26	S + 64 Hr
42. RTC-8 Initiated (Maneuver Inhibit Command)	11:55:00	11:55:00	
43. RTC-6 Initiated (Terminal Maneuver)	12:25:08	12:25:08	
44. CC&S Counter Started (C=0)	12:25:48	12:25:47	C + 0
45. Data Encoder Switched to Mode IV Telemetry	12:52:19		
46. Clock Turn-on of F-Channel (90-Pt Telemetry Received on Channel 8)	13:07:15	13:07:19	S + 37-3/4 Hr
47. F-Channel in Full Power	13:08:35	13:08:35	
48. CC&S Warmup Command (P-Channel in Warmup)	13:10:49	13:10:48	C + 45'
49. P-Channel in Full Power	13:12:09	13:12:09	
50. CC&S Full-Power Command (Backup)	13:15:48	13:15:48	C + 50
51. Impact	13:25:49	13:25:49	

*Approximate times, no definite indication of event.
**Tolerance is + 0 seconds; -15 seconds.

normal performance with the 8- and 16-hour Clock telemetry steps occurring at their predicted times. Midcourse maneuver was initiated at approximately L+17 hours. The 15-point telemetry data from the TV Subsystem was interrupted for 13 minutes and 58 seconds during midcourse maneuver so that propulsion and attitude-control information could be transmitted over the Channel-8 telemetry. When TV telemetry data was returned to Channel 8, the -Y axis shroud temperature had decreased 10°F and the F_a Camera lens temperature had increased 12°F, indicating that the +Y axis of the TV Subsystem was oriented toward the sun during the midcourse maneuver. At the end of midcourse maneuver, the Spacecraft was re-oriented in its normal cruise-mode position, and 4 hours later the temperatures of the TV Subsystem had returned to their pre-midcourse values.

The 24- and 32-hour Clock telemetry steps occurred on time. At the time of the 32-hour step, the Clock also provided an output signal, which removed the Clock-output inhibit and the RTC-5 Clock-turn-off inhibit. Forty hours after launch, the TV Subsystem temperatures stabilized at the following values:

- F_a Camera Lens 66°F
- P-Channel Battery 75°F
- Top Hat (shroud) 82°F
- Lower Shroud 74°F
- F_b Camera Electronics 68°F

The 48- and 64-hour Clock telemetry steps occurred early, by 9 and 17 seconds, respectively. This indicated that the Clock was running fast but still well within its 5-minute overall tolerance. At this time, analysis of the Battery capacities and temperatures indicated that the F- and P-Channels could operate in the full-power mode for 37 and 56 minutes, respectively; the limiting factor being temperature.

d. Terminal Mode

Trajectory information revealed that the television cameras were properly oriented so that no terminal maneuver was required. Thus, an RTC-8 command was sent to inhibit the terminal maneuver, and then an RTC-6 command was sent to start the CC&S counter in the Spacecraft, which supplies the warmup (turn-on) and back-up full-power commands to the TV Subsystem. The terminal sequence of events began with turn-on of the CC&S counter one hour before impact. The Spacecraft Data Encoder switched to Mode IV telemetry 26.5 minutes later indicating that the CC&S

counter was operating. At 13:07:15 GMT, the TV Subsystem Clock turned on the F-Channel into warmup mode and 90-point diagnostic telemetry was transmitted over Channel 8. Eighty seconds after the Clock turn-on pulse occurred, the TV Subsystem sequencer commanded F-Channel into full-power operation. At this time, strong F-Channel video signals were received by the Goldstone Tracking Station. Approximately 3 minutes after the turn-on of the F-Channel, the Spacecraft CC&S commanded the P-Channel into warmup mode, and 80 seconds later the TV Subsystem Sequencer placed the P-Channel in full-power operation. From this time until impact, both TV channels transmitted video pictures of the lunar surface. F-Channel operated for 17 minutes and 14 seconds, and P-Channel for 13 minutes and 40 seconds.

3. RA-7 TV Subsystem Telemetry

a. General

TV Subsystem telemetry was obtained in order to monitor the important Subsystem parameters so that any necessary, real-time adjustments could be made to correct or improve Subsystem performance, and in the event of a failure, an analysis could be made of the telemetry data to isolate the cause. A PAM/FM/FM* system was employed to monitor 104 parameters of the TV Subsystem. Telemetry data was transmitted by the TV Subsystem's two high-power Transmitters on a 225-kc subcarrier, and by the Spacecraft's low-power Transmitter on an I. R. I. G. Channel-8 3-kc subcarrier. Channel 8 was the prime data link. During cruise mode, a 15-point commutator sampled eleven Subsystem parameters and four telemetry references in the TV Subsystem (see figure 3-10. When either F- or P-Channel of the TV Subsystem is turned on into the warmup mode, the cruise-mode telemetry data is switched off of Channel 8 and the diagnostic telemetry sampled by a 90-point commutator is transmitted over Channel 8. The format for the 90-point commutator is the same as for the 15-point commutator shown in figure 3-1, except more and different parameters are sampled. As a backup function, the 90-point commutator also modulates a 225-kc voltage controlled oscillator (VCO) whose output is transmitted over the P-Channel high-power Transmitter. Likewise, the telemetry data from the 15-point commutator is switched to and transmitted over the F-Channel high-power transmitter.

b. Flight Operations Facility

In the Data Analysis Room of the Flight Operations Facility, several devices were employed for monitoring Subsystem telemetry data. During Spacecraft passes over the Goldstone and Woomera tracking stations, the 3-kc analog telemetry

---

*PAM/FM/FM - pulse amplitude modulated/frequency modulated/frequency modulated

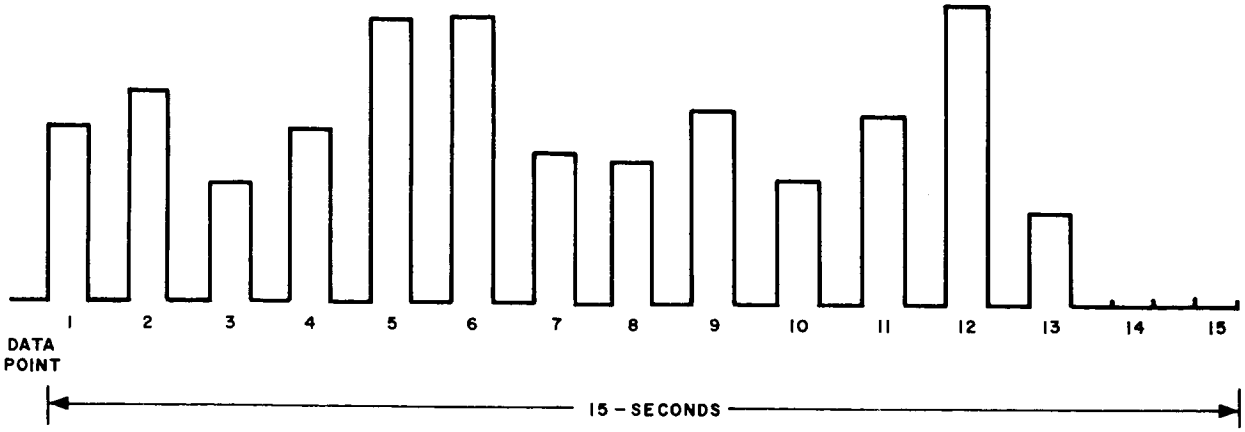

CRUISE-MODE TELEMETRY (15-POINT)

DATA POINT

1. Fa CAMERA LENS TEMPERATURE
2. LOW-CURRENT VOLTAGE REGULATOR OUTPUT VOLTAGE
3. P-BATTERY CURRENT
4. P-BATTERY INTERNAL TEMPERATURE
5. F-BATTERY VOLTAGE
6. P-BATTERY VOLTAGE
7. TOP HAT (SHROUD) TEMPERATURE
8. LOWER SHROUD TEMPERATURE
9. CLOCK TIME STEPS
10. F-BATTERY CURRENT
11. F_b CAMERA ELECTRONICS TEMPERATURE
12. FULL SCALE REFERENCE (4.6 VOLTS)
13. ZERO REFERENCE (0 VOLTS)
14. FRAME REFERENCE
15. FRAME REFERENCE

Figure 3-1. Sample frame of cruise-mode telemetry data from 15-point commutator

signal was sent directly to the Flight Operations Facility and displayed on a Sanborn strip-chart recorder. This telemetry signal was also fed into a computer which sampled each data point and printed out the actual telemetry voltage for that point. The telemetry data was also displayed on strip-chart recorders at the tracking stations, and every 30 minutes, the telemetry was read off the strip charts and the values sent to the SDAT through the administrative teletype network. During Spacecraft passes over the Johannesburg station, the administrative teletype messages were the only source of data available as the analog telemetry signal was not available to the Space Flight Operations Facility from this station.

Prior to the RA-7 flight, the Television Subsystem telemetry was calibrated in accordance with per RTSP 1100A, Appendix N. In the camera telemetry, several of the data points combine two parameters and are not easily calibrated when installed in the Subsystem. Thus, the camera assemblies are calibrated in bench test and verified during the many systems tests performed before flight. The calibration data was fed into a computer which produced tables that converted telemetry voltages into their associated engineering units. These tables were used for conversion of the telemetry data during the flight. Also, at various times during cruise mode, depending on when computer time was available, a tape recording of the received cruise-mode telemetry data was fed into the computer programmed to plot the data as a function of time and also to print out a complete listing of the data in Engineering units as a function of time.

At approximately 7 minutes before TV Subsystem turn-on in terminal mode, the computer was programmed for the reception of the 90-point diagnostic telemetry data. The data outputs available to the TV-SDAT during terminal mode were:

- Strip-chart recording of the analog telemetry signal in real time;
- Real-time computer printouts of selected telemetry points;
- Matrix printouts of all 90-point telemetry data about 1-1/2 to 2 minutes behind real time;
- Phone and administrative teletype messages from the Goldstone Tracking Station of selected telemetry points as read on their strip-chart recorders; and
- Approximately 30 minutes after impact, the computer tabulations and plots of the 90-point telemetry data were available.

4. *SDAT Data Accuracy (Computer Output)*

In order to establish the accuracy of the various data stations, telemetry data point 15-9 (the Clock pulse) was selected as a reference and its incremental change was noted. The following variations were noted:

- Woomera variations averaged 0.3 volt;
- Goldstone variation averaged 0.12 volt; and
- Johannesburg variation averaged 0.3 volt;

Telemetry data from the Woomera, Goldstone, and Johannesburg tracking stations were plotted as minimum and maximum values sampled every hour during Spacecraft view periods. Cruise-mode telemetry data from all tracking stations were further analyzed and compared. Telemetry data from Johannesburg were reading lower than the data from the other stations; the Clock pulse telemetry (15-9) was 200 millivolts lower, LCVR telemetry (15-2) was 100 millivolts lower, and lower-shroud temperature telemetry (15-8) was 100 millivolts lower.

5. *Transition from Cruise-Mode to Terminal-Mode Telemetry*

When terminal-mode operation occurred, 90-point telemetry was transmitted over Channel 8. The terminal-mode (90-point) telemetry included data on the same telemetry points sampled by the cruise-mode (15-point) telemetry and thus provided a basis of reference for determining the consistency of the telemetry readouts.

When the P-Battery voltage (data point 15-6) was readout as data point 90-59, the Primary Data Processor indicated an inconsistency of at least 0.1 telemetry volt in the readouts. In order to ascertain the source of this apparent inconsistency, the hard-line, semi-raw telemetry data from the Goldstone (DSIF-12) tracking station was reviewed. The zero-reference telemetry point was found to have increased from 115 data units as data point 15-13 to 131 data units as data point 90-88 in the terminal-mode telemetry. The full-scale-reference telemetry point (90-35) was also found to be erratic for the first six data points, so the alternate full-scale-reference telemetry point (90-87) was used to establish the gradient for interpreting the terminal-mode telemetry; the full-scale reference was found to have increased from 572 data units as data point 15-12 to 587 data units as data point 90-87. However, the data point in question (P-Battery voltage) increased from 526 data units as data point 15-6 to 556 data units as data point 90-59, a total of 30 data units or approximately 0.150 telemetry volts beyond the previously mentioned increase. The pre-launch tests of July 27, 1964, showed that full-scale reference averaged 573 data units as data point 15-12 and increased to an average value of 590 data units as data point 90-35/87, an increase of 17 data units.

Since the data-converter granularity is one order of magnitude smaller than the error, it would have to be a cumulative effect of programming combined with system noise to account for the entire increase of 30 units for the P-Battery voltage. In order to establish the semi-raw value for a particular data point, the raw pedestal values were sampled on either side of the data point to obtain an average "base band"; this was then subtracted from the raw-data-point value. This amount of programming would not have contributed a change of 30 units, and hence it must be concluded that the overall accuracy at this point is limited to 150 millivolts of telemetry (i.e., ± 75 millivolts).

6. *Telemetry Evaluation of TV Subsystem Performance*

The cruise-mode telemetry was employed to monitor the TV Subsystem temperatures and power-supply operation. The temperatures during cruise and terminal mode were almost exactly as predicted in pre-flight calculations. Graphs of the actual and predicted cruise-mode temperatures are presented in figures 3-2 through 3-11. Terminal-mode temperatures are plotted in figures 3-12 through 3-24 . A discussion of the thermal design of TV Subsystem is presented in Section IV, Paragraph C of this report.

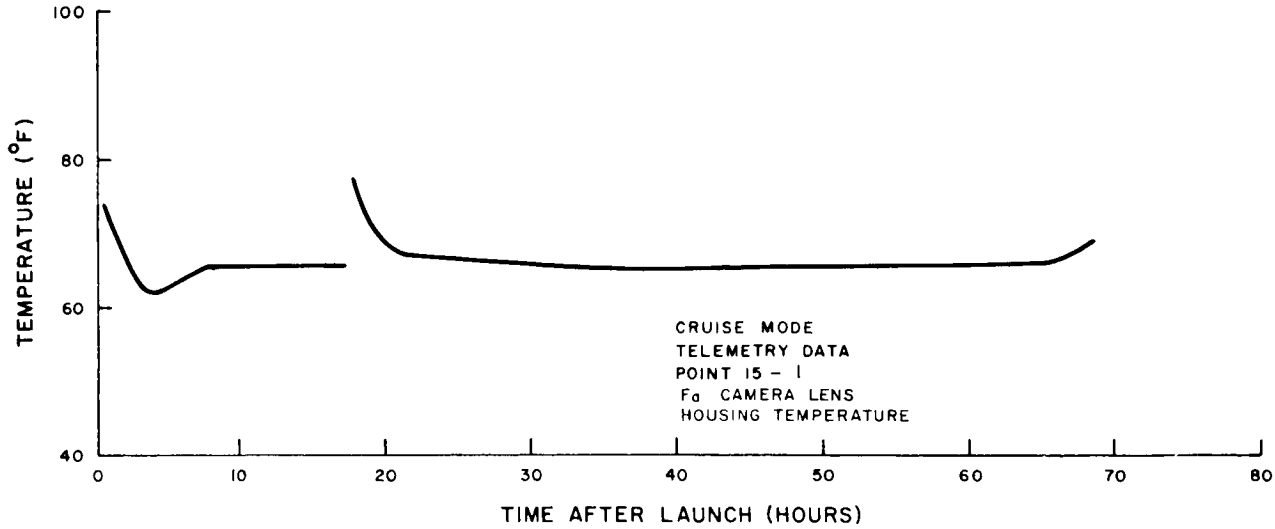

Figure 3-2. Actual F_a Camera Lens Housing temperature during cruise mode

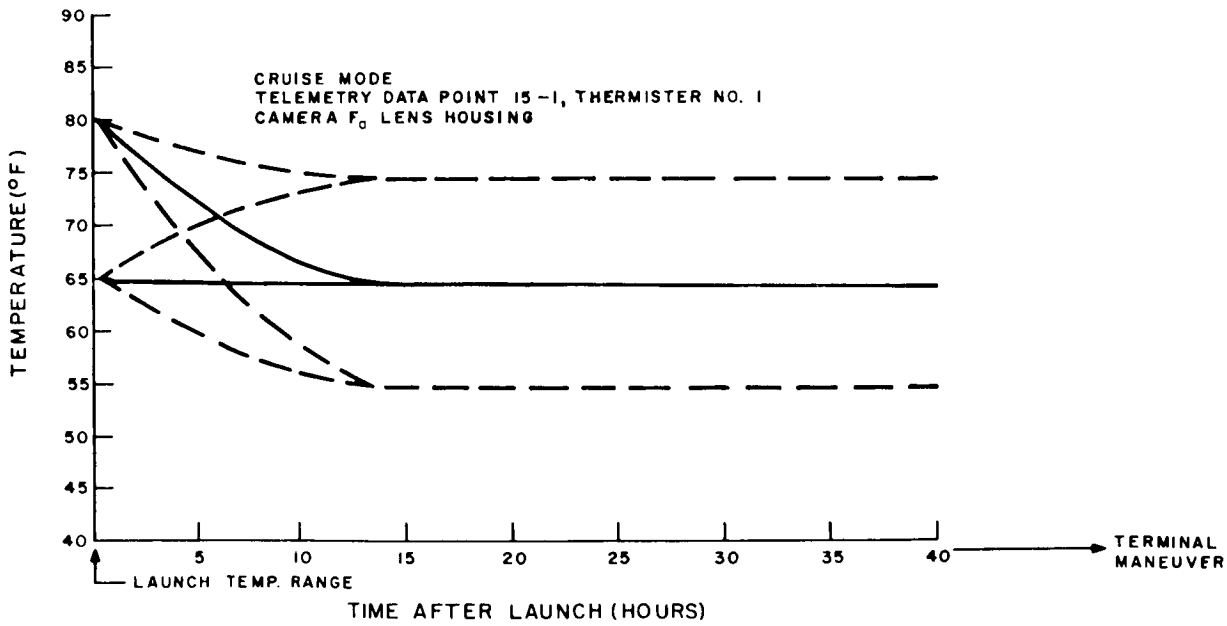

Figure 3-3. Predicted F_a Camera Lens Housing temperature during cruise mode

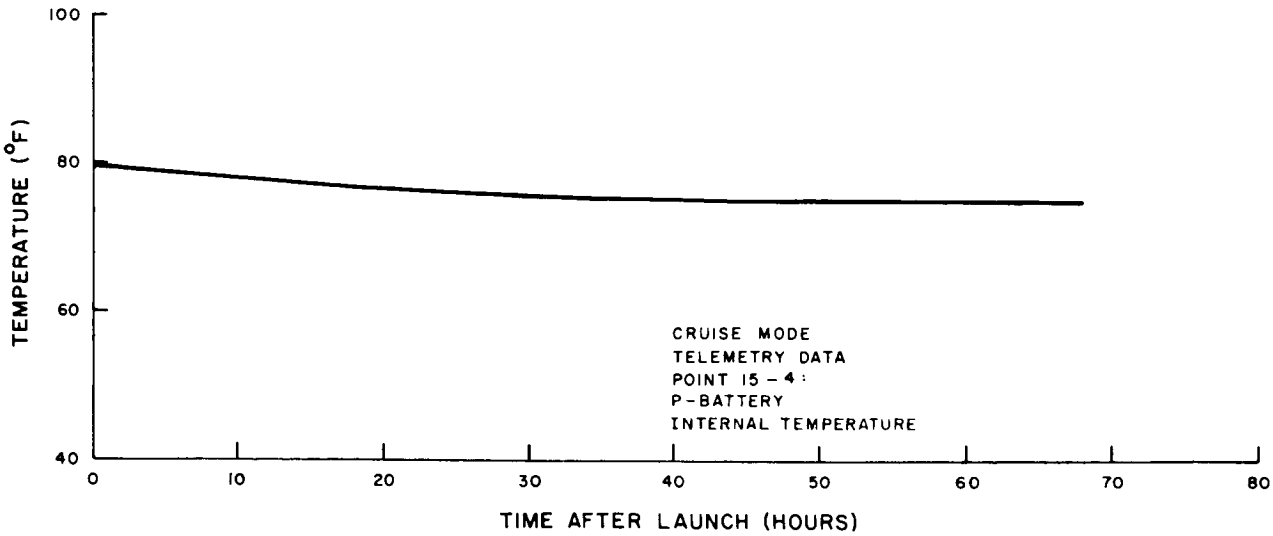

Figure 3-4. Actual P-Battery internal temperature during cruise mode

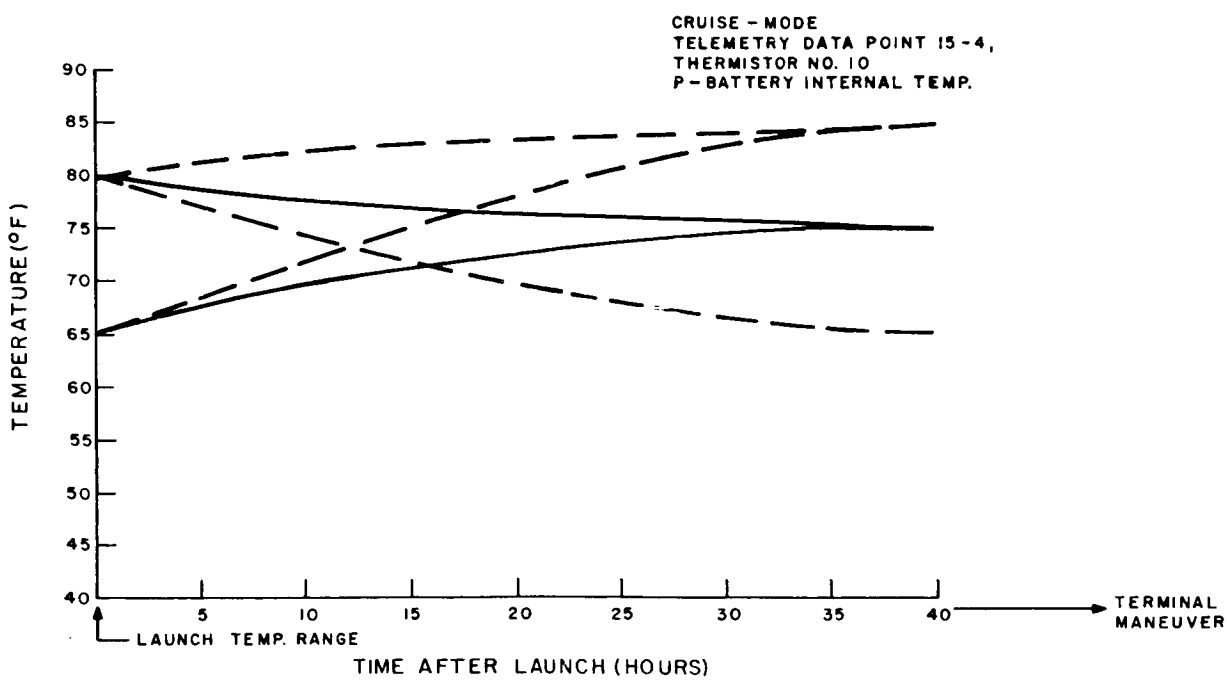

Figure 3-5. Predicted P-Battery internal temperature during cruise mode

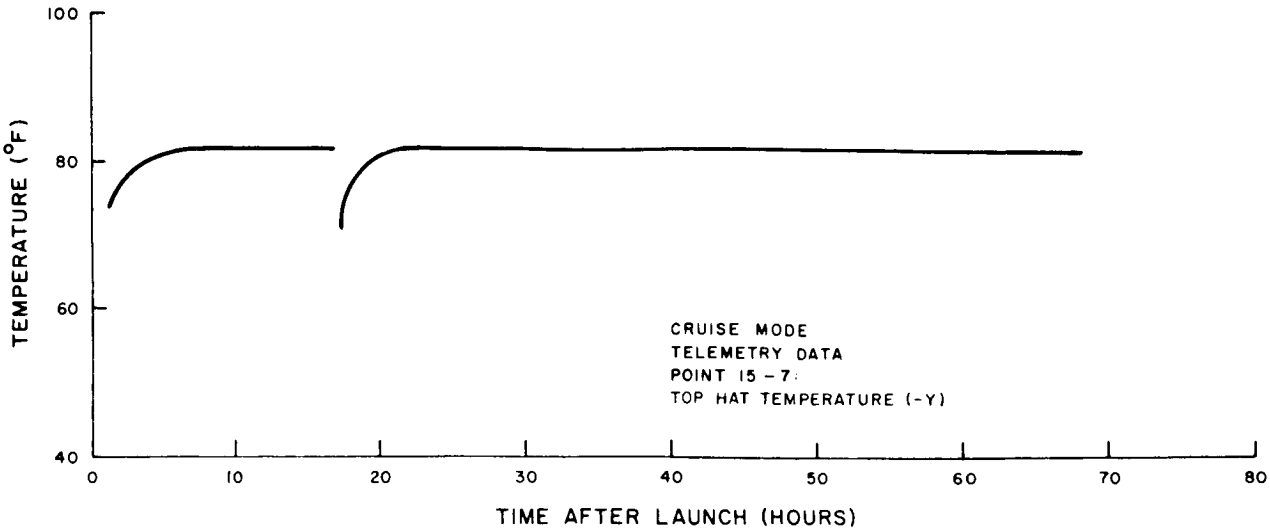

Figure 3-6. Actual Top Hat temperature (-y) during cruise mode

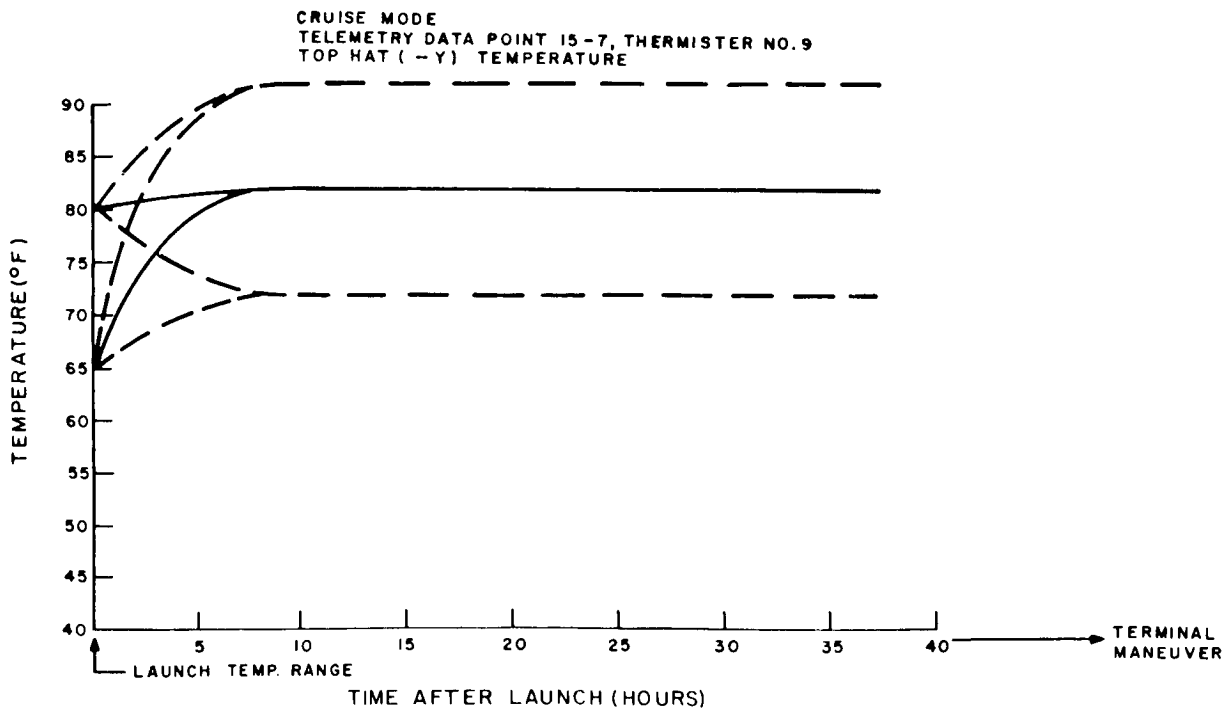

Figure 3-7. Predicted Top Hat temperature envelope during cruise mode

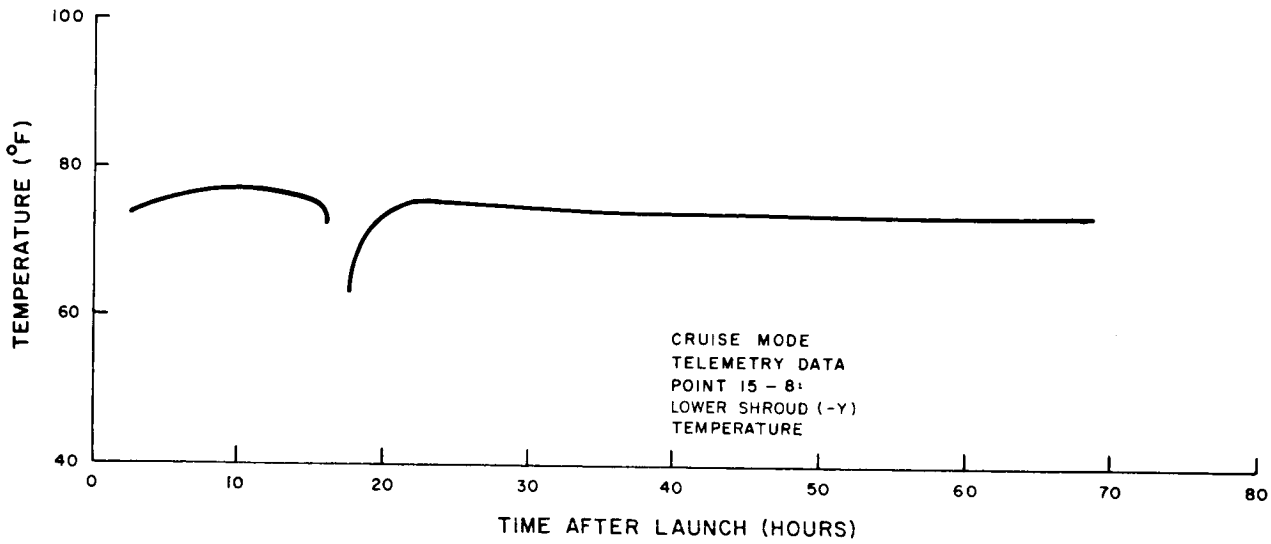

Figure 3-8. Actual Lower-Shroud temperature during cruise mode

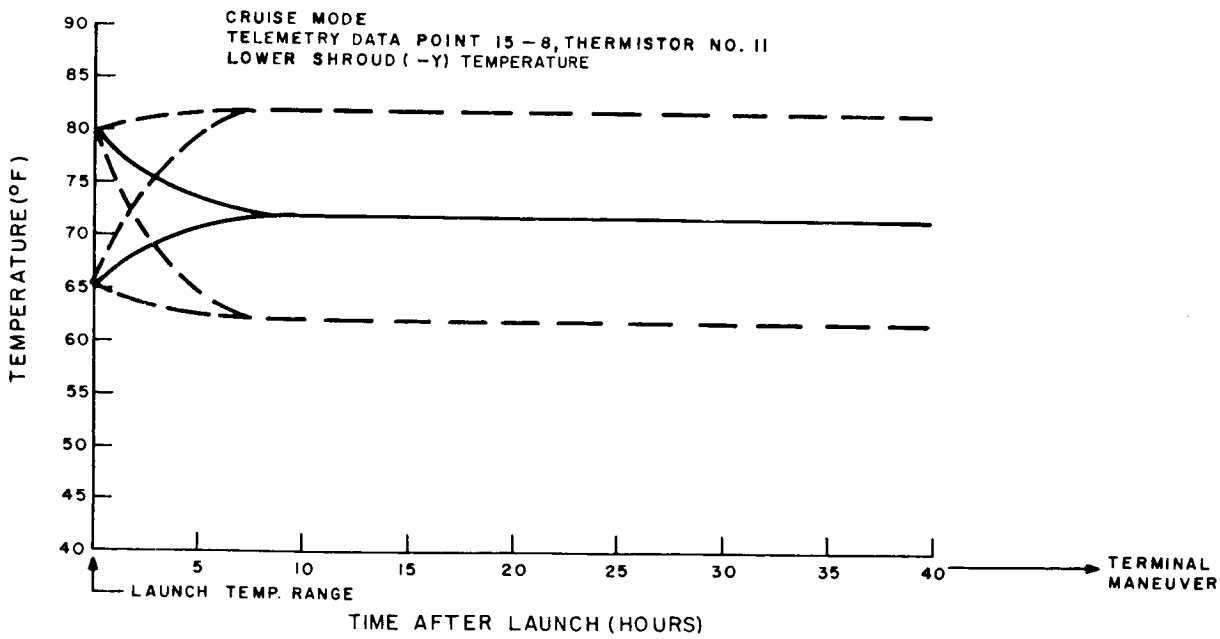

Figure 3-9. Predicted Lower-Shroud temperature during cruise mode

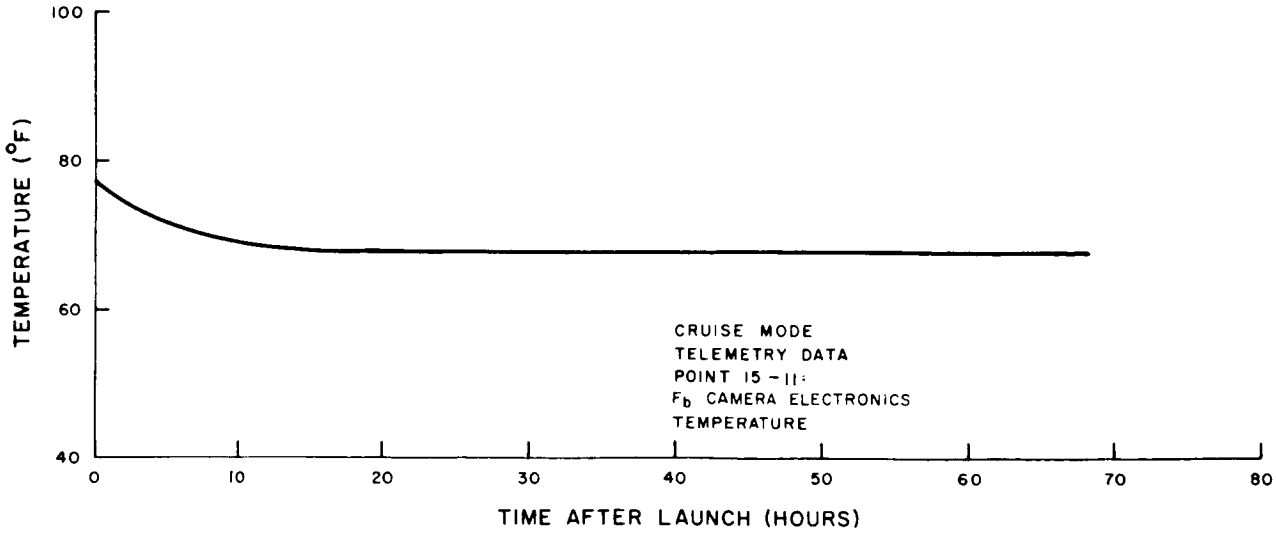

Figure 3-10. Actual F_b Camera Electronics temperature during cruise mode

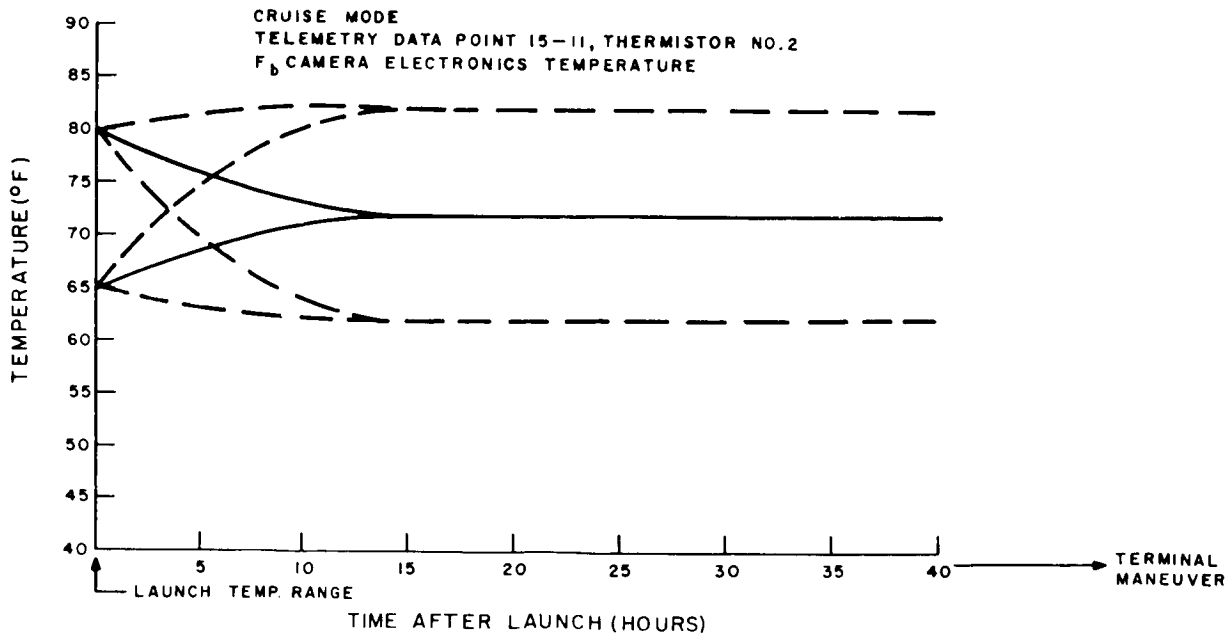

Figure 3-11. Predicted F_b Camera Electronics temperature during cruise mode

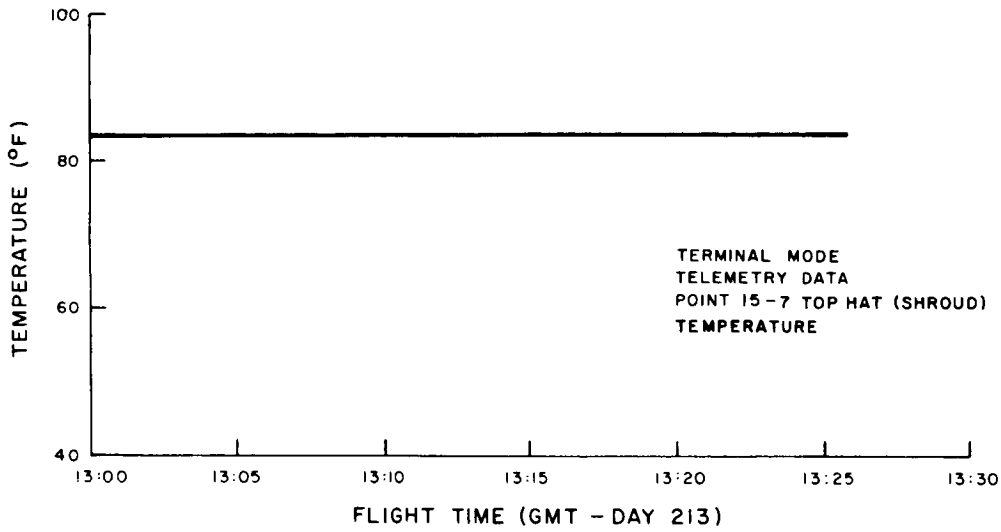

Figure 3-12. Actual Top Hat (Shroud) temperature during terminal mode

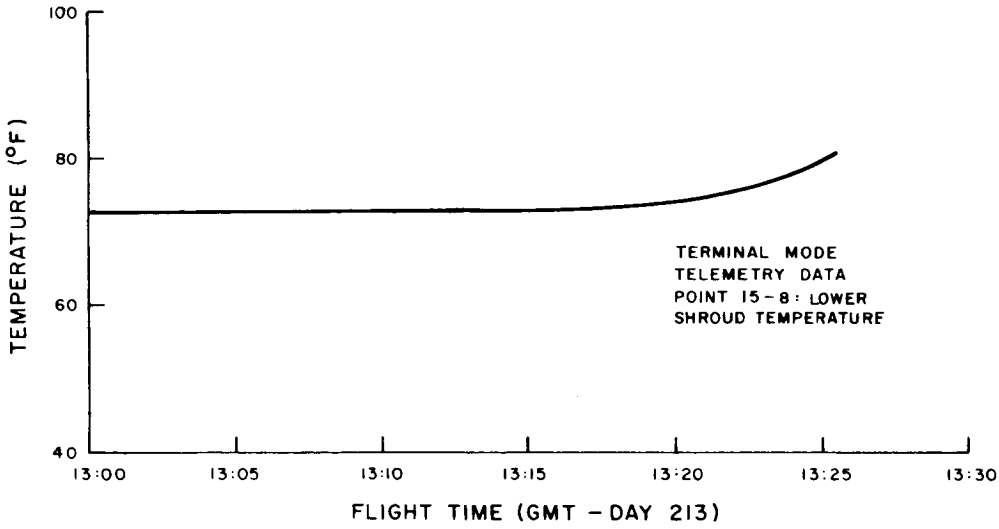

Figure 3-13. Actual Lower Shroud temperature during terminal mode

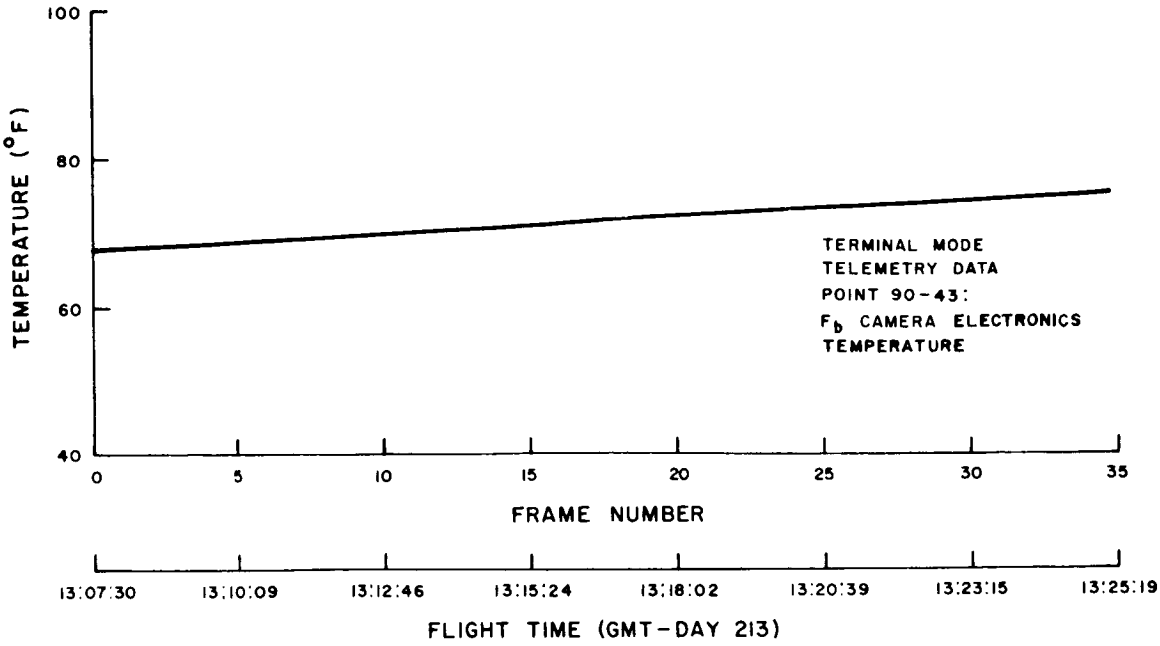

Figure 3-14. Actual F_b Camera Electronics temperature during terminal mode

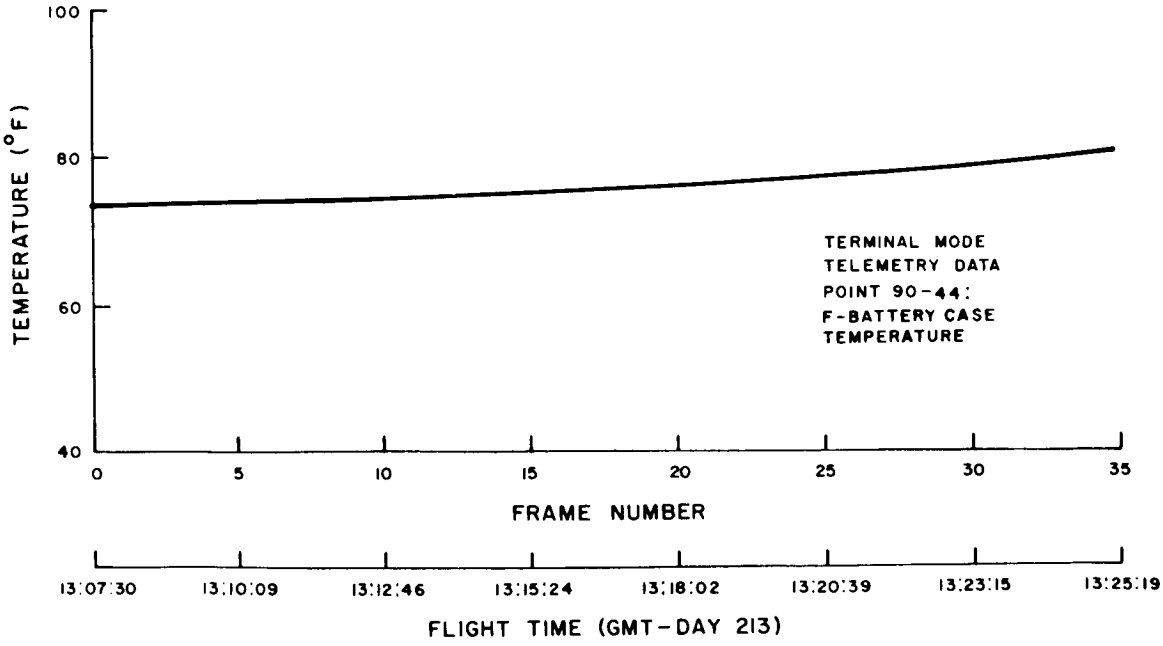

Figure 3-15. Actual F-Battery Case temperature during terminal mode

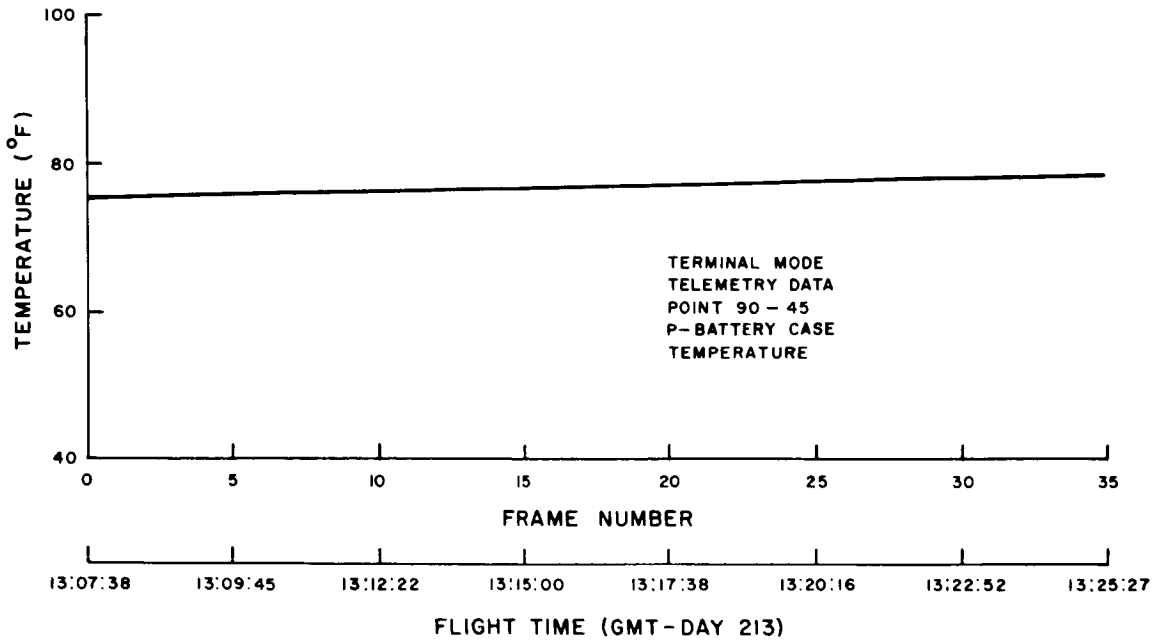

Figure 3-16. Actual P-Battery Case temperature during terminal mode

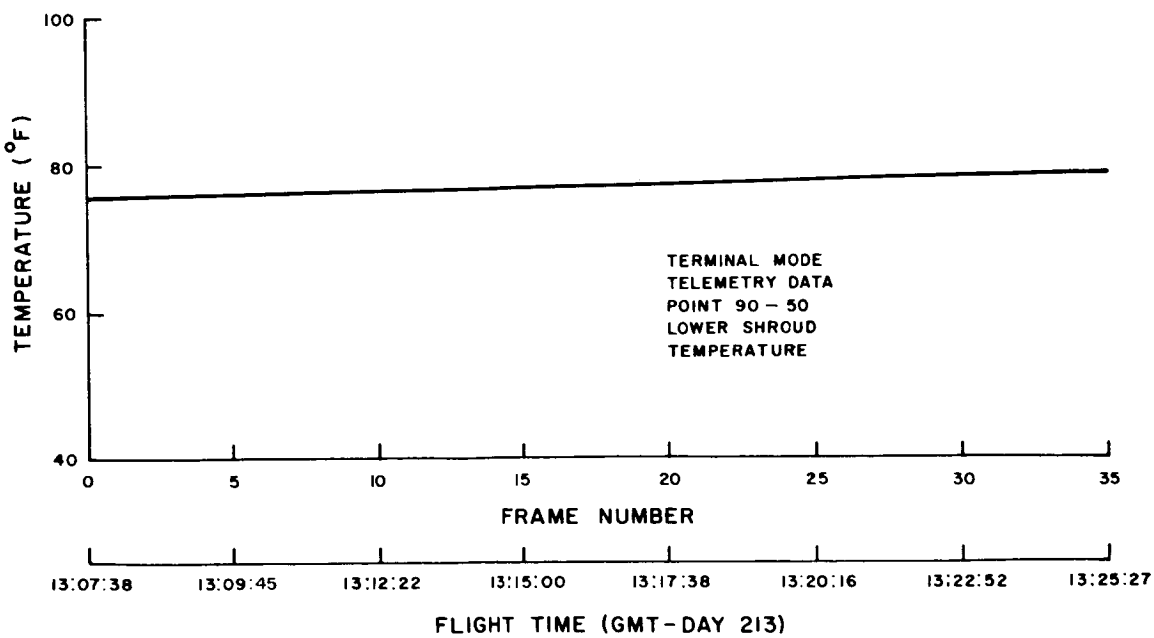

Figure 3-17. Actual Lower Shroud temperature during terminal mode

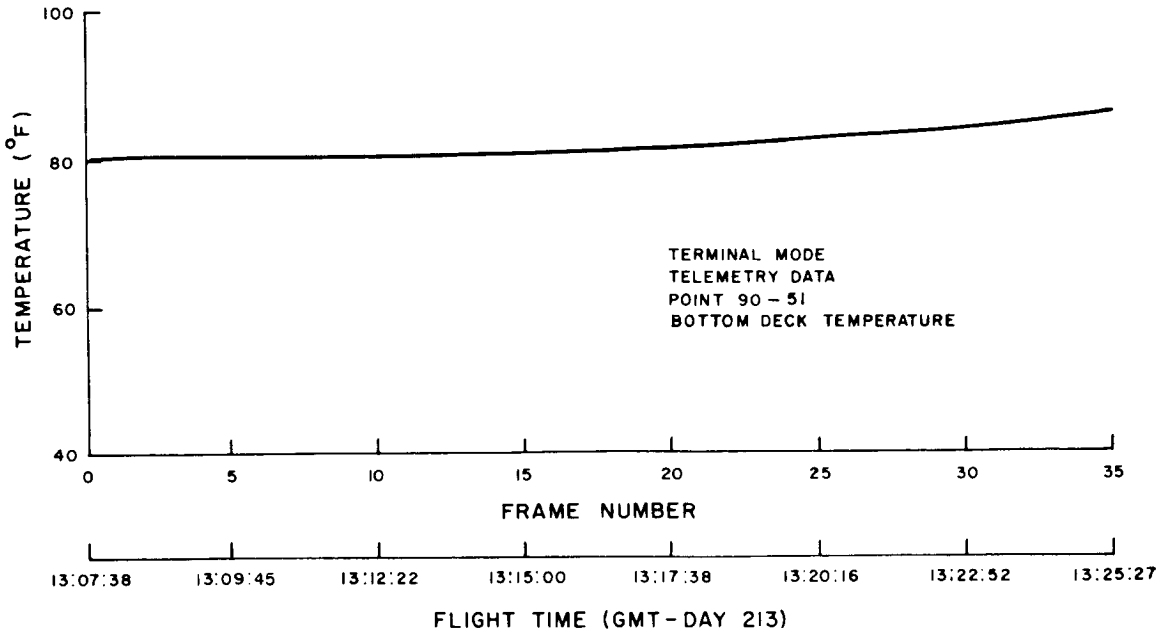

Figure 3-18. Actual Bottom Deck temperature during terminal mode

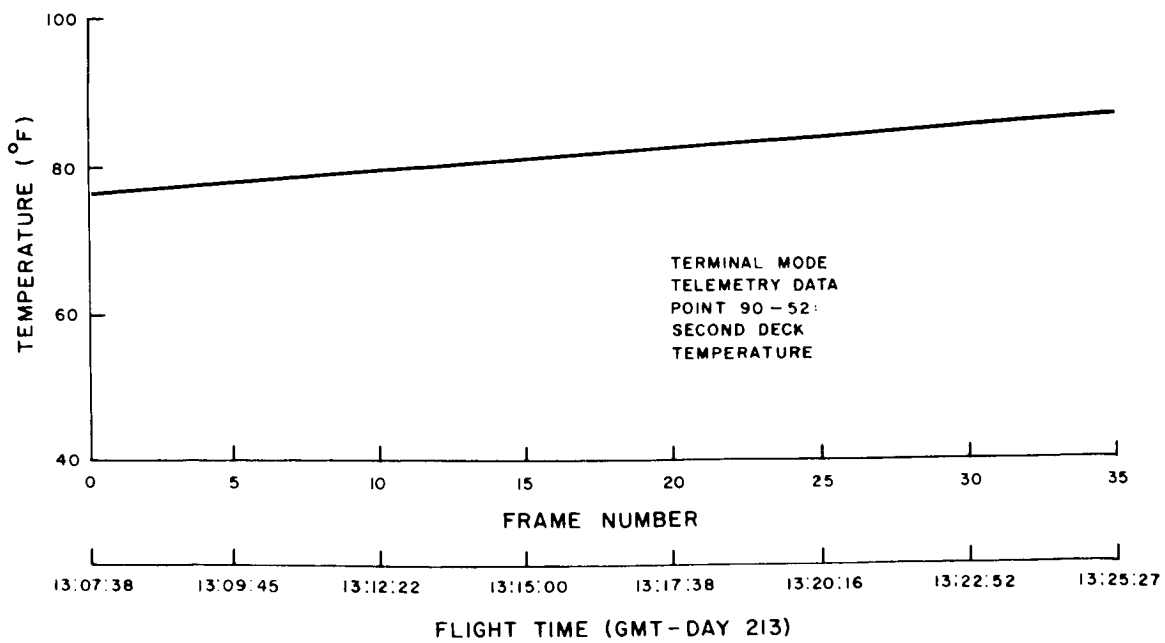

Figure 3-19. Actual Second Deck temperature during terminal mode

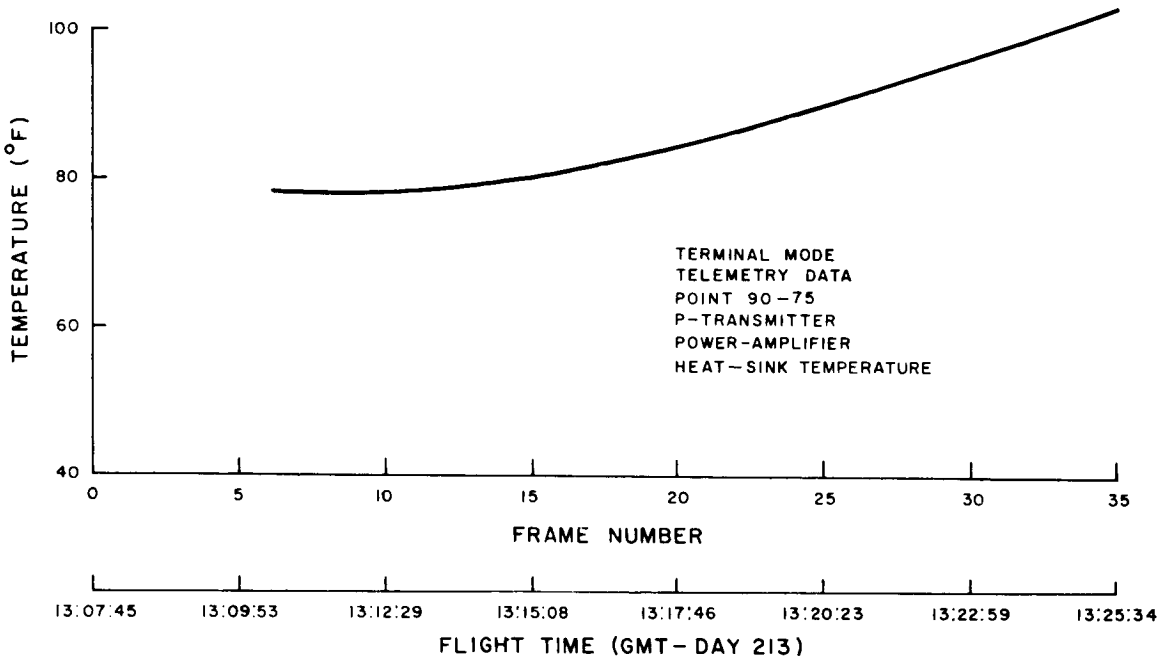

Figure 3-20. Actual P-Transmitter Power-Amplifier Heat-Sink temperature during terminal mode

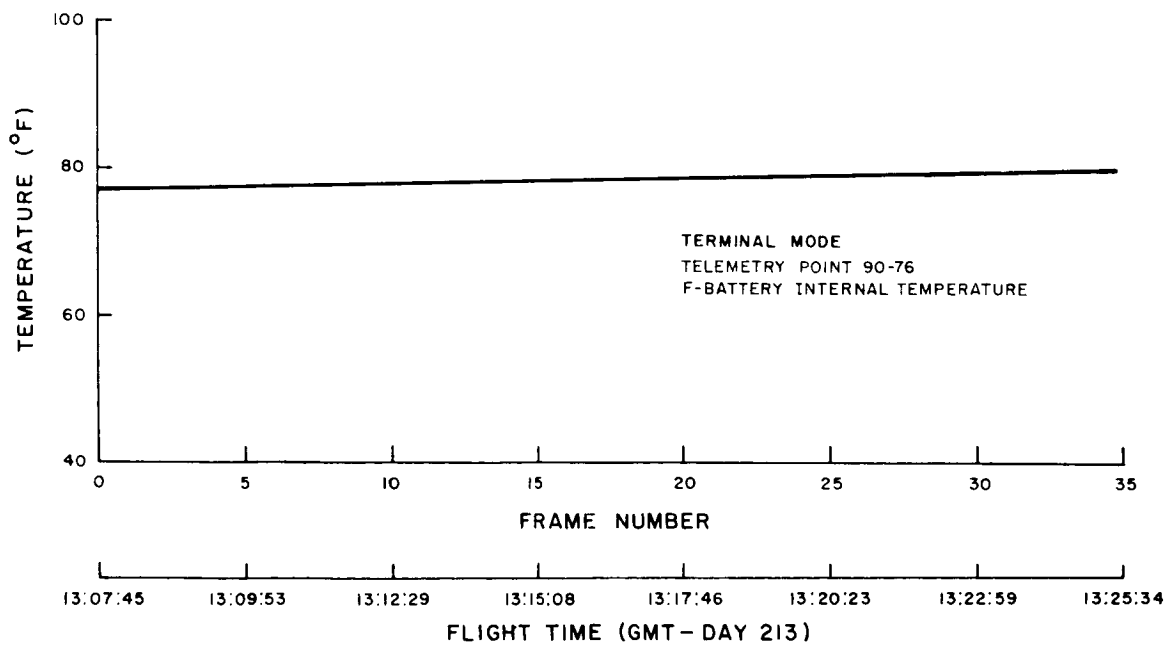

Figure 3-21. Actual F-Battery internal temperature during terminal mode

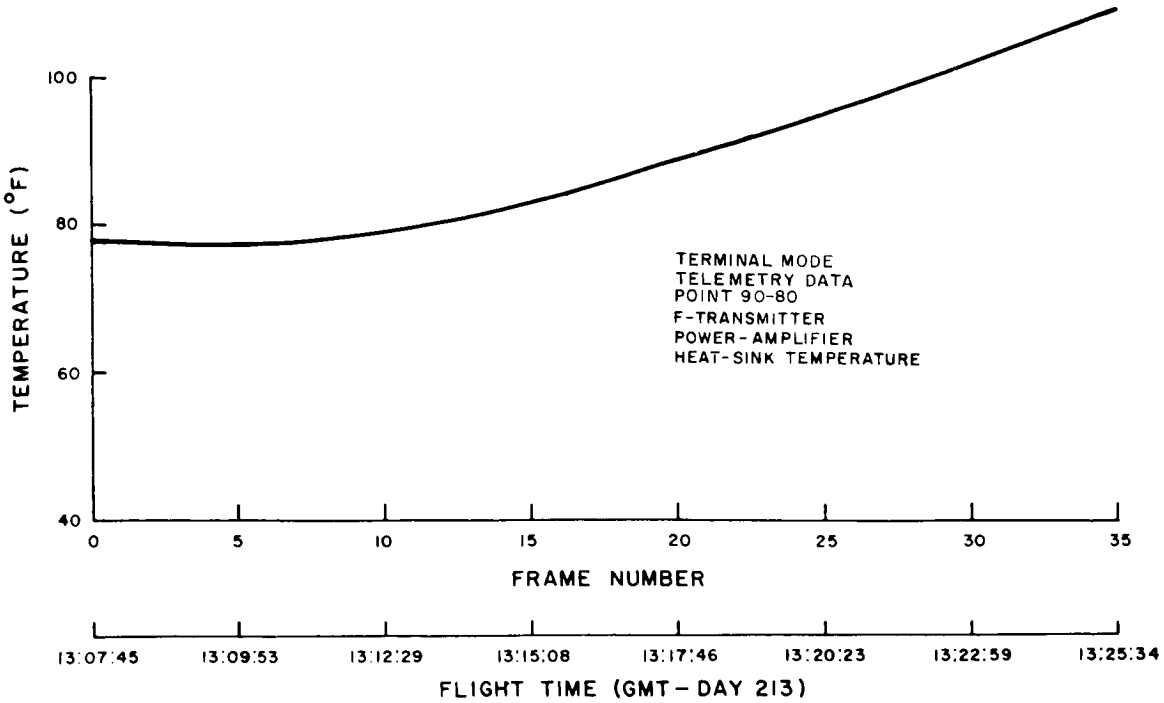

Figure 3-22. Actual F-Transmitter Power-Amplifier Heat-Sink temperature during terminal mode

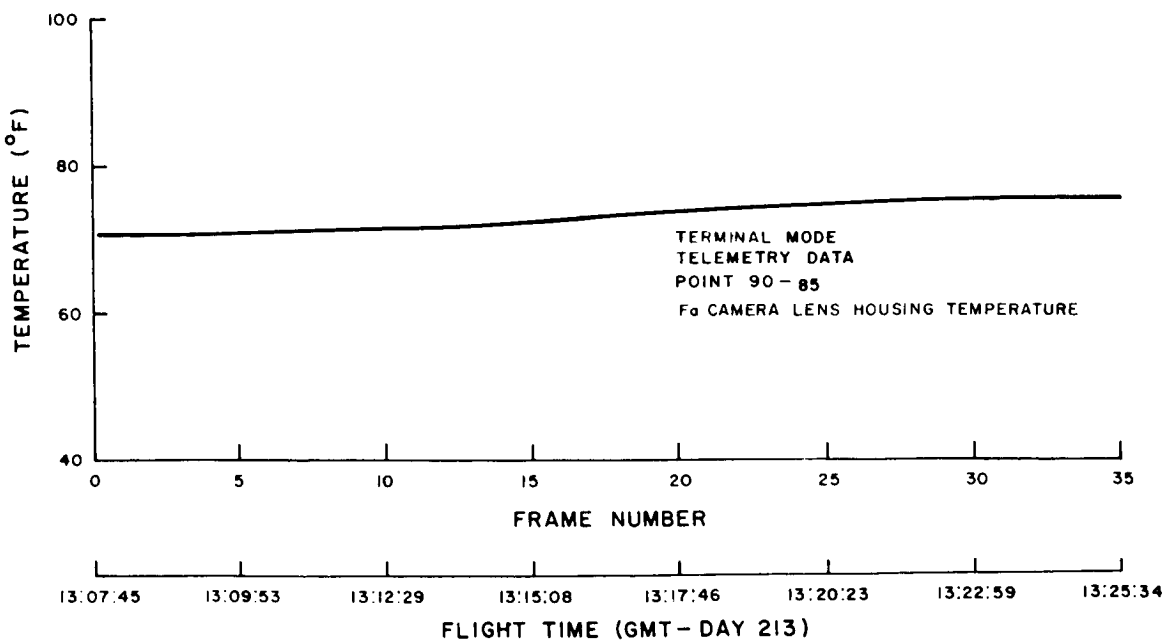

Figure 3-23. Actual F_a Camera Lens Housing temperature during terminal mode

The TV Subsystem power supply consisted of a Battery and a High-Current Voltage Regulator (HCVR) for each of the F- and P-Channels, and a Low-Current Voltage Regulator (LCVR) on the P-Channel only. The power-supply units functioned nominally throughout the mission. Figure 3-25 shows the budgeted and actual ampere-hour Battery capacity for each channel during the various phases of the RA-7 Mission. The total capacity budgeted for the F-Battery was 27.0 ampere-hours, while the actual capacity expended was 12.8 ampere-hours. The F-Battery voltages during cruise mode are shown in figure 3-26. The F-Battery voltages at launch, under a no-load condition, was 39.1 volts. From Clock start (L + 32.5 minutes) until F-Channel turn-on, the F-Battery supplied 0.05* amperes to operate the TV Subsystem Clock. After the initial Battery-voltage drop to 37.4 volts at Clock start, the F-Battery voltage gradually decreased during cruise mode to 34.6 volts. At the start of F-Channel warmup, the Battery voltage dropped to 33.5 volts at 7.7 amperes, and finally to 32.5 volts at 13.5 amperes during full-power operation. (See figure 3-29.)

For the P-Channel, the budgeted and actual Battery capacities were 30.0 and 21.0 ampere-hours, respectively. The P-Channel Battery, which powered the cruise-mode telemetry circuits (0.15 amperes*), had a pre-launch voltage of 35.6 volts, and at 16 hours after launch reached a plateau voltage of 34.4 volts and remained at this voltage until P-Channel warmup (see figure 3-27). The P-Battery voltages and currents were 32.5 volts at 10.5 amperes and 32.0 volts at 15.5 amperes in warmup and full-power modes, respectively.

Both F- and P-Battery voltages remained constant throughout the terminal mode, full-power operation (see figures 3-39 and 3-30).

The Low-Current Voltage Regulator (LCVR) supplied an output voltage of 27.70 volts during cruise-mode (figure 3-28) and 27.78 volts during terminal-mode operation. The reason for the rise during terminal mode was that the Telemetry Power Supply assumed part of the load (see figure 3-31). Both the F- and P-Channel High-Current Voltage Regulators performed as expected. Their output voltages were 27.52 and 27.50 volts for the F- and P-Channels, respectively, as shown in figure 3-32.

At the start of F-Channel warmup, the 90-point diagnostic telemetry data was switched on-to Channel 8. A listing of the terminal telemetry parameters is given in Table 3-2. The signal profile from the full-power command telemetry points (55 and 60) indicated that both channels went into warmup mode for 80 seconds and were then turned on into full-power operation by the TV Subsystem Control Programmer and Sequencer. The Transmitter telemetry data indicated normal supply voltages and operating temperatures for both channels. The Power-Amplifier cathode-current profiles for the transmitters were almost identical to pre-launch full-power tests confirming a high-power output for both channels. All telemetry indications for the TV Camera assemblies, which included four partial-scan Cameras, Video Combiner, and Control Programmer and Sequencer for the P-Channel, and two full-scan Cameras, Video Combiner, and Control Programmer and Sequencer for the F-Channel, were normal.

*These values are based on pre-launch measurements as the cruise-mode telemetry was not sensitive enough to read less than 0.2-ampere changes.

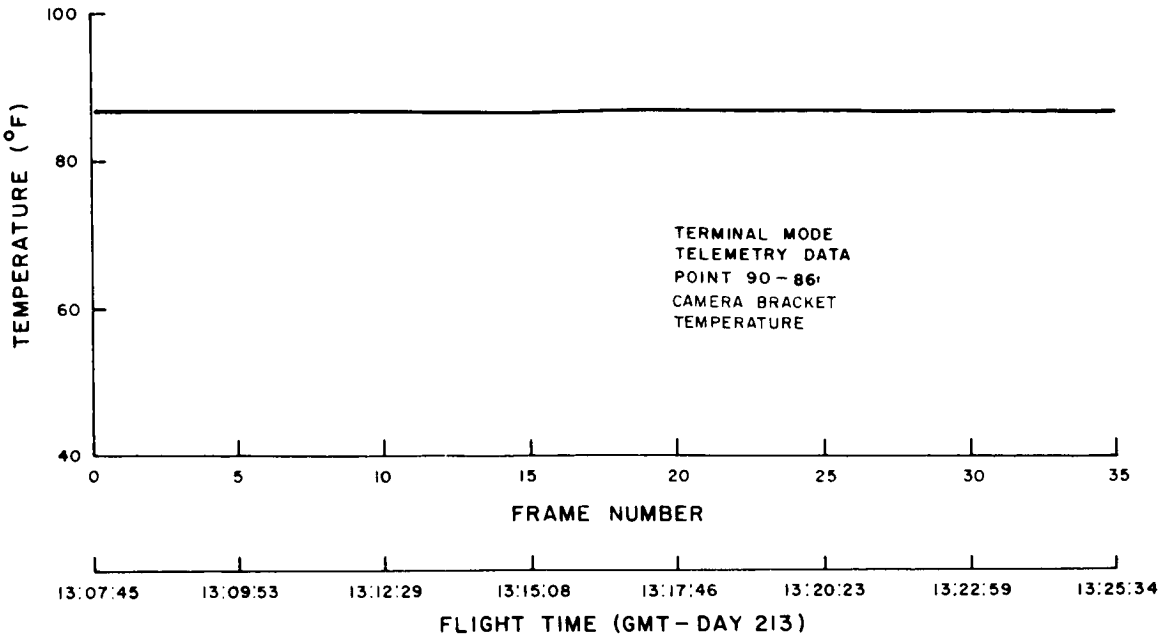

Figure 3-24. Actual Camera Bracket temperature during terminal mode

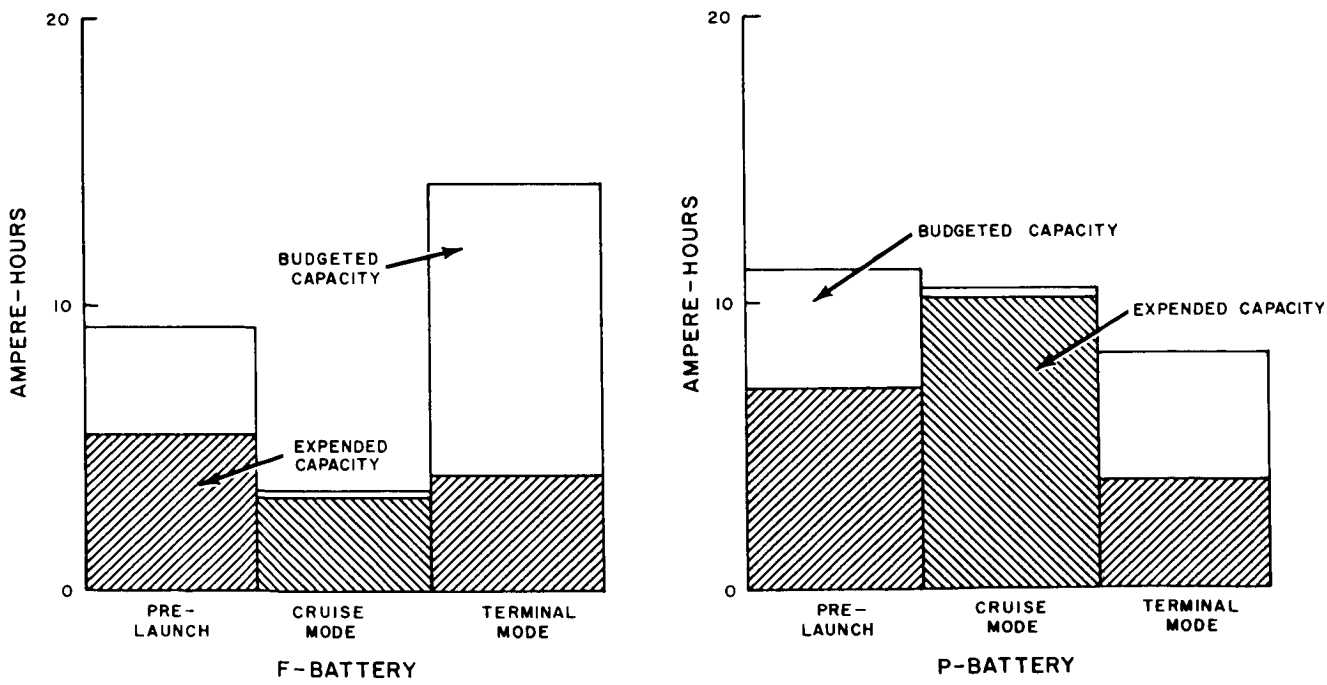

Figure 3-25. F- and P-Channel budgeted and actual battery capacities

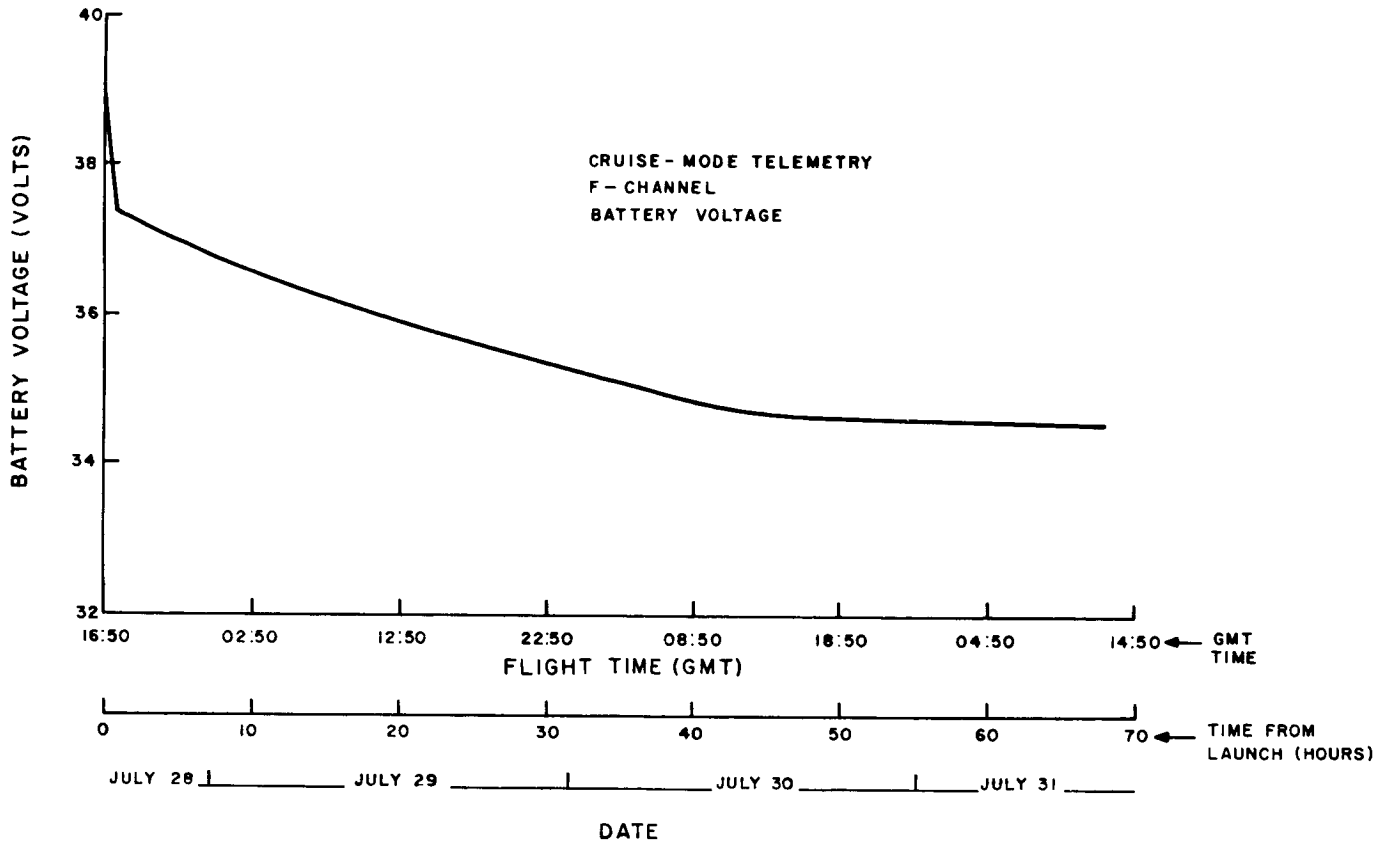

Figure 3-26. F-Channel Battery voltage during cruise mode

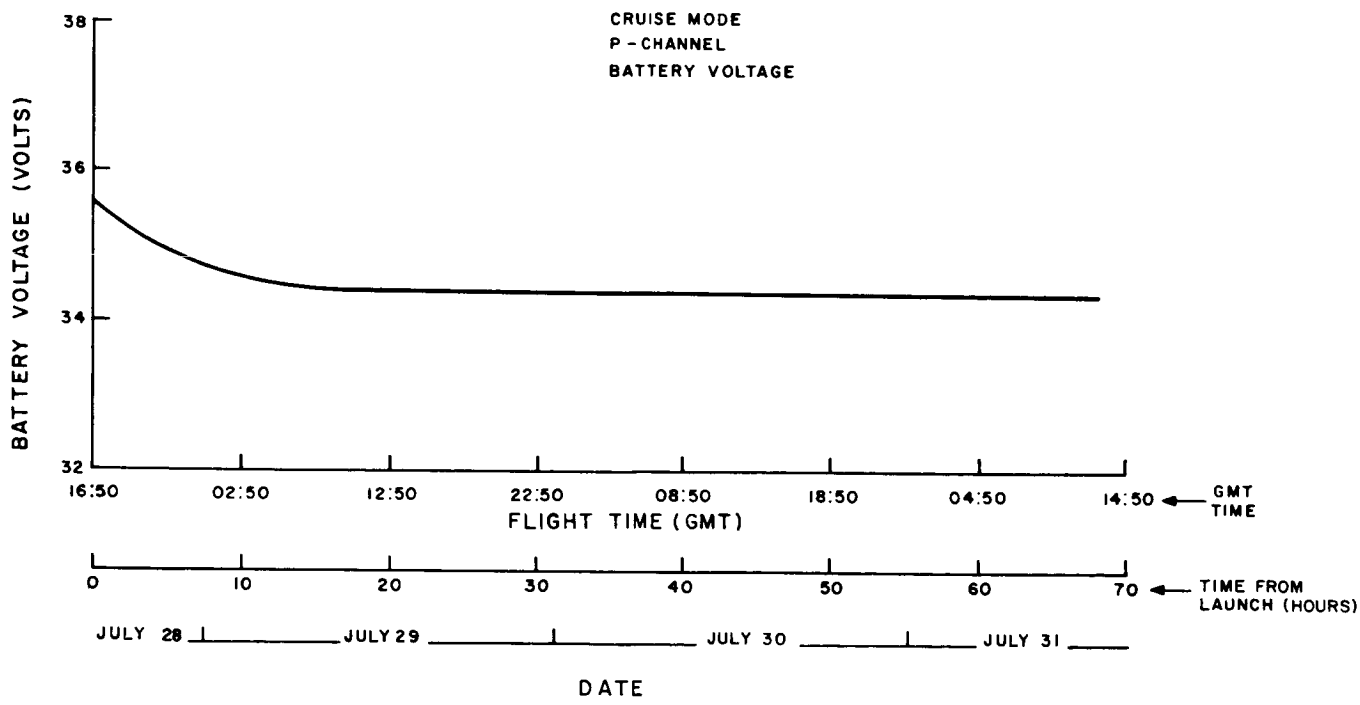

Figure 3-27. P-Channel Battery voltage during cruise mode

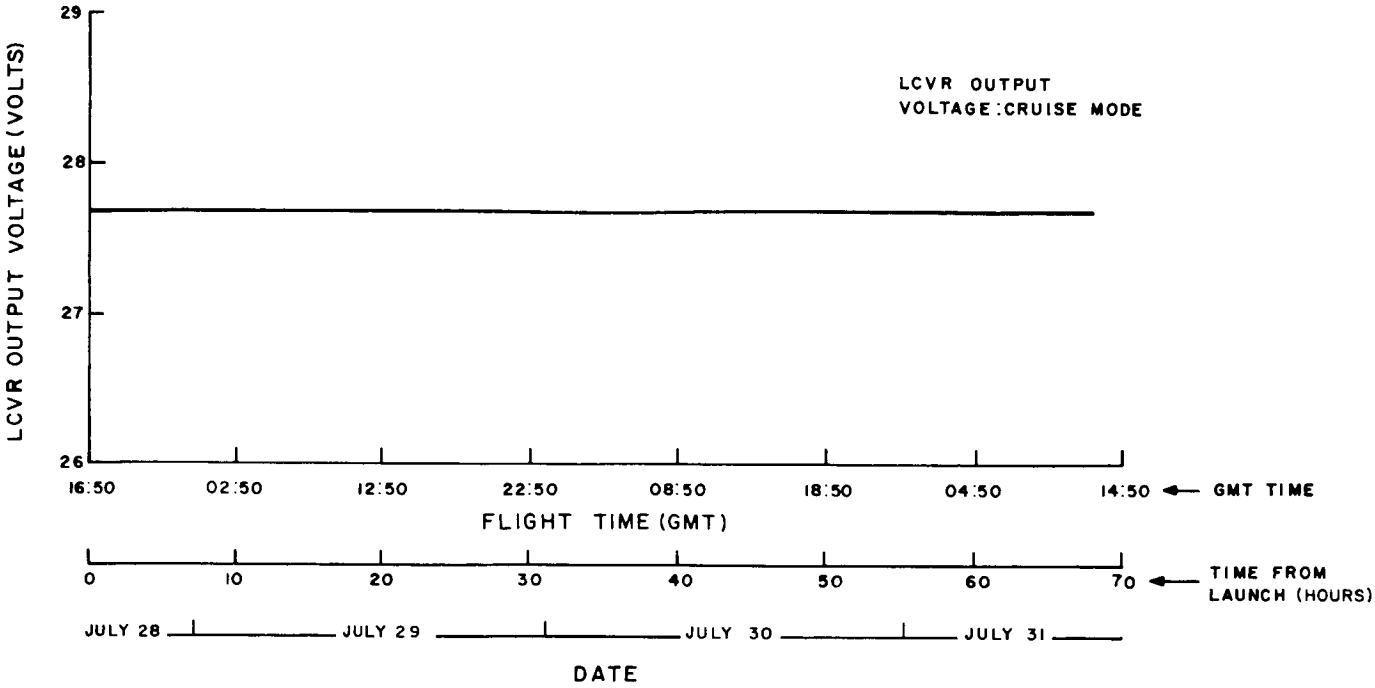

Figure 3-28. Low-Current Voltage Regulator output during cruise mode

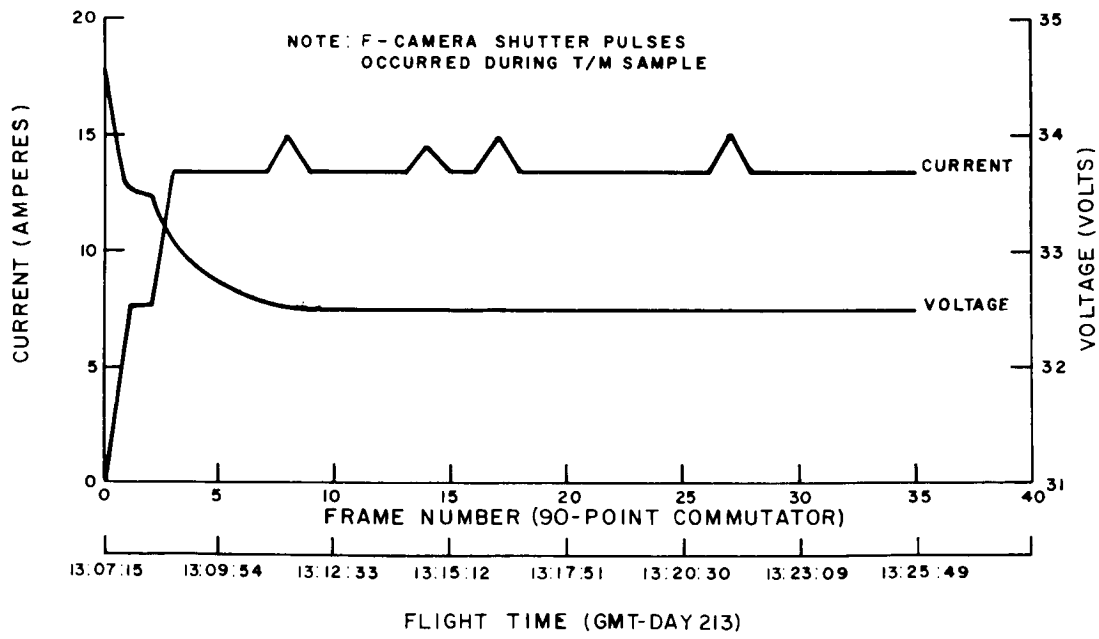

Figure 3-29. F-Channel Battery voltage and current during terminal mode

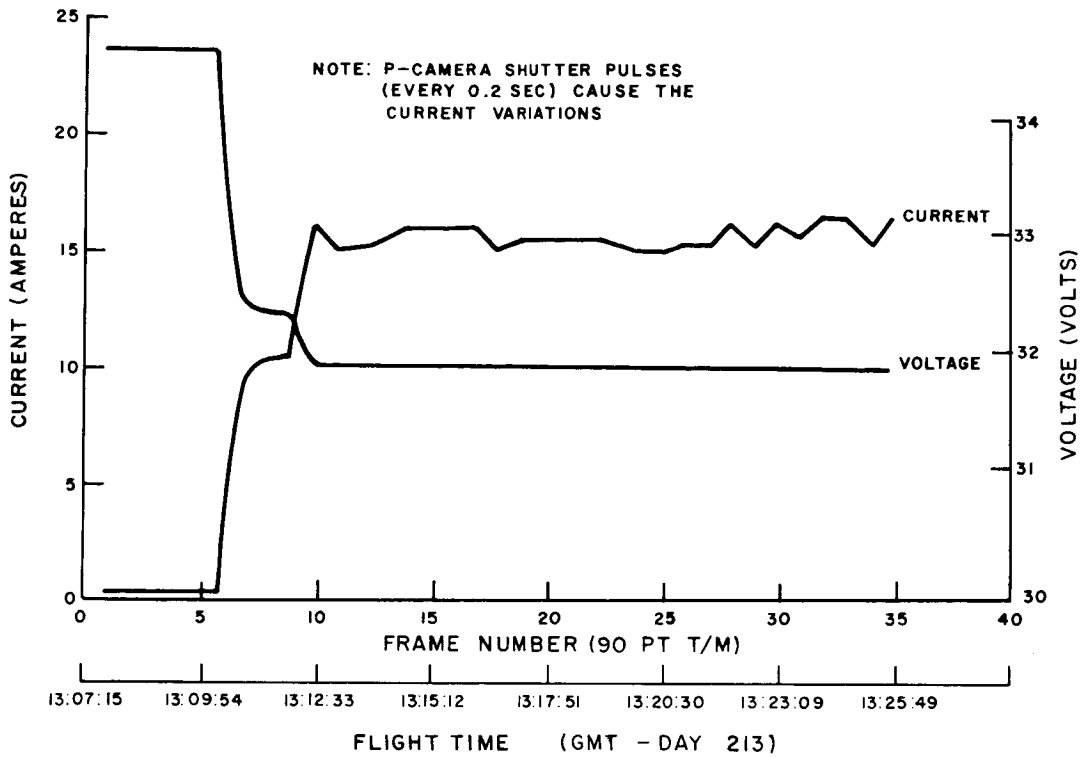

Figure 3-30. P-Channel Battery voltage and current during terminal mode

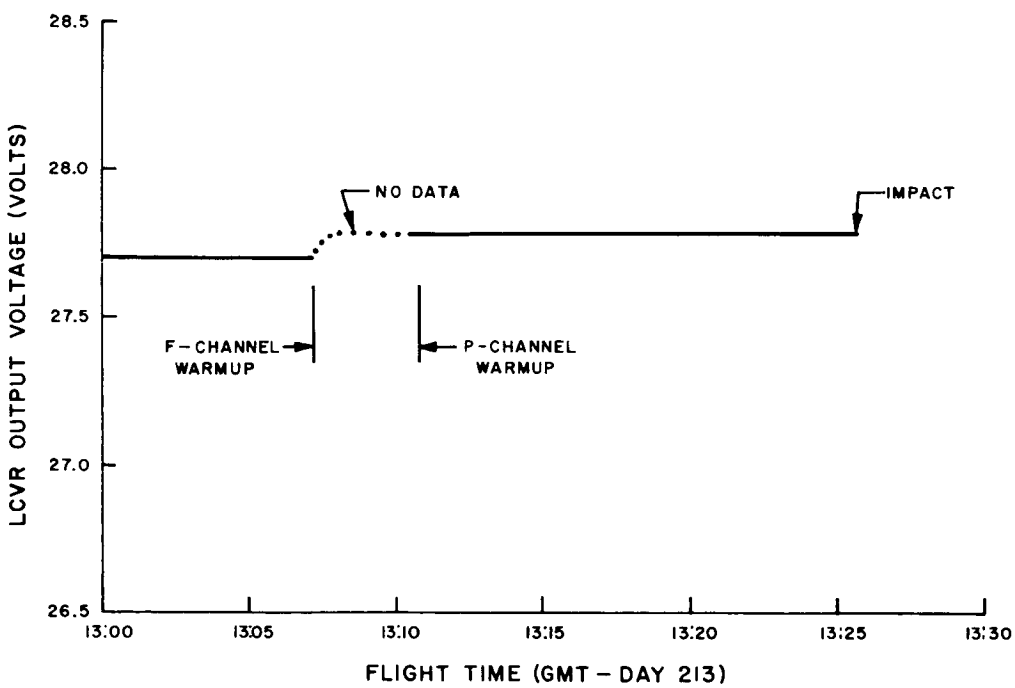

Figure 3-31. Low-Current Voltage Regulator output during terminal mode

TABLE 3-2

TV SUBSYSTEM PARAMETERS MONITORED DURING TERMINAL MODE BY 90-POINT TELEMETRY COMMUTATOR

Data Point No.	Parameter Monitored
1	Camera P1 Vertical Sweep
2	Camera P1 Horizontal Sweep
3	Camera P1 G1 and Focus Current
4	Camera P1 +1000 V and 300 V
5	Camera P1 Shutter and Lamp Drive
6	Camera P1 Vidicon Filament
7	Zero Reference
8 thru 14	Same as 1 thru 7 except for P2 Camera
15 thru 21	Same as 1 thru 7 except for P3 Camera
22 thru 28	Same as 1 thru 7 except for P4 Camera
29 thru 34	Same as 1 thru 6 except for F_a Camera
35	Full Scale Reference
36 thru 42	Same as 1 thru 7 except for F_b Camera
43	F_b Camera Electronics Temperature (Sensor No. 2)
44	F Battery Case Temperature (Sensor No. 4)
45	P Battery Case Temperature (Sensor No. 5)
46	P Unregulated Bus
47	P Regulated Bus (-27.5 V)
48	F Unregulated Bus
49	F Regulated Bus (-27.5 V)
50	Lower Shroud Temperature (+Y) (Sensor No. 12)
51	Bottom Deck Temperature (-X, -Y quadrant) (Sensor No. 13)
52	Second Deck Temperature (-Y) (Sensor No. 14)
53	Second Deck Temperature (+Y) (Sensor No. 15)
54	LCVR Input Voltage
55	F-Channel Full-Power Command
56	P Battery Current
57	F Battery Current
58	F Battery Terminal Voltage
59	P Battery Terminal Voltage
60	P-Channel Full-Power Command
61	F Sequencer "T" Flip-Flop (No. 2)
62	Zero Reference
63	F Sequencer Oscillator (18 Kc)
64	P Sequencer Voltage +12V
65	P Sequencer Voltage -12V
66	P Sequencer Oscillator (18 Kc)
67	F Sequencer Voltage +12V

TABLE 3-2 TV SUBSYSTEM PARAMETERS MONITORED DURING TERMINAL MODE BY 90-POINT TELEMETRY COMMUTATOR (Continued)	
Data Point No.	Parameter Monitored
68	F Sequencer Voltage -12V
69	F Sequencer "T" Flip-Flop (No. 1)
70	P Sequencer "R" Flip-Flop (No. 1)
71	P Sequencer "R" Flip-Flop (No. 2)
72	P Combiner Video Output
73	Zero Reference
74	F Combiner Video Output
75	P-Transmitter PA Heat Sink (Sensor No. 6)
76	F Battery Internal Temperature (Sensor No. 8)
77	F Transmitter PA +1000 V
78	F Transmitter IPA -750 V
79	F Transmitter PA Cathode Current
80	F Transmitter PA Heat Sink (Sensor No. 7)
81	Zero Reference
82	P Transmitter PA +1000 V
83	P Transmitter IPA -750 V
84	P Transmitter PA Cathode Current
85	F_a Camera Lens Housing Temperature (Sensor No. 1)
86	Camera Bracket Temperature (Sensor No. 3)
87	Full Scale Reference
88	Zero Reference
89	Frame Reference
90	Frame Reference

The telemetry data for the F-Channel Video Combiner output shown in figure 3-33, indicated that the video output was greater than expected. This telemetry point (90-72) measures the amplitude of the composite video signal at the video combiner output, which has a range of 1.5 volts from sync tip to peak white for each camera, and is used only to indicate that a video signal is being applied to the modulator input. Its use as a light meter is quite limited, because it monitors two cameras that have a four-to-one difference in their dynamic ranges and the data sample was not synchronized with the camera readouts.

The performance of the TV Subsystem telemetry was nominal throughout the mission. A slow shift in center frequency of the Channel-8 VCO was noted, which amounted to only one or two cycles and was within the ± 2-cps VCO tolerance. The 90-point commutator stopped on data point 69 at the end of the pre-launch test and started on the

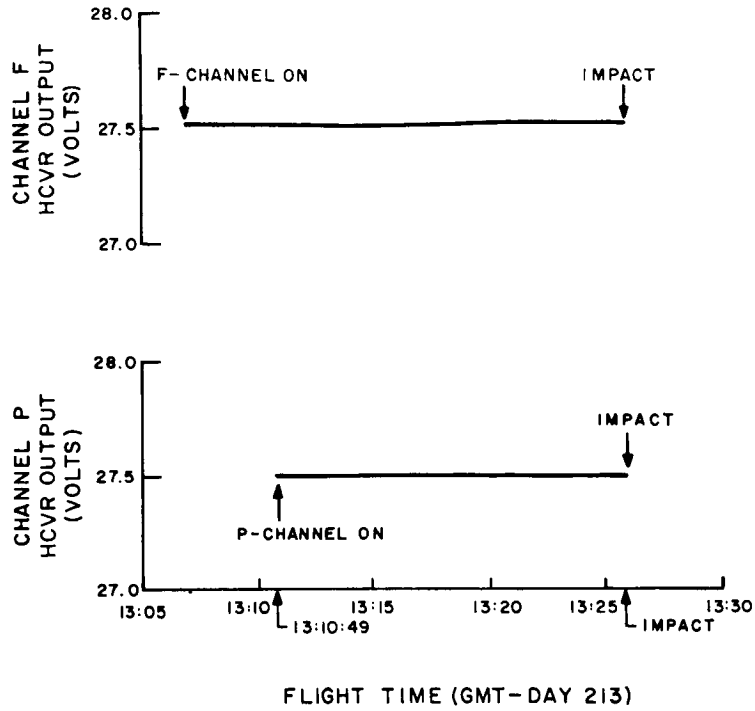

Figure 3-32. F- and P-Channel High-Current Voltage Regulators outputs during terminal mode

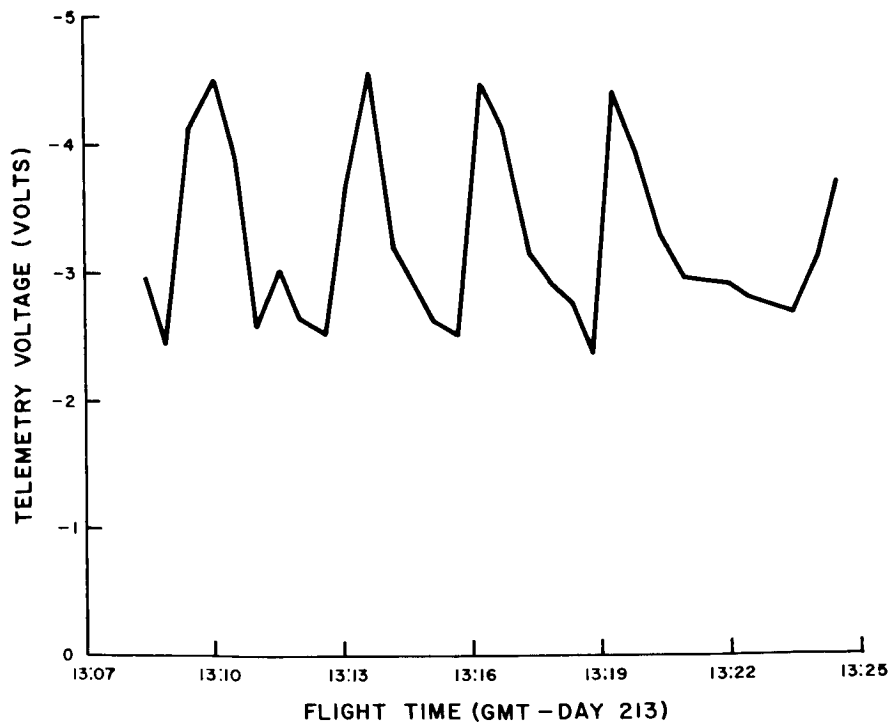

Figure 3-33. F-Channel Video Combiner output during terminal mode

same point at terminal mode, signifying no movement of the commutator during cruise mode. Thus, it may be concluded that the telemetry verified that the TV Subsystem performed a nominal mission.

B. Ground Support Equipment

1. Film Recorder Calibration Procedure

a. General

The function of the Ground Recording Equipment of the Ranger Operational Ground Station at Goldstone was to record on 35-mm film an accurate reproduction of the lunar scene as seen by the TV cameras. All pre-flight calibrations were made to assure that picture detail and photometric characteristics were reproduced faithfully.

With the test specifications, RTSP 1200, 1220, and 1240, the equipment was calibrated to obtain sufficient resolution and linearity to preserve the picture detail.

b. Cathode Ray Tube and High Voltage Power Supply Calibrations

The first step in the Film Recorder Calibration is the designation of mission and backup Cathode Ray Tubes (CRT's) and High-Voltage Power Supplies (HVPS's). At all sites, grid drive as a function of 35-mm density runs were made on the following combinations:

- Mission CRT and Mission HVPS
- Mission CRT and Backup HVPS
- Backup CRT and Mission HVPS

Prior to the mission, a film development gamma was specified and held constant throughout the calibration. Upon initial installation, the lens f-stop was varied and a film record was made of discrete flat-field intensity settings on G1 of the CRT. Succeeding runs verified the results prior to removal of the calibration equipment from the film recorder.

These runs were performed:

- To determine optimum operating conditions;
- For verification of data to ensure proper operation of designated mission and backup components; and
- To determine settings on the backup configurations.

c. Flight Model Calibration

The Film Recorders, in mission configuration, were calibrated with the most recent flight model camera calibration data available. After establishing end-limit densities on 35-mm film at the specified gamma to be 1.9 ± 0.1 for peak whites and 0.35 ± 0.05 for blacks, final adjustments were made on the CRT drives. The resultant film data was submitted to JPL.

2. RA-7 Calibration

a. Grid Drive as a Function of Film Density Curves

For the RA-7 mission, the CRT and HVPS status established is given in Table 3-3.

TABLE 3-3
CRT AND HVPS STATUS

Film Recorder No.	CRT		HVPS	
	Mission	Backup	Mission	Backup
1	1294	032	1007	1015
2	1297	1214	1002	1011
3	1400	025	1008	1012

Data were obtained on all mission-backup combinations and results documented. The mission configuration curves are shown in Figure 3-34.

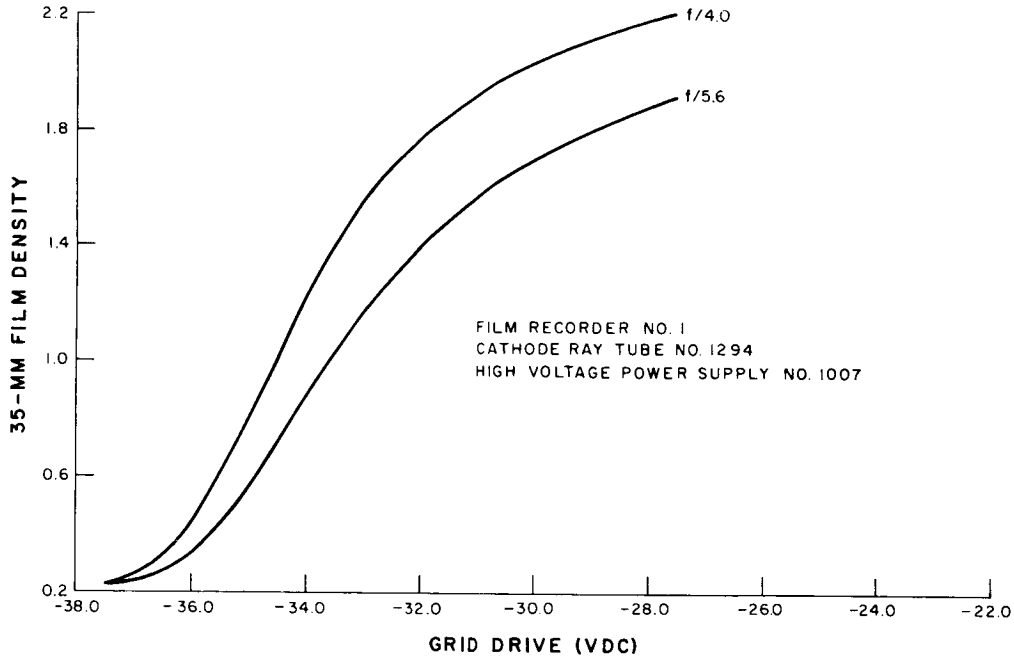

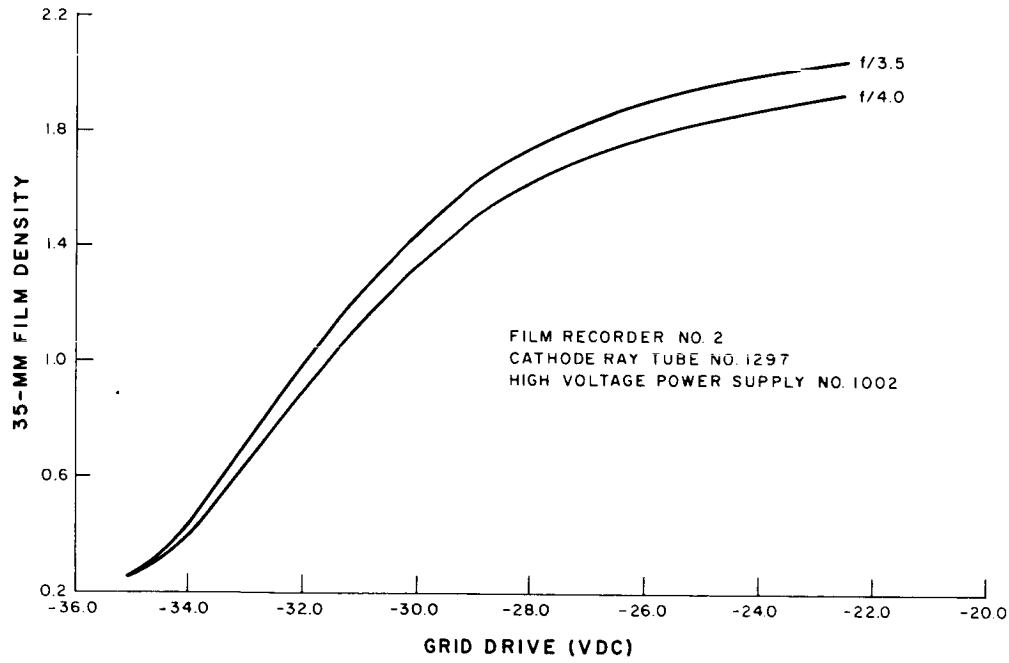

Figure 3-34. Mission configuration curves

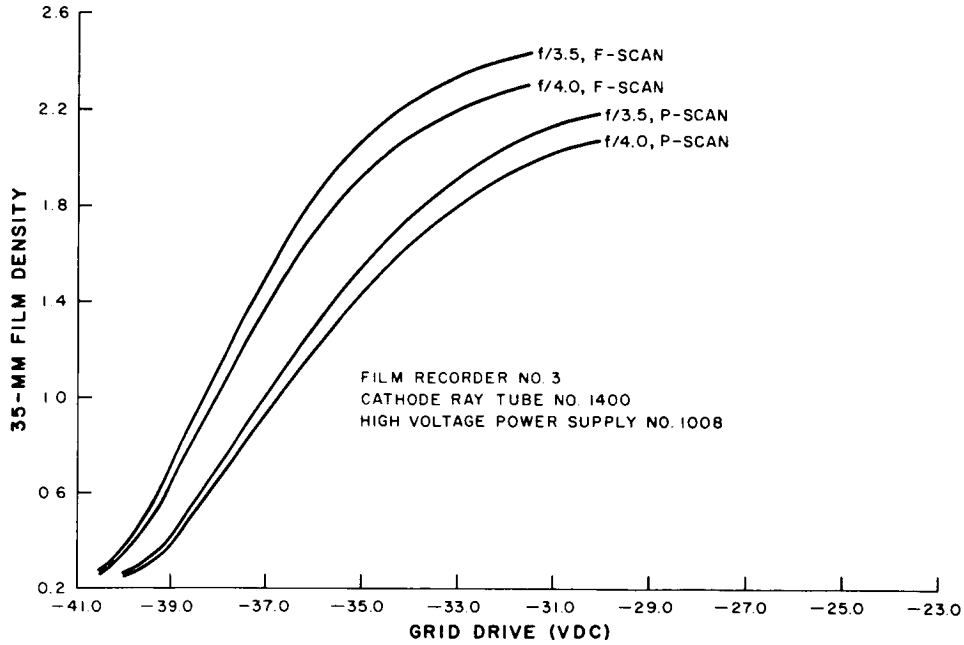

Figure 3-34. Mission configuration curves (Continued)

b. Flight Model Film Calibration Data

A magnetic tape recording was received on July 17, 1964 at the DSIF at Goldstone of the RA-7 camera calibration made at ETR. Final setup was achieved with this data. The following criteria were utilized in the setup:

- Black Level (0.35 ± 0.05 density) was determined by F_b-and-P2 Cameras, which had the lowest black levels.
- White Level (1.9 ± 0.1 density) was determined by F_a-and P-2 Cameras, which had the highest white levels.

A complete transfer curve of the full- and partial-scan cameras for Film Recorders Nos. 1 and 2 was submitted to JPL. Settings were determined in Film Recorder No. 3, but because of the kinescope low-light intensity problems, the calibration data were not submitted to JPL prior to launch. The black and white densities from Film Recorders Nos. 1 and 2 are given in Table 3-4.

TABLE 3-4 BLACK AND WHITE DENSITIES FROM FILM RECORDERS NOS. 1 AND 2						
Level/Cameras	P1	P2	P3	P4	F_a	F_b
Black	0.34	0.32	0.37	0.35	0.35	0.32
Peak White	1.72	1.95	1.80	1.90	1.93	1.73

Calibration prior to terminal mode was completed with the following components:

- Film Recorder No. 1, CRT No. 1294, and HVPS No. 1007 (unchanged)
- Film Recorder No. 2, CRT No. 1214, and HVPS No. 1002
- Film Recorder No. 3, CRT No. 027, and HVPS No. 1008

c. Mission Data

One problem, encountered with the OSE during the RA-7 mission, was corrected before the terminal-mode operation of the Spacecraft. The light intensity of Film Recorders Nos. 2 and 3 decreased. The backup kinescope and high-voltage power supply, which had previously been calibrated, were installed. A set of calibration data was prepared to assure that the density range was correct.

The problem of decrease in kinescope light intensity is currently under investigation by RCA. Initial test results indicate that a relation exists between the decrease in intensity and turning the OSE "off" and then "on" without allowing the equipment sufficient time to cool. The investigation will continue until the actual cause of the decrease in intensity is determined.

As per operational procedure (ROP-4), a film record of the RA-7 camera calibration data was made immediately following the mission, along with a grid drive, as a function of intensity run. From these data, the curves in Figure 3-35 were obtained.

Camera transfer data from the mission film were not immediately available, however, using the available data, the curves shown in Figure 3-36 were derived.

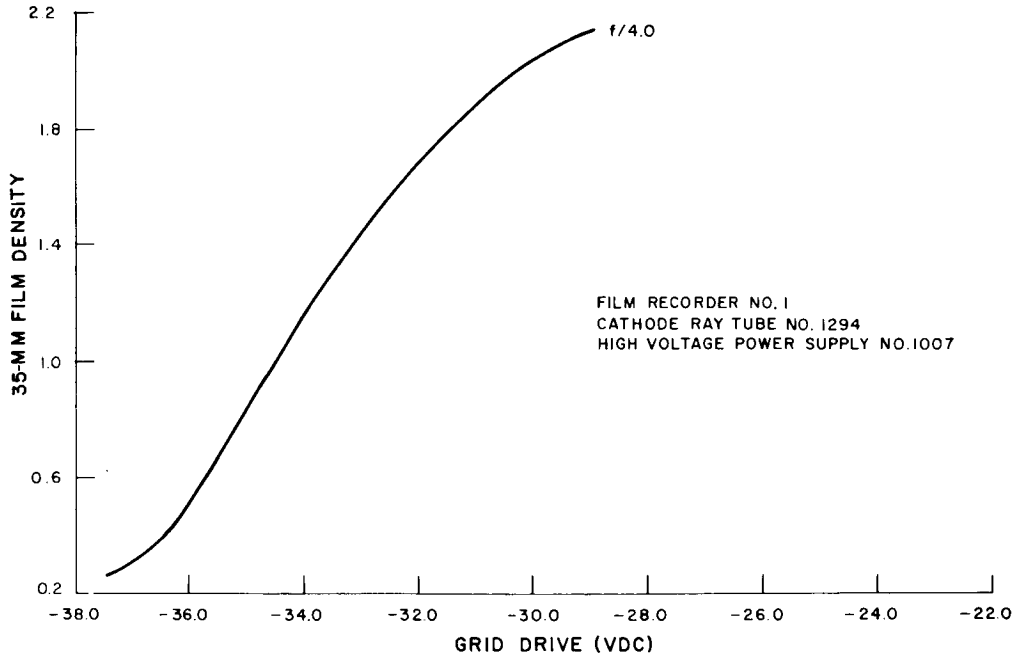

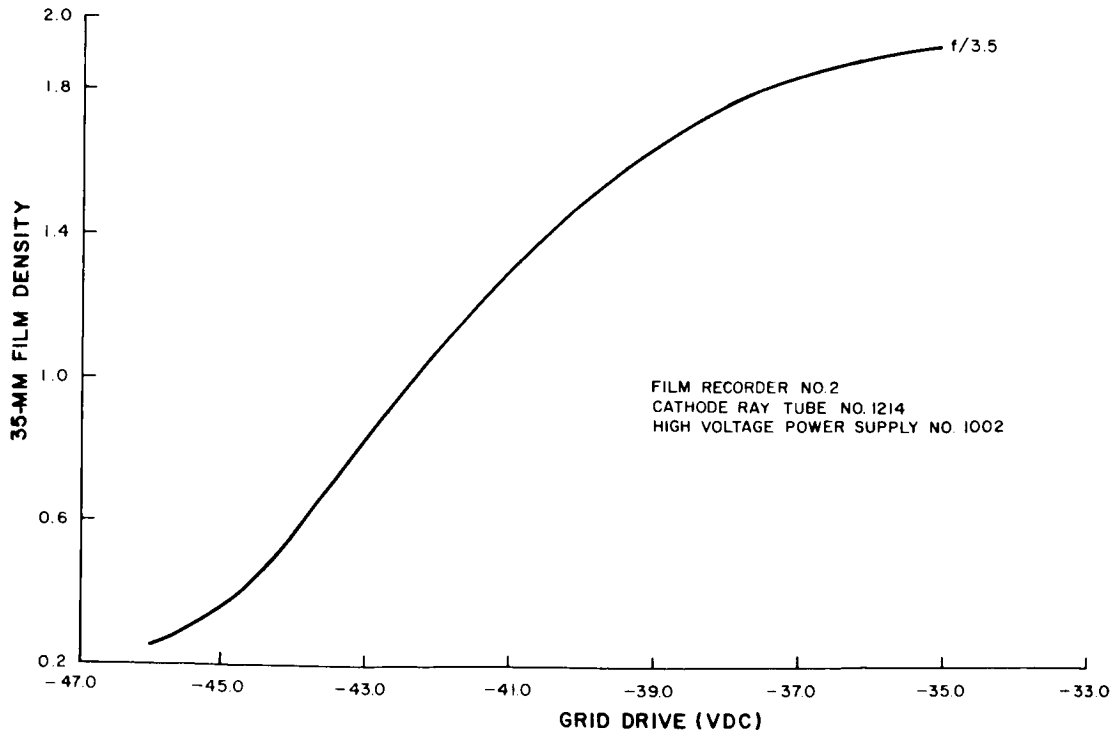

Figure 3-35. Grid Drive as a function of film density after the mission

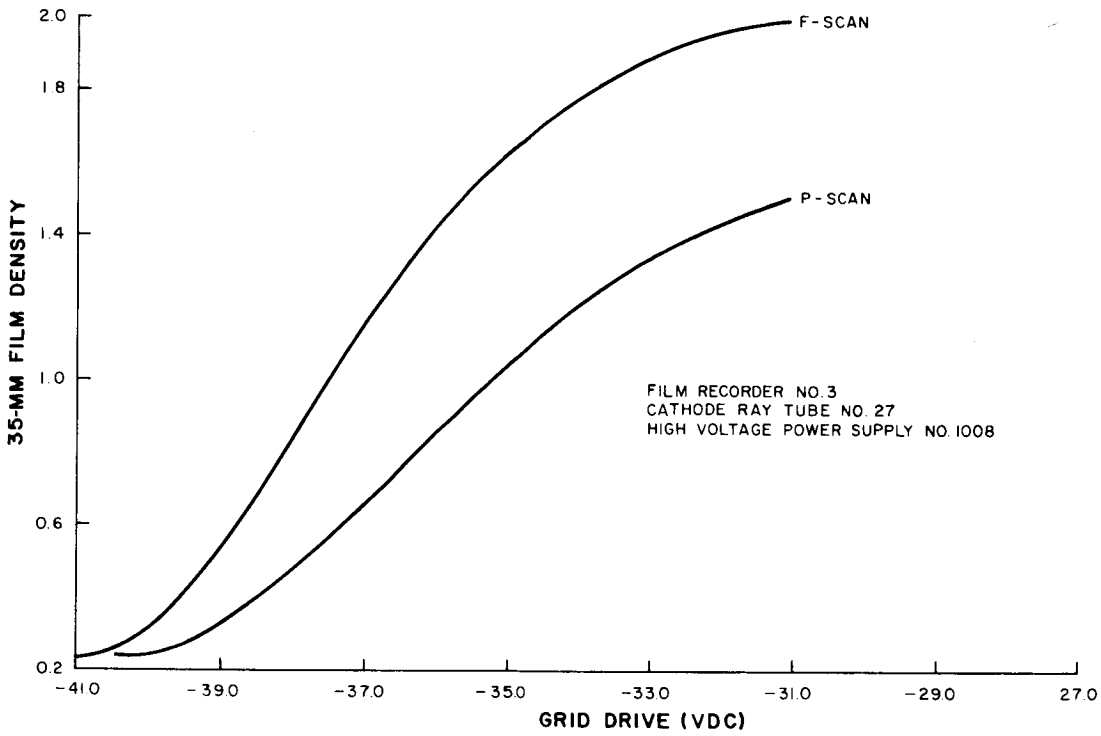

Figure 3-35. Grid Drive as a function of film density after the mission (Continued)

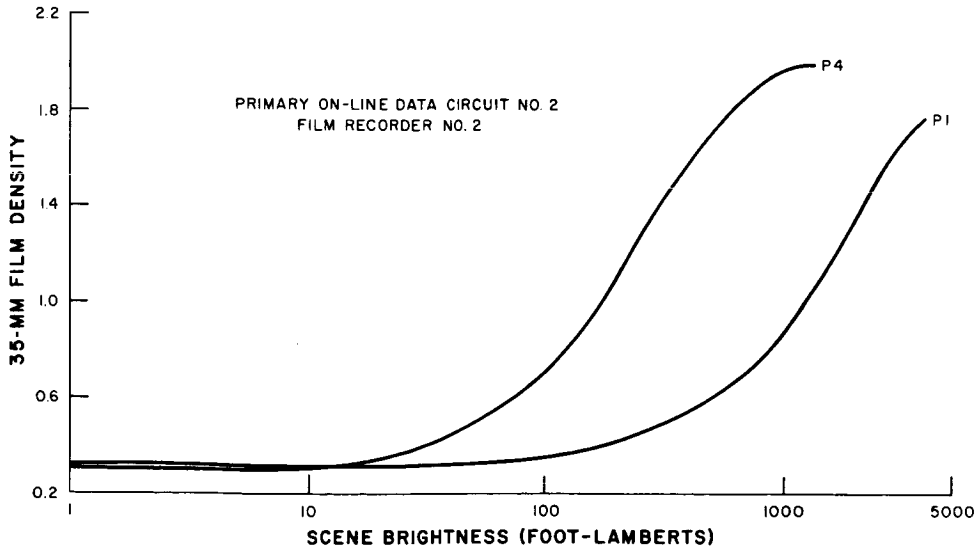

Figure 3-36. Scene Brightness as a function of film density curves

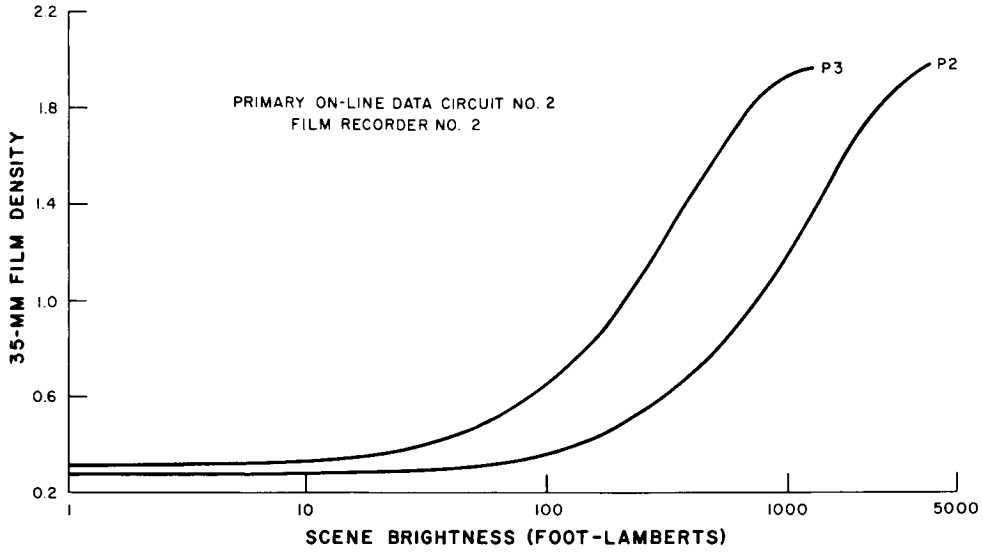

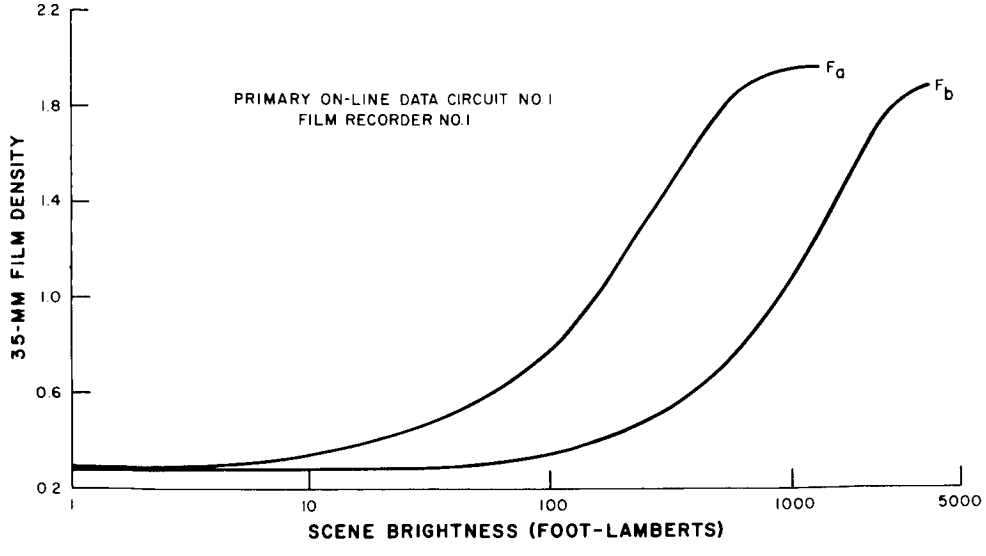

Figure 3-36. Scene Brightness as a function of film density curves (Continued)

d. OSE Modifications

Associated with the localization of the light-intensity problem is a study to improve the capabilities for monitoring the high-voltage power supply and to reduce the time required for its replacement.

Design changes to the high-voltage power supply are currently in process to provide:

- Monitoring points for the 20-kv and 7-kv voltages;
- External adjustment of high voltage; and
- Rapid-disconnect capability through use of a single connector.

These changes will be completed and checked out prior to the RA-8 mission.

As instructed by JPL, a Bandpass Sync Separator will be installed in the OSE at the Pioneer Site. The spare equipment at the Echo Site will be used to accomplish this modification, so that fabrication of new equipment is not required.

Additional modifications that will be incorporated to improve the present OSE configuration for the RA-8 mission include a keyed d-c clamp circuit and a revised trailing-edge sync circuit.

(1) Keyed DC Clamp Circuit — A keyed d-c clamp circuit will be incorporated into the OSE to compensate for the drift in the Spacecraft Transmitter frequency during warmup. The circuit parameters have been finalized and field modification kits have been delivered to JPL.

(2) Revised Trailing-Edge Sync Circuit — During the testing of Flight Model III-2 at RCA, the reticles of the F_b Camera were observed to be within 120 millivolts of the sync tip. At times, this condition resulted in sync tear of the TV picture. To prevent this sync instability, the trailing-edge sync circuit is being modified to reject pulses of 200 microseconds or less, while accepting the slow horizontal sync pulse of 220 microseconds. This prevents the reticles, which are approximately 100 microseconds in width, from affecting the horizontal synchronization of the picture. Tests on this circuit are currently being conducted at AED.

3. *Mission Operation of Telecommunications*

a. Determination of Power Output During Terminal Mode

In the test setup at the Pioneer site, the directional coupler was connected to the 30- to 5-mc converter in the receiver and to the 30-mc preamplifier. The output of the preamplifier was connected to a spectrum analyzer. During the terminal phase of the mission, the peak amplitude of the signal was displayed on the spectrum analyzer. Typical displays are shown in Figure 3-37. After impact, a signal generator was connected to the maser. The generator output was adjusted until the display on the spectrum analyzer was equal to that obtained during the mission. This signal was 4 db higher than anticipated. All complete loop tests of the GSE receivers made at the Pioneer site, prior to the RA-7 mission, were overly optimistic by 2 db. This was assumed to be due to the cable calibrations. The results obtained at the Pioneer site were discounted.

In another effort to determine the power output of the transmitters, the tape recording of the composite signal was examined. The tape was played back through the JPL receiver and displayed on a spectrum analyzer. Using this method it was determined that the F- and P-Channel signals were 21.8 and 22 db, respectively, higher than the beacon signal. Using this information the power output at the Four-Port Hybrid was found to be 40 watts for F-Channel and 42 watts for P-Channel. (The power output at the Four-Port Hybrid is equal to the loss between the Four-Port Hybrid and Case II plus the JPL output at Case II plus the difference between the channel and beacon signals.) The total output was 82 watts. The power output obtained during system tests and thermal-vacuum tests was approximately 60 watts, which was the anticipated output during the mission. The increase in power has been attributed to inaccuracies in the measurements technique.

The telemetry information for the Power-Amplifier cathode current indicated a normal power output and power profile.

The peak-to-peak noise on the sync tip was approximately 30 to 40 mv, which is equivalent to a 42 to 40 db peak-to-peak to rms noise ratio. A signal-to-noise ratio of 39 db was expected for a normal mission.

b. Frequency Stability During Mission

The center frequency of each channel during the RA-7 mission was determined. The F-Channel d-c level, detected within 2 minutes of full-power operation, was approximately 100 mv higher than normal, which corresponds to center-frequency

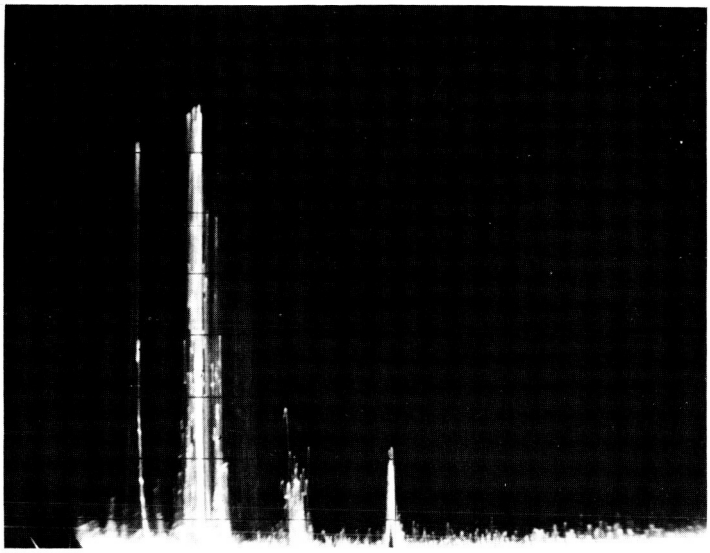

a. F-Channel and beacon signals

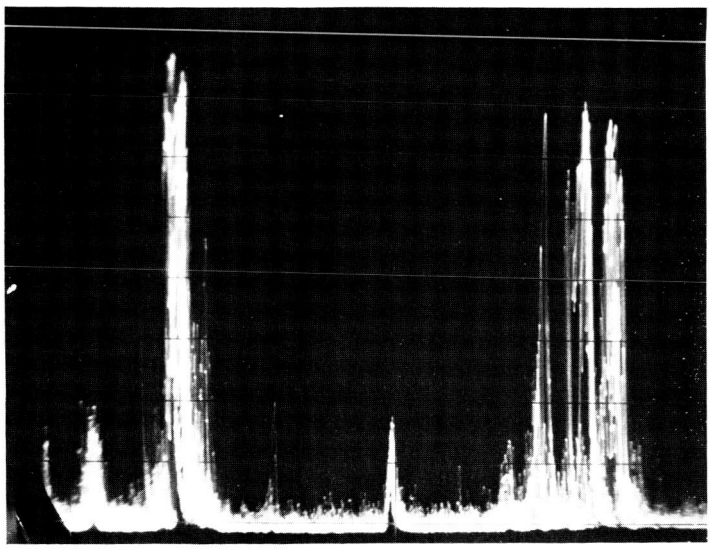

b. F-Channel, beacon, and P-Channel signals

Figure 3-37. Typical displays on typical display

variation of plus 35 kc. During the mission the center frequency remained within 5 kc of this value up to impact. During system test, the center frequency was approximately 20 kc high, and on the launch day, the frequency was 30 to 40 kc high.

The P-Channel center frequency was approximately 17 kc lower than normal at the start of the mission and approximately 25 kc low at impact. During final check on the launch pad, the center frequency was approximately 10 kc high.

c. Deviation

The nominal voltage between the sync tip and the black level is 240 mv ± 10 percent. This voltage was approximately 220 mv for the F_a-Camera, 240 mv for the F_b-Camera, and 250 mv for the P-Cameras.

d. Telemetry

Only the telemetry broadcasted over the F-Channel transmitter was recorded on the strip-chart recorder. There was no noise on the telemetry.

The Channel 8 telemetry had a small amount of noise on the pedestal, however, the noise did not interfere with the data reduction.

e. Recommendations

Because the test setup used at the Pioneer site for the RA-7 Spacecraft produced overly optimistic results, it is recommended that the test setup for the RA-8 Spacecraft be similar to the one used at ETR for the RA-6 and RA-7 Spacecrafts. During full-power and reduced power operations at ETR, the power output was determined to within approximately 0.5 db. In this test setup, a signal generator is permanently connected to the preamplifier through a T-connector. The amplitude of the generator is adjusted to a level equal to that of the peak amplitude for F-Channel, for P-Channel, and for the beacon signals.

This difference in power when added to the power output at Case II and to the loss between the Four-Port Hybrid and Case II results in the individual output of each transmitter during the entire mission.

This test setup could also be used after impact to determine total losses during the mission by inserting a signal generator at the input to the maser.

Section IV

Flight Model III-2 (RA-7) Equipment Performance

A. General

B. Camera Group

C. Thermal Control

Section IV

Flight Model III-2 (RA-7) Equipment Performance

A. General

The receipt of 4316 high-quality pictures of the lunar surface from the Ranger-7 Spacecraft is indicative of the performance of each group of equipment of the Flight Model III-2 Ranger TV Subsystem. The level of performance of some portions of the TV Subsystem can be evaluated on the basis of specific information received during the mission. This is particularly true in regard to the cameras and their associated electronic equipment, since the pictures themselves are evidence of the performance of this equipment. It is also true, although to a lesser degree, of the telemetry equipment, thermal control equipment, power equipment, telecommunications equipment, and OSE equipment. The performance of the command and control circuitry, however, can only be evaluated in absolute terms; that is, all commands were processed and executed on-time and in good order, as expected.

Paragraph B of this section discusses the performance of the cameras and their associated electronic equipment. Paragraph C of this section is devoted to an evaluation of the thermal control equipment and a correlation of the predicted mission temperatures with those actually experienced. The performance of the power equipment, subsystem telemetry equipment, telecommunications equipment, and OSE equipment can only be discussed in terms of the received telemetry data. For this reason the performance of the equipment in these areas must be made in terms of the operational effectiveness of the data as received and as discussed in Section III of this report.

B. Camera Group

1. Summary

a. Satisfaction of Mission Requirements

By observing the 35 millimeter photographs and the magnetic tapes of the video signals it can be said that the Flight Model III-2 camera equipment met the mission requirements. The last partial scan picture was a fragment from the P3-Camera which was outfitted with a one inch, f/0.95 lens. A line selector was used to determine that impact occurred on line 167 approximately 400 μs after the start of scan.

Exposure for the camera actually occurred about 80 milliseconds before the end of readout for the P1 Camera. The total time before impact then is the sum

70	millisecond during P1 readout
6.6	millisecond blanking
111	millisecond of P3 readout
187.1	milliseconds before impact.

A simple geometrical relationship for the 1 inch optical system and for a spacecraft traveling at 2.64 km/sec shows that the final picture was taken at an attitude of 500.0 meters from point of impact on the lunar surface and covered an area about 42 meters by 28 meters. Craters can be recognized that occupy 1/50 of picture height, a diameter of 0.8 meters. The bright rim and shadowed rim constitute image elements of 0.4 meters; hence, the mission resolution requirements were easily satisfied.

For the full scan cameras a fragment of a frame of the F_a Camera was the last to be scanned before impact. Video ceased after 350 microseconds on scan line No. 1074.

The mission requirements of wide area coverage and picture nesting were also satisfied. Examination of an image produced by the F_a Camera at an altitude of 480 miles from the moon shows these two requirements satisfied. This image covers a wide area with several well known features such as the crater Lubiniezky and the Riphaeus Mountains. This image also nests all the remaining sequence of F_a Camera images and records the impact point.

The exposures for both the 76 mm, f/2 cameras and the 25 mm, f/0.95 cameras were such as to provide high signal-to-noise ratios. The peak illuminations appear not to exceed 1800 foot-lamberts with average illuminations between 250 and 450 foot-lamberts. The variations in exposure were noted and examined.

b. Image Degradation

Image degradation due to smear is difficult to assess from an examination of the images. The final P1 and P3 images are oblique views with the major axes of the elliptical images of the round craters being oriented from lower left to upper right.

Image degradation due to residual images from previous exposures is also difficult to assess. By viewing high-contrast crater images of both the F_a and F_b Cameras during the final 20- to 30-picture sequence, sufficient motion and size changing of these images occur to attempt an observation of these residuals. The illuminated portion of craters for succeeding frames shows a break in the highlight, which may be caused by the residual signal from the previous frame. A cautionary note is extended to the photo interpreters to consider this possibility when evaluating the craters for shadow detail.

There is evidence of coherent noise in the images, however, at a decidedly reduced level from pre-launch system tests. The F_a Camera shows the 15 kilocycle crosstalk

from the F_b Camera erase raster. It is more evident in Camera F_b. There are two permanent spots of a detail near the size of the smallest recognizable crater in each full-scan camera. They can be detected as black and white spots with the black opposite to the normal crater shadowing. There is also evidence of four kinescope spots which appear as four tiny white spots on each image. In the Camera F_a pictures there is evidence of shadowing at top left and bottom left of each image which is typical of lens vignetting.

Of the Camera F_a pictures, there are a few images that show evidence of the 12 to 13 nearly evenly spaced disturbances that are characteristic of microphonics excited by partial-scan camera shutter actuations. The Camera F_b pictures show evidence of a loss of a line or lines of video in occasional frames. This is due to the clamp sitting on a noise spike and drawing that line either up to peak white or down to peak black. Some evidence of this exists in F_a Camera video output for a noise pulse caused by the actuation of the P1 and P3 shutters.

The P1 Camera pictures also showed evidence of occasional electrical noise spikes on alternate frames, in a time-coherence with the end of stroke on the P3 shutter.

The P1 and P2 Camera pictures show low level microphonics in time-coherence with the end of stroke of the P3 and P4 shutters respectively.

2. *Evaluation of Performance*

The evaluation of the performance of the Camera group on Flight Model III-2(RA-7) can be made on two levels. The first level would entail a comparison of the informational content and overall performance of the RA-7 cameras to that inherent in the mission requirements and the general specifications. A second level of evaluation would involve a review of each cameras performance against that specific cameras specification.

a. General Specifications

The general specification for the Ranger television cameras was to provide the following:

- High-quality images of the lunar surface at a surface resolution of better than 0.5 meter;
- Wide-area coverage; and
- Picture nesting.

A review of the 4,316 pictures taken by the RA-7 cameras indicates that the general specifications were met. The satisfying of the first specification can be attributed, in part, to the superior performance of the overall system in that (1) the camera platform was placed in an impacting trajectory such that sufficient light and shadow detail was

available for the imaging system and (2) sufficient transmitter power was available to overcome system losses by an ample margin. These facts contributed to a high signal-to-noise ratio video output for each RA-7 camera; this being an essential factor for high-quality images. Resolutions of lunar detail at the level of one-half meter have been conservatively estimated from the image produced by the final two partial-scan exposures made immediately prior to impact. The final fragment of the last partial-scan picture was exposed approximately 530 meters before impact and produced an image of an area 42 meters in width and 28 meters in height. Appendix C provides details concerning the sequencing of the RA-7 Cameras and shows the derivation of the resolution obtained by the last partial-scan pictures. In examining this last image, craters one fiftieth of the picture height, a diameter of 0.8 meters, can be easily recognized. A crater is recognized by its deeply shadowed and brightly luminant image. On the basis of this achieved detail, the resolution requirement of one-half meter was surpassed.

The second and third specifications, wide-angle coverage and picture nesting, were imposed as a basis for correlation of the expected data output of the Ranger cameras to the well-defined telescopic photographs presently on hand. The success with which Ranger-7 cameras met the objectives of these specifications is illustrated by Figure 4-1. This image, produced by the twenty-five-degree camera, was taken 480 miles before impact. It covers a wide area within which several well known features, such as the crater Lubiniezky and the Riphaeus Mountains, can be distinguished by their characteristic images and their geographical relationships. Also indicated on this Figure are the areas covered by pictures taken later in the picture-taking sequence, at a higher level of resolution, including the point of impact as shown in Figures 4-2, 4-3 and 4-4. The realization of the design to satisfy this specification is contained in the interplay of camera fields of view, the camera mounting bracket that physically ties the six-camera array into appropriate overlapping fields of view, the camera exposure sequence, and the design of the impacting trajectory.

b. Detailed Specifications

To achieve high-quality, high-informational content television pictures with the Ranger cameras, detail specifications were imposed on each camera. Some of these detail specifications that can be evaluated from the received pictures are as follows:

- The ratio of the voltage excuusion created by the camera when exposed to illumination ranging from black-to-peak-white to the root-mean-square of the random noise of the camera should exceed 30 db;
- The ratio of the peak-to-peak signal to the peak-to-peak coherent noise should exceed 20 db;
- The scanned area of the tube should maintain an aspect ratio of unity to within four percent; and
- The cameras should have adequate exposure and image distortion due to smear should be minimized.

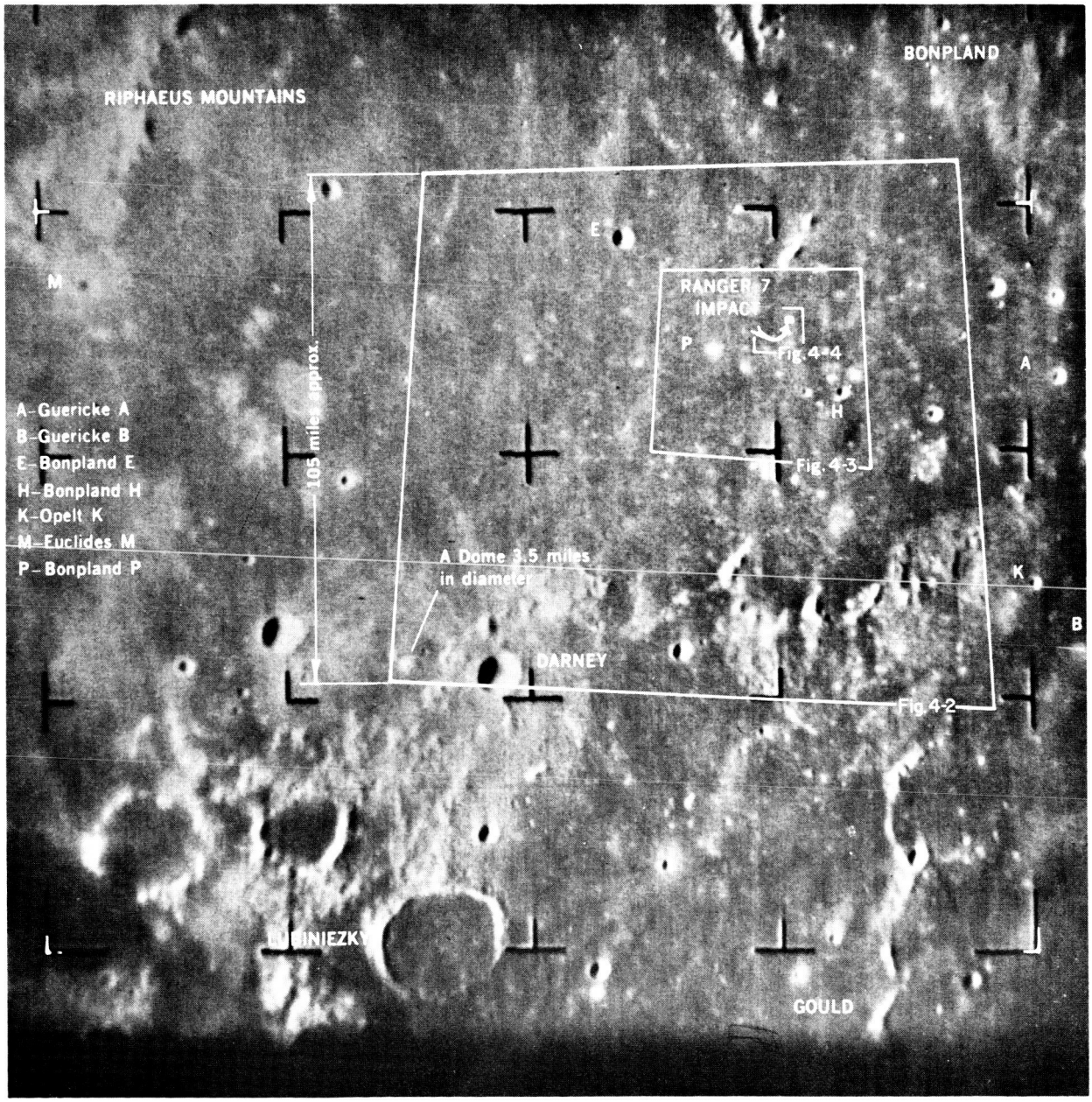

Figure 4-1. Northwest Lobe of Maru Nubium F_a Camera Image with overlays indicating Nesting

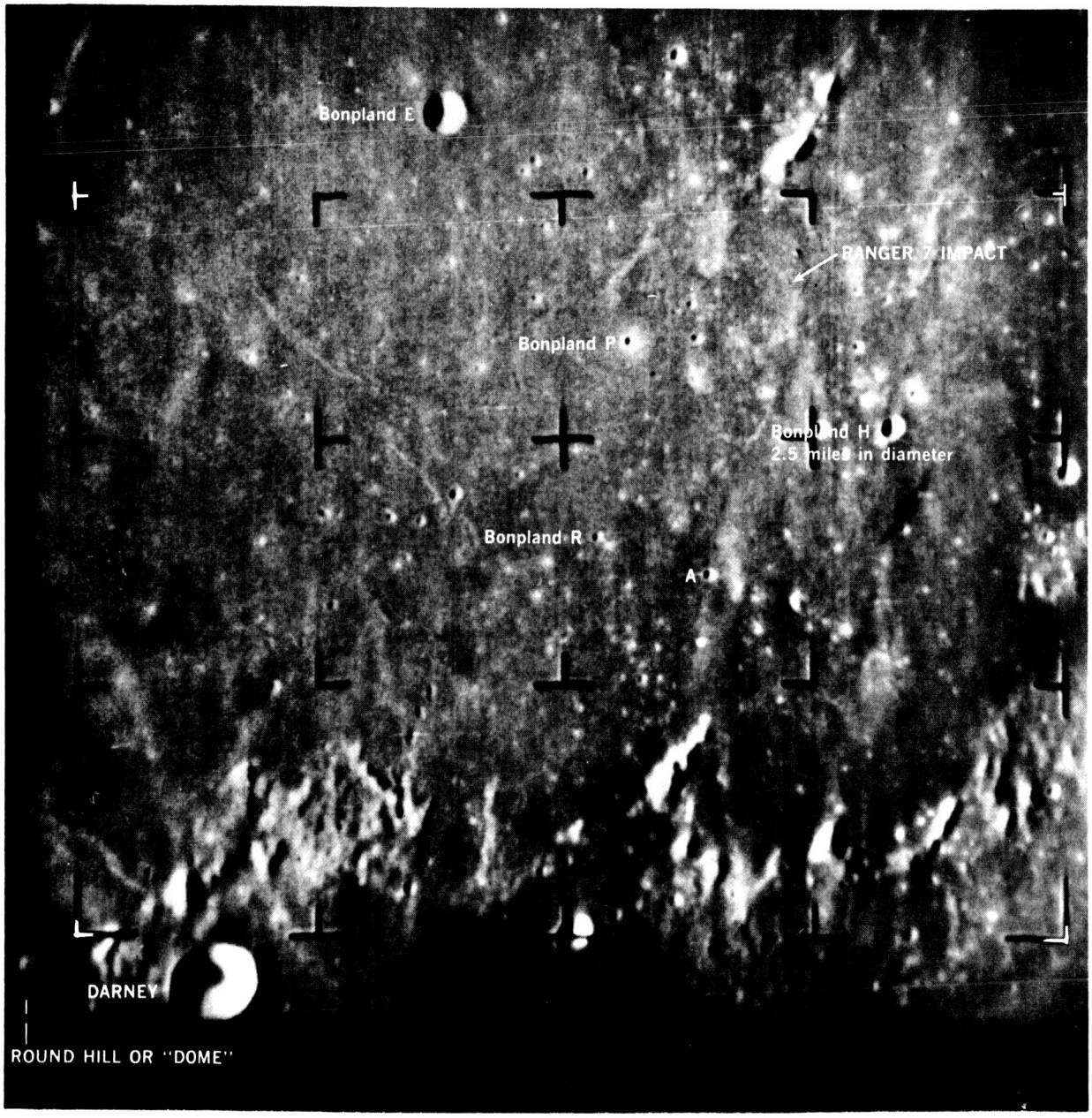

Figure 4-2. Wrinkle Ridges of Northwest Mare Nubium taken by F_a Camera

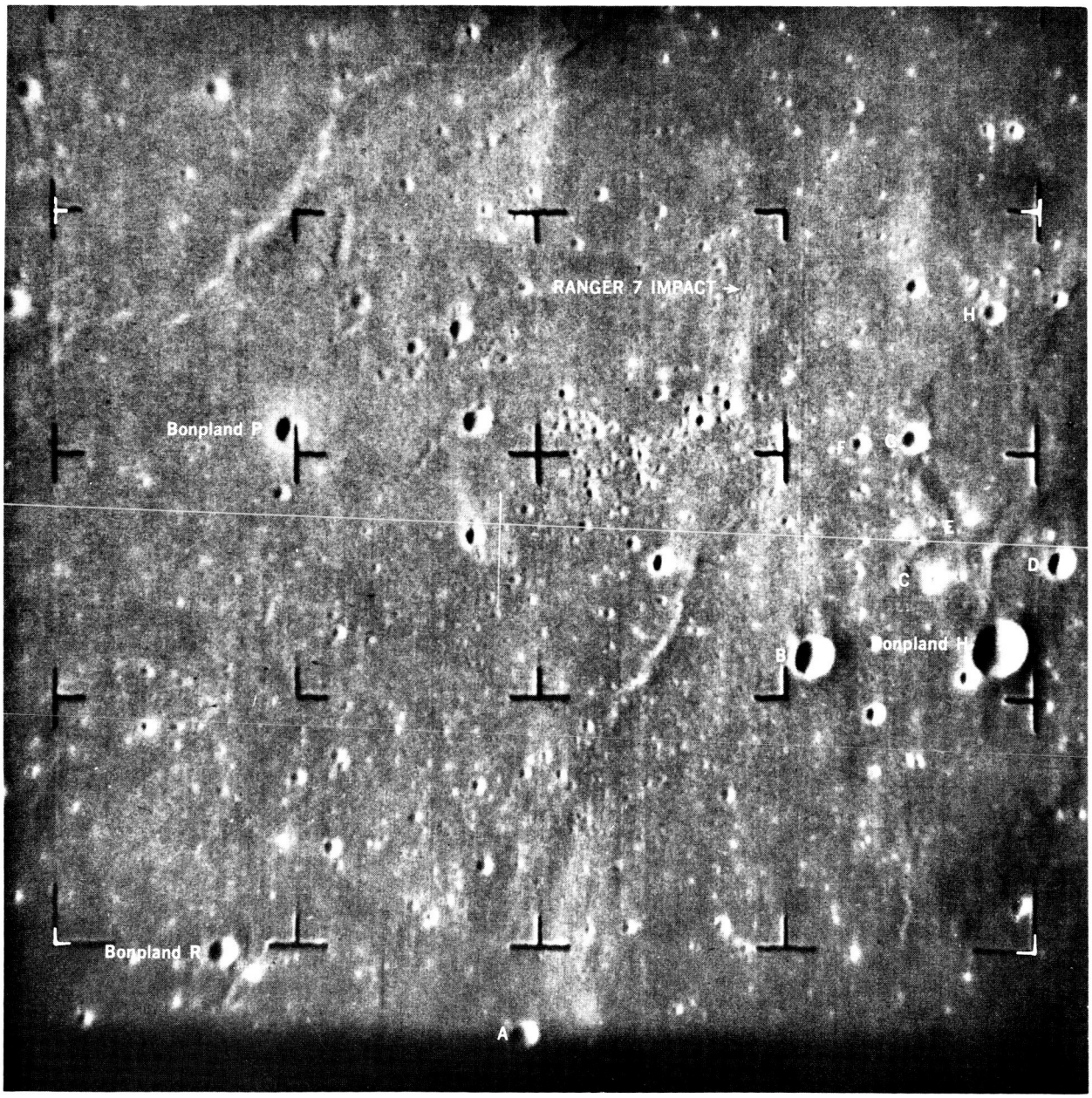

Figure 4-3. Last of Known Craters; Image taken by F_a Camera

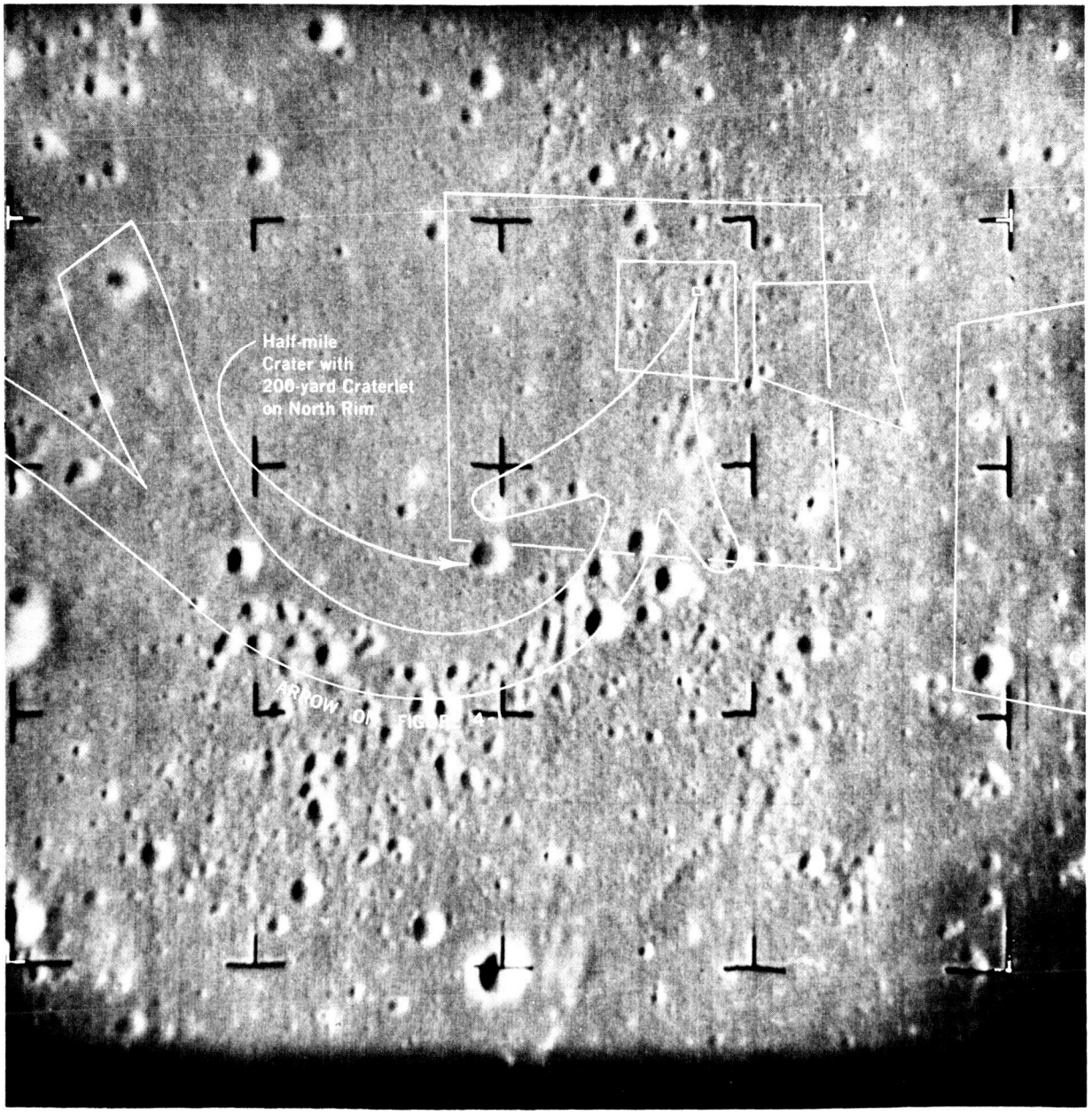

Figure 4-4. Crater rays; Picture taken by F_a Camera

This last specification is a commentary on the ability to calculate and predict the luminance of the lunar surface and the ability of the spacecraft system to direct the cameras to a specific location on the lunar surface. This location must contain the correct mixture of lunar luminance and shadowing to achieve a useful image by the lens, shutter, and vidicon elements of the television camera. The shutter speed was calculated to maintain image smear to less than a TV element. These shutter-actuated exposures were 2 milliseconds for the partial-scan cameras and 5 milliseconds for the full-scan cameras.

The evaluation of how well the cameras performed was conducted by examining, by projection, a duplicate negative of the 35-millimeter primary-on line-film data (P.O.D.). In addition, the dubs of the secondary-on line-magnetic tape data (S.O.D.) were replayed through a Range kinescope recorder and polaroid records were made of the video signals at the input of the kinescope film recorder. These observations and data were evaluated with regard to previous test data and to the detail camera specifications.

One of the procedures imposed on the camera subsystem at the Eastern Test Range, preceding the launch, was a camera alignment and calibration. This procedure utilizes a brightness source simulating the spectral emission and luminance of the moon. For the Ranger-7 cameras, the F_b, P1, and P2 Cameras were aligned for a peak luminance of 2700 foot-lamberts, and the F_a, P3, and P4 Cameras for a peak luminance of 650 foot-lamberts. By varying the luminance of the calibration source, transfer curves, shown in Figures 4-5 and 4-6, for each camera were plotted by recording the corresponding video excursions at the input to the kinescope recorder, as shown in Figure 4-7. Observations of the video excursions at the kinescope recorder were reported during the Ranger-7 mission five minutes after video was received. These values are noted on the transfer curves and are also listed in Table 4-1. These voltage measurements are related to the measured foot-lamberts of the simulated brightness source and provide an indication of how well the cameras were exposed.

TABLE 4-1

LIGHT LEVELS 8 MINUTES BEFORE IMPACT

Camera	Average Light Level (ft.-lamberts)	Peak Light Level (ft.-lamberts)
F_a	520	1300
F_b	600	2100
P1	600	1800
P2	900	2000
P3	410	1350
P4	240	840

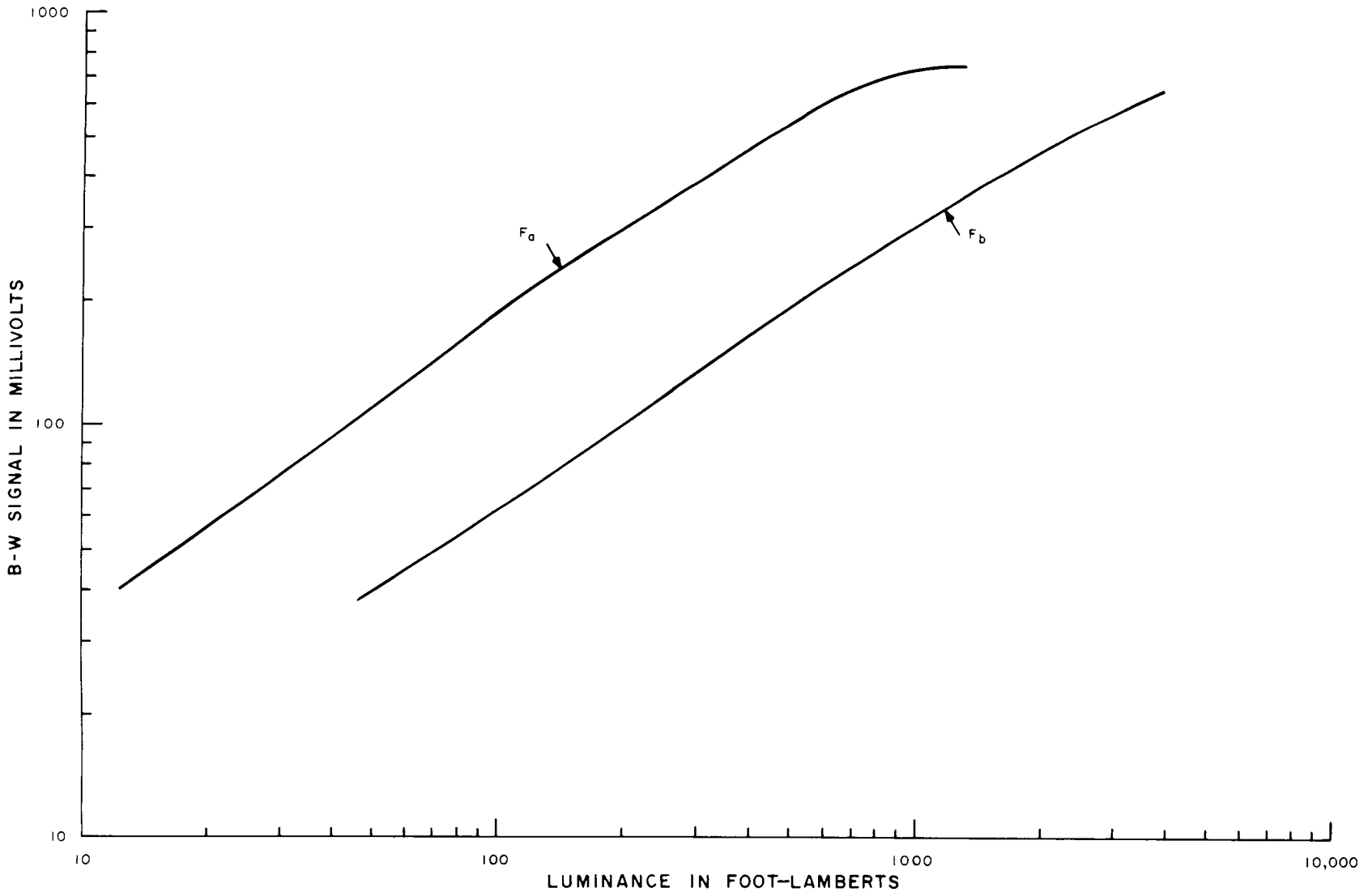

Figure 4-5. Light transfer characteristic curves for Ranger-7 Full-Scan Cameras

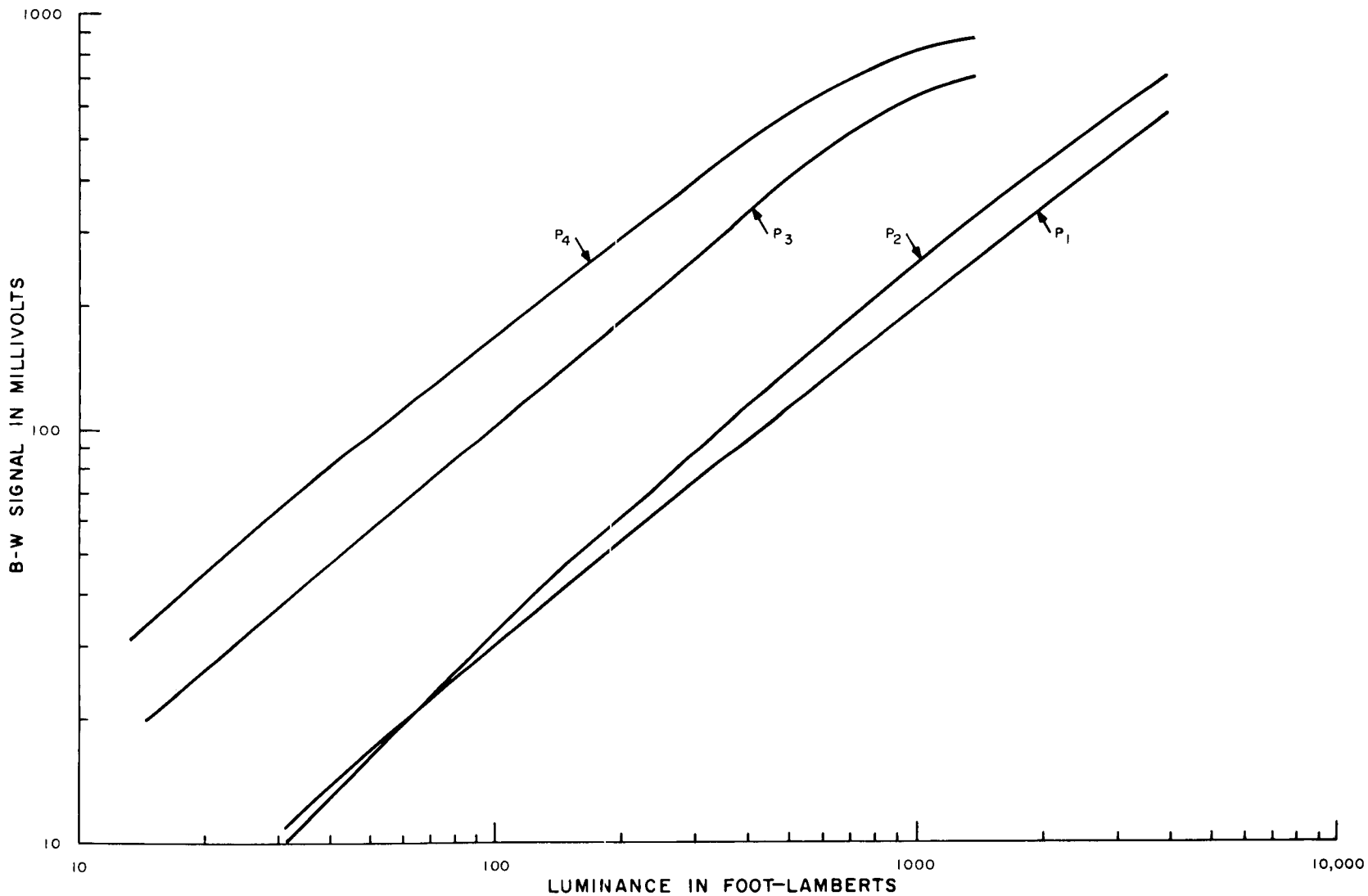

Figure 4-6. Light transfer characteristic curves for Ranger-7 Partial-Scan Cameras

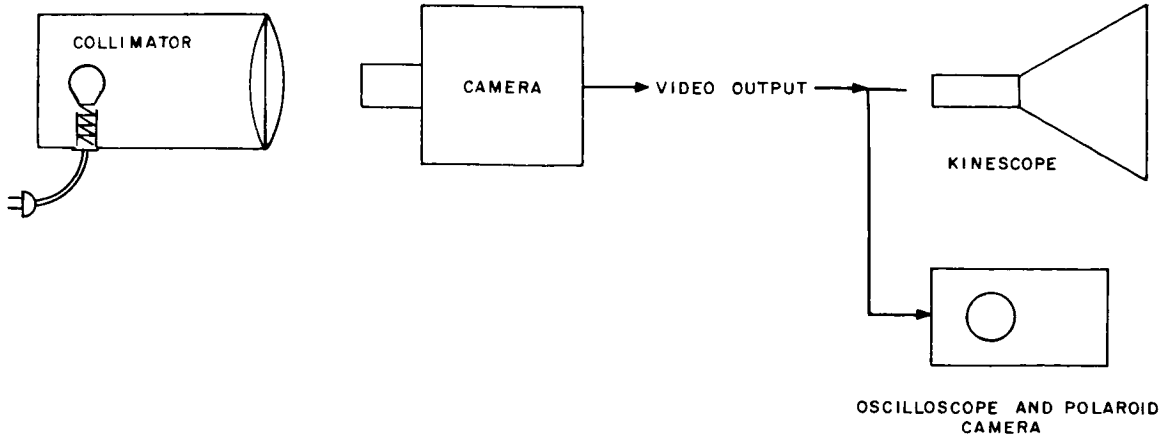

Figure 4-7. Calibration set-up for Ranger-7 Cameras

The choice of the lunar area to be impacted was fortuitous and resulted in maximum use of the optical-to-video conversion capabilities of all six cameras. To this extent, the specification for adequate camera exposure which would result in a high signal-to-noise ratio was satisfied.

Some of the variations in the apparent relative luminancies are due to variations and tolerances of camera components. One of these is the specification which permits a tolerance on the nominal shutter speed and on the variation in shutter speeds for the in-stroke and out-stroke. Camera video output is a measure of this variance, all other parameters remaining constant. From the magnetic-tape playback, oscilloscope traces of alternate exposures were made for each camera. The scene luminance is assumed to be invariant during an alternate exposure sequence, therefore, the primary cause of variance in camera signal amplitude is the difference in speed for the alternate shutter strokes.

The oscilloscope records of the video for each camera, derived from the S.O.D., are shown in Figures 4-8 and 4-9. The variation in exposure for alternate frames is listed in Table 4-2.

TABLE 4-2

VARIATION IN ALTERNATE FRAME EXPOSURE ATTRIBUTABLE TO VARIATION IN SHUTTER SPEED

Camera	Variation in Exposure (percent)
F_a	0+
F_b	8
P1	3
P2	10
P3	25
P4	10

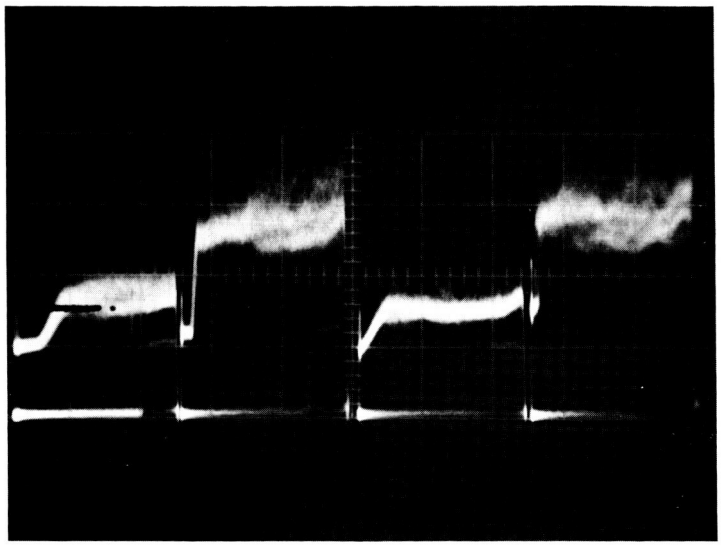

P1 P2 P3 P4

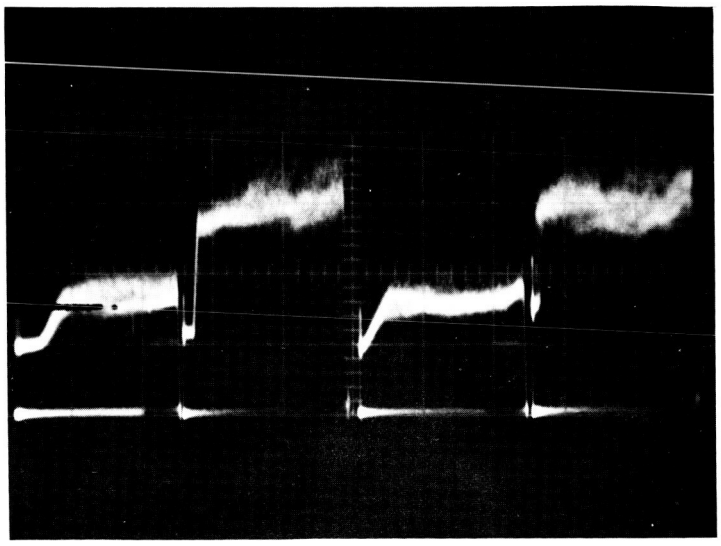

P1 P2 P3 P4

SCALE : 200 mv/cm

Figure 4-8. Partial-Scan Video for alternate exposures

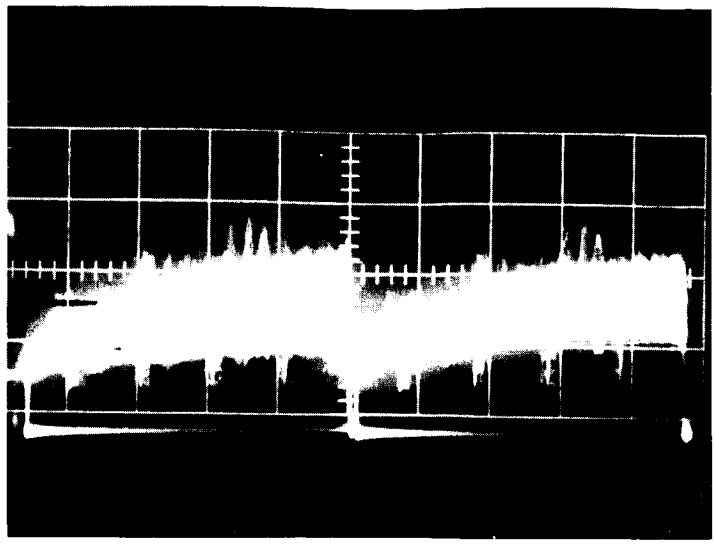

Fb CAMERA

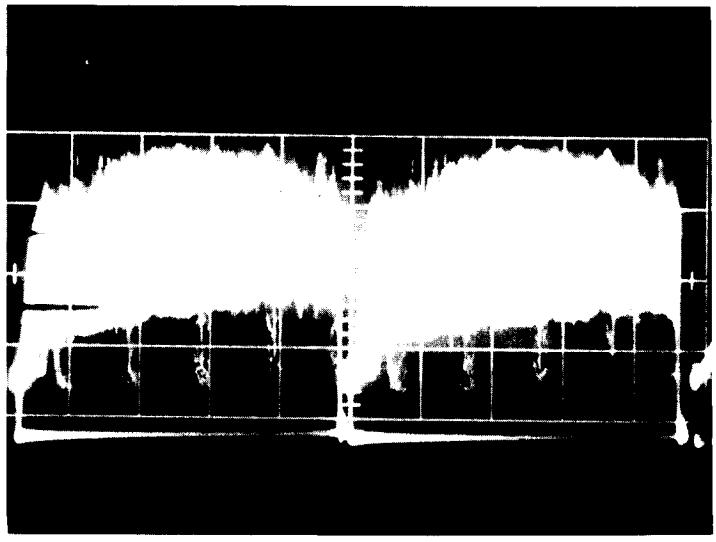

Fa CAMERA

SCALE = 200MV/CM

Figure 4-9. Full-Scan Video for alternate exposures

An examination of the video shows that on the three 25-millimeter, f/0.95 cameras, the peak illuminations are occasionally detected near the saturation level of the camera, but the camera did not actually saturate or clip. Maximum exposure without saturation was then achieved on Cameras F_a, P3 and P4. The remaining three Cameras, F_b, P1, and P2 had average exposures with signal-to-noise ratios three to four db lower than for Cameras F_a, P3 and P4.

Image degradation due to smear is difficult to assess. If image smear is evident, it would have occurred in the final two partial-scan pictures. In these pictures, image motion during the shuttered exposure is near the order of the image element being recorded. One of its effects is to reduce image contrast. These factors are difficult to assess since the final P1 and P3 images are oblique views. The major axes of the elliptical views of all round craters are oriented from lower left to upper right. A sense of motion is revealed by the elongation of the many smaller craters whose major axes are oriented roughly toward the impact point, as shown in Figure 4-10. If the final picture had been taken by either the P1 or P2 Cameras, considerable smear would have been evident for this photogeometry.

The evaluation of the Ranger-7 pictures against specifications for exposure and image smear indicates that all cameras received adequate exposure for high signal-to-noise pictures and that degradation of image smear was minimized during the final sequence of the Ranger-7 mission.

It can be also shown from similar evidence, video line selections from the final F_a and P3 camera frames, shown in Figure 4-11, that the first specification of a high signal-to-noise ratio was also satisfied. A video signal at the input to the kinescope recorder with a signal-to-noise ratio in excess of 30 db will produce a picture acceptable as having high quality. Examination of the video from the final F_a and P3 video shows it to be on the order of 34 db. When this signal is reflected back to the camera output through a communication channel with a signal-to-noise performance of about 39 db, an additional one db is picked up. Thirty-five db then is the average signal-to-noise ratio for the F_a, P3, and P4 Cameras and 31 db is the average signal-to-noise ratio for the F_b, P1, and P2 Cameras. Each of the six cameras then provided video signal with more-than-adequate signal-to-noise ratios to satisfy the first specification and the video criterion for high-quality images.

c. Image Degradation

In the total record of Ranger-7 pictures, other image-degrading factors were noticed that can be described and their effect on the final images evaluated. Some of these factors have remained in the cameras in spite of the best efforts to eliminate them. In general, they were present in the Ranger-7 pictures to a degree considerably reduced from prelaunch test experiences. They are, at worst, nuisance factors and result in a loss of less than 1 percent of actual data. Some of these factors are:

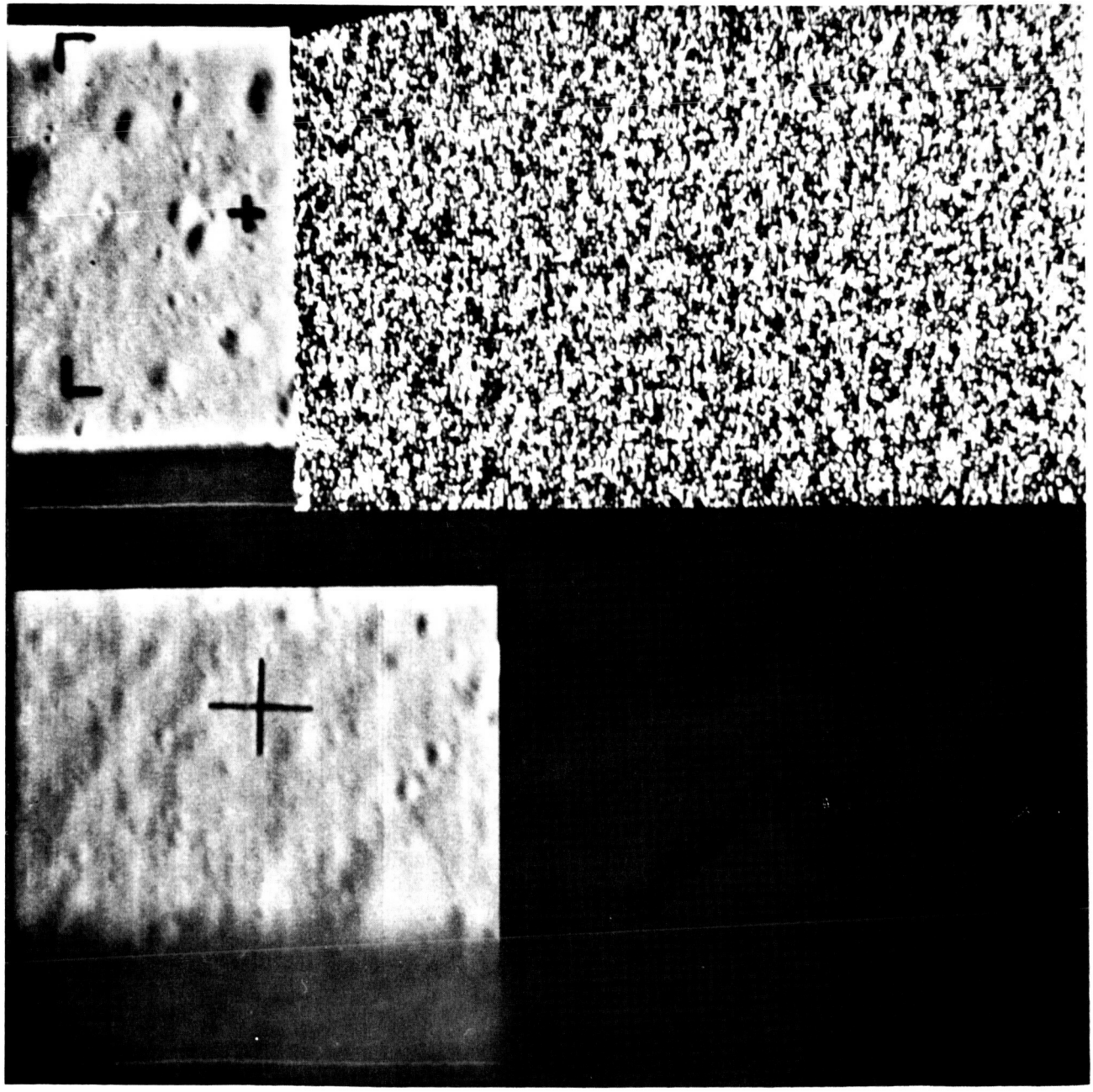

Figure 4-10. Final F_a and P3 Camera Frames taken by Ranger 7

- 15-kilocycle crosstalk;
- Vidicon or nuvister microphonics; and
- Residual images.

Some of these effects will be described in the order of their general occurrence.

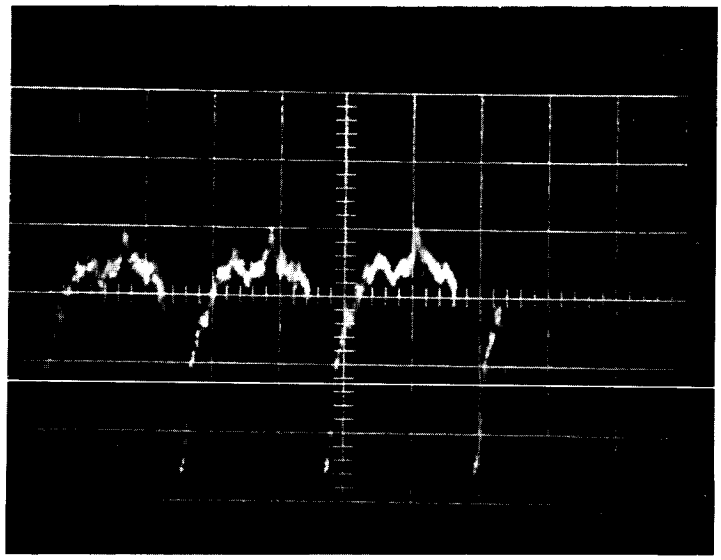

Figure 4-11. Lines 1070, 1072, 1073 and 1074 of last F_a Frame

1. *15-Kilocycle Crosstalk*

In the full-scan Camera channel, Cameras F_a and F_b are exposed and read out in sequence. While Camera F_a is being readout, Camera F_b is being erased and prepared for exposure, as shown in Figure 4-12. Part of this prepare cycle involves switching for exposure, as shown in Figure 4-12. Part of this prepare cycle involves switching the vertical sweep from an 0.39-cycle-per-second read rate to a fifteen-kilocycle-per-second erase rate. This high rate is necessary to cause the scan-erase image to be beyond the bandwidth of the scanning aperture and video amplifier. To insure that sufficient photoconductor area will be scanned at this high rate, the sweep voltages must be increased to a high level. It is this signal which is picked up by the readout

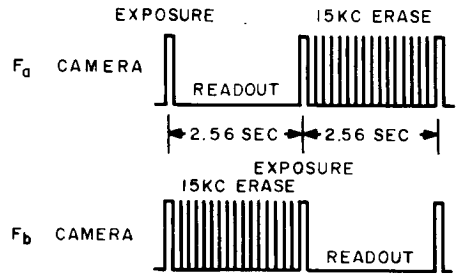

Figure 4-12. Readout sequence, full-scan cameras

camera. The pickup mechanism is not entirely defined; however, it is known that part of it is picked up in the power supply grounds and part by electro-magnetic or electro-static pickup in the vicinity of the camera heads.

The signal produced by this crosstalk is on the order of 20 to 25 millivolts, about 28 db below the peak-white video. It varies in amplitude from 15 millivolts in scene areas that approach black to about 40 millivolts in the peak-white areas. It is evident in each full-scan camera, through its amplitude appears to be slightly higher in Camera F . This signal is identified by vertical marks with the subtitle of a in Figures 4-13 and 4-14.

This high-frequency vertical-erase scan signal is also the dominant source of noise in the P2 Camera. It occurs in the P2 Camera during the erase period of one of the F Cameras. The signal causes 8.5 vertical bars in the picture which persist for three consecutive frames, then are absent for three frames.

2. *Vidicon or Nuvistor Microphonics*

Disturbances in the video signals that can be correlated to exposure sequence are due either to electrical pickup at the high impedance of the vidicon target or actually due to mechanical displacements of either the vidicon or the nuvistor preamplifier. This type of interference is illustrated in Figure 4-14 where twelve disturbances cause by P-Camera shutters is indicated by a subscript b. Microphonic performance was generally satisfactory with occurrences in four-to-five F_a Camera frames showing objectionable levels. Similar disturbances are evident in the lower third of the P1 and P2 frames in time coherence with the end-of-travel of the P3 and P4 shutter strokes.

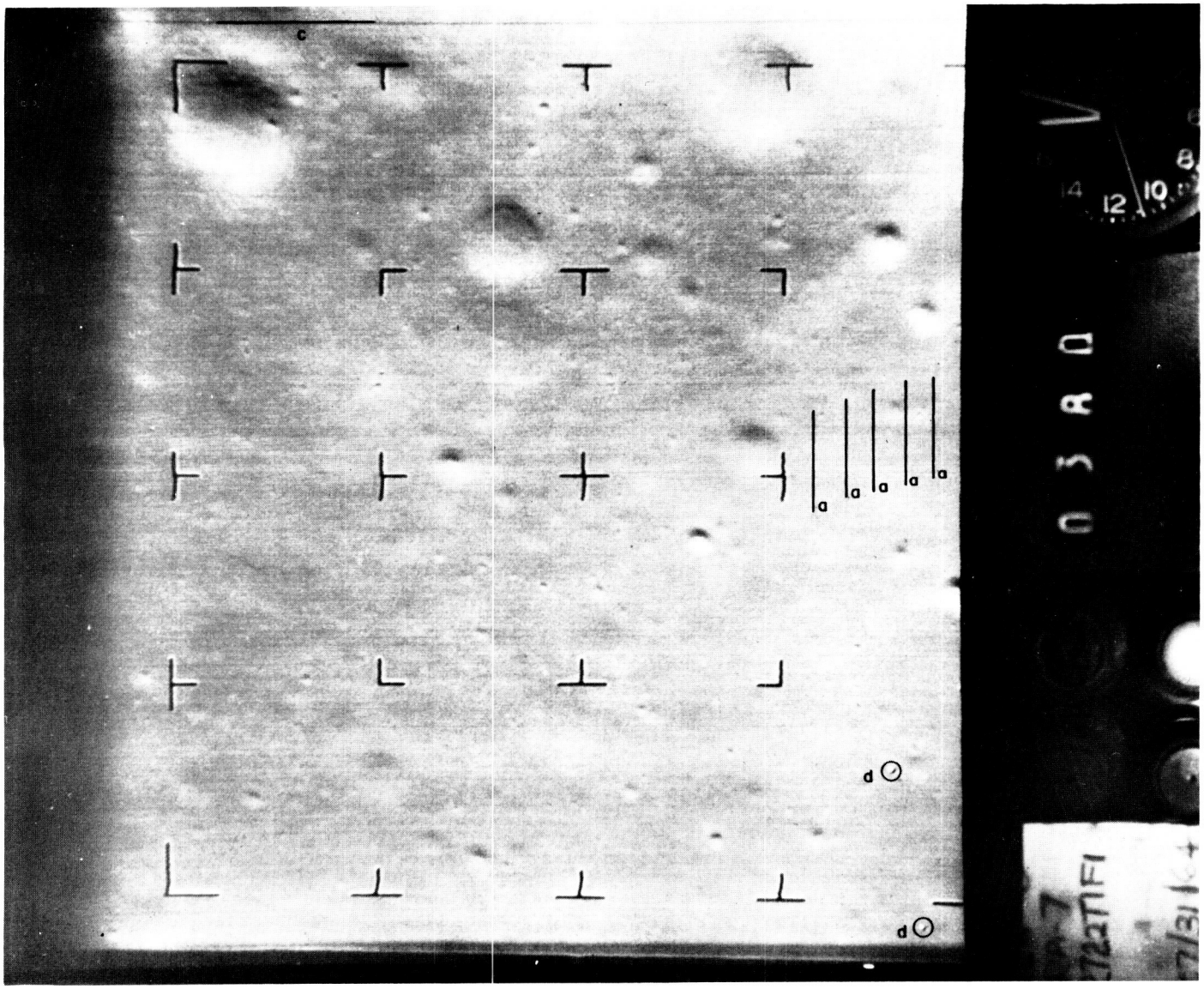

Figure 4-13. F_b Camera Video output (Frame No. 380)

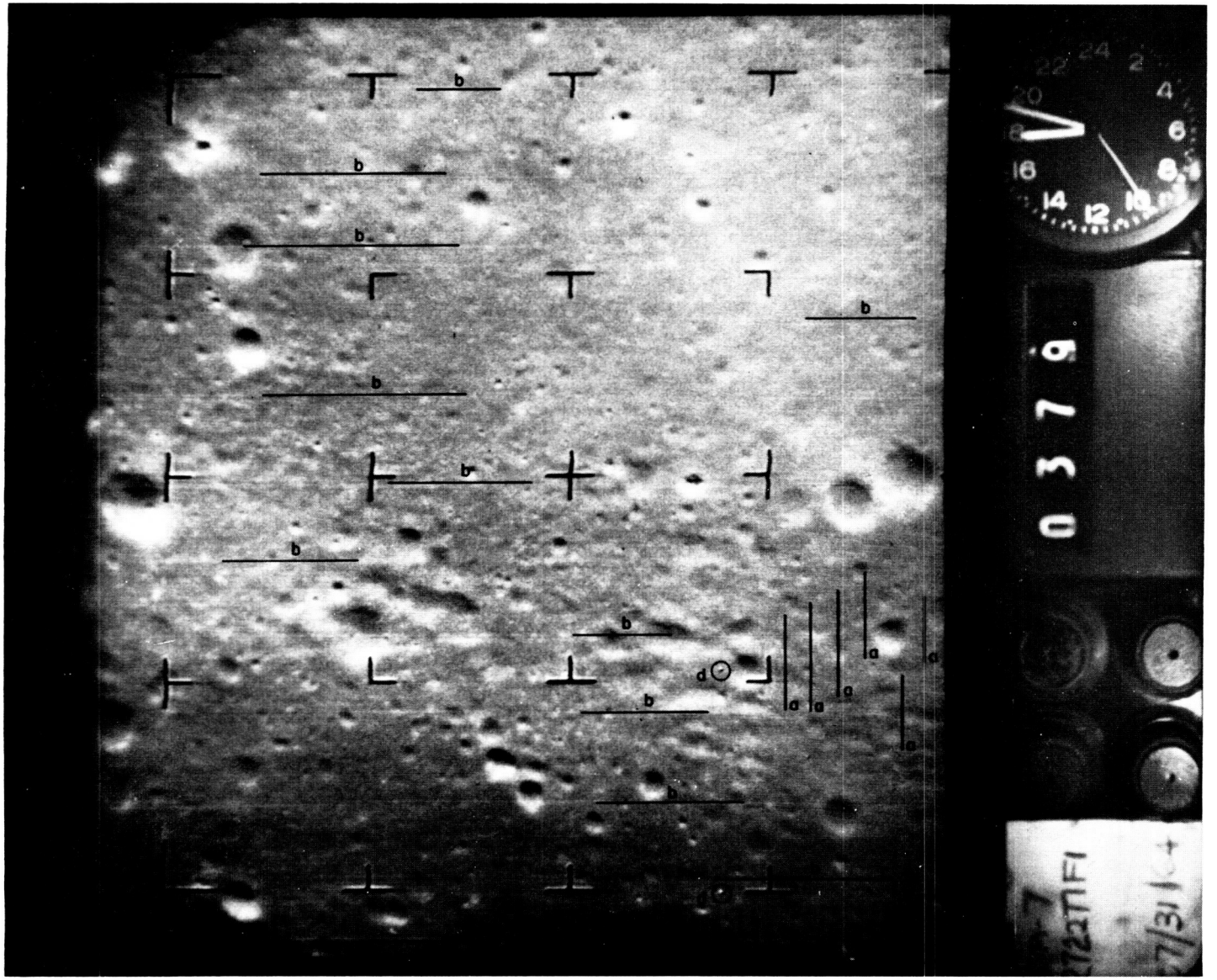

Figure 4-14. F_a Camera Video output (Frame No. 379)

Another noise which is observed occassionally in the Fa camera and P1 camera frames is a very short noise pulse which goes into the saturated white region. While the duration of the noise is only about 15 microseconds, the kinescope beam is overdriven causing an elliptical-shaped spot which appears to be several scan lines wide, as shown in Figure 4-15. In Camera P1 these saturated noise pulses occur during the bottom third of the frame in time coherence with the end-of-shutter stroke of alternate exposures of camera P3. It also occurs about six times in the F_a Camera. In frame 105 of the F-Channel P.O.D. there is a loss of 2 lines of video caused when this shutter-induced noise occurs in time with the clamping action. These noises also appear to be caused by the partial-scan Camera P3, is synchronous with shock-wave microphonics, and is similar to the more prominent noise of Camera P1. Video loss due to clamp displacement is shown as subscript c of Figure 4-13.

A third type of video disturbance due to the shock wave produced by the shutter's end-of-stroke is nuvister microphonics which is the dominant noise present in the P1 camera, as shown in Figure 4-10. The nuvister appears to be excited primarily by its own shutter and by the F-Camera shutters. The microphonic signal is a 13-kilocycle-per-second signal which appears as a series of vertical bands in the picture. There are approximately six-and-a-half bands present in every P1-Camera picture.

3. *Residual Signals*

Perhaps the most difficult image degradation to identify in the Ranger-7 image is that due to residual images. After the normal erase procedure has been applied to a camera, there will generally remain a residual signal amounting to about 5 percent of the previous exposure for the full-scan cameras and as much as 10 percent for the partial-scan cameras. Its effect on the image produced by the subsequent exposure depends on the image contract and the effectiveness of the cameras erasure. The F_b Camera frames number 230 thru 240 of the P.O.D. were observed. The crater in the lower right-hand area appears to be a typical example of image degradation due to residual image. There is a definite brightness discontinuity correlated to the region of high illumination in the previous frame, shown as an increase of white level due to frame-to-frame memory. This is a very subtle degradation and does not effect the over-all image quality; it is categorized here only as a cautionary measure to the image interpretors who may confuse it with image detail.

4. *Vidicon Blemishes*

There are at least two spots in Cameras F_a and F_b that may be due to vidicon blemishes. They are identified by the subscript d in Figures 4-13 and 4-14 and were found to be present also in prelaunch system tests. They have the appearance of the tiniest of craters but betray themselves by having the characteristic white and black rims opposite in-sense to actual craters.

Figure 4-15. Noise pulses induced by end of stroke of shutter in camera P1. Pulse Populations due to Ten overlapping exposures of P1.

5. Shading

Shading is the combined vidicon and lens effect which causes some modification in dynamic range over the scanned area. In the F_a-Camera it is produced primarily by lens vignetting and manifests itself as a dark shadow in three of the four corners of the picture.

6. Summary

In total, image degradations that have been detailed here detract only in a small way from the over-all image quality and information content of the Ranger-7 pictures. They are enumerated here as a guide to the photo-interpreters and as a background for further improvements in future Ranger cameras.

7. *Recommendations*

The analysis and evaluation of the Ranger-7 pictures indicates that modest improvements in camera performance will eliminate several of the more pronounced image disturbances. A program to reduce the shock wave produced by the cameras shutters should eliminate the characteristic vidicon and nuvistor microphonics. The program should culminate in an improved shock-isolator design for the shutter-to-camera mounting. The analysis also indicates that camera effects such as residual images and lens vignetting, previously considered serious, did not, in fact, degrade the image.

In the discussion on camera exposure, it was pointed out that the signal-to-noise ratios for the F_b, P1, and P2 cameras were three-to-four db lower than those for the F_a, P3, and P4 cameras. It was also noted that only few peak-white signals exceeded 1800 foot-lamberts on any of the cameras. The recommendation is to increase the video amplifier gain in the F_b, P1, and P2 cameras to produce the maximum output voltage for an 1800-foot-lambert signal. This will ensure higher signal-to-noise ratios on all cameras for the planned closer-to-the-terminator Ranger-8 picture taking.

The final recommendation is to implement a spectral-response measurement program to accomodate all cameras for Ranger-9 and Spares, to increase the photometric interpretation capability.

C. Thermal Control

The thermal configuration of the RA-6 TV Subsystem is shown in Figure 4-16. Primary temperature-control surfaces are:

- Thermal shroud (polished aluminum vehicle skin)
- Thermal fins
- Thermal shields (insulators)

The construction of the shroud and fin assembly is such that solar energy striking the spacecraft parallel to its axis illuminates only the top surfaces of the fins, i.e., no direct sunlight is incident upon the thermal shroud. The flow of thermal energy with this condition is as follows:

- Sunlight strikes the fin surface at a normal angle of incidence and a portion is absorbed. The remainder is reflected to space and other parts of the spacecraft.
- Part of the energy absorbed by the fin is radiated from the front and rear surfaces of the fin, the remainder flows into the thermal shroud.

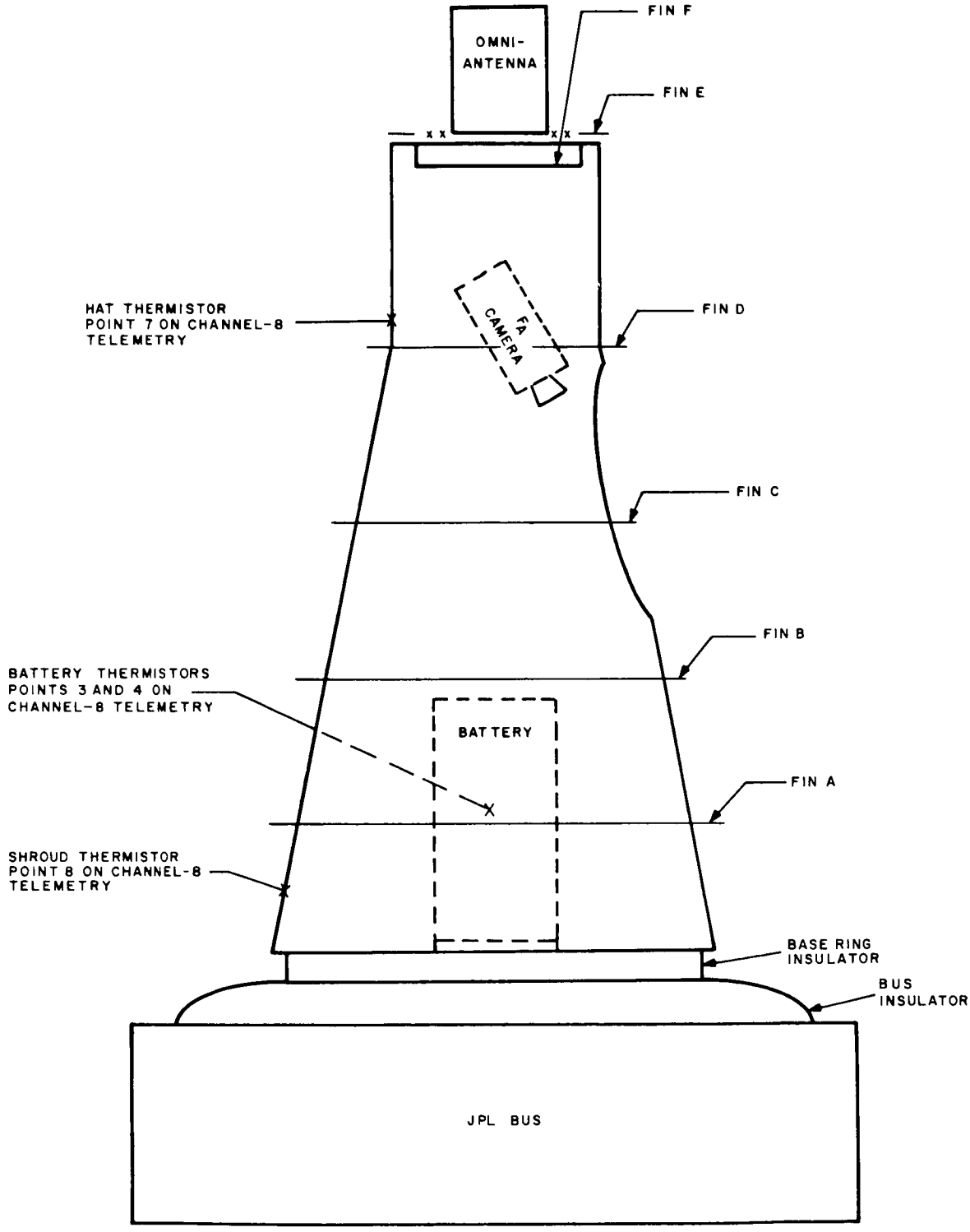

Figure 4-16. Thermal configuration of the TV subsystem

- The energy flowing into the thermal shrouds from the fins is radiated from the shroud surface (polished aluminum), establishing a temperature field on the shroud surface.

- The temperature field established on the shroud is essentially isothermal; since the shroud envelopes all electronic equipment, the equipment will come to this same temperature at steady-state conditions. During full-power operation of the equipment, the temperatures of individual components are maintained below maximum temperature limits due to the "heat-sinking" properties of the spacecraft.

1. Methods Used to Predict Flight Temperatures

Three equilibrium-temperature calculations were performed for the RA-7 flight. The calculation methods used are as follows.

- The energy input to the TV Subsystem was considered to be only direct solar energy which was incident upon the top surfaces of the temperature-control fins. No additional energy input was considered. This is the "direct-input" method.

- The energy input to the TV Subsystem was calculated in essentially the same manner as the "direct-input" method. However, it included calculations for the energy input due to multiple reflections of solar energy from surfaces of the Subsystem to other viewed Subsystem surfaces, and solar energy input from the solar panels and the Bus. This is called the "input including reflections" method.

- The energy input to the TV Subsystem was calculated using ratio factors applied to the results of the "direct-input" method. (These ratio factors were determined from an analysis of the RA-6 flight data and are explained in more detail in Appendix E. The ratio factors emperically account for the greater-than-expected energy input for RA-6 (the discrepancy which was never fully explained). This is called the "input-with-ratio-applied" method.

The use of any of the three methods results in an effective energy input into each of the thermal control fins (identified by letters A, B, C, E and F). Predicted equilibrium temperatures were obtained from the fin-input calculations by utilizing the following equations:

DUMMY VARIABLES

$$X = A + B + C + D + E + F$$

$$Y = -2A - B + D + 2E + 2F$$

$$Z = 2A + B + 2C + D - 2E - 2F$$

where A is the energy input (in watts) to Fin A, B is the energy input to Fin B (in watts), etc.

The cruise-mode telemetry equilibrium temperatures are then given by the following equations.

$$(\sigma T^4)_{HAT} = \left[(1.0934)X + (0.7130)Y + (0.0590)Z\right] \times 10^{-3} \text{ watts/in}^2$$

$$(\sigma T^4)_{VID} = \left[(0.9065)X + (0.6608)Y + (0.1941)Z\right] \times 10^{-3}$$

$$(\sigma T^4)_{SHR} = \left[(1.1656)X - (0.2603)Y - (0.0921)Z\right] \times 10^{-3}$$

$$(\sigma T^4)_{BAT} = \left[(1.0892)X - (0.0762)Y + (0.0559)Z\right] \times 10^{-3}$$

$$(\sigma T^4)_{CAM} = \left[(1.0837)X - (0.1281)Y + (0.1457)Z\right] \times 10^{-3}$$

where

HAT	=	Thermal shroud, hat, -Y side,
VID	=	Camera lens housing,
SHR	=	Thermal shroud, -Y side, below fin A,
BAT	=	Battery, internal, Channel P,
CAM	=	Camera electronics, -Y side, unit (upper),
σ	=	Stefan - Baltzman radiation constant and is equal to 3.657×10^{-11} watts/in^2 $^{o}K^4$, and
T	=	Temperature (in degrees Kelvin).

The temperature equations were obtained by applying a "least-squares" fit to the results of nine thermal-vacuum tests performed on the TV Subsystem and utilizing an IBM 7090 computer for the calculations. Dummy variables (X, Y, Z) were required to reduce the number of effective energy inputs from six to three (necessary because of an insufficient quantity of test data).

The derivation for the "least-squares fit" for determination of spacecraft temperatures is included as Appendix D to this report.

Eleven additional temperature equations were obtained for subsystem locations other than those monitored by cruise-mode telemetry:

$$(\sigma T^4)_{PAF} = (1.0709\,X - 0.0177\,Y + 0.1532\,X) \times 10^{-3} \text{ watts/in}^2$$

$$(\sigma T^4)_{PAP} = (1.0926\,X - .0429\,Y + 0.0888\,Z) \times 10^{-3}$$

$$(\sigma T^4)_{EBR} = (1.010\,X + 0.7780\,Y + 0.2004\,Z) \times 10^{-3}$$

$$(\sigma T^4)_{VREG} = (1.013\,X + 0.0862\,Y + 0.1228\,Z) \times 10^{-3}$$

$$(\sigma T^4)_{TPS} = (1.0778\,X - 0.0127\,Y + 0.004\,Z) \times 10^{-3}$$

$$(\sigma T^4)_{CON} = (1.1388\ X + 1.6419\ Y + 0.1642\ Z)\ X\ 10^{-3}$$

$$(\sigma T^4)_{SHRD} = (1.1013\ X - 0.1818\ Y + 0.0471\ Z)\ X\ 10^{-3}$$

$$(\sigma T^4)_{SHRBC} = (1.1174\ X - 0.0427\ Y + 0.2437\ Z)\ X\ 10^{-3}$$

$$(\sigma T^4)_{DK\ 3} = (1.1583\ X - 0.2385\ Y + 0.0967\ Z)\ X\ 10^{-3}$$

$$(\sigma T^4)_{DK\ 4} = (1.153\ X - 0.1721\ Y - 0.0808\ Z)\ X\ 10^{-3}$$

$$(\sigma T^4)_{DK\ 5} = (1.0865\ X - 0.0157\ Y - 0.0663\ Z)\ X\ 10^{-3}$$

where

PAF	=	Power amplifier, -X side, unit (cavity end) ch. F
PAP	=	Power amplifier, +X side, unit (cavity end) ch. P
CBR	=	Camera mounting bracket
VREG	=	High-current voltage regulator, +Y side, ch. P
TPS	=	Transmitter power supply, +X side, ch. P
CON	=	Temperature control plate, center (fin F)
SHRD	=	Thermal shroud, +Y side, below fin A
SHRBC	=	Thermal shroud, -Y side, between fins B and C
DK 3	=	Deck No. 3, -Y side
DK 4	=	Deck No. 4, -Y side
DK 5	=	Deck No. 5, -Y side

2. *Temperature Predictions for RA-7*

Using the three methods of calculation outlined in the above paragraph and inputs determined from the solar absorptivity values, a set of equilibrium temperatures for the RA-7 flight was predicted for each method. The values of absorptivity were determined by both RCA and JPL/STL; consequently there were six sets of predicted equilibrium temperatures. The resulting dual sets of values are reported in paragraph 3 that follows. All calculations were performed using the minimum solar constant value of 0.87 watts per square inch, which was applicable for the RA-7 flight. The results of the calculations for cruise telemetry data points are tabulated in Table 4-3.

TABLE 4-3

CRUISE MODE EQUILIBRIUM TEMPERATURE PREDICTIONS FOR SUBSYSTEM LOCATIONS MONITORED BY CRUISE-MODE TELEMETRY

Method of Calculation	Hat (-Y)		Vidicon Housing		Shroud		Internal Battery (Ch. P)		Camera Electronics		Remarks
	°F	°C	°F	°C	°F	°C	°F	°C	°F	°C	
RCA values of γ (0.71, 0.50), no reflections included	52	11	34	1	34	1	34	1	32	0	Establishes absolute minimum values - highly unlikely to occur
JPL/STL values of α (0.76, 0.56), no reflections included	66	19	45	7	46	8	45	7	45	7	Unlikely to occur
RCA values of α, reflections included	59	15	39	4	52	11	46	8	46	8	Probable minimal temperature
JPL/STL values of α, reflections included	70	21	48	9	61	16	57	14	55	13	Most probable minimal temperature
RCA values of α using ratio factors from RA-6 (1.37, 0.85)	70	22	55	13	66	19	64	18	68	20	Nominal temperature range (assuming accuracy of RA-6 information)
JPL/STL values of α using ratio factors from RA-6	84	29	66	19	79	26	77	25	79	26	
Telemetry received from RA-6 with α values of 0.41, 0.65, 0.82, and solar constant = 0.93 w/in^2	102	39	84*	29*	97	36	99	37	99*	37*	Establishes absolute maximum values - highly unlikely to occur

*Estimated

The thermal design for RA-7 was primarily based upon the data received from the flight of RA-6. The temperature data in Table 4-3, calculated using the "input with ratio factors applied" method, was considered to be nominal.

It was considered, however, that if the RA-6 temperature data was not accurate, then the remaining entries in the tabulation might become significant. Since emphasis was placed on obtaining battery temperatures of not less than 10°C, conservative methods were employed for selecting the finishes. The calculations indicating battery temperatures of 1 and 8°C for RA-7 were considered highly unlikely in light of the results obtained from the RA-6 flight and the limited adjustment of inputs to this area.

3. *Thermal-Control Paints Applied to RA-7*

Two thermal-control fin paints were to be applied to the TV Subsystem of RA-7. This was at variance with the procedure followed for RA-6 where a third paint was applied to both fin B and the antenna. During final assembly at Cape Kennedy, it was discovered that the RA-7 omni-antenna did not reflect the change from a light grey paint to white paint; it was neither convenient nor practical to repaint at that time since the effect of light grey as compared to the effort of white in that area is almost negligible. All calculations for temperature shown in Table 4-3 (which were made before the launch of RA-7) were made considering Fin E, the antenna ring, as being painted white PV 100. A comparable tabulation that takes the light grey paint on the antenna ring, Fin E, into account in the calculation is shown in Table 4-4.

The thermal-control paints used on the fins of RA-7 were a mixture of PV-100 white paint and Mil-E-5557 type III black paint and are identified as follows:

Description	Drawing Number
Light Gray (antenna)	1758619-19
Light Gray	1758619-27
Dark Gray	1758619-28

Mixtures of gray paints were prepared in March 1964 for RA-7. The desired values of solar absorptivity (α) for the paints were 0.58 and 0.77 (as compared to 0.62 and 0.82 for RA-6). Samples of the paints were sent to JPL for spectral evaluation by JPL/STL. The values of α measured by JPL/STL on the RA-7 samples were 0.04 to 0.05 higher than those measured at RCA and resulted in values that were almost the same as measured on RA-6. It was decided, therefore, to use JPL/STL solar absorptivity measurements as the design reference values or "true" values and the RCA values were used as a lower bound.

TABLE 4-4

CRUISE-MODE EQUILIBRIUM TEMPERATURE PREDICTIONS* FOR FLIGHT MODEL III-2

Location on TV Subsystem	RCA Calculations			JPL/STL Calculations		
	σT^4	Temperature		σT^4	Temperature	
		0^oC	0^oF		0^oC	0^oF
Thermal Shroud, Hat, -Y Side	0.294	26	78	0.317	32	90
Camera Lens Housing	0.257	16	61	0.276	22	72
Thermal Shroud, -Y Side, Below Fin A	0.271	20	68	0.297	27	81
Battery (Internal), Channel P	0.269	20	68	0.293	26	79
Camera Electronics, -Y Side, Unit (upper)	0.273	21	70	0.296	27	81
Power Amplifier, -X Side, Unit (cavity end) Channel F	0.273	21	70	0.297	27	81
Power Amplifier, +X Side, Unit (cavityend) Channel P	0.273	21	70	0.297	27	81
Camera Mounting Bracket	0.286	24	75	0.307	30	86
High Current Voltage Regulator, +Y Side, Channel P	0.260	18	64	0.281	23	73
Transmitter Power Supply, +X Side, Channel P	0.264	19	66	0.288	25	77
Temperature Control Plate, Center (Fin F)	0.341	38	10	0.364	43	109
Thermal Shroud, +Y Side, Below Fin A	0.268	20	68	0.293	26	79
Thermal Shroud, -Y Side, Between Fins B and C	0.290	25	77	0.315	32	90
Deck No. 3, -Y Side	0.284	24	75	0.296	30	86
Deck No. 4, -Y Side	0.272	21	70	0.298	27	81
Deck No. 5, -Y Side	0.257	17	63	0.281	23	73

* Considering Gray Paint with α of 0.41 on the antenna ring, using Ratio Factors from the RA-6 Spacecraft.

New mixtures of gray paint were prepared for spectral analysis to obtain the new values of 0.55 and 0.75. The discrepancy between RCA and JPL/STL measurements indicated that the RCA values of 0.51 and 0.71 were reversed. The spectral-measurement history of these paints is given in Table 4-5.

TABLE 4-5
SPECTRAL-MEASUREMENT HISTORY

Description	Desired Design Values Absorptivity	Samples Painted at RCA 5/8/64	Samples Painted at JPL 5/26/64	Samples Prepared During Painting of RA-7 Fins at JPL 6/12/64	Values Measured on RA-7 Fins at ETR with Portable Reflectometer 6/24/64
Light Gray	RCA 0.51	RCA 0.522	RCA 0.513	RCA 0.517	RCA 0.50
RCA 1758619-27	JPL/STL 0.55	-	JPL/STL 0.56	JPL/STL 0.56	-
Dark Gray	RCA 0.71	RCA 0.716	RCA 0.720	RCA 0.716	RCA 0.71
RCA 1758619-28	JPL/STL 0.75	-	JPL/STL 0.76	JPL/STL 0.76	-

Measurements of absorptivity at AMR on the RA-7 thermal shroud fins were obtained using the Lion Model 25A portable reflectometer and RCA prepared calibration standards. The accuracy of this reflectometer is estimated to be $\pm$ 5% percent. The light gray paint on the antenna was prepared and measured in a series of spectral measurements similar to those employed for RA-6 and checked at ETR on RA-7. Therefore, the measurements program data indicates the values of solar absorptivity on the RA-7 fins to be as given in Table 4-6.

TABLE 4-6
VALUES OF SOLAR ABSORPTIVITY ON THE RA-7 FINS

Location	Solar Absorptivity
Fins A, B, F	0.50 to 0.56
Fins C, D	0.71 to 0.76
Fin E (White Paint)	0.19 to 0.22

4. RA-7 Cruise-Temperatures vs. Flight Predictions

a. Thermal Shroud Hat

The temperature of the hat was monitored during cruise mode by channel 8, data point 7. Immediately after launch, the Spacecraft traveled into the shadow of Earth. The hat, being of low thermal mass, dropped steadily from a launch temperature of 78° to 61°F before the spacecraft was out of the shadow and exposed to solar radiation. Within 10 hours after launch, the temperature of the shroud hat had reached equilibrium at 82°F, but took a drop again during midcourse when it went to about 75°F. One hour after midcourse maneuver was initiated, the temperature of the hat was back to equilibrium at 84°F.

Using the "input-with-ratio-applied" method, the predicted temperature was calculated to range from 76°F (RCA α) to 90°F (JPL/STL α). The hat, being large in area and low in thermal mass reacts significantly to small changes in energy input and it is for this reason that the temperature drops occurred within Earth's shadow and during midcourse maneuver. (See Section III of this report for graphs of the cruise mode telemetry).

b. Camera Lens Housing

The temperature of the camera lens housing was monitored during cruise mode by channel 8, data point 1. This point indicated a decrease in temperature of about 10°F while the vehicle was in the Earth's shadow. Temperature drifted still lower to 62°F until about an hour after spacecraft exposure to solar radiation at which time the temperature began to rise and reached equilibrium at 66°F, 14 hours after launch.

During midcourse maneuver, the spacecraft was rotated in such a way as to subject the lens housing to an increased solar input, as indicated by a sharp rise in temperature to 76°F. A large mass, such as the six cameras and the bracket, took this rise as indicated by the time required to reestablish equilibrium at 66°F (8 hours from the time midcourse maneuver was initiated).

Using "the input-with-ratio-applied" method the predicted temperature was calculated to range from 61°F (RCA α) to 72°F (JPL/STL α). The camera lens housing remained steady at 66°F after midcourse maneuver until the final few hours of flight at which point a slight rise occured due to lunar inputs, as described in paragraph 5 that follows.

c. Thermal Shroud (-Y side, below Fin A)

The temperature of the thermal shroud in this area was monitored during cruise mode by channel 8, data point 8. Passage through Earth's shadow allowed the temperature of the lower portion of the shroud to drop to 65°F before exposure to solar radiation which allowed this area to stabilize at 74°F. Temperature equilibrium was reached within 8 hours from launch.

Analysis of the data indicates the (-Y) side of the vehicle was shadowed during midcourse maneuver and a decrease to 70°F occured at this time. This apparent shadowing is somewhat substantiated by the increased input to the cameras since the field-of-view hole is on the (+Y) side. Within 90 minutes, however the shroud in this area was once again at a stable 74°F.

Using the "input-with-ratio-applied" method the predicted temperature at this data point was calculated to range from 68°F (RCA α) to 80°F (JPL/STL α). Flight temperature fell at the midpoint of this range.

d. Battery—Ch. P

The temperature of the Battery is monitored during cruise mode by an internally located thermistor on channel 8, data point 4.

The batteries were not affected by transient changes in solar input as occurs when the Spacecraft is in the Earth's shadow and during midcourse maneuver, due to their high thermal mass and location.

Battery temperature decreased steadily and reached equilibrium at 75°F within the 40-hour time constant determined from thermal-vacuum testing. From using "the input-with-ratio-applied" method, the predicted temperature of the batteries ranged from 66°F (RCA) to 79°F (JPL/STL).

e. Camera Electronics

The Camera Electronics temperature was monitored during cruise mode by channel 8, data point 11. Reaction to brief changes in solar input, as during passage through Earth's shadow and midcourse maneuver, was limited by the thermal mass location within the Subsystem.

Temperature of this component decreased steadily and obtained equilibrium within 24 hours from launch. Stability was reached at 68°F, 12° below the launch temperature of 80°F. The predicted temperature range, calculated by the "input-with-ratio-applied" was 70°F (RCA α) to 81°F (JPL/STL α). Flight temperature fell slightly below the lower limit of the prediction. This can be explained only as being an inaccuracy of the prediction equation due possibly to insufficient knowledge of the temperature of this area from the flight of RA-6. This data point was not telemetered on Channel 8 and during the RA-6 mission no information was obtained from that flight.

f. Summary

Of the five points which were monitored for temperature during cruise mode, four points were close to the midpoint temperature of the predicted range.

Three were right at midpoint, the Hat being 2° below mid-temperature. The Camera Electronics was $7^{o}F$ below the midpoint of the predicted range, but well within the range of desirable operation temperature. A comparison of predictions to actual flight temperatures obtained from Channel-8 telemetry is listed in Table 4-7.

TABLE 4-7

COMPARISON OF PREDICTED TO ACTUAL FLIGHT TEMPERATURES

Location	Data Point	Predicted By RCA α (^{o}F)	Predicted By JPL/STL α (^{o}F)	Flight (^{o}F)
Hat	7	78	90	82
Lens Housing	1	61	72	66
Shroud	8	68	81	74
Battery	4	68	79	75
Camera Elect.	11	70	81	68

5. Temperature Rise of RA-7 Camera Lens Housing During Final Hours Prior to Lunar Impact

As the Spacecraft approaches the moon, the effects of lunar solar reflections and moonshine begin to be noticed. These factors will not affect the over-all spacecraft temperature to any noticeable extent due to the high reflectance of the surfaces which face the moon. The solar cell paddles and the cameras, however, have a highly absorptive surface facing the moon, and both these areas experienced heating during the final hours of flight.

The thermal energy flux is a summation of the reflected solar radiation and the IR radiation of the moon, referred to as moonshine. Calculations of the flux density at various distances from the moon were plotted to provide the curve in Figure 4-17. The curve is not absolute due to the approximations that were used in the calculations, but it is accurate enough to explain the conclusions that were reached by its useage.

From the curve, the average flux during the last three hours of flight can be reasonably approximated at 0.01 watts per square inch to within 1000 miles from the moon's surface. Within 1000 miles to impact, the average flux is 0.12 watts per square inch for a period of 15 minutes. Using these values as an input, the increase in temperature of the camera lens housing can be calculated. Although the entire projected area of the cameras is exposed to this energy flux, the front end of the camera can be treated separately due to its limited conductivity to the balance of the mass. This is evident by the fact that the camera bracket does not rise in temperature at the same rate as the lens housing. The temperature increase, ΔT, during the last 15 minutes can be calculated from:

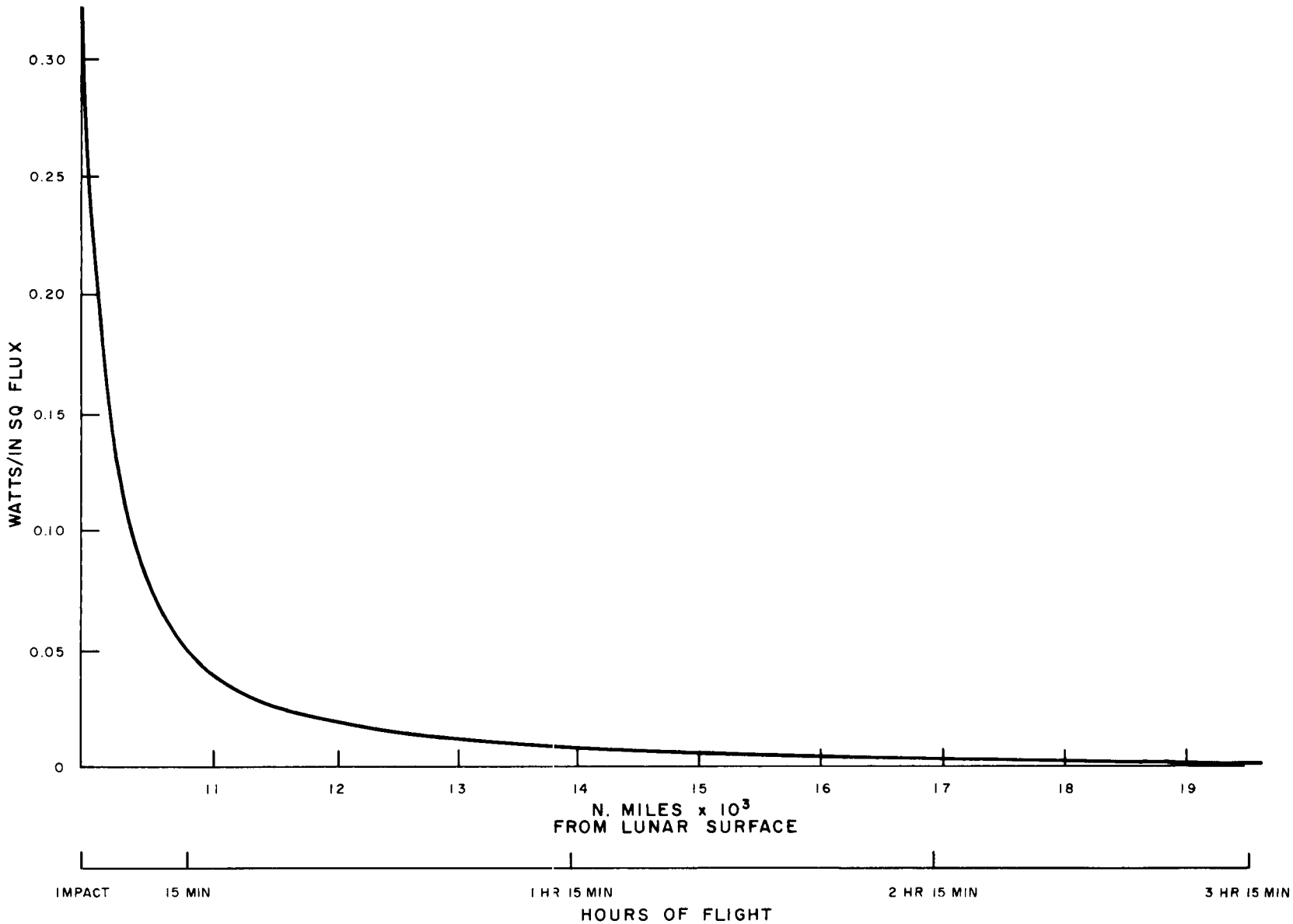

Figure 4-17. Reflected solar radiation and moonshine θ_s=40°, 11°S. Lat. 21°W Longitude

$$\Delta T = \frac{Q}{mc}$$

$$= \frac{\text{(flux) (area) (minutes)}}{\text{(weight) (specific heat)}}$$

$$= \frac{(0.12 \frac{w}{in^2})\ (0.0569 \frac{BTU}{min/w})\ (12.5\ in^2)\ (15\ min)}{(1.5\ lbs)\ (0.22 \frac{BTU}{lb^oF})}$$

$$\Delta T = 3.8^oF$$

and the ΔT for the previous three hours using the same relationship:

$$\Delta T = \frac{(0.01 \frac{w}{in^2})\ (0.0569 \frac{BTU}{min/w})\ (12.5\ in^2)\ (180\ min)}{(1.5\ lbs)\ (0.22 \frac{BTU}{lb^oF})}$$

$$\Delta T = 3.9^oF$$

These calculations indicate a rise in temperature of the front end of the cameras on the order of 7 to 8^oF. Using this approach, the increase of 6 to 10^oF from telemetry, in the area of the camera lens during Ranger-7 flight can be explained. Lunar inputs can provide heating on the same order as that experienced by the Ranger-7 spacecraft.

Other data points indicate little or no temperature increase due to the lunar inputs since conditions of mass and high reflectance limit the effects.

Section V

Conclusions and Recommendations

A. Conclusions

B. Recommendations

Section V

Conclusions and Recommendations

A. Conclusions

Based upon an analysis of the data returned from the flight of the Ranger-7 spacecraft, it may be concluded that the flight performance of the RA-7 TV Subsystem (III-2) met or surpassed all design and mission requirements.

B. Recommendations

In view of the highly satisfactory performance of the RA-7 TV Subsystem, it is not recommended that major design or operational changes (other than those changes implemented prior to the flight of RA-7) be considered for the RA-8 and RA-9 TV Subsystems. However, the following minor recommendations are made with a view towards effecting small improvements in reliability or performance of the TV Subsystem, or in the operational techniques used to control or evaluate the flight performance:

1. It is suggested that the CTU/CSU be modified from the linear amps/volt telemetry relationship used in RA-7 to a non-linear relationship that will provide improved reading accuracy for current drains in the vicinity of the cruise and full-power currents.

2. In the event that it is desired to obtain pictures closer to the lunar terminator it is suggested that the gain of the cameras fitted with 76mm F/2.0 lenses be increased to provide a peak video signal for scene illumination of 1800 foot lamberts. The implementation of this recommendation will effectively narrow the failure mode capability of the TV Subsystem in the event of a nonstandard mission; however, this recommendation is consistent with the results of the RA-7 mission.

3. Although the microphonics observed during the RA-7 mission were considerably less then the microphonics seen during system taking of the RA-7 TV Subsystem, it is recommended that present efforts aimed to reducing microphonics be continued in order to minimize the effects of this noise on system performance.

4. An improved method of r-f signal level calibration and measurements should be used at Goldstone in order to enable a more accurate measurement of the TV Subsystem r-f power during flight.

5. It is suggested that the possibility of improving communications facilities between SFOF and the Johansbury DSIF station be investigated, as flight experience with RA-7 indicates the desirability of receiving direct analog TV Subsystem telemetry from all remote DSIF stations.

Appendix A

Testing of Ranger Flight Model III-2 TV Subsystem at JPL

Appendix A

Testing of Ranger Flight Model III-2 TV Subsystem at JPL

This appendix describes the tests performed on the Ranger Flight Model III-2 TV Subsystem at JPL. A total of 18 tests were performed on the TV Subsystem either while mated to the JPL Spacecraft Bus, or on the Subsystem alone. The tests performed at JPL are listed in Table A-1.

A. Post-Shipment Electrical Test (RTSP-1100A, Appendix R)

When the Ranger Flight Model III-2 TV Subsystem arrived at JPL on May 2, 1964, it was mounted on a test stand and the shrouds and impactograph were removed. The Subsystem was then visually inspected for any damage that might have occurred during shipment. Following this, the Post-Shipment Electrical Test was performed.

1. Purpose of Test

The purpose of the Post-Shipment Electrical Test was to verify that no damage was incurred by the TV Subsystem during shipment from RCA to JPL.

TABLE A-1
TV SUBSYSTEM TESTS AT JPL

Title of Test	Date	Test Procedure
Post-Shipment Electrical Test	5/2/64	*RTSP 1100A Appendix R
Matchmate Test	5/2/64	JPL No. 3R 212.04
System Test No. 8	5/4/64	JPL No. 3R 300.11
RF Link Test	5/5/64	JPL No. 3R 315.00

TABLE A-1 TV SUBSYSTEM TESTS AT JPL (Continued)		
Title of Test	Date	Test Procedure
Vibration-Post X-Axis	5/8/64	JPL No. 3R 311.03
Vibration-Post Y-Axis	5/8/64	JPL No. 3R 311.03
Vibration-Post Z-Axis	5/12/64	JPL No. 3R 311.03
Vibration-Modal Test	5/12/64	JPL No. 3R 311.03
System Test No. 9	5/14/64	JPL No. 3R 300.12
Subsystem Verification Test	5/21/64	*RTSP 1100A, Appendix R
Pre-Thermal-Vacuum Verification Test	5/24/64	JPL No. 3R 302.05
Mission Verification Test Nos. 4 and 5	5/28-31/64	JPL No. 3R 302.05
Special TV Subsystem Test	6/8/64	*RTSP 1100A, Appendix
Space-Simulator Operational Check-Precount	6/8/64	JPL No. 3R 320.01
Space-Simulator Operational Check-Precount	6/9/64	JPL No. 3R 320.01
ESA Test No. 1	6/10/64	JPL No. 3R 235.00
ESA Test No. 2 (RF1 Test)	6/10/64	JPL No. 3R 235.00
Back-Up Function Test No. 3	6/11/64	JPL No. 3R 305.06
*TV Subsystem not mated to JPL Spacecraft bus.		

2. *Description of Test*

The Post-Shipment Electrical Test was performed by RCA personnel with JPL observers in attendance. The test procedure was that of RTSP-1100A, Appendix R, and was performed with the following conditions:

- Subsystem thermal shroud removed;
- Subsystem power provided by external sources (separate supply for F- and P-Channel);

- Collimators installed on the Subsystem; and
- Test terminated at T + 14'.

With the TV Subsystem mounted on its test stand, interconnection cables were connected between the Subsystem and the Ground Support Equipment (GSE), as specified in RTSP-1100A, Appendix R. The total test time was 14 minutes.

The test sequence for the Post-Shipment Electrical Test is given in Table A-2.

TABLE A-2
POST-SHIPMENT ELECTRICAL TEST SEQUENCE

Time	Operation Function
T* + 0	Main power turned on. External Power was selected on GSE console. F- and P-Channels were prepared for full-power operation. Light source for illumination of Cameras was prepared.
T + 1'	Cruise-mode operation activated by Cruise Mode switch on GSE.
T + 3'	F- and P-Channel warmup mode activated by RTC-7F and RTC-7P switches.
T + 4'20"	F- and P-Channels went into full-power operation. Film Recorder turned on. Cruise-mode telemetry received over r-f link and recorded on strip-chart recorder. Note: An illumination source (light gun) was used to verify the operation of the TV Cameras and was calibrated before use. It was then used to illuminate each Camera separately. Polaroid photographs of the Camera video outputs were taken for rapid evaluation of Camera performance. The Camera video output received over the r-f link was also recorded on 35-mm film as a permanent record for future evaluation.
T + 8'	F- and P-Channels turned off by RTC-5 switch.
T + 8'30"	Cruise mode turned off by Cruise Off switch.
T + 9'	Cruise mode activated by Cruise On Test switch.
T + 9'30"	F- and P-Channel reset activated by Reset F and Reset P switches.

TABLE A-2 POST-SHIPMENT ELECTRICAL TEST SEQUENCE (Continued)	
Time	Operation Function
T + 11'20"	F- and P-Channel full-power operation activated by CC&S Full-Power switch. Recorder started on P-Channel 225kc and P-Channel 90-point telemetry recorded.
T + 12	After the sync separator in Unit 5 of GSE was prepared for sync-failure mode, Sync Disable was activated by Sync Disable switch. P1-Camera illuminated with 2700-foot-lambert light source. A Polaroid picture of P1-Camera video output taken.
T + 13'30"	Camera sync re-established by Sync Disable Switch, and sync separator (Unit 5 of GSE) restored to normal operation.
T + 14'	Light source removed and turned off. Returned to warmup mode by CC&S Full-Power Switch. TV Subsystem turned off by the RTC-5 switch. Tape recorder turned off and tape reviewed in accordance with RTSP-1100A, Appendix Q. F- and P-Channels reset by F- and P-Channel Reset switches.
* T represents time of primary power application.	

3. *Test Data Evaluation*

a. Video Performance

The video signals obtained during this test were considered satisfactory; however, the following problems in the GSE Test Equipment detracted from the quality of the video signals recorded on the 35-mm film.

- Collimator alignment was not optimum; this resulted in low video-output level from the P1- and F_b-Cameras;
- GSE sync level in F-Channel was not adjusted for best horizontal sync. Most frames of F-Channel video output contained horizontal-line offsets where black-to-white transitions occurred at the trailing edges of the line. (See Figure A-1).

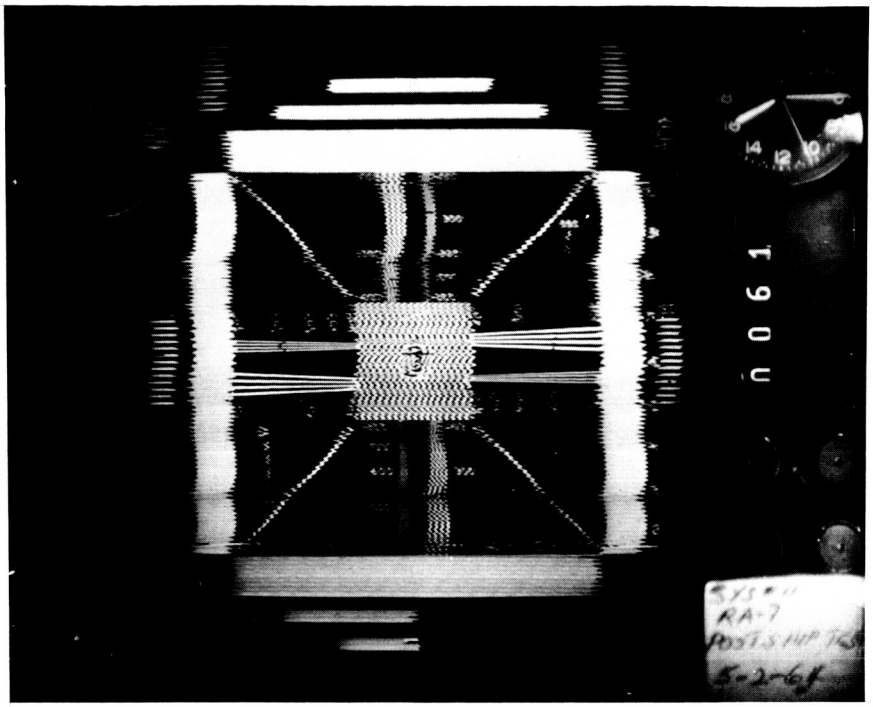

Figure A-1. Video output of F_a Camera showing poor horizontal sync level in GSE

Several frames of P1-Camera video output exhibited a single, very-fast noise spike. Although these noise spikes were not considered a serious degradation to the video performance, they were noted for observation during future testing, since they had not been previously encountered.

b. Communications Performance

RF power output was satisfactory, with 59 watts combined power after one minute of full-power operation and a peak r-f power output of 60 watts after 3 minutes of full-power operation. Several 1-watt increases in r-f power output occurred at approximately T + 6' and T + 13'. RF power increases of this magnitude are not considered serious, however, instantaneous changes in power are not desirable. This problem was noted as a potential failure area, if the changes in power increased in magnitude.

c. Telemetry Performance

All telemetry data obtained indicated that TV Subsystem performance was normal. There were no anomalies in the telemetry data.

B. Matchmate Test (JPL Procedure 3R212.04)

The Matchmate Test was performed at JPL on May 2, 1964. For this test, the TV Subsystem was mated to the JPL Spacecraft Bus.

1. Purpose of Test

The Matchmate Test was performed to verify the electrical compatibility of the TV Subsystem with the Spacecraft Bus; to establish operational readiness of the TV Subsystem by performing a functional checkout; and to verify r-f compatibility with the TV Subsystem operating in the full-power mode and with the high-gain antenna radiating.

2. Description of Test

The configuration of the TV Subsystem for this test was as follows:

- Collimators were not mounted;
- Thermal shroud was removed; and
- Power from external sources was utilized.

The test setup for the Matchmate Test was as shown in Figure A-2. The Matchmate Test can be divided into five specific areas;

- Voltage and resistance checks performed on the TV Subsystem prior to mating with the Spacecraft Bus;
- Functional checkout of the TV Subsystem using simulated CC&S (programmed) and command (real-time) signals;
- Functional checkout of the TV Subsystem operating in the full-power mode by TV commands from the Operational Support Equipment (OSE); proper operation of the 890-Mc Transponder Receiver on the JPL Bus is also verified during the full-power mode of the TV Subsystem to assure that no interference exists between the two links. The output level of the Channel-8 VCO's are also adjusted, and the loss of the TV sequence sync pulses is simulated to check the free-running mode of the P1-Camera; and

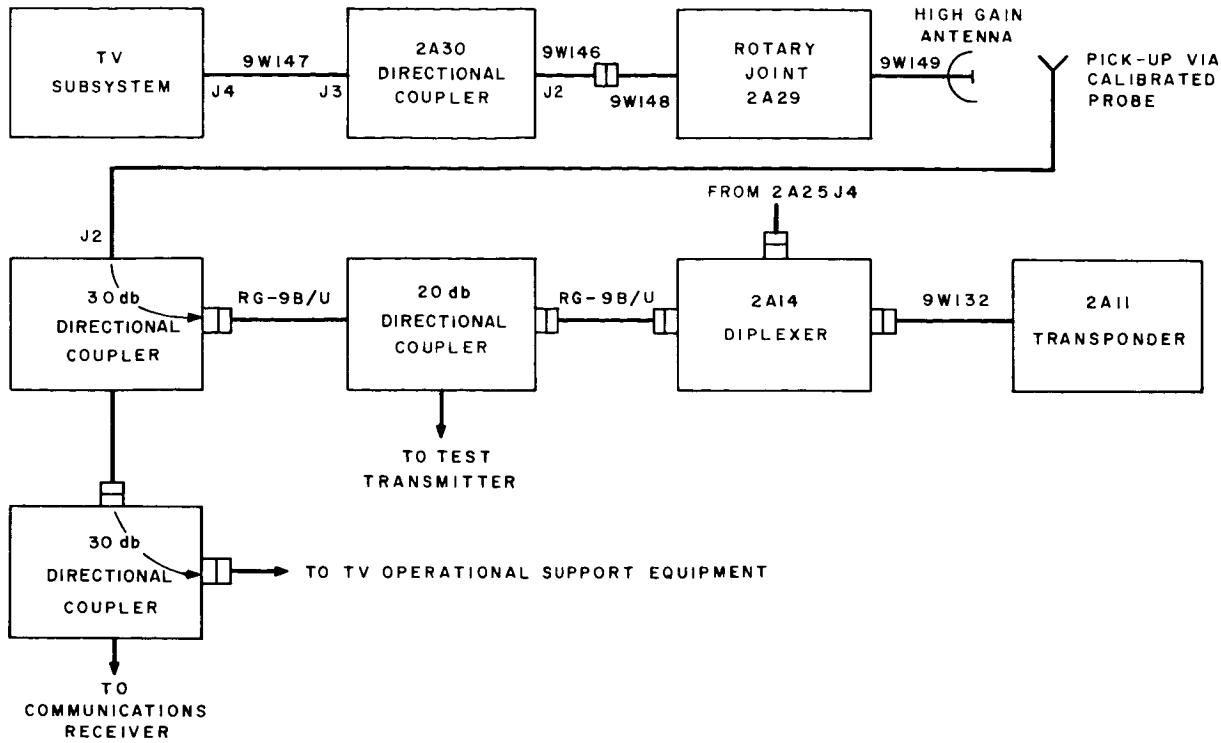

Figure A-2. Matchmate Test set-up

- Functional checkout of the TV Subsystem operating in the full-power mode by Spacecraft real-time commands; operation of the JPL 960.05-Mc Transmitter during the TV Subsystem full-power mode is also monitored during this portion of the test to assure that no interference exists between the two links.

The r-f data link for the functional checkouts was established by:

- Verification of the JPL Transponder via the r-f link through the high-gain antenna. The output is fed hard-line to the OSE;
- Monitoring the outputs of the Spacecraft Transmitter and feeding them hard-line to the Communications OSE from an r-f link antenna;
- Routing the television r-f signals to the Television OSE.

3. *Test Evaluation*

a. Video Performance

Performance of the TV Subsystem was considered satisfactory with one exception. Radio-frequency interference (rfi) was observed on the outputs of the

F_a- and F_b-Cameras and very slightly on the output of the P3-Camera. The rfi was identified as cross-channel interference, with P-Channel video horizontal-sync rate being detected by the F-Camera Heads, and F-Channel video sync rate being detected by the P3-Camera Head. The specific mechanism of detection could not be established although it is logical to expect some a-m detection of r-f signals in the Camera Preamplifier circuits. This test was performed with the TV Subsystem thermal shrouds removed which probably accounted for the increased susceptibility of the Camera Heads to stray r-f radiation. In addition, the r-f output of the TV Subsystem was fed into the high-gain antenna which was radiating into the floor of the test area. This setup generated a much higher level of stray r-f radiation than is normally experienced when the TV Subsystem is operated in its normal configuration with the r-f cable terminated by a dummy load.

Collimators were not employed for Camera evaluation during this test; however, through the use of a calibrated light gun, it was noted that the output video level of the P1-Camera was approximately 150 millivolts below normal. Very slight microphonics were observed on the P1-Camera video output; this condition was attributed to the shutter action of an F-Camera. An occasional slight microphonic condition was also observed in the video output of the P4-Camera and was attributed to the shutter action of the P1-Camera.

The GSE sync-level for F-Channel was not properly adjusted during the test. This resulted in sync tearing in approximately 25 percent of the frames of F-Channel video output.

b. Communications Performance

The r-f power output was 59.7 watts after one minute of full-power operation and peaked at 63.1 watts at 8 minutes of full-power operation. The input voltage to the P-Channel Transmitter Power Supply was 30.3 volts, d-c and 31.0 volts, d-c to the F-Channel Transmitter Power Supply. The r-f power profile and 3-watt fluctuations in r-f power at the F-Camera rate during most of the test. These fluctuations in the power recording were attributed to r-f reflections, from the high-gain antenna radiating into the floor, being detected in the TV Subsystem.

c. Telemetry Performance

All telemetry points indicated that the TV Subsystem operated normally throughout the test. Channel-8 telemetry had approximately 300 millivolts of noise when the received signal level at the JPL Beacon Receiver was at the threshold level of -130 dbm. It was determined after the test that the Channel-8 Discriminator in the GSE was not operating properly.

d. Conclusions

The test was considered successful although some problems were experienced with stray r-f radiation. It was estimated that the rfi problems probably would not recur when the TV Subsystem had shrouds, and the radiated energy from the high-gain antenna was properly absorbed or radiated into free space.

4. Changes to Flight Model III-2

Upon completion of the Matchmate Test (JPL Procedure 3R 212.04), several items were replaced in the Flight Model III-2 TV Subsystem. These replacements occurred on May 4, 1964, and included the P1-Camera Shutter, the Four-Port Hybrid output cable, and the Telemetry Assembly.

P1 Shutter, Serial No. 3065, was replaced by Shutter, Serial No. 3076. The new shutter speeds were 2.1 milliseconds in both directions with an operating time of about 7 hours.

The flight r-f cable from the output of the Four-Port Hybrid to the input of Case II in the JPL Bus was removed for replacement of its Mylar shielding.

It was also decided to replace Telemetry Assembly, Serial No. 008, with Serial No. 007. The replacement actually contained new-design Fifth Dimension, Inc. Commutators, but the other subassemblies in the telemetry assembly were original units (225-kc VCO's, Channel-8 VCO, and AC amplifier).

At this time, the following Batteries were also installed to provide power for the TV Subsystem during the pre-vibration and vibration tests that were to be performed later in the test series:

- F-Channel: Battery, Serial No. 79; V_{oc} = 40 VDC
- P-Channel: Battery, Serial No. 63; V_{oc} = 40.5 VDC

A brief test was then performed to verify proper operation after the installation of the new items.

The shrouds were then installed on the TV Subsystem to conform with the required configuration for System Test No. 8 (JPL Procedure 3R 300.11). Once again, the system was given a thorough informal system test to assure proper performance.

C. System Test No. 8 (JPL Procedure 3R300.11)

System Test No. 8 was performed on May 4, 1964, with the TV Subsystem mated to the JPL bus. Collimators were attached to the TV Subsystem and an external electrical source provided the power to operate the Subsystem equipments.

1. Purpose of Test

System Test No. 8 was an accelerated mission simulation to verify that all equipment of the Ranger Spacecraft operated properly. In this test, the TV Subsystem underwent simulated-launch electrical operation and was commanded through a simulated-terminal-mode operation.

2. Description of Test

Batteries had been installed on the TV Subsystem prior to this test, however, an external power source was employed during the test. The r-f meter calibration setup is shown in Figure A-3, and Figure A-4 shows r-f test configuration employed during this system test.

Table A-3 describes the test sequence.

3. Test Evaluation

a. Video Performance

Camera operation was considered satisfactory during System Test No. 8, although the previously observed low video-output levels on the F_b-and P1-Cameras were again encountered. The below-normal level of F_b-Camera video output was attributed to misalignment and brightness of the collimator. The low video-output level from the P1-Camera was again the result of improper gain adjustment on the GSE.

b. Communications Performance

The measured r-f power output from the TV Subsystem was 57.6 watts after 2 minutes of full-power operation, and reached a peak of 58.3 watts at 3 minutes

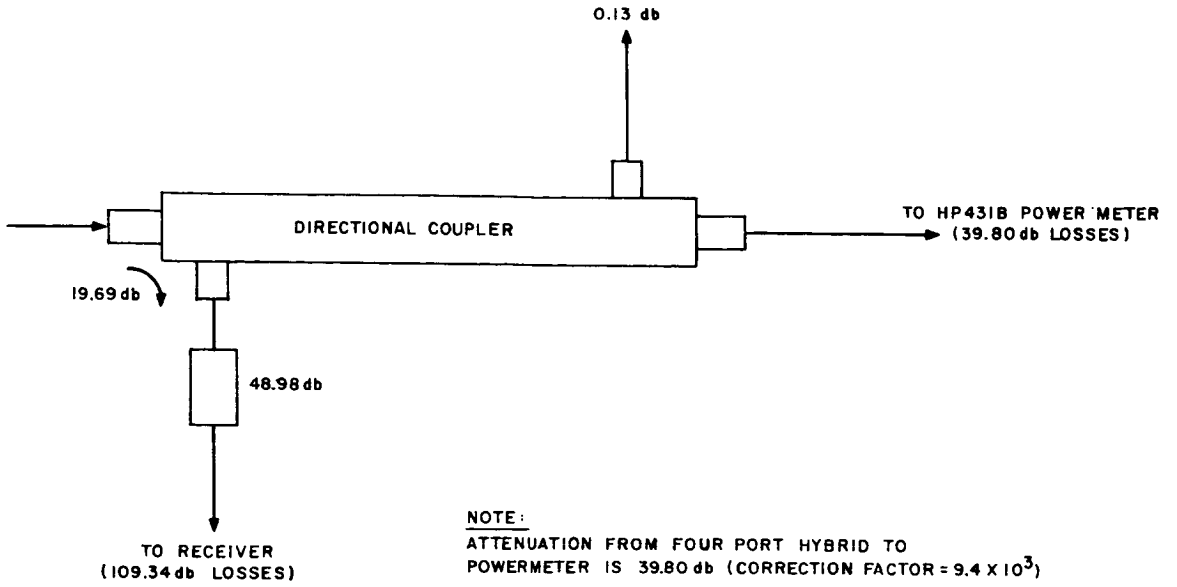

Figure A-3. RF meter calibration for System Test

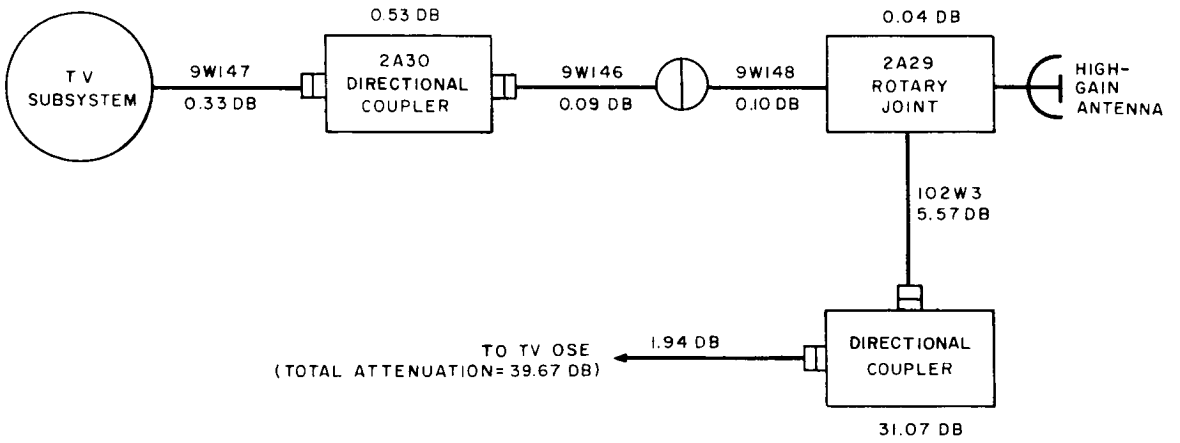

Figure A-4. RF test set-up

TABLE A-3

SYSTEM TEST NO. 8 TEST SEQUENCE

Time	Operation Function
A*-5'	Cruise On Test switch depressed twice. This allows Cruise-Mode telemetry to be received over Channel 8.
A + 38'40" S** + 5'	Bus-Agena microswitch closed. This activates the TV Subsystem Clock.
A + 63'40" S + 30'	Hydraulic timer enabled the TV turn-on bus by grounding the SCR-gate resistors in preparation for the SCR turn-on command. (No indication from TV Subsystem)
C*** + 44'	RTC-7 command turns on F- and P-Channels into warmup mode.
C + 45'20"	Both channels are turned-on in full-power mode by TV Sequencer full-power command.
C + 50'	TV operation and sync-disable activated This disables the P-Channel Sequencer and verifies operation of the free-running mode of the P1-Camera.
C + 51'30"	Sync disable removed. This restores the proper P-Channel sync signals for all P-Channel Cameras.
C + 54'30"	F- and P-Channel full-power command in TV Sequencer reset. TV Subsystem remains in full power by CC&S full-power command. This verifies activation of the CC&S Full-Power switch.
C + 55'	CC&S Full-Power switch reset. TV Subsystem goes into warm-up mode.
C + 56'	RTC-5 switch turns off F- and P-Channels.
C + 56'10"	Cruise On Test switch depressed twice. This resets the TV Subsystem Clock.
C + 56'20"	Cruise Off switch activated. This turns off Cruise-Mode telemetry.

*represents time of launch.
**represents time of Agena separate.
***represents time of terminal mode.

of full-power operation. At the end of the test, the r-f power output was 58.2 watts. The input voltage to the F-Channel Transmitter Power Supply was 31.4 volts, and the input to the P-Channel Transmitter Power Supply was 30.6 volts.

c. Telemetry Performance

All telemetry data obtained during the test indicated that the operation of the TV Subsystem was normal. No abnormal values were observed in a review of the telemetry data.

D. RF Link Test (JPL Procedure 3R315.00)

The RF Link Test was performed on May 15, 1964. The TV Subsystem was mated to the JPL Spacecraft Bus for this test, and power for the TV Subsystem was provided by batteries installed in the Subsystem. Prior to the test, the cell voltages of the batteries were checked and measured as follows

- Each cell (22) of the F-Battery measured 1.86 volts, and
- Each cell (22) of the P-Battery measured 1.62 volts.

Jumper plug 30P13 was installed to complete the normal Battery-load flight configuration of the TV Subsystem.

1. Purpose of Test

The RF Link Test was an accelerated mission-simulation test in which all OSE and ground cables were disconnected from the TV Subsystem. All communications with the Spacecraft were accomplished by r-f link only. The purpose of the RF Link Test was to verify the operation of all Spacecraft equipments in their true-flight configuration.

Two simulated terminal maneuvers were performed. One was to verify the Subsystem turn-on command from the Spacecraft Bus (CC&S Warmup); the second was to verify the RTC-7 commands (real-time warmup commands).

2. *Description of Test*

The RF Link Test was performed with the TV Subsystem mated to the JPL Spacecraft Bus. For this test, no cables were attached to the Spacecraft, and instead of mounted collimators, a white material, illuminated with flood lamps, provided exposure for the six cameras. The TV Subsystem was powered internally by two non-flight batteries and with the jumper plug 30P13 installed.

To prevent any radio-frequency interference (rfi) problems, the directional antenna was deployed so that it pointed from the side of the Spacecraft to a wall (10 feet away) lined with microwave-absorption material. This configuration, in the path of the antenna radiation, eliminated any r-f reflections back to the Spacecraft.

The sequence of events in the RF Link Test is presented in Table A-4.

TABLE A-4
RF LINK TEST SEQUENCE

Time	Operation Function
A-5	Cruise On Test switch depressed twice; this allows Cruise-Mode telemetry to be received over Channel 8, and simultaneously resets the Clock on the TV Subsystem while disabling the SCR gates in the High-Current Voltage Regulators.
A + 33'40" (S + 0)	Simulated Spacecraft operation. Back-up-command hydraulic timer is started.
A + 38'40" (S + 5)	Television Clock microswitch is closed. Clock starts.
A + 62'	Solar panels are deployed. Switch contact closure serves a back-up for the hydraulic-timer operation.
A + 63'40" (S + 30)	The hydraulic-timer switch closure enables the television SCR gate turn-on circuits and serves as a back-up for Cruise-On command.
	First Terminal Maneuver
C + 45'	CC&S Warmup command (TV-2) turns on F- and P-Channels in warmup mode. (Camera illumination on).
C + 46'20"	F- and P-Channels turned-on in full-power mode by TV Sequencer full-power command.
C + 51'37"	RTC-5 command from OSE turns off F- and P-Channels.

TABLE A-4 RF LINK TEST SEQUENCE (Continued)	
Time	Operation Function
	Second Terminal Maneuver
C + 44'	RTC-7 Command from OSE turns on F- and P-Channels into warm-up mode.
C + 45'20"	F- and P-Channels are turned on into full-power mode by TV Sequencer full-power command.
C + 51'30"	Camera illumination removed for dark-field photographs.
C + 53'30"	Camera illumination restored.
C + 56	RTC-5 Command from OSE turns off F- and P-Channels.
	Test (GSE)
	Cables are connected to the TV Subsystem and the following sequence performed. (a) Cruise On Test switch depressed twice to stop & reset Clock. (b) Cruise Off switch depressed to turn off Channel-8 Cruise Mode telemetry.

3. *Test Evaluation*

a. Video Performance

Since collimators were not employed during this test, a detailed evaluation of the video output could not be made. However, it was concluded that camera operation was normal in that no excessive noise was evident on the recorded video output.

b. Communications Performance

The r-f link was not calibrated for this test; therefore, no absolute measurement of r-f power output could be made. The r-f power profile recorded during the test was normal.

c. Telemetry Performance

The telemetry data obtained during test indicated that TV Subsystem operation was normal. The only discrepancy was that telemetry point no. 8 on the 15-point Commutator (Shroud Temperature, -Y-axis) indicated a telemetry value of 0.8 volt, which is equivalent to approximately 40°F. The actual temperature of the shroud during this test was approximately 70°F, indicating that a malfunction had occurred in thermistor No. 11, or its associated circuitry.

Noise spikes were noted in the Channel-8 strip-chart recording at low r-f power levels. It was later determined that the Channel-8 Discriminator in the GSE had failed.

E. X-Axis Vibration Test (JPL Procedure 3R311.03)

The X-Axis Vibration Test was performed at JPL on May 8, 1964, with the TV Subsystem mated to the JPL Spacecraft Bus. Power for operation of the TV Subsystem equipments was provided by non-flight Batteries installed in the Subsystem.

1. Purpose of Test

The purpose of the X-Axis Vibration Test was to verify that the TV Subsystem capable of withstanding X-axis vibrations equivalent to or greater than the vibrations imparted by the Atlas and Agena vehicles during the launch and orbit-injection operations. The Cruise-Mode portion of the Subsystem operation, which was to be operated during the launch phase, was required to operate satisfactorily during the vibration test. Since the TV Subsystem was to perform its picture-taking function during the terminal phase of the mission, proper operation after the specified levels of vibration was also required as part of this test.

2. Description of the Test

The following Batteries were installed in the TV Subsystem for the vibration tests:

- F-Battery: Serial No. 79
- P-Battery: Serial No. 63

The TV Subsystem was mated with the Spacecraft Bus for this test, and the entire Spacecraft was mounted on a special test fixture so as to simulate the shear and tension ties normally utilized to mate the Spacecraft to the Agena adapter (Reference JPL Procedure 3R 115).

During the vibration, the Spacecraft was monitored by a two-way r-f link. A Stoddard antenna was positioned adjacent to the Spacecraft omni-antenna and interconnected to a directional antenna located on the roof of the Environmental Test Laboratory (ETL) at JPL for transmission to the system test complex located in the Spacecraft Assembly Facility. The r-f losses encountered with this arrangement are calculated in Figure A-5, which shows the basic r-f link for this test.

a. Preliminary Test Preparation

Prior to actual vibration of the Spacecraft, the following operations were performed from the Preliminary Conditions Checklist:

(1) Proper Spacecraft configuration verified;

(2) OSE verified as ready for start of test;

(3) TV Subsystem enabled by Cruise On Test switch;

(4) 15-point telemetry recorded on Channel 8;

(5) Modal Survey conducted in accordance with JPL Procedure 3R 117.

(6) Cruise On Test switch activated, then Cruise Off Test activated to inhibit TV Subsystem;

(7) No reception of 15-point telemetry verified;

(8) End of Modal Survey

b. Test Sequence

The X-Axis Vibration test sequence is presented in Table A-5.

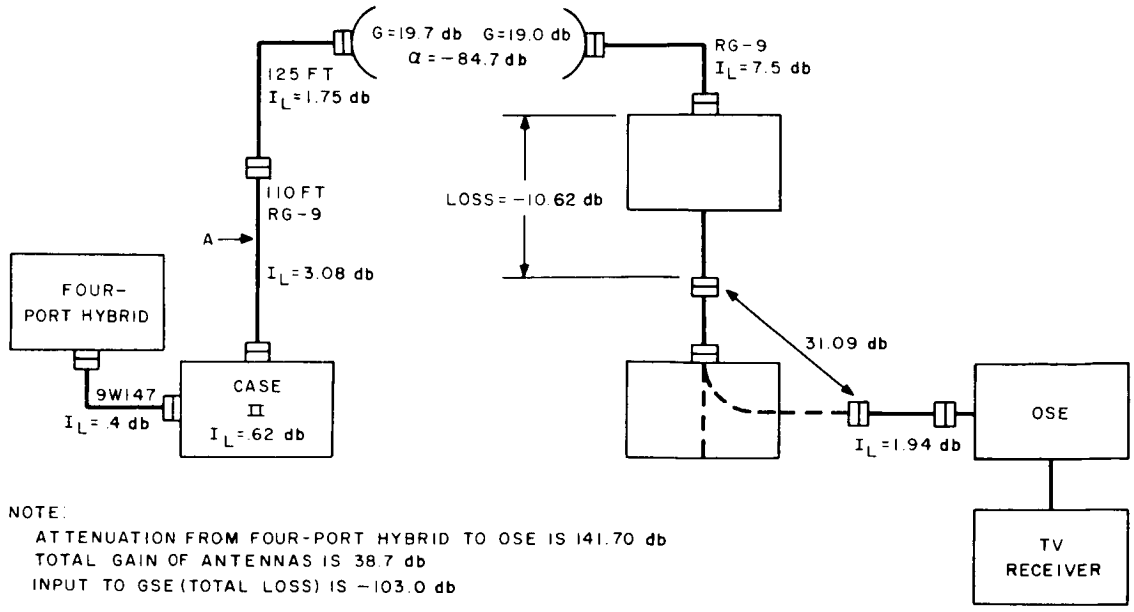

Figure A-5. RF losses for vibration test arrangement at JPL

TABLE A-5
X-AXIS VIBRATION TEST SEQUENCE

Time	Operation Function
	Cruise Mode activated by Cruise On Test switch. Cruise-mode telemetry received on Channel-8. Vibration preparation started. Mode III Spectrum Analysis started. Preparations made for emergency TV turn-off.
A - 5'	Transfer from external to internal Subsystem power.
A - 2'30"	Channel-8 telemetry recorder started.
A = 0	Launch (simulated).
	Vibration turned off. Cruise Off switch activated. No reception of Cruise-Mode telemetry received.
	End of Vibration Test.

c. *Post-Vibration Functional Verification of the TV Subsystem*

Following the X-Axis Vibration Test, a functional verification test was performed on the TV Subsystem. As a preliminary condition of a full-power test of the TV Subsystem, a white reflective surface was placed within the field of view of the Cameras, with a source of illumination provided incident to the viewed surface.

The OSE was connected in hard-line mixed-signal configuration, and was then made ready to receive r-f signals from the TV Subsystem.

The post-vibration functional verification test sequence is presented in Table A-6.

TABLE A-6
POST-VIBRATION FUNCTIONAL VERIFICATION TEST SEQUENCE

Time	Operation Function
T - 3'	Cruise On Test switch activated to obtain Channel-8 telemetry modulation.
T - 0'38"	Subsystem turned-on into warmup mode by RTC-7 switch.
T = 0	Stopwatch countdown to full-power-mode turn-on started. Channel-8 90-point telemetry recorded.
T + 10"	Cruise On switch released.
T + 60"	Power-Output Recorder started.
T + 80"	Full-power operation verified. Tape-Recorder started. Film-Recorder started on P-Channel. F-Channel 225-kc telemetry recorded. Polaroid picture of P-Camera video output taken.
T + 4'	Recording and Polaroid-picture-taking activities switched over to F-Channel.
T + 6'	TV Subsystem turned off by RTC-5 switch.

3. *Test Evaluation*

a. *Video Performance*

Collimators were not employed in this test, so that a detailed evaluation of the cameras and output video was not possible. Based on the video information received, all cameras appeared to function normally.

b. Communications Performance

RF power output was measured as 59.0 watts after one minute of full-power operation, and peaked at 59.5 watts after 1.5 minutes of operation. At termination of the 6-minute test, the r-f power output was 57.2 watts. The input voltage to the F- and P-Channel Transmitter Power Supplies was approximately 31.0 volts.

After one minute of full-power operation, the r-f power output increased from 54.2 to 59.0 watts in less than one second. Data point No. 79 (F-Channel Power Amplifier cathode current) of the 90-point telemetry decreased in value from 3.5 to 1.9 volts, verifying a change in operation of the F-Channel Power Amplifier.

c. Telemetry Performance

With the exception of data point No. 8 (shroud temperature) of the 15-point telemetry, which had previously malfunctioned, all telemetry indicated that operation was normal.

F. Y-Axis Vibration Test (JPL Procedure 3R311.03)

The Y-Axis Vibration Test was performed at JPL on May 8, 1964, with the TV Subsystem mated to the JPL Spacecraft Bus. Power for operation of the TV Subsystem equipments was provided by non-flight Batteries installed in the TV Subsystem.

1. Purpose of Test

The purpose of this test was the same as that of the X-Axis Vibration Test described in Paragraph D, except that the Y-axis was tested.

2. Description of Test

The Test setup and procedure for the Y-Axis Vibration Test was the same as for the X-Axis Vibration Test described in Paragraph E, except that modal survey was not required as a prerequisite.

3. Test Evaluation

a. Video Performance

The cameras of the TV Subsystem performed satisfactorily during the test, except that the previously encountered sync-tearing problem was again evident on the 35-mm film of the F-Channel video output. Playback of the F-Channel video output recorded on magnetic tape showed no evidence of this problem.

b. Communications Performance

The r-f power output was measured as 57 watts after one minute of full-power operation, peaked at 59.2 watts after two minutes, and was 56.0 watts at termination of the 7-minute test. The input voltages to the F- and P-Channel Transmitter Power Supplies were 31.0 and 30.1 volts, respectively. Performance of all communications assemblies was satisfactory.

c. Telemetry Performance

The telemetry obtained during this test indicated that the performance of the TV Subsystem was normal. However, data point No. 8 (shroud temperature) of the 15-point commutator again malfunctioned.

d. Post-Vibration Verification

At conclusion of the Y-Axis Vibration Test, the TV functional verification procedure described in Table A-6 was performed. The TV Subsystem responded satisfactorily to all commands except the Cruise Off command. Investigation revealed that connector JB30 at the blockhouse junction box was not properly mated.

G. Z-Axis Vibration Test.

The Z-Axis Vibration Test was performed on May 12, 1964, with the TV Subsystem mated to the JPL Spacecraft Bus. Power for the TV Subsystem equipment was provided by non-flight batteries installed in the TV Subsystem.

1. Purpose of Test

The purpose of the Z-Axis Test was the same as that described in Paragraph D for the X-Axis, except that the vibrations were imparted to the Z-axis of the Spacecraft.

2. Description of Test

The test setup and procedure for the Z-Axis Vibration Test was the same as for the X-Axis Vibration Test, except that a modal survey was not required as a prerequisite.

3. Test Evaluation

a. Video Performance

The 35-mm film recording of the F-Channel video output again exhibited the sync-tearing problem, while the playback of the magnetic tape of the video information did not. This indicated that the GSE horizontal sync input was not properly adjusted, and it was decided to monitor the d-c level into the GSE F-Channel sync circuits continuously to insure proper F-Channel video synchronization.

Due to an accumulation of TV Subsystem and GSE video-level and r-f drift tolerances, it became necessary to track the d-c video level at the GSE to maintain the correct synchronization of the F-Channel video signals.

Also, single lines of video information from the P1, P3, and P4 Cameras were missing on several frames of the 35-mm film. This problem did not exist on the magnetic tapes of the recorded video information, indicating that the problem originated in the GSE. Further investigation revealed that a minor adjustment was required in the P-Channel horizontal sweep circuitry of the GSE. Once this adjustment was made, no further problems were experienced with lost lines in the P-Channel video output.

b. Communications Performance

The r-f power output was normal with 60.5 watts measured after 2 minutes of full power operation, dropping off to 57.0 watts at 3 minutes of full-power operation, and rising to 60.5 watts at termination of the 6-minute test. The input voltages to the F- and P-Channel Transmitter Power Supplies were 31 and 30 volts, respectively.

The power profile was considered satisfactory. Very small fluctuations were observed in the r-f power recording at the F-Shutter rate, but were not considered serious.

c. Telemetry Performance

The telemetry obtained during the test indicated that the TV Subsystem performed normally. Data point No. 8 (shroud temperature) of the 15-point commutator continued to malfunction.

H. Vibration-Modal Test (JPL Procedure 3R311.03)

The Vibration-Modal Test was performed on May 12, 1964, with the TV Subsystem mated to the JPL Spacecraft Bus. Power for operation of the TV Subsystem equipments was provided by non-flight Batteries installed in the TV Subsystem.

1. Purpose of Test

The purpose of this test was primarily the same as that described in Paragraph E for the X-axis, except that the torsional mode of vibration was simulated.

2. Description of Test

The test setup and procedure for this test is the same as that for the X-Axis Vibration Test, except that the modal test is the final operation following the X-, Y- and Z-Axis Vibration Tests.

3. Test Evaluation

Following the modal test, a post-vibration inspection of the TV Subsystem was performed. The shutter of F_a-Camera was found to be loose, with all four top mounting screws not tight. However, the shutter was in the proper-position, that is, there was a 50/1000-inch clearance from the camera housing. New mounting screws were installed and retorqued.

One mounting screw on the shutter of the F_b Camera was also loose, and it was replaced.

The battery voltages following the modal test measured as follows:

	Total Voltage	Cell Voltage
• F-Battery	34.99 volts	1.61 volts/cell
• P-Battery	34.69 volts	1.60 volts/cell

I. System Test No. 9 (JPL Procedure 3R300.12)

System Test No. 9 was performed on May 14, 1964, with the TV Subsystem mated to the JPL Spacecraft Bus. Collimators were installed on the Subsystem, and power for the Subsystem equipments was provided by an external source.

1. Purpose of Test

This test was an accelerated mission simulation to verify that all Spacecraft equipments operate as intended. The TV Subsystem was required to function properly during a simulated launch and through a simulated terminal-mode operation.

2. Description of Test

In all respects, the procedure for this test is the same as the test procedure given in Table A-3 for System Test No. 8 (paragraph C).

3. Test Evaluation

a. Video Performance

The GSE F-Channel sync problem recurred during this test, causing the F_a-Camera video output to exhibit sync tearing as shown in Figure A-1. Except for this problem, F-Camera performance was satisfactory.

Noise spikes appeared in approximately 5 percent of the frames of the 35-mm film recording of P1-Camera video output. In 35-mm frame No. 252, shown in

Figure A-6, the outputs of the P2- and P4-Cameras were read out in the P2 position. It was determined that the GSE did not switch sweep positions correctly, since the tape playback showed no evidence of this problem. No problems could be found in the GSE switching circuits, and therefore, it was assumed that the switching malfunction was the result of a noise pulse of unknown origin in the GSE. This problem did not recur during testing of Flight Model III -2 TV Subsystem. Except for the minor problems noted, P-Channel video output was satisfactory.

b. Communications Performance

The r-f power output during this test was measured at 49.7 watts after one minute of full-power operation, and reached a peak of 51.8 watts after 2 minutes of full power operation. At termination of the 6-minute test, the r-f power output was 51.0 watts. The input voltages to the F- and P-Channel Transmitter Power Supplies were 30.1 and 29.4 volts, respectively. The lower input voltage (about 1 volt) probably accounted for the low r-f power output obtained, compared to the 59 watts obtained during System Test No. 8. The r-f power-profile was normal during this test.

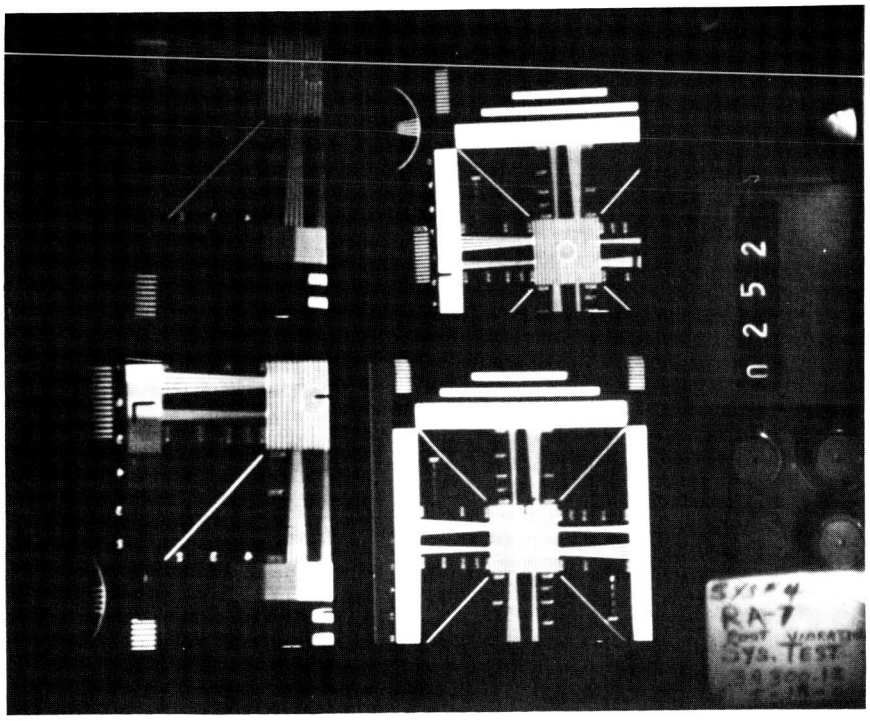

Figure A-6. P2- and P4-Cameras read out in P2 position (35-mm Frame No. 252)

c. Telemetry Performance

The telemetry obtained during the test indicated that the TV Subsystem functioned normally. Data point No. 8 (shroud temperature) of the 15-point commutator failed again.

J. Subsystem Verification Test (RTSP 1100A, Appendix R)

The Subsystem Verification Test was performed on May 21, 1964. The TV Subsystem was not mated to the JPL Spacecraft Bus for this test.

1. Purpose of Test

The Subsystem Verification Test was an abbreviated operation of the TV Subsystem to ensure proper operation prior to mating with the JPL Spacecraft Bus, after a storage period of approximately one week.

2. Description of Test

Before the start of the Subsystem Verification Test, some preliminary inspections and minor modifications of Flight Model III-2 were performed. These were:

- Spare Temperature Sensor Unit, Serial No. 7, was inspected with the cover off, and then replaced the original Temperature Sensor Unit, Serial No. 6, in the Subsystem;
- The 67-3/4 hour Clock plug was installed and torqued;
- The pressure-vessel covers of the F- and P-Channel Power Amplifier were removed to check their internal connectors for safety wiring. All communications coaxial connectors were found to be safety wired, including the connectors of the Resdel Intermediate Power Amplifiers (IPA). The covers were then replaced on the Power-Amplifier pressure vessels, and the Power Amplifiers and Dummy Load pressurized to 15 psi; and

- The TV Subsystem was mounted on the JPL Bus, and a camera-alignment check was performed by JPL personnel. The Subsystem was then demated and returned to its test stand.

The test sequence for the Subsystem Verification Test was the same as that described in Table A-2 for the Post-Shipment Electrical Test, with the following exceptions:

- Collimators were installed;

- The fields of view of all P-Cameras were illuminated simultaneously, eliminating the necessity to illuminate cameras individually with a light gun; and

- F-Channel Battery, Serial No. 85, with an open circuit voltage of 41.0 volts, and P-Channel Battery, Serial No. 76, with an open-circuit voltage of 40.9 volts, were installed in the TV Subsystem.

The test setup for the Subsystem Verification Test is shown in Figure A-7.

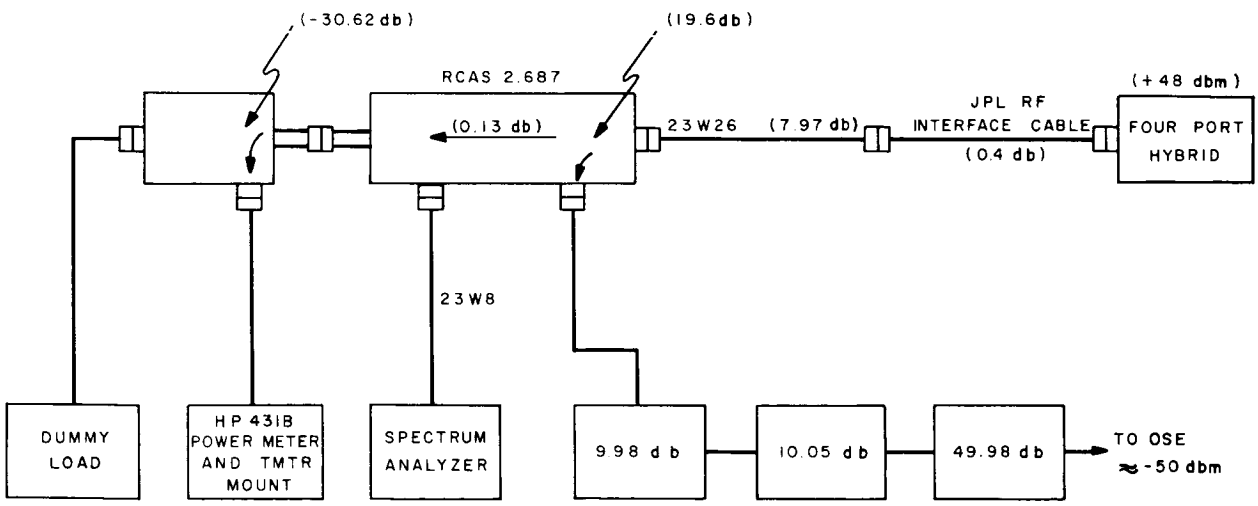

NOTE:
ATTENUATION FROM FOUR-PORT HYBRID TO POWER METER = 39.12 db
POWER METER CORRECTION FACTOR = 8.2×10^3

Figure A-7. Test setup for Subsystem Verification Test

3. *Test Evaluation*

a. Video Performance

The TV Cameras performed satisfactorily during this test. Several minor abnormalities were observed, but were not considered serious. Approximately 30 percent of the frames of 35-mm film recording of the P1-Camera video output exhibited noise spikes. Frame No. 202 (Figure A-8) showed a single line lost in the P2-Camera video output. Frame Nos. 68 and 132 (Figure A-8) showed single lines lost from the P4 Camera video output.

Although continuous tracking of the F-Channel video sync signal is now standard GSE procedure, the sync of F_a Camera was observed to tear during 35-mm frame Nos. 40, 42, 44 and 52 (see Figure A-9). It was determined that the GSE operator failed to track the d-c level to the required accuracy. The F_a-sync during this test showed an improvement over prior tests, but the peak white level of the F_b-Camera video output appeared lower than during previous tests, probably due to poor collimator alignment.

b. Communications Performance

The r-f power output was 50.5 watts after one minute of full-power operation, and peaked at 53.5 watts at T + 11-1/2 minutes. The r-f power output at the end of test was 52.2 watts. The input voltages to the F- and P-Channel Transmitter Power Supplies were 29.3 and 28.5 volts, respectively. These intput voltages were below the specified minimum of 29.5 volts, which accounts for the lower-than-normal r-f power output. The power profile during this test was normal.

c. Telemetry Performance

The telemetry obtained during the test indicated that the TV Subsystem performed normally, considering that the d-c input voltage to both channels was lower than specified.

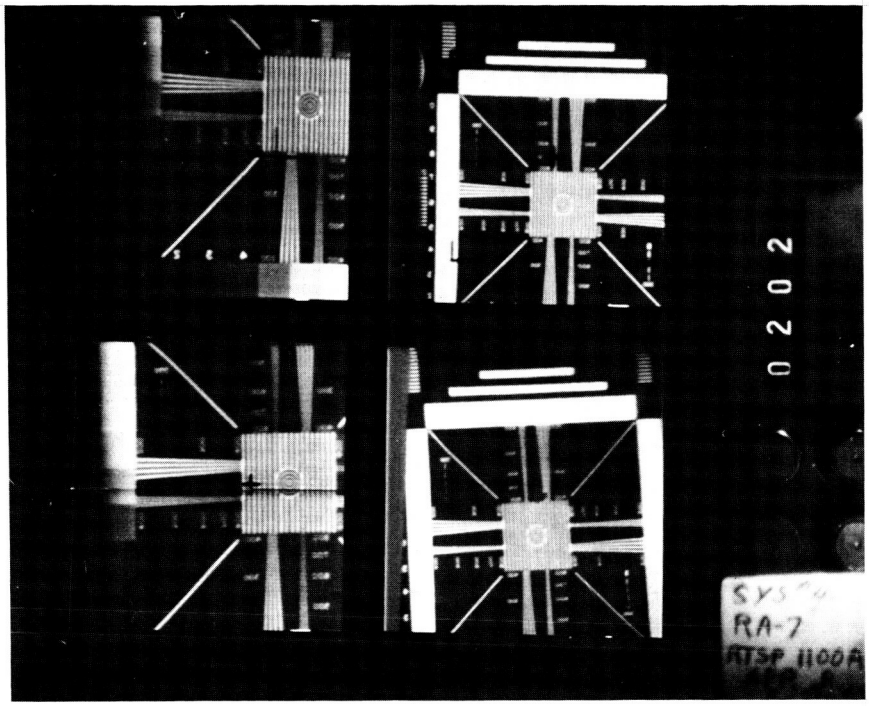

a. P2-Camera video output (Frame No. 202)

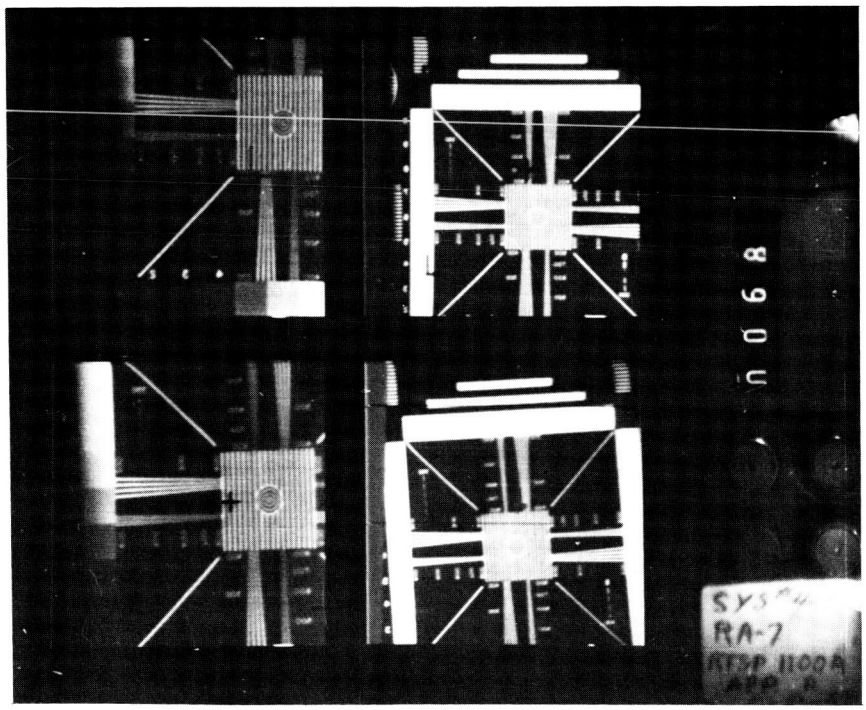

b. P4-Camera video output (Frame No. 68)

Figure A-8. Single Video lines of P-Camera outputs lost during Subsystem Verification Test

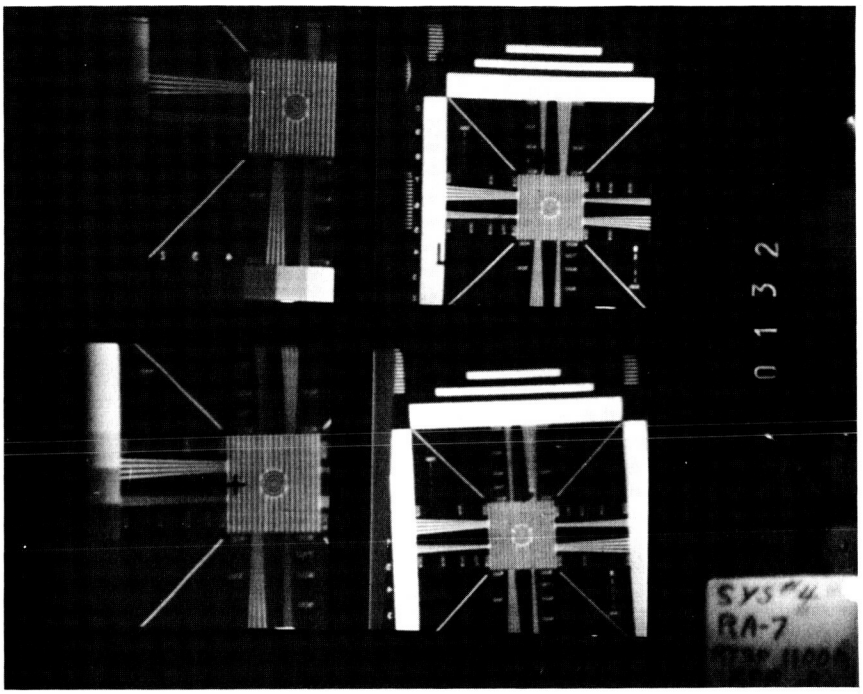

c. P4-Camera video output (Frame No. 132)

Figure A-8. Single video lines of P-Camera outputs lost during Subsystem Verification Test (Continued)

K. Pre-Thermal-Vacuum Verification Test (JPL Procedure 3R302.05)

The Pre-Thermal-Vacuum Verification Test was performed on May 24, 1964, with the TV Subsystem mated to the JPL Spacecraft Bus.

1. Purpose of Test

The Spacecraft had just been moved to the thermal-vacuum area and the reason for the Pre-Thermal-Vacuum Verification Test was to ensure that the system was still operable after transportation.

The Spacecraft was installed in the vacuum chamber and connected to the OSE through the vacuum-chamber bulkhead connectors. A second reason for this test was to verify that the proper connections had been made and that system operation was satisfactory prior to committing the Spacecraft to the simulated space environment.

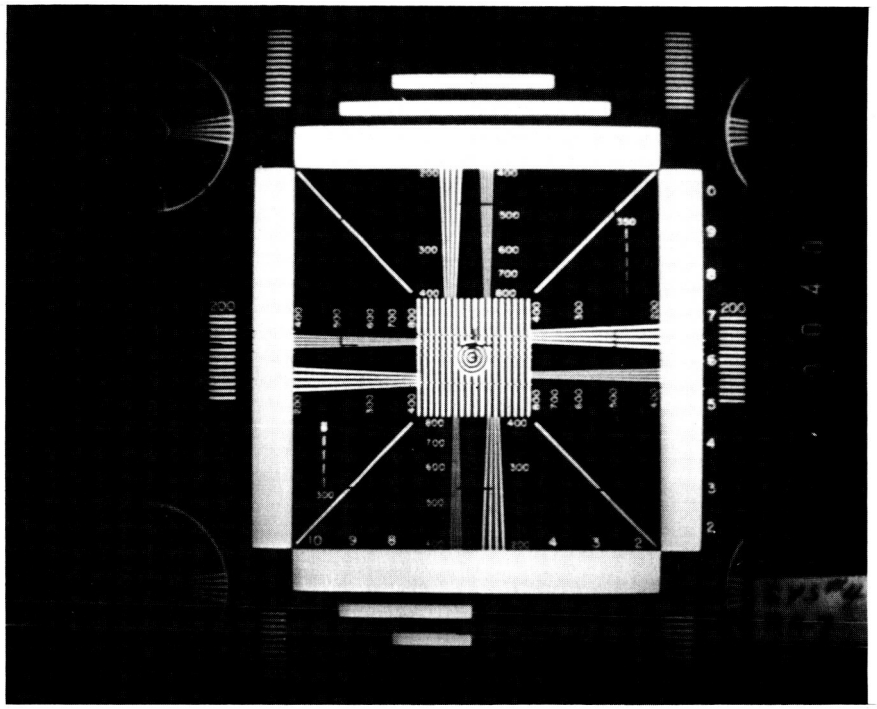

a. 35-mm Frame No. 40

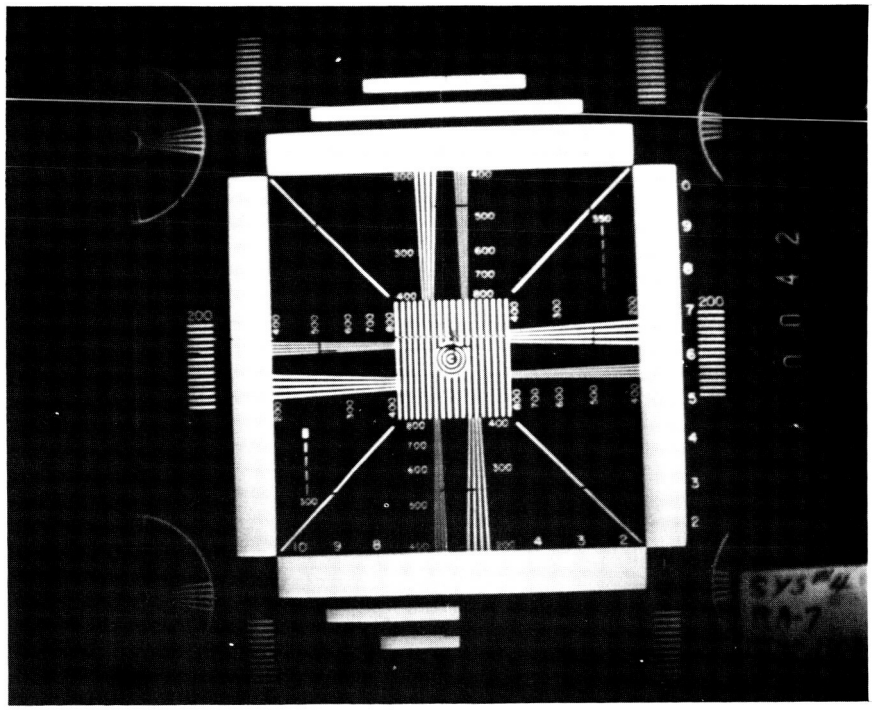

b. 35-mm Frame No. 42

Figure A-9. Sync tearing observed on F-Camera video output during Subsystem Verification Test

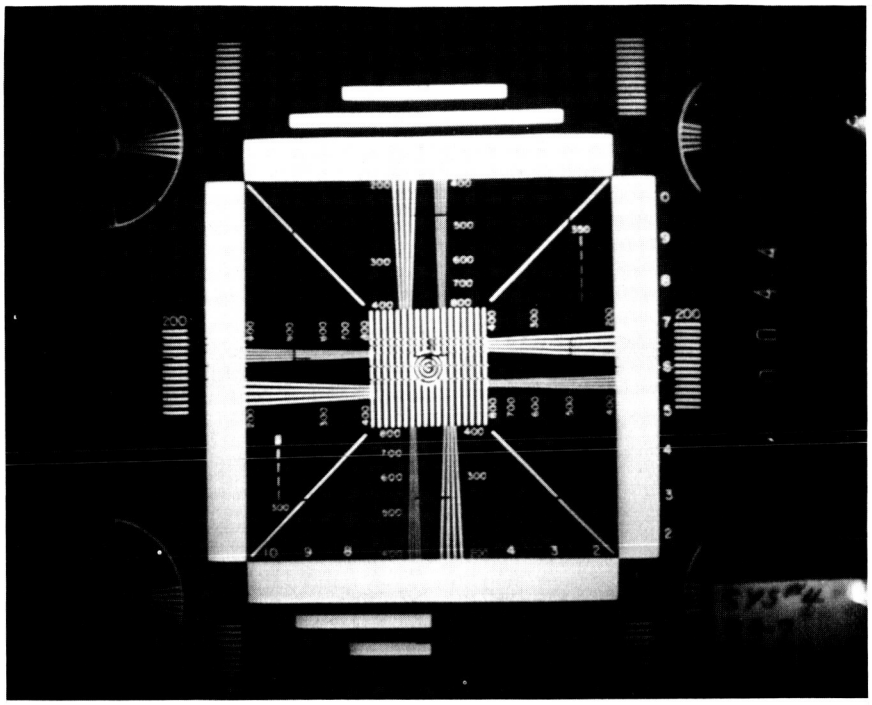

c. 35-mm Frame No. 44

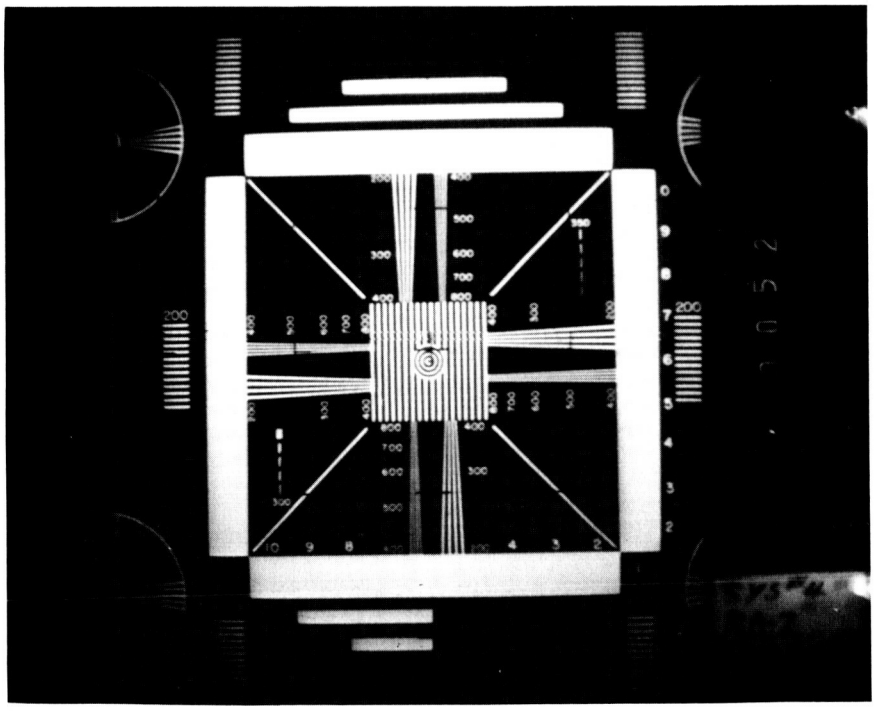

d. 35-mm Frame No. 52

Figure A-9. Sync tearing observed on F-Camera video output during Subsystem Verification Test (Continued)

2. *Description of Test*

For this test, collimators were installed on the TV Subsystem, and batteries were installed (P-Battery, Serial No. 76; F-Battery, Serial No. 85), although external power was used to operate the Subsystem equipments.

Prior to the start of tests, the battery-cell voltages were checked and measured as indicated in Table A-7.

Although JPL Procedure 3R 302.05 contains a complete test sequence wherein the Spacecraft is exercised at near space temperatures and vacuum environment, the purpose of this test is adequately served by performing only the electrical system tests described in that procedure. The procedures for this test are the same as those performed in the real environmental tests described in Paragraph L "Mission Verification Test Nos. 4 and 5." It should be noted that the tests were performed in rapid succession for this verification test, eliminating the indicated time intervals, but holding to the same sequence of events. The power measurement test setup for this test is shown in Figure A-10.

TABLE A-7

BATTERY-CELL VOLTAGES PRIOR TO START OF PRE-THERMAL-VACUUM VERIFICATION TEST

Battery	Cell Voltage (volts)		Total Battery Voltage (volts)
	Cell No.	Voltage	
F-Battery, Serial No. 76	3	1.75	
	4	1.81	39.95
	6, 10, 11		
	all others	1.86	
P-Battery, Serial No. 85	all	1.86	40.82

3. *Test Evaluation*

a. Video Performance

Examination of the 35-mm film of the video output received showed that noise spikes occurred in approximately 50 out of 400 frames of the P2-Camera video output. Noise spikes were also evident on two frames (Nos. 90 and 322) of P2-Camera

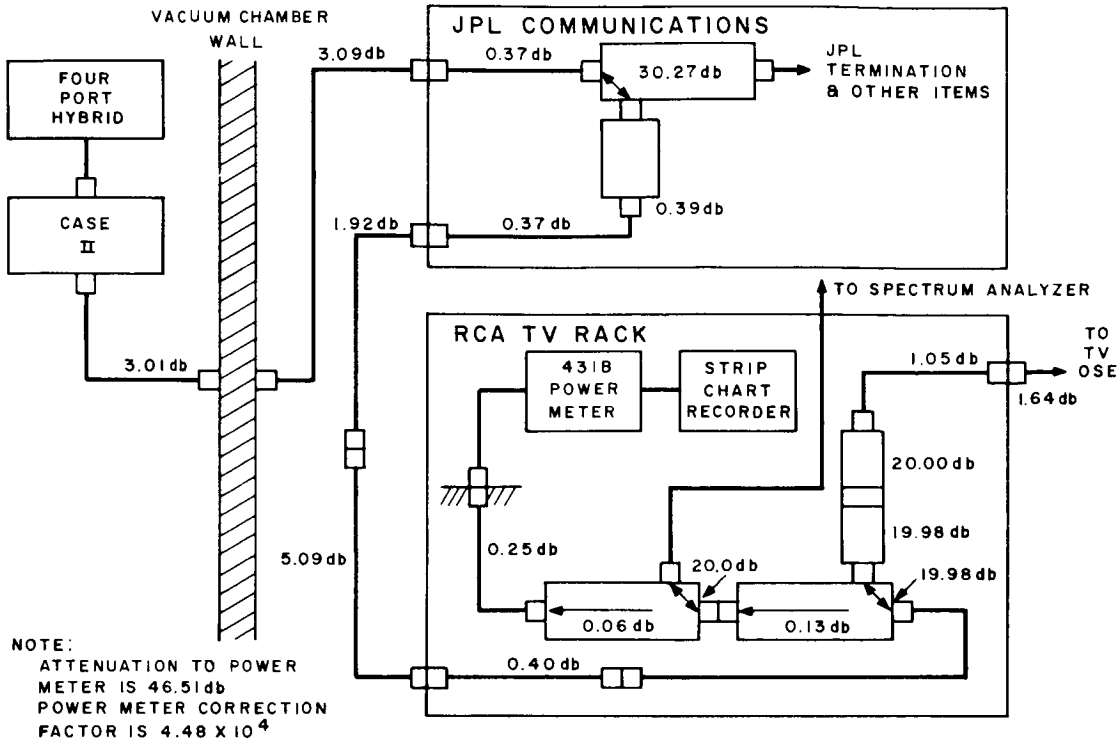

Figure A-10. Power measurement test set-up for the Pre-Thermal-Vacuum verification test

video output. Frame No. 90 is shown in Figure A-11. The P3-Camera video output showed a noise spot in the mask, which was shifting the d-c level in that region slightly toward white. Approximately 1 percent of the frames of P4-Camera video output exhibited severe microphonics induced by an F-shutter.

The F-Cameras performed normally. The video-output level of the F_b-Camera was slightly low as observed in previous tests, and there was some evidence of slight sync tearing on the video output of the F_a-Camera.

b. Communications Performance

The r-f output power was measured at 56.2 watts after two minutes of full-power operation. It remained at this level until 6 minutes of full-power operation had elapsed and then slowly decreased to 55.4 watts at the end of the 9-minute test. The input voltage to the Transmitter Power Supplies was 31.5 volts on both the F- and P-Channels.

Small flunctuations were observed in the r-f output power recording until C + 47 minutes (one minute of full-power operation).

The telemetry point for the cathode current of the P-Channel Power Amplifier indicated 3.0 volts or higher during this period. This is not an abnormal condition but an undesirable one, and could represent system degradation should consistent performance of this nature occur.

c. Telemetry Performance

All telemetry recorded during this test indicated that the TV Subsystem operated normally.

d. Conclusions

The objectives of this test were accomplished in that the initial performance conditions of the TV Subsystem were established prior to the start of the mission verification tests.

Battery-cell voltage were checked at the conclusion of the Pre-Thermal-Vacuum Test. The results are presented in Table A-8.

TABLE A-8
BATTERY-CELL VOLTAGES AT CONCLUSION OF PRE-THERMAL-VACUUM VERIFICATION TEST

Battery	Cell Voltage (volts)		Total Battery Voltage (Volts)
	Cell No.	Voltage	
F-Battery, Serial No. 76	3	1.68	
	4	1.81	39.89
	6, 10, 11	1.62	
	all others	1.86	
P-Battery, Serial No. 85	all cells	1.87	40.87

L. Mission Verification Test No. 4 (JPL Procedure 3R302.05)

Mission Verification Tests Nos. 4 and 5 were performed during the period from May 25, 1964 to May 31, 1964. For these tests, the TV Subsystem was mated to the JPL

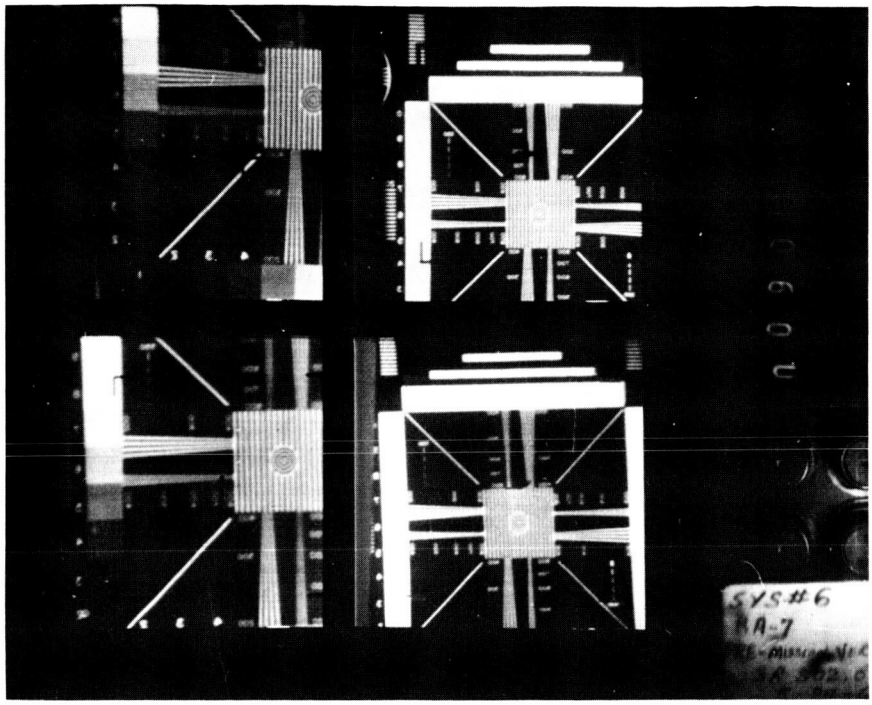

Figure A-11. P2 Camera video output showing noise spikes (35-mm frame No. 90)

Spacecraft Bus. Power for operation of the Subsystem equipments was provided by an external power source, although batteries were installed in the Subsystem. The test sequence and evaluation of Mission Verification Test No. 5 is described in Paragraph M.

Mission Verification Test No. 4 (thermal-vacuum) initially commenced on May 24, 1964. Soon afterward, however, the Test Director decided to return the vacuum chamber to ambient and break vacuum because of a gas leak in the Attitude Control System. The Clock was turned off by a Cruise Test command, and cruise mode was turned off. Power was also removed from the TV Subsystem.

The gas leak was traced to an improperly attached hose in the Pressure Instrumentation System. Test preparations were resumed on May 25, 1964.

1. Purpose of Test

The purpose of the Mission Verification Tests was to functionally test the Ranger Spacecraft as an integrated electronic system while operating in a near space vacuum and temperature environment.

This test series had the following prime objectives:

- To detect all system interactions that may result from operation in a normal flight sequence while exposed to a space environment;
- To demonstrate that the Spacecraft is capable of operating for an extended period of time as required during the assigned mission; and
- To evaluate the long-term operation of electronic and mechanical subsystems in a modified flight sequence.

2. *Description of Mission Verification Test No. 4*

As the first test to be performed, Mission Verification Test No. 4 was a real-time mission at higher-than-average payload temperature (+37°C).

The test was based on a nominal mission; that is, most backup functions were not checked, and expected signal-strength levels were adjusted prior to the midcourse and terminal phases when commands were sent to the Spacecraft. At the end of the high-temperature test, the Spacecraft was recycled to the pre-launch mode, and the Spacecraft temperatures adjusted to lower values for Mission Verification Test No. 5. Spacecraft power was not turned off between tests nor was the vacuum-chamber pressure or chamber-wall temperature changed.

The power-measurement configuration for this test was similar to that used in the Pre-Thermal-Vacuum Verification Test, shown in Figure A-10.

The test sequence for Mission Verification Test No. 4 is presented in Table A-9.

TABLE A-9
MISSION VERIFICATION TEST NO. 4 TEST SEQUENCE

Time	Operation Function
	Launch Phase
	Spacecraft external power turned on. OSE F- and P-Channel Power Supplies set to 36.0 vdc, and Power Select On switch activated.
A-5'	Cruise On Test (Clock off) switch depressed twice. Reception of 15-point telemetry verified via strip-chart recorder.
A=0	Simulated launch start.
A+1'	Squib firing assembly armed.
A+33' 40"	Simulated Spacecraft separation.

TABLE A-9

MISSION VERIFICATION TEST NO. 4 TEST SEQUENCE (Continued)

Time	Operation Function
	Terminal Phase (RTC-7)
C+42'	Collimators turned on.
C+43'	Full-power operation selected at OSE.
C+44'	F- and P-Channel Warmup activated by RTC-7F and RTC7-P commands. Channel-8 telemetry switches from 15-point telemetry to 90-point telemetry.
	Full-scan video observed hardline at the Video Combiner by test video cable.
	Terminal Phase (Clock Turn-On)
C+38'	TV collimators turned on.
C+39'	Full-power operation selected at OSE.
C+40'	F-channel warmup mode activated by Clock turn-on
C+41' 20"	F-channel full-power mode activated by Sequencer turn-on.
	F-channel video verified and recorded on 35-mm film. Polaroid and 35-mm pictures of F_a- and F_b-Camera video output taken.
C+44'	P-Channel warmup mode activated by RTC-7P command.
C+45' 20"	P-Channel full-power mode activated by Sequencer turn-on.
C+46'	Polaroid and 35-mm pictures of P-Camera video outputs taken.
C+49'	Polaroid and 35-mm pictures of P-Camera video outputs (black field) taken.
C+50'	Polaroid and 35-mm pictures of F_a- and F_b-Camera video output (black field) taken.
	Collimators turned-on and black-field procedure repeated with TV fields illuminated.

TABLE A-9 MISSION VERIFICATION TEST NO. 4 TEST SEQUENCE (Continued)	
Time	Operation Function
	Terminal Phase (Clock Turn-On) (Cont)
C+53'	F- and P-Channels of Sequencer reset. TV Subsystem remains in full-power operation, indicating that the TV-3 override function of the Sequencer is effective.
C+54'	F- and P-Channels returned to warmup mode by TV-2 and TV-3 hold-on commands.
C+55' 10"	Cruise Test mode activated; Channel - 8 telemetry turned-off. Subsystem Power remains on. End of Mission Verification Test No. 4.

3. *Test Evaluation*

a. Video Performance

Noise spikes were observed in approximately 10 percent of the 35-mm frames of P1-Camera video output received during this test. This represented a reduction in noise from the previous tests. A slight increase in mesh noise was evident in the video output of the P2- and P4-Cameras, and was probably due to the high operating temperature. The spot in the mask of P3-Camera increased (toward white) the clamp level in the region of the spot. This effect was observed only at high temperature, and was considered an acceptable departure from normal TV Subsystem performance.

A slight increase in 15-kc noise occurred in the F_a-Camera video output exhibited a slight white video level of the F_b-Camera was slightly below normal. The increase in 15-kc noise was considered an effect produced by the high operating temperature. The low value of the F_b-Camera white level had been observed during previous testing.

At the OSE, the monitor presentation of the F-Camera video output exhibited a slight bounce which was not completely taken out by the kinescope clamp circuit. It was later determined that this was caused by the failure of one of the OSE power supplies. An additional OSE problem encountered during this test was that the data display clock was not illuminated on the 35-mm film. This was attributed to the failure of the lamp-drive circuit for the clock lamp.

b. Communications Performance

The r-f power output profile for this test is presented in Table A-10.

TABLE A-10
RF POWER OUTPUT PROFILE FOR MISSION VERIFICATION TEST NO. 4

Time (minutes)	RF Power Output (watts)	Input to Transmitter Power Supplies (volts)	
		F-Channel	P-Channel
C+41	27.0	30.9	-
42	28.2	30.9	-
43	29.5	30.9	-
44	31.5	30.85	-
45	31.5	30.86	-
46	60.0	30.9	30.58
47	59.0	30.86	30.57
48	59.0	30.86	30.56
49	59.0	30.85	30.53
50	59.0	30.84	30.5
51	58.5	30.89	30.5
52	58.0	30.89	30.5
53	57.2	30.89	30.5
54	57.2	30.89	30.55

c. Telemetry Performance

All telemetry data recorded during this test indicated that the TV Subsystem performance was normal.

At the conclusion of Mission Verification Test No. 4, the battery cell voltages were checked. The results of this measurement are presented in Table A-11.

TABLE A-11 BATTERY-CELL VOLTAGES AT CONCLUSION OF MISSION VERIFICATION TEST NO. 4			
Battery	Battery Cell Voltages (volts)		Total Battery Voltage (volts)
	Cell No.	Cell Voltage	
F-Battery	17	1.50	
	all other cells	1.57	34.55
P-Battery	all cells	1.495	34.60

M. Mission Verification Test No. 5 (JPL Procedure 3R302.05)

Mission Verification Test No. 5 was started on May 28, 1964, immediately following conclusion of Mission Verification Test No. 4, and was completed on May 31, 1964.

1. Purpose of Test

This test had the same objectives as Mission Test No. 4, but was performed under different temperature conditions.

2. Description of Test

This test was performed in real mission time at a lower-than-average payload temperature of +10°C. The test sequence for the Mission Verification Test No. 5 is presented in Table A-12.

3. Test Evaluation

a. Video Performance

Noise spikes were exhibited in approximately 25 percent of the 35-mm frames of P1-Camera video output recorded during the test. The video output of all other cameras was particularly free of noise, due to the low operating temperature.

TABLE A-12 MISSION VERIFICATION TEST NO. 5 TEST SEQUENCE	
Time	Operation Function
C+42'	Collimators turned on.
C+43'	Full-Power operation selected at OSE.
C+45'	F- and P- Channel warmup mode activated by CC & S Warmup command.
	Video signals were observed hardline at the output of the Video Combiner with a video test cable.
C+46'20"	F- and P-Channel full-power mode activated by 80-second timer output pulse from Sequencer. F-Channel video output recorded on 35-mm film. Two Polaroid pictures of F_a - and F_b-Camera video output taken.
	P-Channel video output recorded on 35-mm film. One Polaroid of the video output of each P-Camera taken.
C+51'30"	Collimators turned off and Polaroid and 35-mm pictures of the P-Camera video output (black fields) taken.
C+53'	Switched to F-channel and Polaroid and 35-mm pictures of F-Camera video output (black fields).
C+54'30"	F- and P-Channels of the Sequencer reset. Continued full-power operation verified, indicating the effectiveness of the CC & S full-power override function of the Sequencer.
C+55'	Subsystem reset to warmup mode by switching CC & S Warmup and Full-Power Hold On Commands.
C+55'23"	TV Subsystem turned-off by RTC-5 switch.
	End of Mission Verification Test No. 5

The d-c video level of the F_b-Camera was approximately 100 mv lower than normal; this was expected, based on the results of previous tests.

b. Communications Performance

The r-f power output profile recorded during this test is presented in Table A-13.

TABLE A-13 RF POWER OUTPUT PROFILE DURING MISSION VERIFICATION TEST NO. 5			
Time	RF Power Output (watts)	Input to Transmitter Power Supplies (watts)	
		F-Channel	P-Channel
C+42'	16.0	29.7	-
43'	13.7	29.7	-
44'	16.0	29.7	-
45'	17.7	29.7	-
46'	21.2	29.7	-
47'	55.0	29.7	29.0
48'	55.8	29.7	28.9
49'	55.8	29.7	28.9
50'	56.5	29.7	28.9
51'	56.5	29.7	28.9
52'	56.5	29.7	29.0
53'	56.2	29.7	29.0
54'	56.2	29.8	29.0

The F-Channel r-f power output was below the specified minimum value of 19.5 watts after 2 minutes of full-power operation. This condition was primarily attributed to two causes:

- F-channel was tuned to rise more slowly in output power in order to hold power for a mission of one hour. The power rise is slower for a colder ambient temperature; and

- The battery voltage was marginally low on F-channel (29-7 volts at the input to the Transmitter Power Supply).

Also, the telemetry for the cathode current of the F-Channel Power Amplifier indicated that the power output of the F-Channel Power Amplifier was below normal.

c. Telemetry Performance

All telemetry data recorded during this test indicated normal TV Subsystem performance.

d. Post-Test Measurements

At completion of Mission Verification Test No. 5, the battery ampere-hours for Mission Verification Tests Nos. 4 and 5 were calculated to be 26.1 ampere-hours for the P-Battery (Serial No. 76), and 14.1 ampere-hours for the F-Battery (Serial No. 85).

The Spacecraft was removed from the vacuum chamber on June 2, 1964. Collimators were removed from the TV Subsystem, and the Subsystem was demated from the Spacecraft Bus. After the TV Subsystem was mounted on a tillstand, Batteries, Serial Nos. 76 and 85, were removed and Batteries, Serial Nos. 87 and 84, installed. The shrouds were removed and pressure checks performed with the following results:

Unit	Pressure
• Dummy Load, Serial No. 024	13.2 psi
• F-Channel Power Amplifier, Serial No. 011	16.0 psi
• P-Channel Power Amplifier, Serial No. 021	14.9 psi

N. Special TV Subsystem Test (RTSP 1100A, Appendix G)

This test was performed on June 8, 1964, The TV Subsystem was not mated to the JPL Spacecraft Bus for the test.

1. Purpose of Test

The Special TV Subsystem Test was performed to ascertain that the TV Subsystem was still operable after several components had been removed for inspection and

modifications, and then replaced. The F- and P-Channel High Current Regulators, Serial Nos. 10 and 14, and the Temperature Sensor Unit, Serial No. 007, were removed on June 1, 1964 and were reinstalled on June 2, 1964.

2. Description of Test

The Special TV Subsystem Test employed an external power source to operate the Subsystem equipments. The power-measurement setup for the test presented in Figure A-12.

The test sequence for the Special Subsystem Test is given in Table A-14.

3. Test Evaluation

a. Video Performance

Noise spikes were evident in approximately 20 percent of the 35-mm frames of P1-Camera video output. The video output of all other P-Cameras was normal, in that it was free of noise. No evaluation of resolution could be made since collimators were not employed in this test.

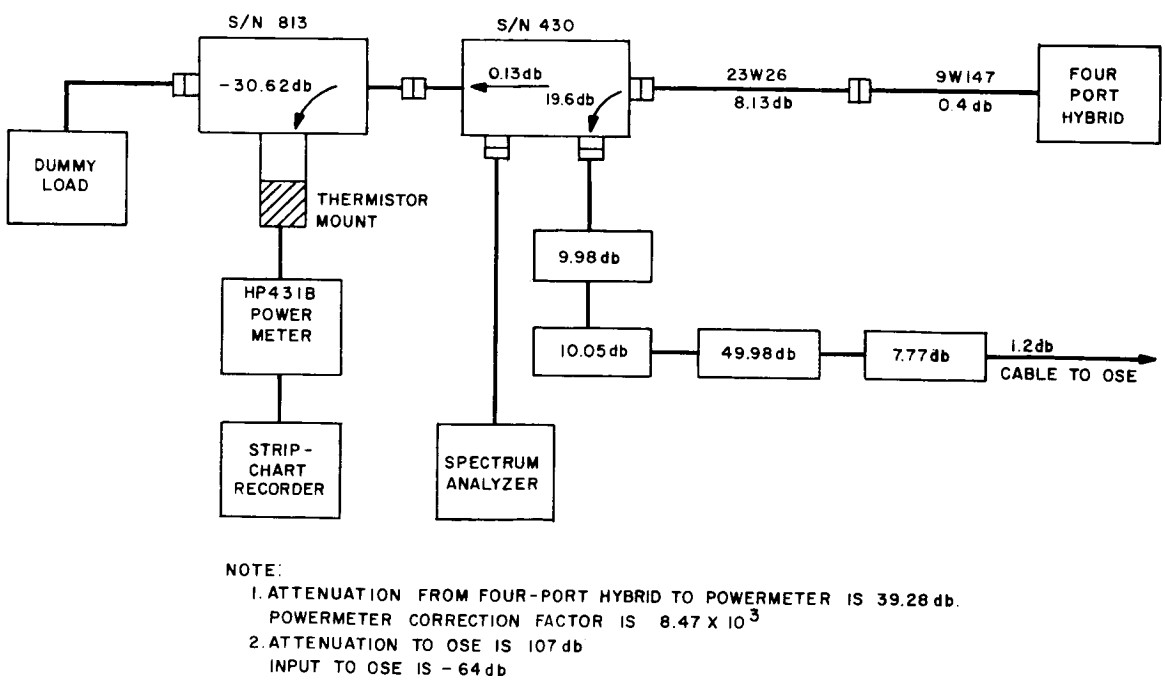

Figure A-12. Power-measurement test setup for special subsystem test

TABLE A-14 SPECIAL TV SUBSYSTEM TEST SEQUENCE	
Time	Operation Function
T+0'	External power applied to TV Subsystem.
T+1'	Cruise mode activated by Cruise On Test switch.
T+2'	F-Channel warmup mode activated by RTC-7F switch.
T+3'20"	F-Channel full-power mode activated by output from Sequencer.
T+8'	Polaroid picture of F_a- and F_b-Camera output video taken, using a light box as the video source.
T+10'40"	P-Channel warmup mode activated by RTC-7P switch.
T+12'	P-Channel full-power mode activated by output from Sequencer
T+17'	TV Subsystem returned cruise-mode operation by RTC-5 command. Subsystem turned off by Cruise-Off Test switch.

Approximately 100 mv of mesh noise existed on the last 2 percent of the 35-mm frames of F_b-Camera video output. It was determined that this condition had always existed in the F_b-Camera, and although it was not desirable, it did not constitute a failure mode.

b. Communications Performance

The r-f power output was 26.3 watts after 2 minutes of full-power operation, with only the F-Channel operating at this time. The input voltage to the F-Channel Transmitter Power Supply was 29.5 volts. At T + 7 minutes (4 minutes of full-power operation), the input voltage to the F-Channel Transmitter Power Supply was increased to 31.0 volts, resulting in an attendant increase in r-f power output to 29.6 watts from 27.1 watts.

The r-f power output was 54.2 watts at T + 13' (2 minutes after P-Channel full-power operation). At termination of the test (T + 17 minutes), the r-f power output was 55.7 watts.

c. Telemetry Performance

All telemetry data recorded during the Special Subsystem Test indicated that the Subsystem performance was normal.

4. Post-Test Measurements

Upon completion of the Special Subsystem Test, the shrouds were installed on the TV Subsystem, and the cell voltages of the Batteries measured. These are listed in Table A-15.

TABLE A-15
CELL VOLTAGE OF BATTERIES MEASURED AFTER SPECIAL SUBSYSTEM TEST

Battery	Battery-Cell No.	Voltage (volts)
F-Battery	1 to 8	1.62
	9 to 10	1.85
	11 to 22	1.62
P-Battery	all cells	1.86

Upon completion of the Special Subsystem Test, the shrouds were installed on the TV Subsystem, and the cell voltages of the Batteries measured. These are listed in Table A-15.

The TV Subsystem was mated to the Spacecraft Bus and placed in the thermal-vacuum chamber in preparation for the Space Simulator Functional Checkout.

O. Space Simulator Operational Checkout; Pre-Countdown Phase (JPL Procedure 3R320.01)

This test was performed on June 8, 1964, with the TV Subsystem mated to the Spacecraft Bus.

1. Purpose of Test

The Space Simulator Operational Checkout is an accelerated-mission simulation to verify that all equipment of the Spacecraft operates properly. All communications

with the Spacecraft is accomplished through r-f link, with all but necessary OSE and ground cables disconnected after simulated Spacecraft separation.

This pre-countdown phase accomplishes the test objectives on the basis of a non-space environment (chamber door open) to demonstrate operational capability of the Spacecraft before committing the system to the space environment. The test is then repeated to demonstrate similar performance in near space conditions (vacuum-chamber closed). This is referred to as the Terminal Phase and is described in Paragraph P.

2. *Description of Test*

The test configuration for the Space Simulator Functional Checkout is shown in Figure A-13.

The Pre-Countdown Phase of the test is performed on an accelerated basis wherein all steps are in proper sequence, but no time delays are inserted between steps to simulate actual mission intervals.

The test on the Spacecraft is performed in four distinctive parts as follows:

(1) Preliminary preparations for the test ensure that all equipment (spacecraft and test) are properly calibrated and operating, and that the Spacecraft (bus and TV Subsystem) is in the proper configuration for the start of test;

(2) Spacecraft pre-launch and simulated-launch operations are completed at this time. Telemetry measurements of the Spacecraft are monitored throughout the test. This part is performed as follows:

- The Spacecraft is controlled from the blockhouse trailer until A=O (Separation);
- The separation connectors are removed and the special P1 relay box is installed; and
- The Spacecraft is then commanded through a flight sequence.

(3) The midcourse phase of the test includes a midcourse maneuver and return to cruise mode; and

(4) The terminal mode is performed and the TV Subsystem is commanded through sequence to checkout all of its functions.

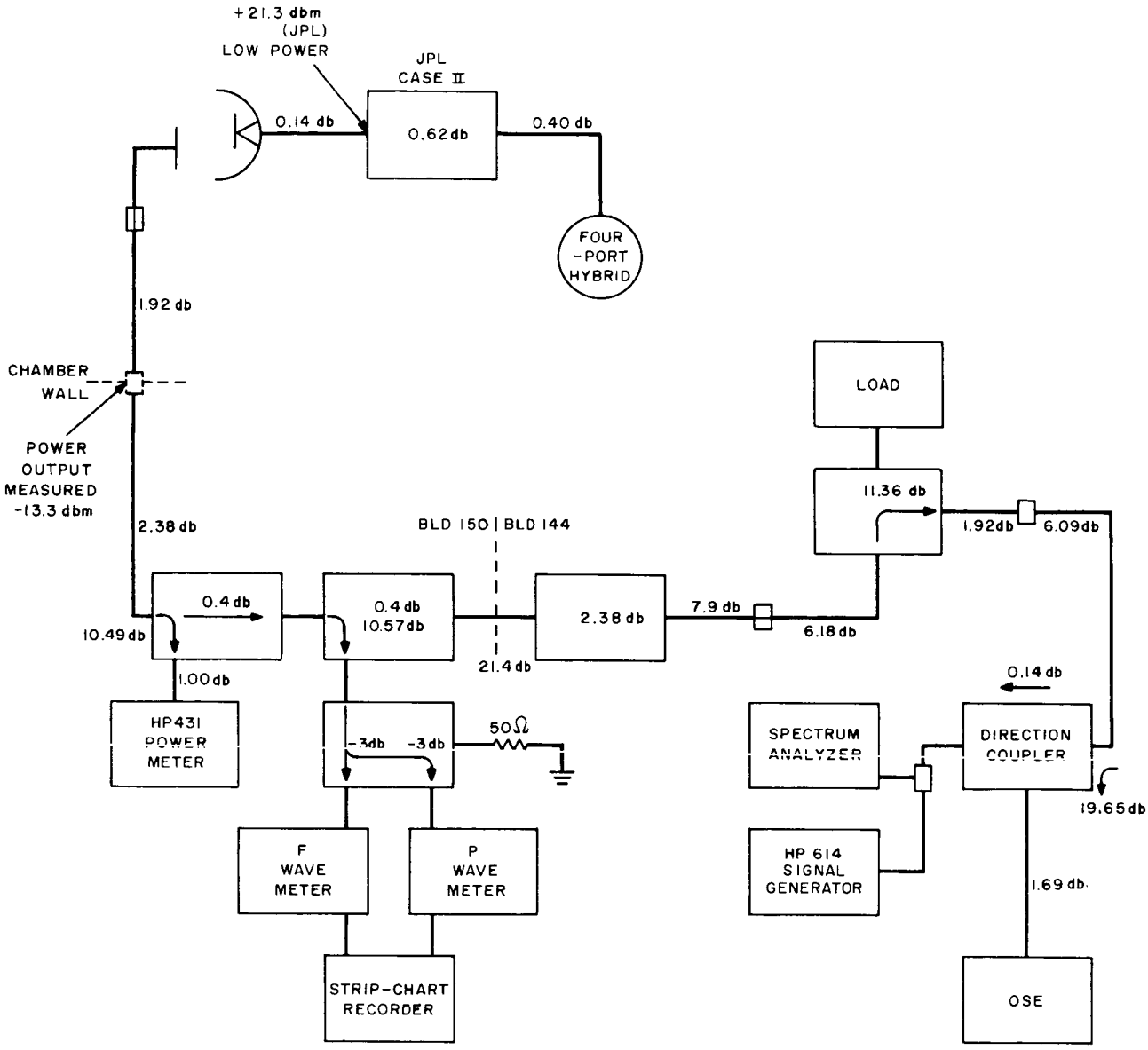

NOTES:

1. ATTENUATION FROM FOUR-PORT HYBRID TO SPECTRUM ANALYZER IS 95.57 db
2. ATTENUATION TO WAVEMETERS IS 35.00 db
3. ATTENUATION TO POWER METER IS 49.49 db. POWER METER CORRECTION FACTOR IS 8.9×10^4

Figure A-13. Spacecraft test configuration

The Pre-Countdown phase of the test is performed at a nominal temperature of 85° F at the Spacecraft Bus, and 78° F at the TV Subsystem. The test sequence for the terminal-mode portion of the Pre-Countdown phase, where the TV Subsystem is exercised, is presented in Table A-16.

3. Test Evaluation

a. Video Performance

Very fast noise spikes were observed in approximately 30 percent of the 35-mm frames of P1-Cameras video output recorded during the test. The video output of the P2-Camera exhibited more noise than observed in previous tests. Approximately 10 percent of the 35-mm frames of P2-Camera video output contained noise spikes.

Radio-frequency interference was noted in the video output of the P3-and F_b-Cameras, and was probably due to reflected r-f power being detected in the Cameras. All other cameras appeared to function normally.

b. Communications Performance

The r-f power output was 62.1 watts after 2 minutes of full-power operation, and increased to 63.3 watts at the end of the 7-minute test. The r-f power recording showed fluctuations at the camera rates, which probably were the result of the detected radio-frequency interference. The input to the F- and P-Channel Transmitter Power Supplies at the end of the test was 28.5 volts.

c. Telemetry Performance

Noise was observed on the telemetry outputs of the F- and P-Channel 225-kc Voltage Controlled Oscillators. The noise appeared to be synchronous with the camera operations, indicating that it was rfi induced.

The Channel 8 telemetry recorded was normal and indicated normal TV Subsystem performance.

TABLE A-16 TEST SEQUENCE FOR TERMINAL-MODE PORTION OF PRE-COUNTDOWN PHASE OF SPACE SIMULATOR OPERATIONAL CHECKOUT	
Time	Operation Function
C=O	Clock Start
C+42'	TV Cameras illuminated
C+45'	F- and P-Channel warmup mode activated by CC & S warmup command. Channel 8 output switches from 15-point to 90-point telemetry.
C+46'	Power output recording starts.
C+46'20"	F- and P-Channel full-power mode activated by TV Sequencer output Video output of F-Channel recorder 35-mm film One Polaroid picture of F_a- and F_b-Camera video output taken.
C+48'30"	35-mm film recorder switched to P-Channel and P-Channel video output recorded. Also, one Polaroid picture of P-Channel video output taken.
C+51'30"	Camera illumination turned off. 35-mm pictures and one Polaroid picture of P-Channel video output taken (black field).
C+52'	35-mm film recorder switched to F-Channel and 35-mm pictures of F-Channel video output (black field) taken. Also, one Polaroid each of F_a- and F_b-Cameras video output (black field). Camera illuminated turned on and black-field sequence repeated, taking pictures of illuminated field in this case.
C+55'23"	F- and P-Channels turned off by RTC-5 command. End of Test.

d. Conclusions

The rfi problems experienced were not considered an abnormality or malfunction of the TV Subsystem, since these problems were the result of test conditions and were anticipated.

P. Space Simulator Operational Checkout; Terminal Phase (JPL Procedure 3R320.01)

The Terminal Phase of the Space Simulator Operational Checkout was performed on June 9, 1964, with the TV Subsystem mated to the JPL Spacecraft Bus.

1. Purpose of Test

The purpose of the Terminal Phase is exactly the same as the Pre-Countdown Phase described in Paragraph O, with the exception that the test is performed at near-space environment. This test is also performed on an accelerated-operation basis; however, proper time is taken to exhaust the vacuum chamber.

2. Description of Test

The description of this test is the same as that for the Pre-Countdown Phase described in Paragraph O. The test sequence for the TV Subsystem is described in Table A-16. The test configuration is the same as shown in Figure A-13.

3. Test Evaluation

a. Video Performance

Fast noise spikes were observed in the P1-Camera video output, similar in quantity to that observed during the Pre-Countdown Phase of the test. The video outputs of all other P-Cameras appeared to be normal. Slight radio-frequency interference (rfi) was suspected in the video output of the P3-Camera; however, identification could not be confirmed.

The video output of the F_a-Camera contained very-low-level diagonal lines which appeared to be rfi induced (possibly slight defocussing of the vidicon). The F_b-Camera video output contained severe radio-frequency interference, as previously observed. As noted in the Pre-Countdown Phase, the rfi is probably due to stray r-f radiation in the closed vacuum chamber.

b. Communications Performance

The r-f power output was 65.0 watts after 2 minutes of full-power operation, peaked at 69 watts after 7 minutes of full-power operation, and gradually decreased to 65 watts at the end of the 10-minute test. Slight fluctuations that appeared in the r-f power recording were probably rfi induced. The input voltages to F- and P-Channel Transmitter Power Supplies were 27.5 and 28.2 volts, respectively.

c. Telemetry Performance

Several telemetry values were not within their specified limits, probably as a result of low-battery voltage. A check of the cell voltages of the Batteries show that each F-Battery cell was 1.60 volts, and each P-Battery cell was 1.62 volts -- both below normal voltage.

All calibrated telemetry points indicated that the TV Subsystem performance was normal.

d. Conclusions

The problems resulting from the low Battery voltages and radio-frequency interference were anticipated. No abnormalities, other than those expected, were observed.

Q. Explosive-Safe Area Test No. 1 (JPL Procedure 3R235.00)

This test was performed on June 10, 1964 with the TV Subsystem mated to the JPL Spacecraft Bus.

1. *Purpose of the Test*

The purpose of this test was to educate Spacecraft test personnel in the procedure for determining the effect of TV full-power radio-frequency (960 mc) on the pyrotechnics to be installed in the midcourse-propulsion system of the Spacecraft at ETR. This "dry run" also provided an opportunity to verify the test procedure in advance of the actual pyrotechnics installation.

2. *Description of Test*

During this test, the high-power, TV radio-frequency signal was radiated from the Spacecraft high-gain antenna, which is nested under the Spacecraft Bus, into "Echo-sorb" material located directly in line with the directional antenna. The test sequence performed for this test is presented in Table A-17.

The test setup for ESA Test No. 1 is shown in Figure A-14.

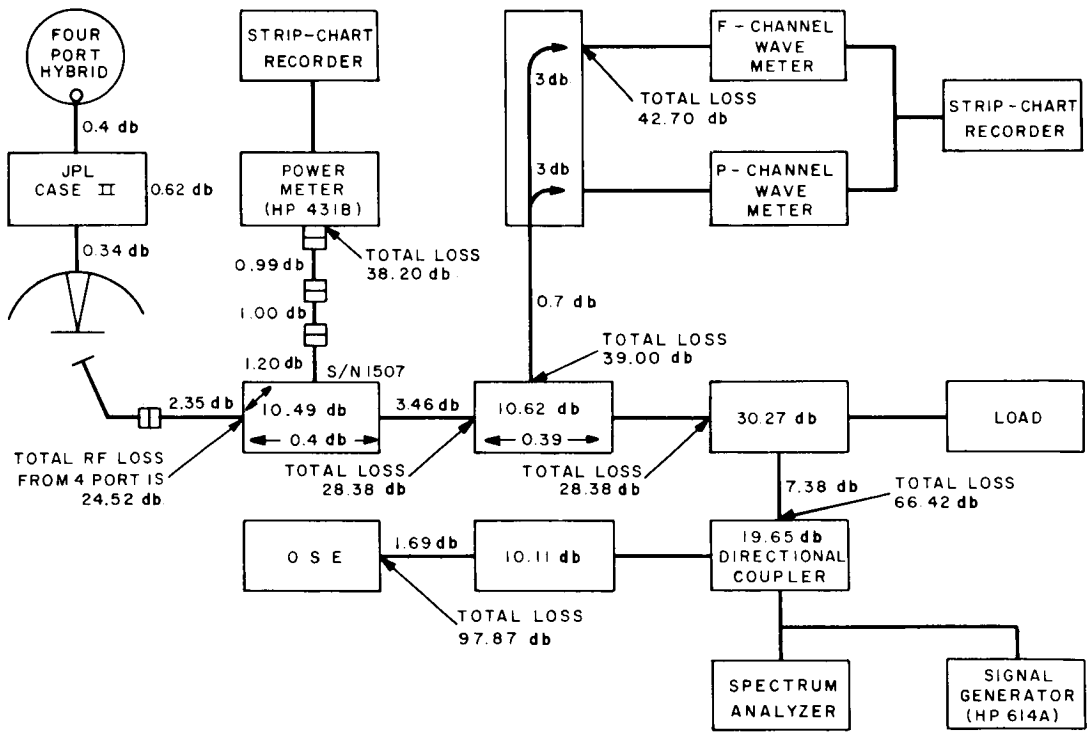

Figure A-14. Radio frequency test connections for ESA test No. 1

TABLE A-17 ESA TEST NO. 1 TEST SEQUENCE	
Time	Operation Function
T-5'	Cruise mode activated and the SCR gate circuits in the High-Current Voltage Regulators enabled by Cruise on Test switch.
T+0	F- and P-Channels turned on in warmup mode by RTC - 7F and RTC-7P command.
T+1'20"	F- and P-Channels full-power mode activated by 80-second timer output from TV Sequencer. 35-mm and Polaroid pictures taken of the video output from the F_a- and F_b-Cameras.
T+8'	35-mm film recorder switched to P-Channel, and 35-mm and Polaroid pictures taken of the P-Channel video output.
T+16'	F- and P-Channel turned off by RTC-5 command. Power removed from TV Subsystem.

3. Test Evaluation

a. Video Performance

The video output of the P1-Camera exhibited fast noise spikes in approximately 30 percent of the 35-mm frames recorded. All other cameras functioned normally, and the quality of their performance remained stable.

b. Communications Performance

The r-f power output was 64.7 watts after one minute of full-power operation, and peaked at 68.0 watts after 5 minutes of full-power operation. At the end of the 10-minute test, the r-f power output was 66.0 watts. The input voltage to the F- and P-Channel Transmitter Power Supplies during the test was 32.2 and 32.0 watts, respectively.

c. Telemetry Performance

All telemetry data recorded during the test indicated that the TV Subsystem performance was normal.

d. Conclusions

All objectives of ESA Test No. 1 were accomplished and the TV Subsystem was prepared for ESA Test No. 2.

R. Explosive-Safe Area (ESA) Test No. 2 (JPL Procedure 3R325.00)

This test was performed on June 10, 1964, with the TV Subsystem mated to the JPL Spacecraft Bus.

1. Purpose of Test

During ESA Test No. 1, radio-frequency interference (rfi) appeared in the video-output displays, so the test was repeated, as ESA Test No. 2, to determine the effect that varying the pointing angle of the high-gain antenna would have on the radio-frequency interference.

2. Description of Test

For this test, the high-gain antenna was detached from its drive mechanism so that it could be easily maneuvered through its rotational limits. The test sequence is the same as used in ESA Test No. 1 and is described in Table A-17.

3. Test Evaluation

a. Video Performance

Fast noise spikes were observed in approximately 20 percent of the 35-mm frames of video output from the P1-Camera; this was an appreciable improvement over the results in ESA Test No. 1. The video output from all other cameras was normal.

b. Communications Performance

The r-f link was not calibrated for this test because of the variations in power loss expected between the high-gain antenna and the pickup probe. However, measurement of the relative amplitude of the r-f signals was made and is presented in Table A-18.

TABLE A-18
RELATIVE AMPLITUDE OF RF SIGNALS RECORDED DURING ESA TEST NO. 2

Time	Measured Amplitude of RF Signals (dbm)		
	F-Channel	Spacecraft Beacon	P-Channel
C + 46' 30'	-45.0	-65	-42.0
49'	-40.5	-63	-40.5
51'	-43.0	-66	-43.0
T + 3'	-40.0	-	-40.0
4'	-50.0	-70	-50.0
8'	-45.0	-70	-52.0

It is evident from the data of Table A-17 that there was an apparent variation in the relative amplitudes of the F- and P-Channel carrier signals. This variation was attributed to the test setup, and particularly to the fact that the probe antenna was not within the beam width of the radiating antenna. The probe was detecting signals from the back lobes of the directional antenna which presents an apparent bandwidth problem.

There was no evidence of rfi observed during this test, indicating that it is not a problem when the high-gain antenna is radiating into free space or a good microwave absorber.

Several r-f dropouts were observed at the OSE as the antenna hinge angle was varied. This was caused by r-f nulls resulting from the relative positions of the high-gain antenna and probe.

c. Telemetry Performance

All telemetry data recorded during this test indicated normal TV Subsystem performance. However, there were several telemetry dropouts when the r-f level was below receiver threshold, as noted in the communications evaluation.

d. Conclusions

ESA Test No. 2 showed that the TV Subsystem does not experience any rfi difficulties when the high-gain antenna is radiating into free space or an efficient microwave absorber.

Following this test, the cell voltages of the Batteries were measured, and each cell read 1.62 volts for each Battery.

S. Backup Functions Test No. 3 (JPL Procedure 3R305.06)

This test was performed on June 11, 1964, with the TV Subsystem mated to the JPL Spacecraft Bus. An external power source was employed to supply operating power for the Subsystem equipments, and TV Collimators were installed.

JPL Procedure 3R 300.12A was listed as the controlling specification for TV Subsystem turn-on procedure; however, investigation revealed that JPL Procedure 3R 305.06 contained the necessary procedures.

1. *Purpose of Test*

This test was performed to verify the backup command functions of the Spacecraft Bus, some of which are used for control of the TV Subsystem. Only those backup commands that cannot be feasibly checked during normal systems tests are verified here. The following is a list of these commands, which affect the TV Subsystem, and their function:

- Agena-Separate Switch —

  Activation of this switch initiates a command to start the TV Subsystem Clock;

- Hydraulic-Timer TV Contact Closure —

  Activation of this switch provides a ground enable for the current-limiting resistors of the SCR gates in the High-Current Voltage Regulators turn-on of the TV Cruise mode; and

- Solar Panel TV Arming Microswitch —

  Activation of this switch also provides a ground enable for the SCR-gate current-limiting resistor. It also activates turn on of the TV cruise mode.

This function is in parallel with the hydraulic-timer contact closure;

- CC&S Warmup Command —

  This command turns on F- and P-Channels into warmup mode; it is in parallel with the RTC-7F and RTC-7P commands and is a backup for these commands; and

- Cruise On Test (Clock OFF) Command —

  This command is initiated from the GSE. Initiating cruise test on removes power from the TV Clock and disables it.

2. *Description of Test*

The Backup Functions Test was performed with the TV Subsystem mated to the Spacecraft bus. The Subsystem had collimators mounted, and was powered from an external source. The test sequence for the test is presented in Table A-19.

TABLE A-19

BACKUP FUNCTIONS TEST NO. 3 TEST SEQUENCE

Time	Operation Function
A-5	Cruise-On Test switch depressed twice. Cruise-mode telemetry received on Channel 8.
A+0	Simulated Launch
[A+38'40" S+5]	Agena - Separate microswitch activated to initiate command for TV Clock.
A+40'	Cruise Off switch activated, turning off 15-point telemetry on Channel 8.
[A+63'40" S+30]	Hydraulic-timer closure. TV command enabled the SCR gate resistors and 15-point telemetry received on Channel 8. (Reset hydraulic timer.)
A+64	Cruise-Off switch activated, turning off 15-point telemetry on Channel 8.
[A+78'45" S+45]	Solar-Panel-Deploy-Back-Up microswitch closes, enabling SCR gate.
C+42'	TV collimators turned on.
C+43'	Full-power operation selected at OSE.
C+45'	CC&S Warmup command turns on F- and P-Channels in warmup mode of operation.
C+46'20"	F- and P-Channel full-power mode activated by 80-second timer output from Sequencer. Polaroid and 35-mm pictures taken of F- and P-Channel video outputs.
C+48'	F- and P-Channels turned off by RTC-5 command.
C+49'	F- and P-Channels turned on in warmup mode by RTC-7F and RTC-7P commands.
C+50'20"	F- and P-Channel full-power mode activated by 80-second timer output from Sequencer. Polaroid and 35-mm pictures taken of F- and P-Channel video outputs.
C+53'	Collimators turned off. 35-mm pictures of F- and P-Channel video output (black field) taken.

TABLE A-19 BACKUP FUNCTIONS TEST NO. 3 TEST SEQUENCE (Continued)	
Time	Operation Function
C+56'10"	Cruise-On switch depressed twice, turning off TV backup Clock.
C+57'10"	Cruise-Off switch depressed; cruise-mode telemetry turned off.

3. Test Evaluation

a. Video Performance

Fast noise spikes were observed on approximately 40 percent of the 35-mm frames of P1-Camera video output. Only one frame of P2-Camera video output exhibited a fast noise spike. The video output from all other cameras was normal during this test.

b. Communications Performance

The r-f power output was 60.1 watts after 2 minutes of full-power operation, and dropped to 58.2 watts at the end of the 12-minute test. The d-c input voltages to the F- and P-Channel Transmitter Power Supplies were 31.0 and 30.5 volts, respectively.

c. Telemetry Performance

All telemetry data recorded during the Backup Functions Test No. 3 indicated normal TV Subsystem performance.

d. Conclusions

The objectives of this test were successfully accomplished. Following the completion of the Backup Functions Test No. 3, the last test performed at JPL, the TV Subsystem was placed in a shipping container for transport to the launch site at the Eastern Test Range. The results of the Pre-launch Checkout Tests at ETR are described in Appendix B.

Appendix B

Prelaunch Testing of Flight Model III-2 At Eastern Test Range (ETR)

Appendix B

Prelaunch Testing of Flight Model III-2 At Eastern Test Range (ETR)

On June 21, 1964, the Ranger 7 Spacecraft arrived at ETR for a final series of tests prior to launch. This appendix covers all testing performed on the Spacecraft during the period from arrival at ETR to launch from ETR. The tests performed are given in Table B-1.

These tests were performed on the TV Subsystem, on the Spacecraft, and on the Spacecraft when adapted to the launch vehicle to ensure correct Spacecraft operation, to train the test personnel in Spacecraft and launch-vehicle procedures, and to verify these procedures.

A. Post-Shipment Electrical Test (RTSP 1100A, Appendix R, Abbreviated Subsystem Test)

This test was performed on June 23 prior to the mounting of the TV Subsystem on top of the JPL Ranger Bus. RCA personnel performed the test with JPL personnel observing.

1. Purpose of Test

After a mechanical inspection of the TV Subsystem, the Post-Shipment Electrical Test was performed to ensure proper electrical performance within the various assemblies of the TV Subsystem after shipment from JPL.

2. Description of Test

The post-shipment verification electrical test performed on the TV Subsystem was in accordance with a modified version of Appendix R. The command function portion of

TABLE B-1 TESTS PERFORMED AT ETR		
Date	Procedure	Title of Test
June 23, 1964	RTSP 1100A, Appendix R	Post-Shipment Electrical Test
June 25, 1964	JPL No. 3R305.07	Back-up Functions Test
June 27, 1964	JPL No. 3R300.13	System Test No. 10
June 29, 1964	JPL No. 3R315.02	Operational Checkout, RF Link Test
July 1, 1964	JPL No. 3R235.01	ESA High-Power Test
July 2, 1964	JPL No. 3R317.02	ESA Low-Power Tests
July 2, 1964	JPL No. 3R317.02	Special RFI Test
July 6, 1964	JPL No. 3R317.02 (1-A)	Special ESA Test
July 6, 1964	JPL No. 3R304.04	Precountdown Dummy Run
July 7, 1964	JPL No. 3R310.02	Combined Radiation Test
July 10, 1964	JPL No. 3R309.05	Joint Flight Acceptance Composite Test
July 11, 1964	JPL No. 3R220.02	Camera Calibration
July 15, 1964	JPL No. 3R300.13	Preflight System Test No. 11
July 20, 1964	JPL No. 3R235.02	ESA High-Power Test
July 22, 1964	JPL No. 3R317.03	ESA Low-Power Test
July 23, 1964	JPL No. 3R304.05	Precountdown Test
July 25, 1964	JPL No. 3R309.06	Simulated Launch
July 27, 1964	JPL No. 3R309.06	Countdown on First Day
July 28, 1964	JPL No. 3R309.06	Countdown on Second Day

Appendix R was not performed because the TV commands were to be tested in the Back-up Functions Test. The Ground Support Equipment (GSE), Serial No. 3, was used in this test. The test sequence is given in Table B-2.

3. *Test Evaluation*

a. Video Performance

The P1-Camera had noise spikes similar to those observed during the RA-7 tests at JPL. The spikes appeared as saturation on a single line of video. The duration of the spike was between 1 and 10 percent of the video line. The spikes, observed only on alternate 35-mm frames, did not appear to be more numerous during this test than during previous tests.

The P2-Camera video output was normal with the exception of noise spikes on four frames of 35-mm film (2 percent of the photographs). This noise was similar to that

TABLE B-2 POST-SHIPMENT ELECTRICAL TEST SEQUENCE	
Elapsed Time (minutes and seconds)	Operation
T + 1'	Cruise Mode activated via Cruise Mode Switch
T + 3'	F- and P-Channels placed in warmup via RTC-7F and RTC-7P switch.
T + 4'20"	F- and P-Channels placed in full-power operation.*
T + 8'	F- and P-Channels turned off via RTC-5 switch.
T + 8'30"**	Cruise mode turned off via Cruise Off switch.

*A calibrated illumination source (Light Gun) was used to illuminate each camera. Polaroid photographs were taken for a quick evaluation of camera performance. A 35-mm film was taken of the video received over the r-f link during the test.

**Total test time.

observed on this camera during previous tests and to that observed on the P1-Camera video.

The P3-Camera video output was normal during the entire test. No anomalies were observed while analyzing the 35-mm film.

The P4-Camera video output was normal with the exception of noise spikes on two frames of 35-mm film (1 percent of the photographs). These noise spikes were similar to those observed on the P4-Camera during previous tests on RA-7 and to those observed on P1.

The F_a- and F_b-Camera video outputs were normal. Analysis of the 35-mm film showed no unexplained anomalies during the test.

b. Communications Performance

The communication performance was normal. Figure B-1 shows the r-f connection between the Four-Port Hybrid of the TV Subsystem to the GSE and power meter.

The voltage input to the transmitter power supply is determined by subtracting 0.5 volt from the unregulated bus voltage. The 0.5 volt is the difference in potential between the unregulated bus telemetered point, which is at the High-Current Voltage

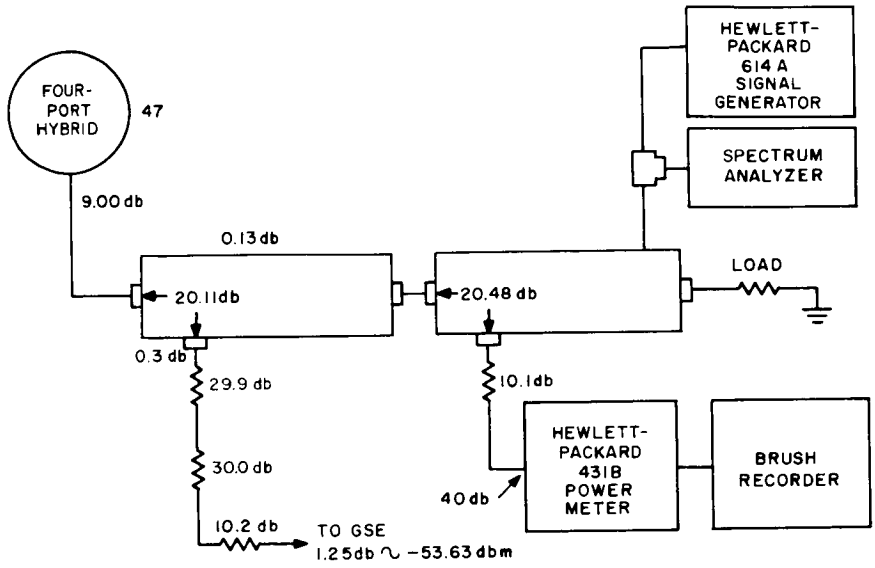

Figure B-1. RF Setup for the Post-Shipment Electrical Test

Regulator (HCVR) output, and the input to the transmitter power supply. During this test the average input voltage for the transmitter power supplies was 30.8 volts for F-Channel and 30.5 volts for P-Channel.

The Subsystem went into full power at T + 4 minutes 20 seconds and was shut off at T + 8 minutes. The power profile taken during this test is given in Table B-3.

TABLE B-3
POWER PROFILE TAKEN DURING POST SHIPMENT ELECTRICAL TEST

Elapsed Time (minutes and seconds)	Power Out at Four-Port Hybrid (watts)
T + 4'30"	56
T + 6'	56
T + 7'	58
T + 8'	58

c. Power Performance

The GSE supplied power to the TV Subsystem. The GSE power supplies were set for approximately 32.3 volts input to the F-Channel HCVR and approximately 32.0 volts input to the P-Channel HCVR.

d. Telemetry Performance

The telemetry during this test was normal. No discrepancies indicating a malfunction in either the telemetry system or in the monitored systems were observed.

4. Conclusions

No damage was incurred by the TV Subsystem during shipment from Pasadena, California, to Cape Kennedy, Florida.

The batteries, Serial Nos. 85 and 76, were installed in F-Channel and P-Channel respectively. The top hat, shrouds, collimators, and counter balance were installed on the TV Subsystem, which was then mated with the Ranger Bus in preparation for the RA-7 Back-up Functions Test.

B. Back-up Functions Test (JPL Procedure 3R305.07)

1. Purpose of Test

This test was performed on the RA-7 Spacecraft on June 25, 1964, to verify the back-up command functions in the Bus for the TV Subsystem. Only those back-up commands which cannot be checked during regular systems tests were checked. These commands are listed in Table B-4.

TABLE B-4 COMMANDS TESTED DURING BACK-UP FUNCTIONS TEST	
Command	Function
Agena Separate Microswitch	Starts the Clock
Hydraulic Timer Command	Provides a ground enable for the SCR gate current-limiting resistors. Activates Cruise Mode.
Solar Panel TV Arming Microswitch	Switch activation provides a ground enable for the SCR gate current-limiting resistors. Activates Cruise Mode. (This command is in parallel with the Hydraulic Timer Command.)
CC and S TV2 Command	Places F- and P-Channels into warmup. (This command is in parallel with and is a back-up command for RTC-7.)
Cruise On Test Command	Removes power from the Clock. (This command is from the GSE.)

2. *Description of Test*

The Back-Up Functions Test was performed with the TV Subsystem mated with the Ranger 7 Bus. The Subsystem had the collimators mounted, and it was powered externally. The test sequence is given in Table B-5.

TABLE B-5 BACK-UP FUNCTIONS TEST SEQUENCE	
Elapsed Time (minutes and seconds)	Operation Function
A - 5'	Cruise On Test switch depressed twice. Cruise mode (15-point) telemetry on Channel 8.
A + 38' 40" (S + 5)	Agena separation microswitch activated. Command for the Clock initiated.
A + 40'	Cruise Off switch depressed. Cruise-mode telemetry turned off.
A + 63' 40" (S + 30)	Hydraulic timer closure activated. Ground provided for the SCR gate resistors and 15-point telemetry turned on Channel 8. (Reset hydraulic timer.)
A + 64'	Cruise Off depressed. Cruise-mode telemetry turned off.

TABLE B-5 BACK-UP FUNCTIONS TEST SEQUENCE (Continued)	
Elapsed Time (minutes and seconds)	Operation Function
A + 78' 45" (S + 45)	Solar panel deploy back-up microswitch activated. Ground enable provided to the SCR gate resistors and 15-point telemetry turned on.
C + 45'	CC and S TV-2. F- and P-Channels placed in warmup.
C + 46' 20"	Both channels placed in full-power operation.
C + 48'	RTC-5 Command. Both channels turned off.
C + 49'	RTC-7 Command. Both channels placed in warmup.
C + 50' 20"	Both channels placed in full-power operation.
C + 56'	RTC-5 Command. Both channels turned off.
C + 56' 10"	Cruise On Test switch depressed twice. Clock is stopped.
C + 57' 10"	Cruise Off switch depressed. Cruise-mode telemetry turned off.

3. *Test Evaluation*

a. Video Performance

During the test, no hard-line video was received during warmup. After the test, this problem was traced to a faulty minus 6.3-volt d-c power supply for the GSE video amplifier. The individual cameras were evaluated for proper performance.

The P1–Camera video output had noise spikes similar to those observed in the previous test in approximately 50 percent of the frames. Typical examples of the noise spikes observed throughout the test are shown in Figure B-2.

Analysis of the 35-mm film on the P2-Camera revealed noise spikes similar to those previously observed. The noise spikes appear in only four frames, are not large (approximately 1 percent of a video line or less), and are very infrequent. The video output from this camera was considered normal.

Slight microphonics were observed in the video output of the P3-Camera. The microphonics were similar to those observed during previous tests at AED.

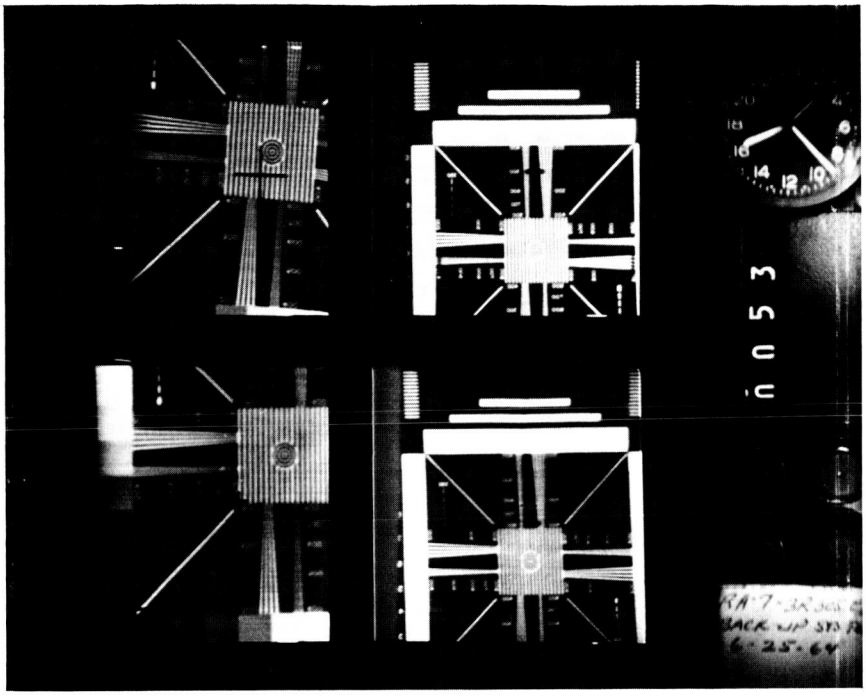

a. Noise spikes seen through RETMA pattern

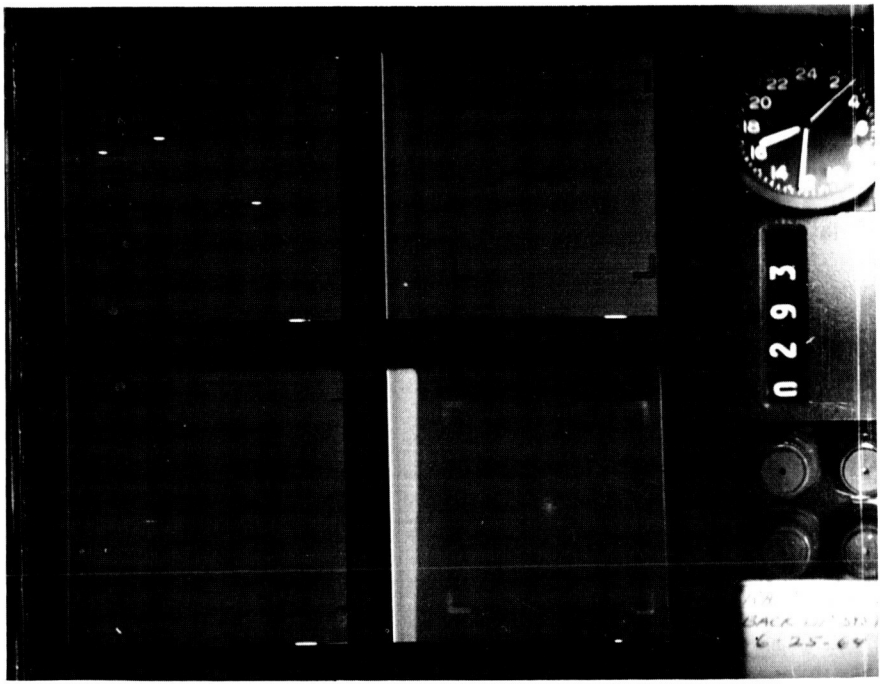

b. Noise spikes on black field

Figure B-2. P1-Camera video output during Back-up Functions Test

The 35-mm film of the P4-Camera revealed noise transients in approximately 2 percent of the frames. These marks appear as a wedge in the frame. The camera was considered ready for the next test. Typical frames of the P-Channel video output are shown in Figure B-3.

The F_a-Camera video output appeared normal for this test. There were no anomalies observed when the 35-mm film was analyzed. Figure B-4a is a typical frame of the observed video output. The tearing in the center square of the pattern is caused by the white bars at the edge of the pattern interferring with the GSE sync. This condition was corrected for the Systems Test No. 10. Figure B-4b is a typical frame of the video output with no pattern.

The F_b-Camera operation was normal. There were no anomalies observed in the video. Typical frames of F_b-Camera video output are shown in Figure B-5.

b. Communications Performance

The communication performance for this test was normal. Figure B-6 shows the r-f connection from the Four-Port Hybrid of the TV Subsystem to the GSE and power meter.

The voltage input to the transmitter power supply is determined by subtracting the line loss between the unregulated bus telemetry point and the input to the transmitter power supply (0.5 volts) from the converted telemetry unregulated bus voltage. The average input voltage for this test was minus 31.7 volts for F-Channel and minus 30.9 volts for P-Channel.

The power profile taken during this test is given in Table B-6.

c. Power Performance

The GSE supplied power to the TV Subsystem. The ground power supplies were set for approximately 33.2 volts input to the F-Channel HCVR and 32.4 volts input to the F-Channel HCVR.

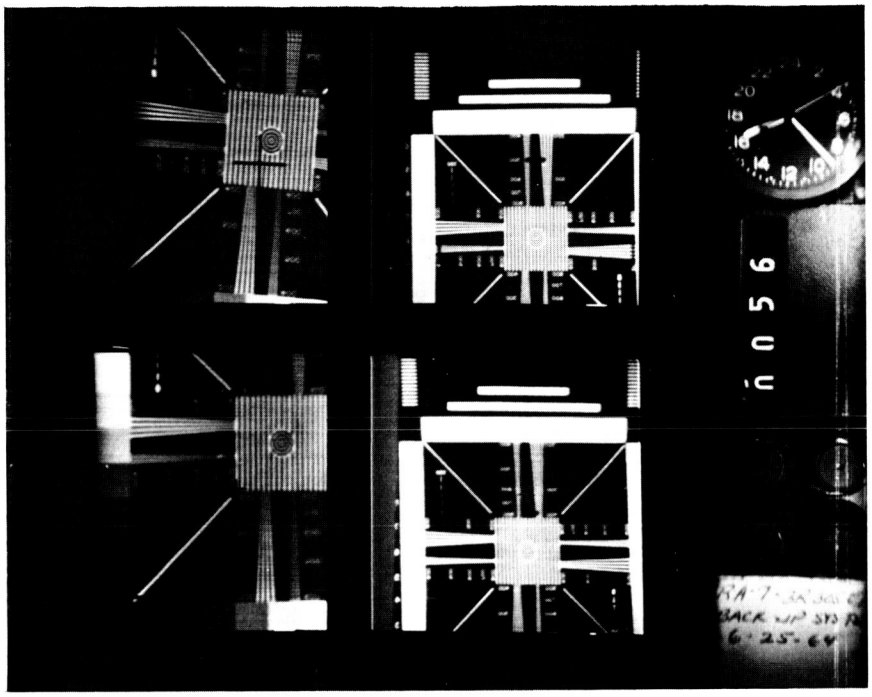

a. With RETMA chart

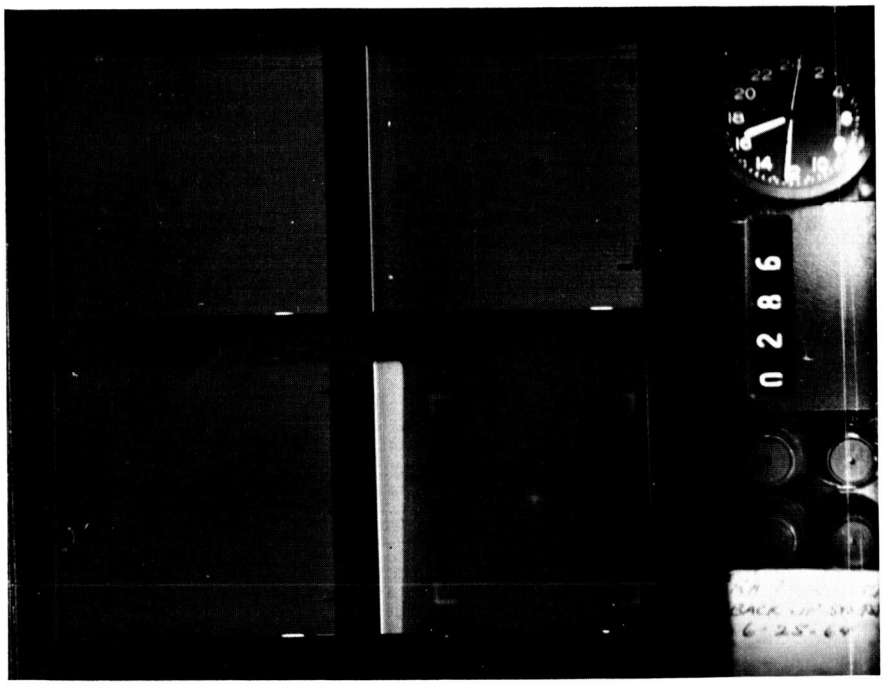

b. Black field

Figure B-3. Typical frames of P-Camera video output during Back-up Functions Test

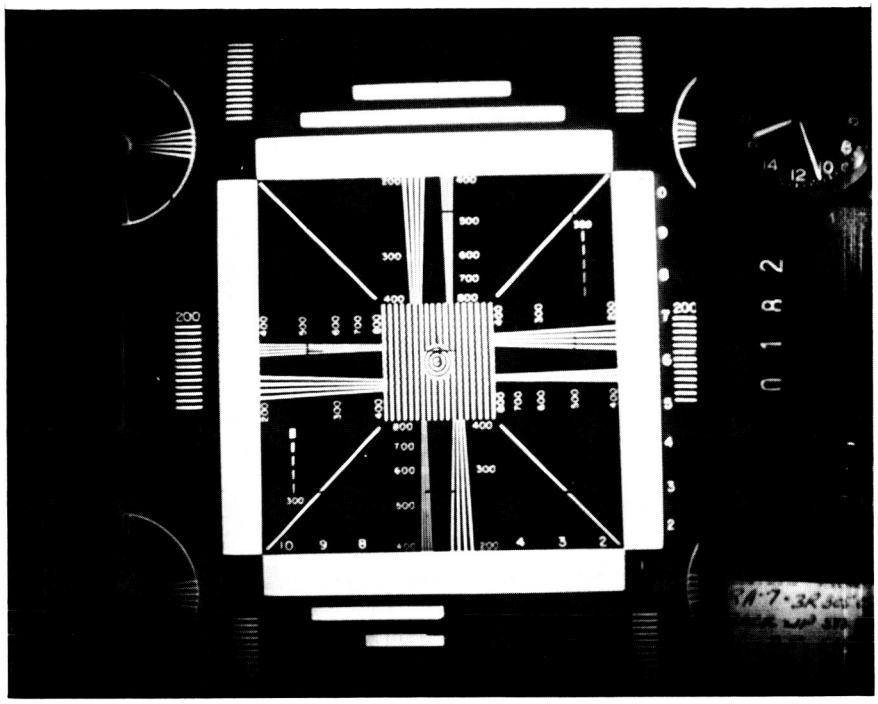

a. With RETMA chart

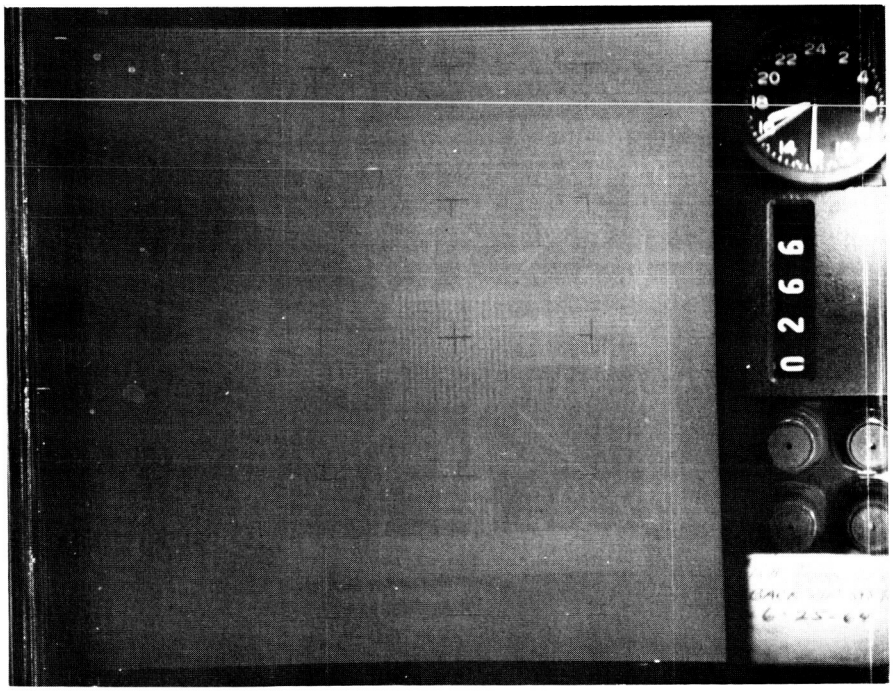

b. Black field

Figure B-4. Typical frames of F_a-Camera video output during Back-up Functions Test

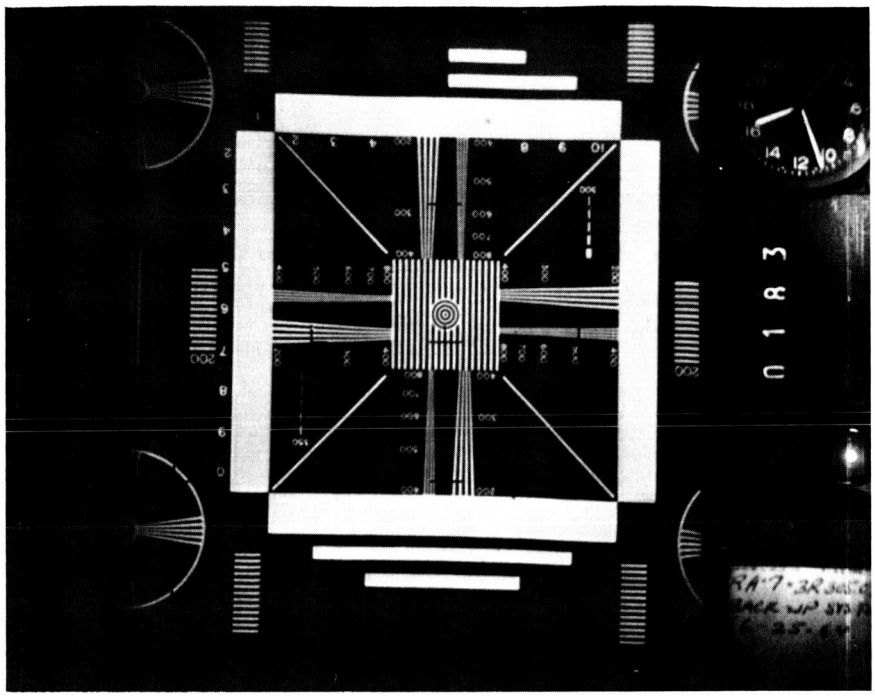

a. With RETMA chart

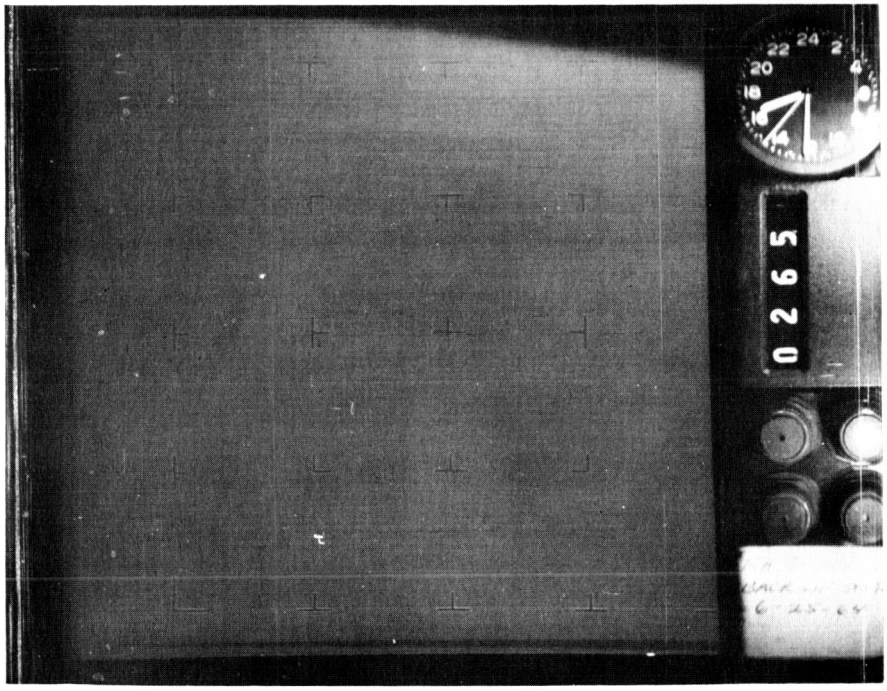

b. Black field

Figure B-5. Typical frames of F_b-Camera video output during Back-up Functions Test

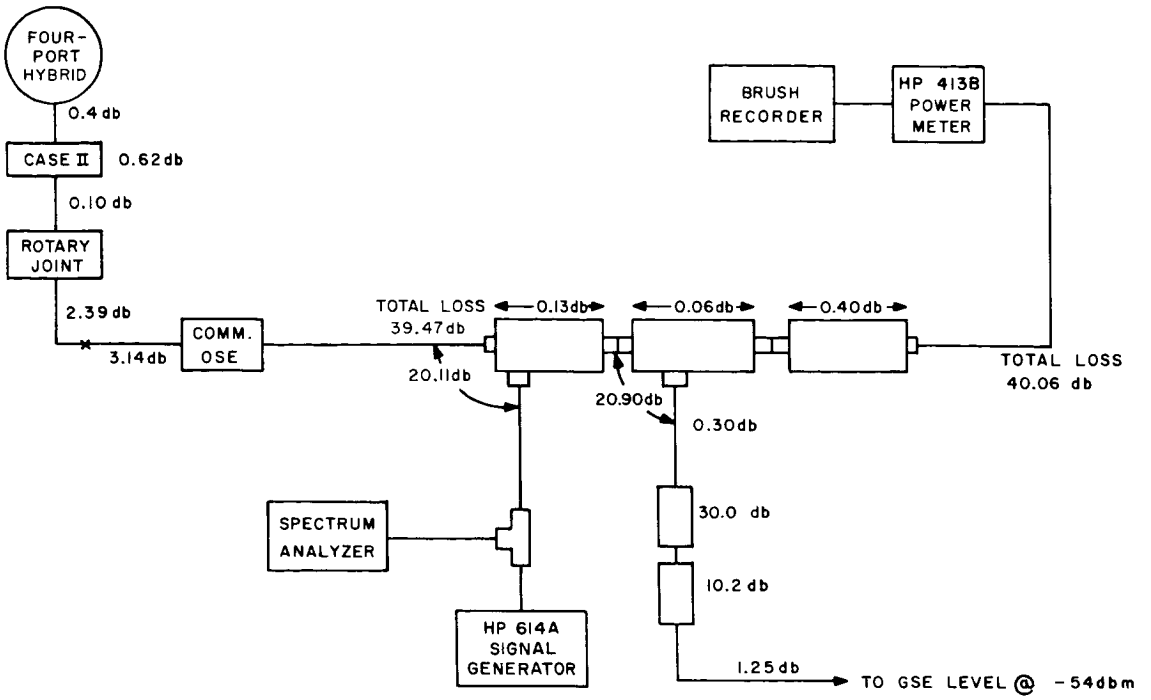

Figure B-6. RF Connection for Back-up Functions Test

TABLE B-6
POWER PROFILE TAKEN DURING BACK-UP FUNCTIONS TEST

Elapsed Time (minutes and seconds)	Power Out at Four-Port Hybrid (watts)
C + 47	57
48	60
C + 50' 20"	59.5
51	58
52	60
53	60
54	60
55	59.5
56	59.0

d. Telemetry Performance

The telemetry over Channel 8 appeared noisy. The noise did not appear up on the JPL Channel 8 recording. This noise was traced to the GSE, which was re-adjusted; the noise disappeared.

The P-Channel 225-kc telemetry output was compressed and clipped at the base line. This malfunction was traced to the GSE. A discriminator was replaced in the GSE, and the P-Channel telemetry output was then observed as normal.

In both of these cases, the corrective action was accomplished through the use of the tape recording of the test for diagnostic purposes. The tape recordings in both cases showed that the TV Subsystem telemetry had been good during the test, indicating that the telemetry and the circuits telemetered were operating normally.

4. Conclusions

The TV Subsystem and the Subsystem back-up functions performed normally. No new problems were observed.

The collimator for the P-4 Camera slipped from its bracket during preparations for the System Test No. 10. However, the collimator supported by wires, did not fall onto the floor. It was checked prior to the next test and found to be in good working condition. The TV Subsystem was committed to the next test.

C. System Test No. 10 (JPL Procedure 3R300.13)

1. Purpose of Test

This test, performed on the Ranger-7 Spacecraft on June 27, 1964, was an accelerated mission simulation to verify that all Spacecraft equipment operated in a proper manner.

2. Description of Test

The TV Subsystem was mounted on the Ranger Bus. The Subsystem batteries were installed. However, for this test, power for the Subsystem was supplied externally.

The TV Subsystem underwent simulated launch electrical performance and was commanded through a simulated terminal mode operation. The sequence of events for this test is given in Table B-7.

TABLE B-7
SEQUENCE OF EVENTS DURING SYSTEM TEST NO. 10

Elapsed Time (minutes and seconds)	Operation
A – 5'	Cruise On Test switch depressed twice. Cruise telemetry obtained over Channel 8.
A + 38' 40" (S + 5)	Agena microswitch activated. The TV Subsystem Clock starts.
A + 63' 40" (S + 30)	Hydraulic timer activated. TV turn-on bus enabled by grounding the SCR gate resistors in preparation for SCR turn-on command. (No indication from Subsystem.)
C + 44'	RTC-7 Command. F- and P-Channels placed in warmup.
C + 45' 20"	Both channels placed in full-power operation via TV Sequencer full-power command.
C + 50'	TV Subsystem operation placed in sync-disable mode. This disables the P Channel Sequencer and verifies P1 free-run mode.
C + 51' 30"	Sync disable removed. Proper P-Channel sync restored for all P-Channel cameras.
C + 54' 30"	F- and P-Channel full-power commands were reset in TV Sequencer. TV Subsystem in full power via CC and S TV-3. This verifies TV-3 actuation.
C + 55'	CC and S TV-3 was reset. TV Subsystem in warmup.
C + 56'	RTC-5 Command. F- and P-Channels off.
C + 56' 10"	Cruise On Test switch depressed twice. The TV Subsystem Clock is stopped.
C + 56' 20"	Cruise Off switch is depressed. Cruise telemetry is turned off.

3. Test Evaluation

a. Video Performance

Hardline video was not received during this test. After the test, it was discovered that the GSE video amplifier had to be readjusted because the output d-c level was incorrect. Video output from the Subsystem was confirmed by observing the 35-mm film obtained via r-f link.

The P1-Camera video output exhibited noise spikes similar to those previously observed. However, less than 10 percent of the frames showed these spikes. Interference at a rate of approximately 12.5 kc was observed in the video output. This interference appeared in less than 1 percent of the frames of the 35-mm film. The video output obtained from the P2-, P3-, and P4 cameras was normal in all cases.

The video output obtained from both the F_a- and F_b-Cameras was normal. See Figures B-7 and B-8 for typical frames of F-Camera output.

b. Communications Performance

The performance of the TV Subsystem communications was normal. The r-f connection is the same as shown in Figure B-6. The input to the transmitter power supplies is determined in the same manner as in the previous test. Subtracting the 0.5-volt drop between the unregulated bus output at the HCVR and the input to the transmitter power supplies from the telemetered unregulated bus, the input voltage to the transmitter power supplies was 30 volts for F-Channel and 30.1 volts for P-Channel. The power profile obtained during this test is given in Table B-8.

c. Power Performance

The TV Subsystem was supplied power from the GSE. The ground power supplies were set for approximately 32 volts on F-Channel and 32 volts on P-Channel. No problems were encountered during this test.

d. Telemetry Performance

The telemetry was normal during this test indicating no problem in either the telemetry assembly or in the circuits monitored.

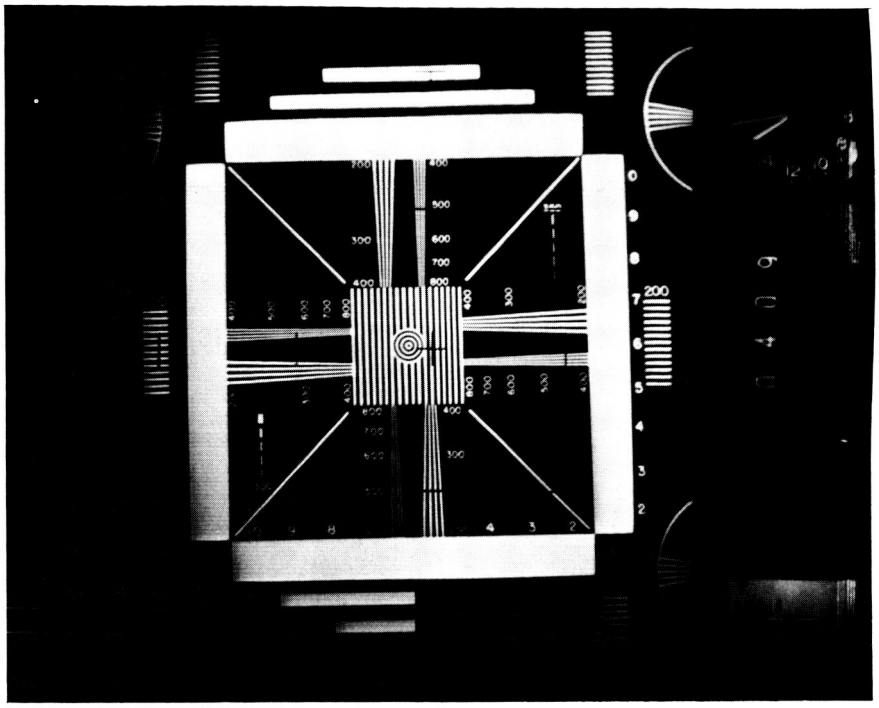

Figure B-7. F_a-Camera video output during System Test No. 10

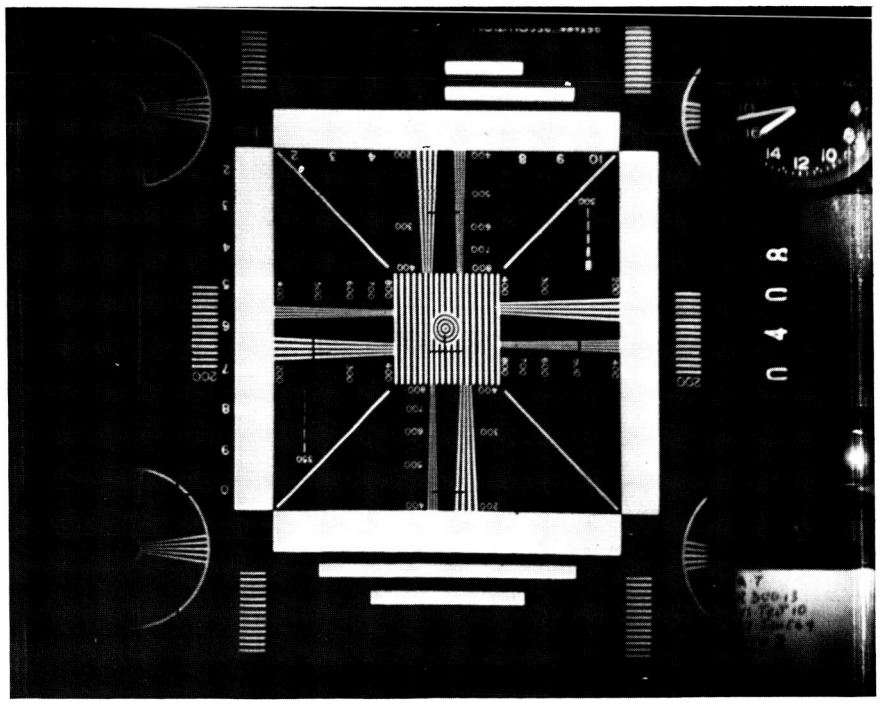

Figure B-8. F_b-Camera video output during System Test No. 10

TABLE B-8 POWER PROFILE TAKEN DURING SYSTEM TEST NO. 10	
Elapsed Time (minutes and seconds)	Power Out at Four-Port Hybrid (watts)
C + 45' 30"	57
C + 46	57.5
47	60
48	60.5
49	60
50	60
51	60
52	59.5
53	59
54	58.7
55	58.4

4. *Conclusions*

The TV Subsystem operated properly. The TV battery jumper plug was installed in 30J13 in preparation for the start of the Operational Checkout Test.

D. Operational Checkout, RF Link Test (JPL Procedure 3R315.02)

1. *Purpose of Test*

The operational checkout test performed on June 29, 1964, in the AM hangar at ETR, was an accelerated mission simulation test with all OSE and ground cables disconnected from the Spacecraft. Communication with the Spacecraft was conducted via r-f link. The purpose of this test was to verify that all Spacecraft equipment operated in a proper manner when in flight configuration (with cables off).

Two terminal maneuvers were performed in sequence. The first one checked out the turn-on command from the Bus (CC&S warmup), and the second maneuver checked out the RTC-7 turn-on command.

2. Description of Test

a. Spacecraft Configuration

This test was performed with the TV Subsystem mounted on the RA-7 Bus. No cables were attached to the Spacecraft. Instead of mounted collimators, a white material illuminated with flood lamps provided exposure for the six cameras. The TV Subsystem was powered by non-flight batteries, and the jumper plug 30P13 was installed.

To prevent radio-frequency interference problems, the directional antenna was hung in a normally deployed position pointing out from the side of the Spacecraft. Microwave absorption material lined a portion of a nearby wall, which was in the path of the antenna radiation, to eliminate r-f reflections back to the Spacecraft.

b. Test Procedure

The sequence of events for this test is given in Table B-9.

At the end of the test, the cables were reconnected, the Cruise On Test switch was depressed twice to stop and reset the Clock, and the Cruise Off switch was depressed once to turn off Channel-8 cruise-mode telemetry.

3. Test Evaluation

a. Video Performance

Camera video performance was of satisfactory quality. In the P1-Camera video output, noise spikes, similar in appearance to those reported in previous tests, were observed in approximately 40 percent of the P-Camera video frames, an increase over that for the system test. Occasionally, when a spike occurred in the mark portion of the signal, it upset the clamp operation and caused some lines of the video output to go black as shown in Figure B-9. An interference

TABLE B-9 SEQUENCE OF EVENTS FOR THE OPERATIONAL CHECKOUT	
Time (minutes and seconds)	Operation Function
A - 5'	Cruise On Test switch on console was depressed twice to start cruise-mode telemetry (Channel 8) and to reset the Clock. With Cruise On Test switch in the off condition, the SCR gates were not enabled from the console.
A + 33' 40" (S + 0)	Simulated Spacecraft separation. The backup-Command Hydraulic Timer was started.
A + 38' 40" (S + 5)	Microswitch for Clock was closed. Clock started.
A + 62'	Solar panels were deployed. Switch contact closure is backup for the Hydraulic Timer.
A + 63' 40"	The Hydraulic Timer switch closure enabled the SCR gate turn-on circuits and served as a backup for cruise mode on.
First Terminal Maneuver	
C + 45'	CC&S warmup command (TV-2). F- and P-Channels placed in warmup (camera illumination on).
C + 46' 20"	Both channels in full-power operations by Sequencer full-power command
C + 51' 37"	RTC-5 command. Both channels were turned off.
Second Terminal Maneuver	
C + 44'	RTC-7 command. F- and P-Channels placed in warmup
C + 45' 20"	Both channels placed in full-power operation by Sequencer full-power command.
C + 51' 30"	Camera illumination off for dark-field photographs.
C + 53' 30"	Camera illumination on.
C + 56"	RTC-5 Command. Both channels turned off.

beat pattern, which was believed to be caused by microphonics of the preamplifier nuvistor tube, appeared either at the top or bottom of the raster at approximately a 13-kc rate.

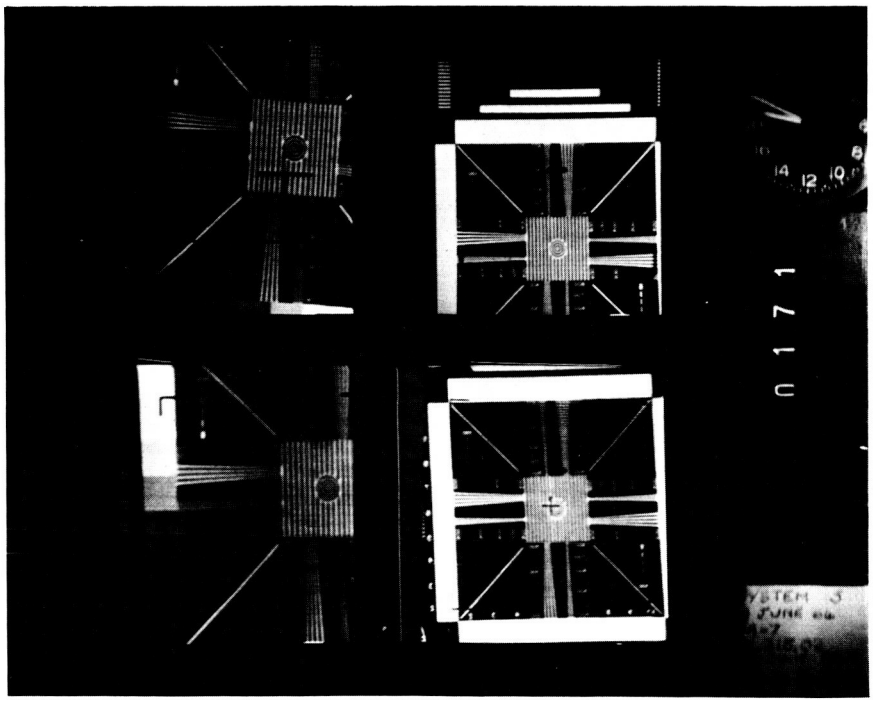

Figure B-9. Effect of noise spike in mask portion of signal

The video output obtained from the P2- and P3-Cameras appeared normal throughout the run. A noise transient which is shown in Figure B-10, was observed near the center square in one of the P4-Camera frames.

The video output from the F_a- and F_b-Cameras appeared normal.

b. Communications Performance

The performance of the TV Subsystem communications was normal. Power variations, which were less than 2 watts, were within specifications. The r-f connection is shown in Figure B-11. Since this test was performed without cables, the r-f was picked up with a Stoddard antenna probe placed near the high-gain antenna dipole.

The input voltage to the Transmitter Power Supplies, which was determined by subtracting line losses from the telemetered data on the HCVR input, was 31.3 volts d-c for F-Channel and 30.9 volts d-c for P-Channel.

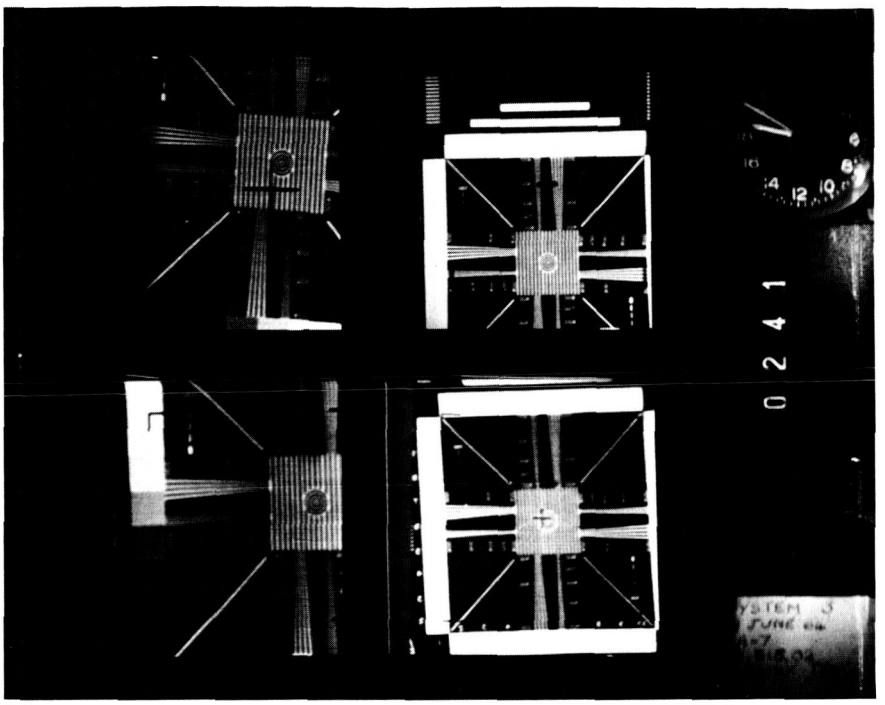

Figure B-10. Noise transient observed in one P4-Camera frame during r-f Link Test

c. Power Performance

The r-f power output taken during these two terminal operations is shown in Table B-9A. The corresponding battery (terminal) voltages and computed voltages at the input to theTransmitter Power Supplies are also given. The r-f test configuration used for this test is shown in Figure B-11. The batteries performed normally, maintained satisfactory voltage input levels to the Transmitter Power Supplies throughout both terminal missions. The total discharge for F-Battery was 4.07 amperes and for P-Battery was 5.75 amperes.

d. Telemetry Performance

The telemetry performance was normal.

TABLE B-9A
RF POWER DURING TERMINAL MANEUVER

	Time (minutes and seconds)	Input to HCVR		Input To Transmitters		Power Output at Four-Port Hybrid (watts)	Operating Mode
		F-Battery (volts)	P-Battery (volts)	F-Channel (volts)	P-Channel (volts)		
Terminal Operation No. 1	C + 46'	33.6	33.5	32.6	32.5	-	Warmup
	C + 47'	33.3	32.9	31.8	31.4	59.64	Full-Power
	C + 48'	-	-	-	-	59.64	Full-Power
	C + 49'	-	-	-	-	61.87	Full-Power
	C + 50'	32.8	32.7	31.3	31.7	61.87	Full-Power
	C + 51'	32.9	32.8	31.4	31.3	61.87	Full-Power
	C + 52'	35.1	35.06	0	0	-	Off
Terminal Operation No. 2	C + 44'	33.9	33.5	32.4	32.5	-	Warmup
	C + 45'30"	-	-	-	-	61.87	Full-Power
	C + 46'	33.3	32.9	31.8	31.4	60.7	Full-Power
	C + 47'	-	-	-	-	60.5	Full-Power
	C + 48'	-	-	-	-	61.87	Full-Power
	C + 49'	-	-	-	-	61.87	Full-Power
	C + 50'	-	-	-	-	60.7	Full-Power
	C + 51'	-	-	-	-	61.4	Full-Power
	C + 52'	32.6	32.3	31.1	30.8	60.9	Full-Power
	C + 53'	-	-	-	-	60.7	Full-Power
	C + 54'	32.8	32.4	31.3	30.9	61.4	Full-Power
	C + 55'	-	-	-	-	60.7	Full-Power
	C + 57'	34.6	34.2	0	0	-	Off

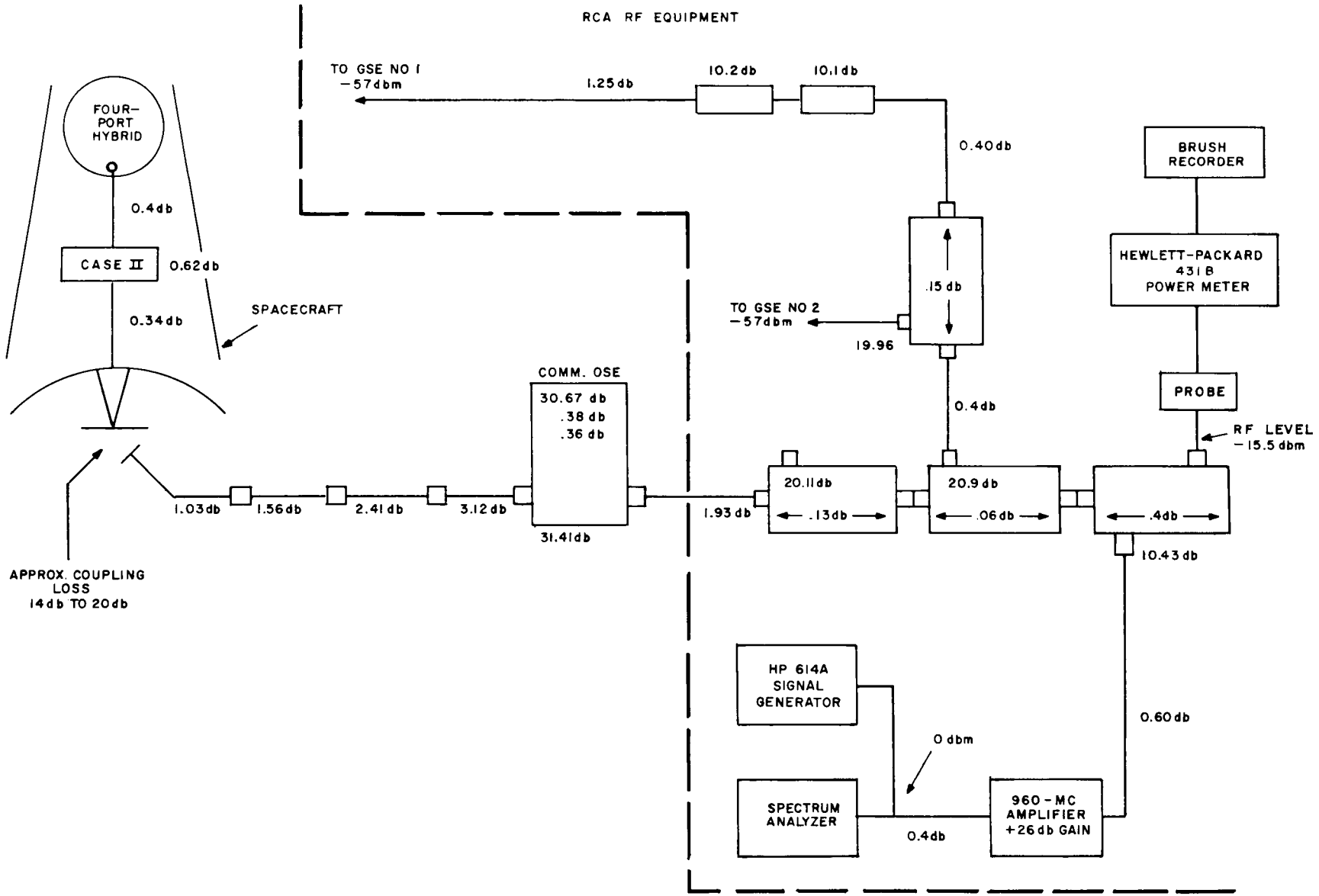

Figure B-11. Operational checkout, RF Link Test configuration

4. Conclusions

The TV Subsystem without external cables attached, performed satisfactorily as part of the RA-7 Spacecraft. It was, therefore, considered ready for the Explosive Safe Area (ESA) tests and the prelaunch tests.

E. Explosive Safe Area High-Power Test (JPL Procedure 3R235.01)

The TV Subsystem was transported to the Explosive Safe Area (ESA) on June 30, 1964. It was removed from the shipping container, was mounted on the Ranger Bus, and was prepared for the ESA High-Power Test on July 1, 1964. The test was performed using TV Subsystem batteries for power.

1. Purpose of Test

The purpose of this test was to determine the effect the TV Subsystem high-power r-f signal has on the pyrotechnics installed in the Ranger Bus midcourse propulsion system.

2. Description of Test

The test is performed in the ESA. The high-power r-f signal is radiated from the high-gain antenna. The antenna is nested under the Bus, and the r-f signal is radiated into the Echo-sorb material, which is directly in line with the directional antenna. The test sequence is given in Table B-10.

3. Test Evaluation

a. Video Performance

The F-Channel video output could not be recorded in real time because a failure in the GSE caused a level shift in the channel. The video signal was recorded on tape, and F-Channel evaluation was obtained from the tape playback. The

TABLE B-10 ESA HIGH-POWER TEST SEQUENCE	
Elapsed Time (minutes and seconds)	Operation
T - 5'	Cruise On Test switch depressed. Cruise mode turned on and the SCR gate firing circuits enabled.
T + 0	RTC-7 Command. F- and P-Channels in warmup.
T + 1' 20"	Both channels in full-power operation.
T + 5' 30"	RTC-5 Command. Both channels off.
T + 6'	Cruise Off switch depressed. Cruise-mode telemetry stops.

P1-Camera output exhibited noise spikes in approximately 30 percent of the frames recorded on 35-mm film. The performance of the P2- and P3-Cameras was normal. The video output from the P4-Camera exhibited noise transients in approximately 2 percent of the frames recorded on 35-mm film. These had been observed previously on this camera.

b. Communications Performance

The performance of the TV communications system was normal throughout the test. Subtracting 0.5 volt from the telemetered unregulated bus to compensate for the voltage drop between the output of the HCVR and the input to the Transmitter Power Supplies gave input voltages of 30.6 (F-Channel) and 30.7 volts (P-Channel) for the communications system. The test configuration is given in Figure B-12. The power profile obtained for this test is given in Table B-11.

TABLE B-11 POWER PROFILE TAKEN DURING THE ESA HIGH-POWER TEST	
Elapsed Time (minutes and seconds)	Power Out at Four-Port Hybrid (watts)
T + 1' 30"	55
T + 2'	58
T + 3'	58
T + 4'	58
T + 5'	58

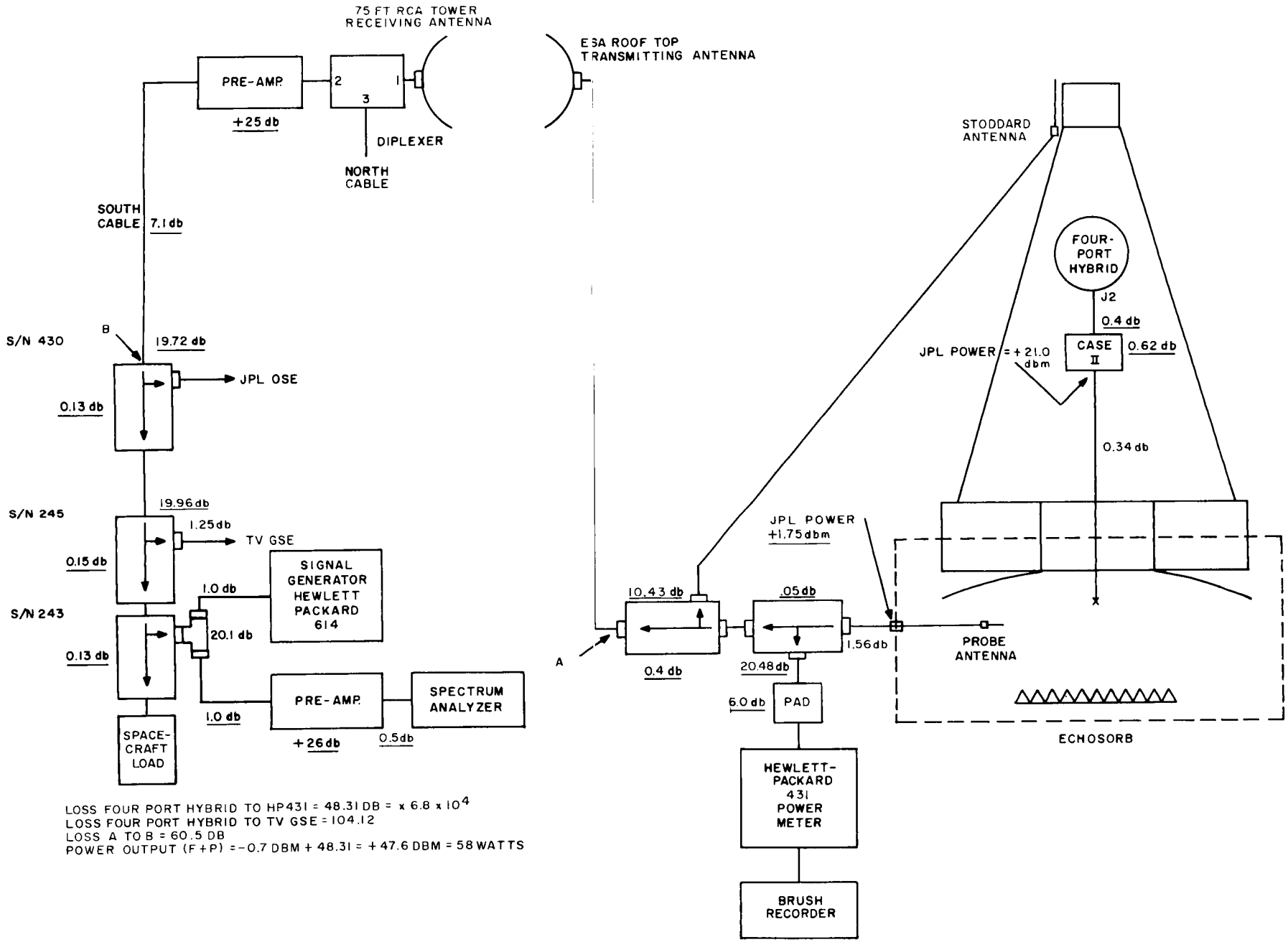

LOSS FOUR PORT HYBRID TO HP431 = 48.31 DB = x 6.8 x 10^4
LOSS FOUR PORT HYBRID TO TV GSE = 104.12
LOSS A TO B = 60.5 DB
POWER OUTPUT (F+P) = -0.7 DBM + 48.31 = +47.6 DBM = 58 WATTS

Figure B-12. Test configuration for ESA High-Power Test

c. Power Performance

Power was supplied to the TV Subsystem for this test by batteries. The profile obtained from telemetry during this test is given in Table B-12.

TABLE B-12
POWER PROFILE OBTAINED FROM TELEMETRY DURING ESA HIGH-POWER TEST

Elapsed Time (minutes)	Input to F-Channel HCVR		Input to P-Channel HCVR	
	Voltage (volts)	Current (amperes)	Voltage (volts)	Current (amperes)
T + 0	35.4	0	34.5	0.15
T + 1	33.6	7.8	33.5	9.4
T + 2	33.3	13.4	32.9	15.6
T + 4	32.9	13.7	32.8	16.3
T + 6	32.7	13.4	32.4	15.3
T + 7	34.6	0	34.5	0.15

Battery discharge during this test was 1.46 ampere-hours for a F-Battery, Serial No. 85, and 1.80 ampere-hours for P-Battery, Serial No. 76.

d. Telemetry Performance

Telemetry during this test was normal. No discrepancies indicating a malfunction in either the telemetry system or in the monitored system were observed.

4. Conclusions

The TV Subsystem performed properly, and it was committed to the next test. Prior to the ESA Low-Power Test, Ranger 7 was mounted on the Agena adapter ring.

F. Explosive Safe Area Low-Power Test (JPL Procedure 3R317.02)

The Low-Power Test (no TV Subsystem full power) was performed at the ESA on July 2, 1964.

1. *Purpose of Test*

The purpose of this test was to verify the compatibility of the Blockhouse Trailer and the hanger OSE with the Spacecraft. This test also provided a sequence of tests to verify the readiness of the Spacecraft for launch-pad operation.

2. *Description of Test*

The sequence of events comprising the Low-Power Test at the ESA is given in Table B-13.

TABLE B-13
LOW-POWER TEST SEQUENCE

Elapsed Time (minutes and seconds)	Operation Function
T + 84'	Cruise On Test switch depressed twice. Cruise-mode telemetry on, SCR gate circuits not enabled.
T + 86'	RTC-7 Command. F- and P-Channels did not go into warmup. (Gates were not enabled.)
T + 89'	Cruise On Test switch activated. The SCR gate circuits were enabled.
T + 90'	RTC-7 Command. Both channels in warmup.
T + 0' 10"	Cruise On Test switch depressed.
T + 91' 20"	Subsystem on in reduced-power mode.
T + 94' 40"	RTC-5 Command and Cruise Off switch depressed. Cruise mode turned off.

3. Test Evaluation

a. Video Performance

Most of the received video output exhibited rfi. During this test, the shroud lamp was not visible to the P1-Camera. It was discovered, prior to the special test at the ESA on July 6, that the hole in the shroud, which allows the P1-Camera to view the shroud light, was not in the line-of-sight of the camera. This was corrected. The noise spikes, which had been seen previously in the P1-Camera video output, were in approximately 10 percent of the recorded frames.

The P2-Camera output was normal with the exception of noise transients similar to those observed previously. These marks occurred in 50 percent of the frames just below the center reticle. The duration of the mark was 10 to 20 percent of a video line.

The P3-Camera video output exhibited a large amount of rfi as shown in Figure B-13. The video output from the P4-Camera was normal and the video output from the F_a- and F_b-Cameras exhibited rfi as shown in Figures B-14 and B-15. The source of the rfi was not apparent. However, it was thought that the interference was caused by

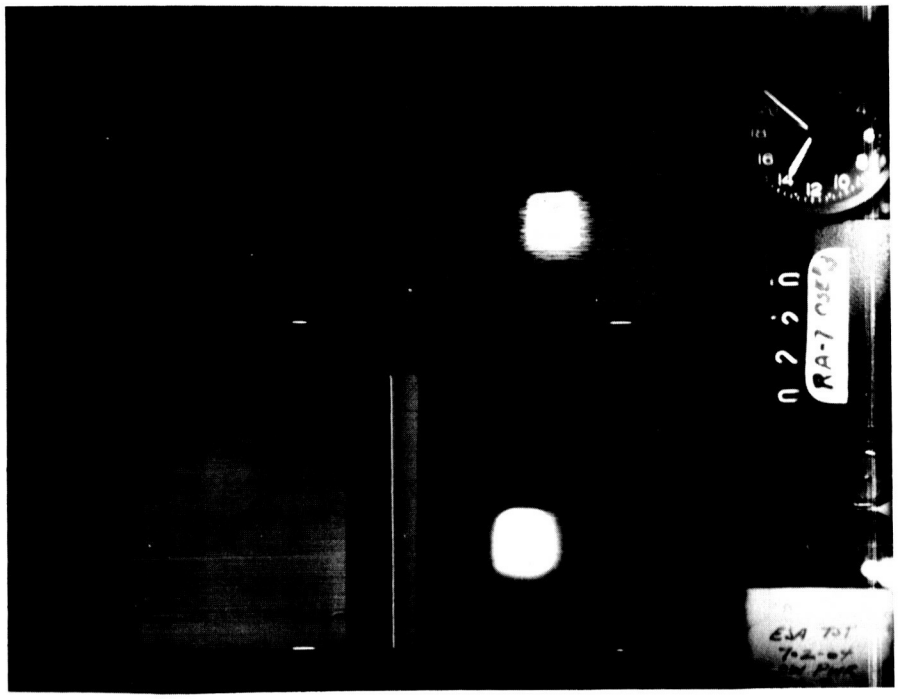

Figure B-13. RFI in P3-Cameras video output during ESA Low-Power Test

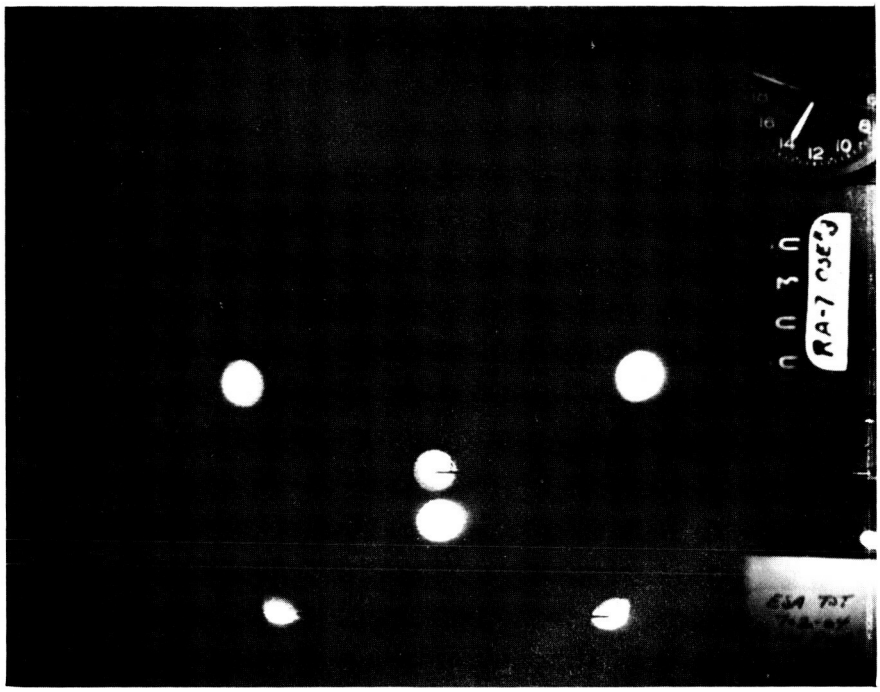

Figure B-14. RFI in F_a-Camera video during ESA Low-Power Test

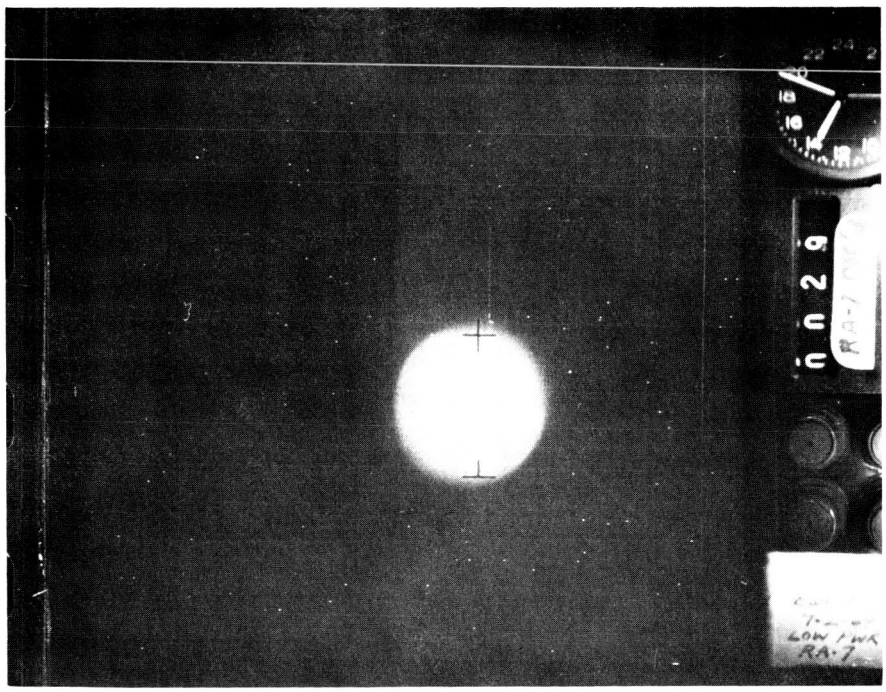

Figure B-15. RFI in F_b-Camera video output during ESA Low-Power Test

the r-f from the high-gain antenna reflecting under the Agena shroud and being detected in the camera front-end. A second test was proposed using the same r-f configuration and using Echo-sorb under the high-gain antenna. This test was the ESA Low-Power Test No. 2 performed on July 2, 1964.

b. Communications Performance

The communications test setup is shown in Figure B-16. There was no Echo-sorb under the high-gain antenna, and the r-f output was transmitted into a steel plate directly under the antenna.

The input to the Transmitter Power Supply was approximately 1.1 volts less than the input voltage to the HCVR in the reduced-power mode which gave an input voltage of 32.2 volts for the F-Channel and 31.8 volts for the P-Channel.

The power profile taken during this test is given in Table B-14.

TABLE B-14
POWER PROFILE TAKEN DURING THE ESA LOW-POWER TEST

Elapsed Time (minutes and seconds)	Power Out at Four-Port Hybrid (milliwatts)
T + 92' 30"	88.5
T + 93'	142.0
T + 93' 30"	159.0
T + 94'	143.0
T + 94' 30"	136.0

c. Power Performance

This test was performed using battery power and the overall performance was normal. The battery profile is given in Table B-15.

d. Telemetry Performance

The low r-f signal level for the first 30 seconds of low-power operation introduced noise in the telemetry. The noise cleared, and the telemetry was observed to be normal.

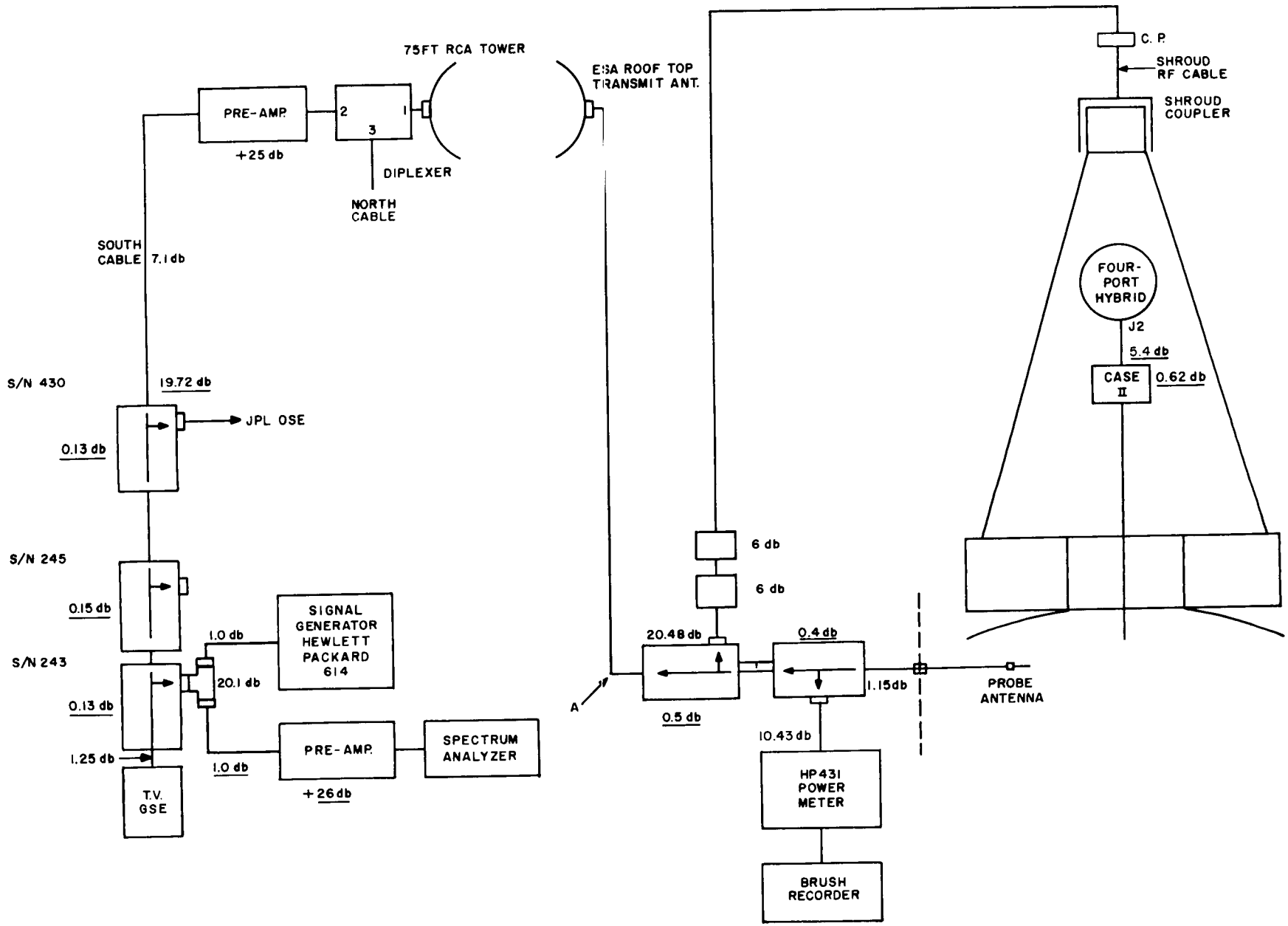

Figure B-16. Test configuration for ESA Low-Power Test

TABLE B-15 BATTERY PROFILE FOR ESA LOW POWER TEST				
Elapsed Time (minutes)	Input to F-Channel HCVR		Input to P-Channel HCVR	
	Voltage (volts)	Current (amperes)	Voltage (volts)	Current (amperes)
T + 83	35.12	-	34.78	-
T + 90	34.02	7.86	33.68	9.37
T + 92	33.87	9.61	33.51	11.95
T + 94	33.32	8.97	32.95	10.85
T + 97	34.57	-	34.51	-

4. *Conclusion*

The r-f type of interference observed in this test lead to the performance of the ESA Low-Power Test, No. 2. The shroud was not removed at this time, therefore, the obstruction in the line-of-sight on the P1-Camera could not be removed. The second low-power test commenced soon after the first low-power test data had been analyzed.

G. ESA Low Power Test No. 2 (JPL Procedure 3R317.02)

1. *Purpose of Test*

The second low-power test was performed on July 2, 1964, to determine whether or not the rfi observed in the video in the first test could be reduced by putting Echo-sorb in the path of radiation from the high-gain antenna.

2. *Description of Test*

The test was performed in the same manner as in the first low-power test. The Spacecraft was seated on the Agena adapter ring with the high-gain antenna nested and the adapter ring was on a metal plate.

3. *Test Evaluation*

a. Video Performance

There was no change in the video characteristics from those observed in the first low-power test at the ESA. The P1-Camera shroud lamp was still not visible to the P1-Camera.

b. Communications Performance

The r-f test setup was the same as that for the Low Power Test No. 1 with the following exceptions: (1) the signal from the JPL omni-antenna was reduced by 6 db, and (2) 2 minutes after reduced power was on, Echo-sorb was placed under the high-gain antenna. The Echo-sorb was not put directly in the radiated beam, because of the limited space between the nested antenna and the metal plate. Therefore, it was of minimal effect in that it only caused the r-f output power level to fluctuate. The input voltage to the Transmitter Power Supplies for the test was 31.8 volts for the F-Channel Power Supply and 31.9 volts for the P-Channel Power Supply.

A power profile taken during this test is given in Table B-16.

TABLE B-16
POWER PROFILE TAKEN DURING LOW-POWER TEST NO. 2

Elapsed Time (minutes and seconds)	Power Out at Four-Port Hybrid (milliwatts)
T + 1' 30"	88.2
T + 2'	90.0
T + 3'	100.0
T + 4'	160.0
T + 5'	135.0
T + 5' 30"	124.0
T + 6'	117.0
T + 7'	106.0
T + 8'	100.0

A power fluctuation of considerable magnitude, recorded at T + 3 minutes, distorted the power profile. This fluctuation was due to the movement of the high-gain antenna when the Echo-sorb was being placed under it.

c. Power Performance

The TV Subsystem was powered by batteries, and the battery profile obtained during the test is given in Table B-17. The voltage is obtained from telemetry at the input to the HCVR.

TABLE B-17
BATTERY PROFILE DURING ESA LOW-POWER TEST NO. 2

Elapsed Time (minutes)	Input to F-Channel HCVR		Input to P-Channel HCVR	
	Voltage (volts)	Current (amperes)	Voltage (volts)	Current (amperes)
T + 0	35.12	-	34.78	-
T + 1	33.60	7.86	33.51	9.37
T + 3	33.47	9.24	33.40	11.95
T + 5	33.04	8.97	32.95	10.85
T + 7	33.00	-	32.80	-
T + 9	34.69	-	34.69	-

The total battery drain for the ESA Low-Power Tests is 2.16 ampere hours for F-Battery, Serial No. 85, and 2.84 ampere hours for P-Battery, Serial No. 76. The overall power performance was normal through the test.

d. Telemetry Performance

The telemetry for this test was normal. The noise observed in the previous tests was not as predominant during this test.

4. Conclusion

After the test had been completed, it was found that the Echo-sorb was not put directly in line with the radiated r-f power from the high-gain antenna, but had been put at the rim of the dish. Because of this placement, there was no noticeable difference in the rfi observed in the video. It was then decided to perform another low-power test at the ESA in which the Spacecraft was to be installed on a stand to eliminate the metal sheet directly under the nested high-gain antenna, and the Echo-sorb material was to be put in line with the radiated r-f power to absorb most of the signal, thereby preventing, as much as possible, signal reflection.

The Agena shroud was removed. It was found that the obstruction in the P1-Camera line-of-sight was the metal liner inside the shroud. The opening that allowed the P1 shroud light to be visible to the P1-Camera was too small. The opening was enlarged and the P1 shroud light was observed in the next text.

H. Special RFI Test (JPL Procedure 3R317.02 Revision 1-A)

1. Purpose of Test

This test was performed at the ESA on July 6, 1964, to determine (1) whether or not the rfi previously observed with the TV Subsystem in reduced-power operation could be reduced by absorbing the r-f output from the high-gain antenna, (2) the repeatability of the rfi, and (3) whether the interference was a flight problem or a test problem.

2. Description of Test

The test configuration was the same as in the Low-Power Test No. 1 with the following exceptions:

- The Spacecraft with the Agena shroud in place was placed on a test stand. The microwave absorbent material, Echo-sorb, was placed under the Spacecraft to absorb the r-f energy radiated from the nested high-gain antenna;

- The signal from the omni-antenna was 3 db less than that obtained in the ESA Low Power Test No. 1; and

- The test was modified so that only the functions required for the operation of the TV Subsystem were exercised.

3. *Test Evaluation*

a. Video Performance

In general, the rfi was less in this test than in the previous low-power tests at the ESA. The P1-Camera video output was normal with very few noise spikes observed (less than 10 percent of the recorded frames showed these spikes). The shroud light was clearly visible, and the camera operation was normal.

The P2- and P4-Camera video output was normal.

The P3-Camera video output exhibited a strong r-f type of interference, and there was no decrease in the amount of interference throughout the test. A typical example of the interference observed throughout the test is shown in Figure B-17.

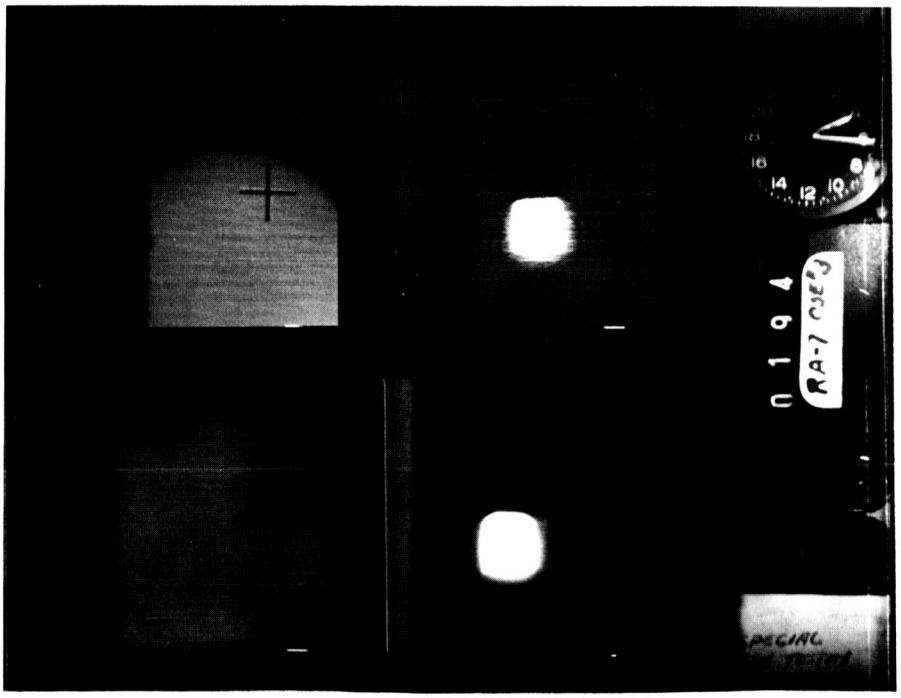

Figure B-17. P3-Camera video output with interference during the Special RFI Test

At the start of the test, when the TV communications power output was low, the F_a-Camera video output exhibited large amounts of rfi. The interference took the form of a checker-board pattern in the background with marks similar to noise spikes appearing throughout the picture as shown in Figure B-18a. As the communications power output increased, the r-f type of interference lessened. The background pattern became insignificant and did not interfere with the picture quailty, and the marks disappeared as shown in Figure B-18b.

The F_b-Camera video output had the same interference as that in the output of the F_a-Camera. When the power output was low, the rfi was very strong and the quality of the received video signal was poor. The checker-board pattern in the background and the multiple noise-spike type of marks were clearly visible. As the power output increased, the r-f type interference was reduced to an insignificant level. See Figure B-19 for a sample of the F_b-Camera video output.

Evaluation of the video output after this test indicated that this interference was probably a test problem. The high-frequency interference observed in the P3-Camera did not appear to be controlled by the absorbent placed in the path of the r-f radiated power (from the high-gain antenna). However, the repeatability in the low-power test indicated that it was not a flight problem. It was noted that in full-power operation, the video output did not exhibit this r-f type of interference.

b. Communications Performance

The r-f test configuration is shown in Figure B-20. The Spacecraft was installed on a stand with the Echo-sorb under the nested antenna. The input voltage to the Transmitter Power Supplies was minus 31.0 volts for F-Channel and minus 31.1 volts for P-Channel. The power profile for this test is given in Table B-18.

TABLE B-18
POWER PROFILE TAKEN DURING THE SPECIAL RFI TEST

Elapsed Time (minutes and seconds)	Power Output at Four-Port Hybrid (milliwatts)
T + 91' 30"	88
T + 93'	147
T + 94'	140
T + 95'	130

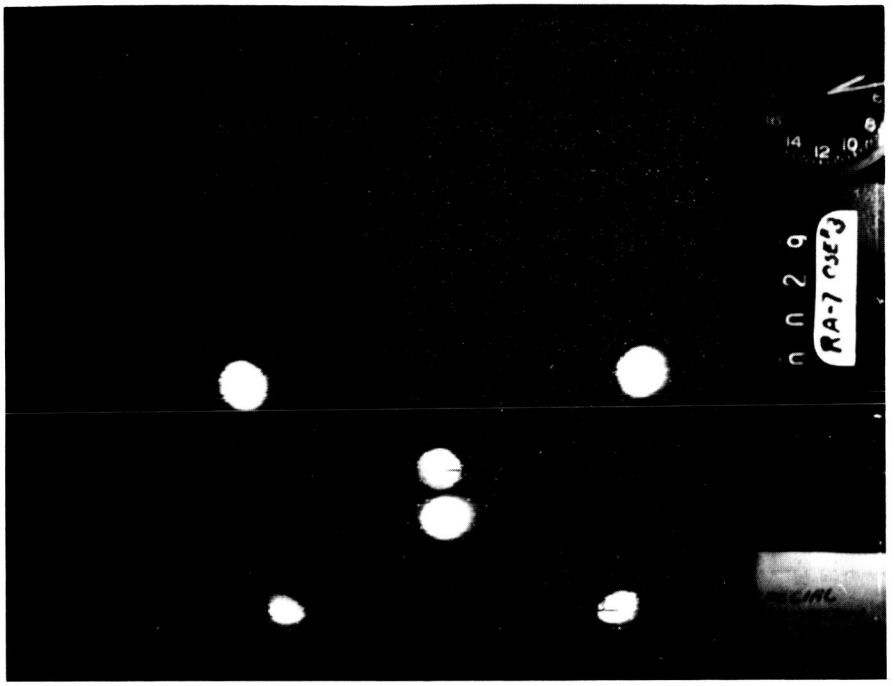

a. With interference

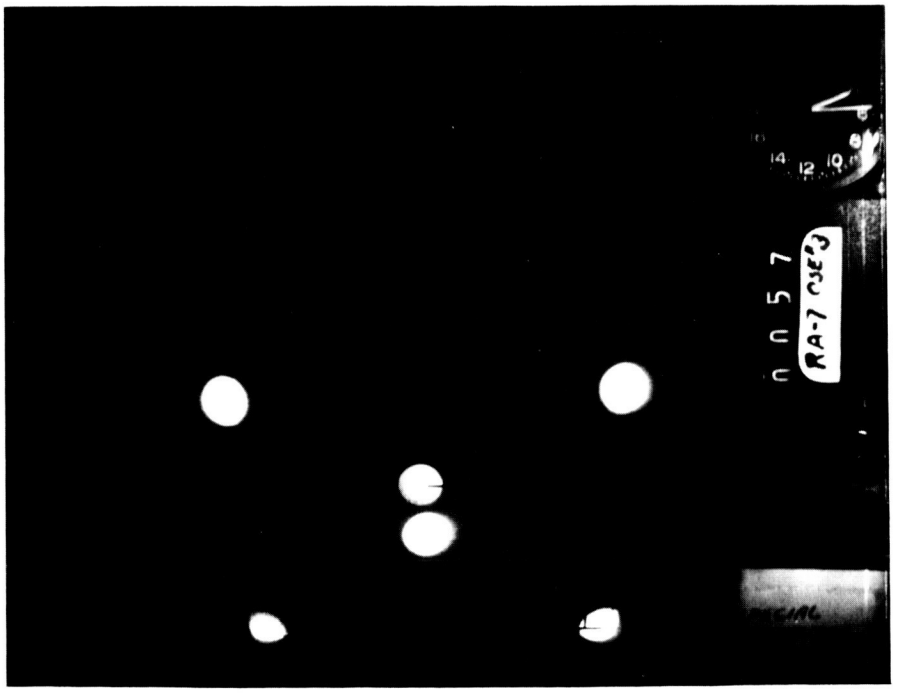

b. Without interference

Figure B-18. F_a-Camera video output during the Special RFI Test

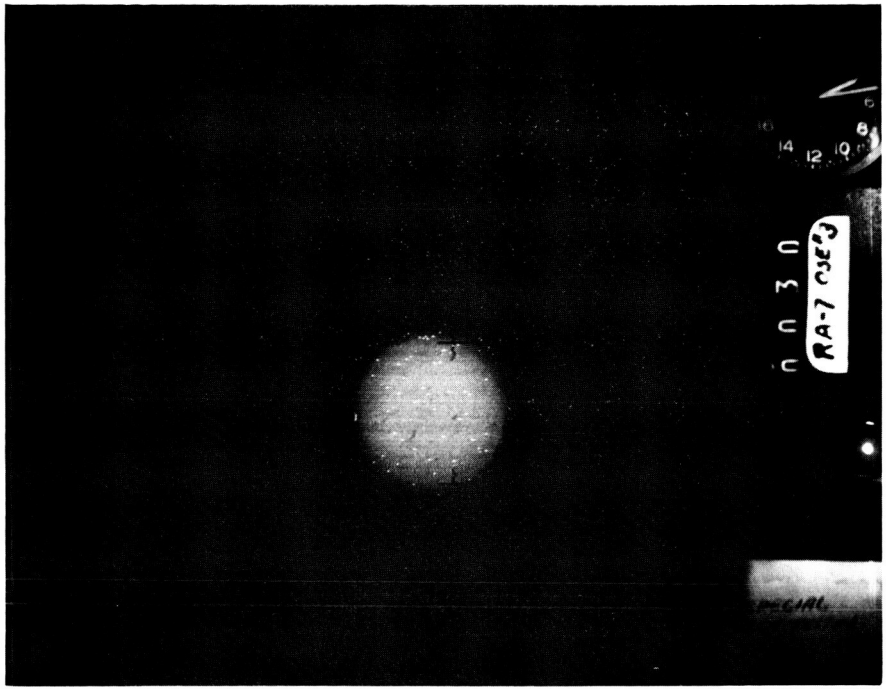

a. With interference

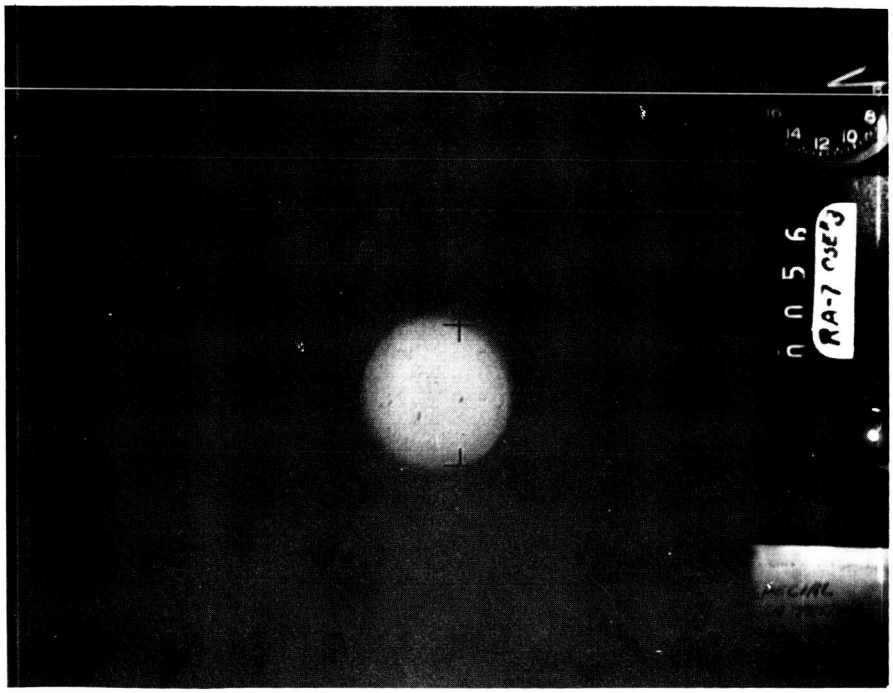

b. Without interference

Figure B-19. F_b-Camera video output during Special RFI Test

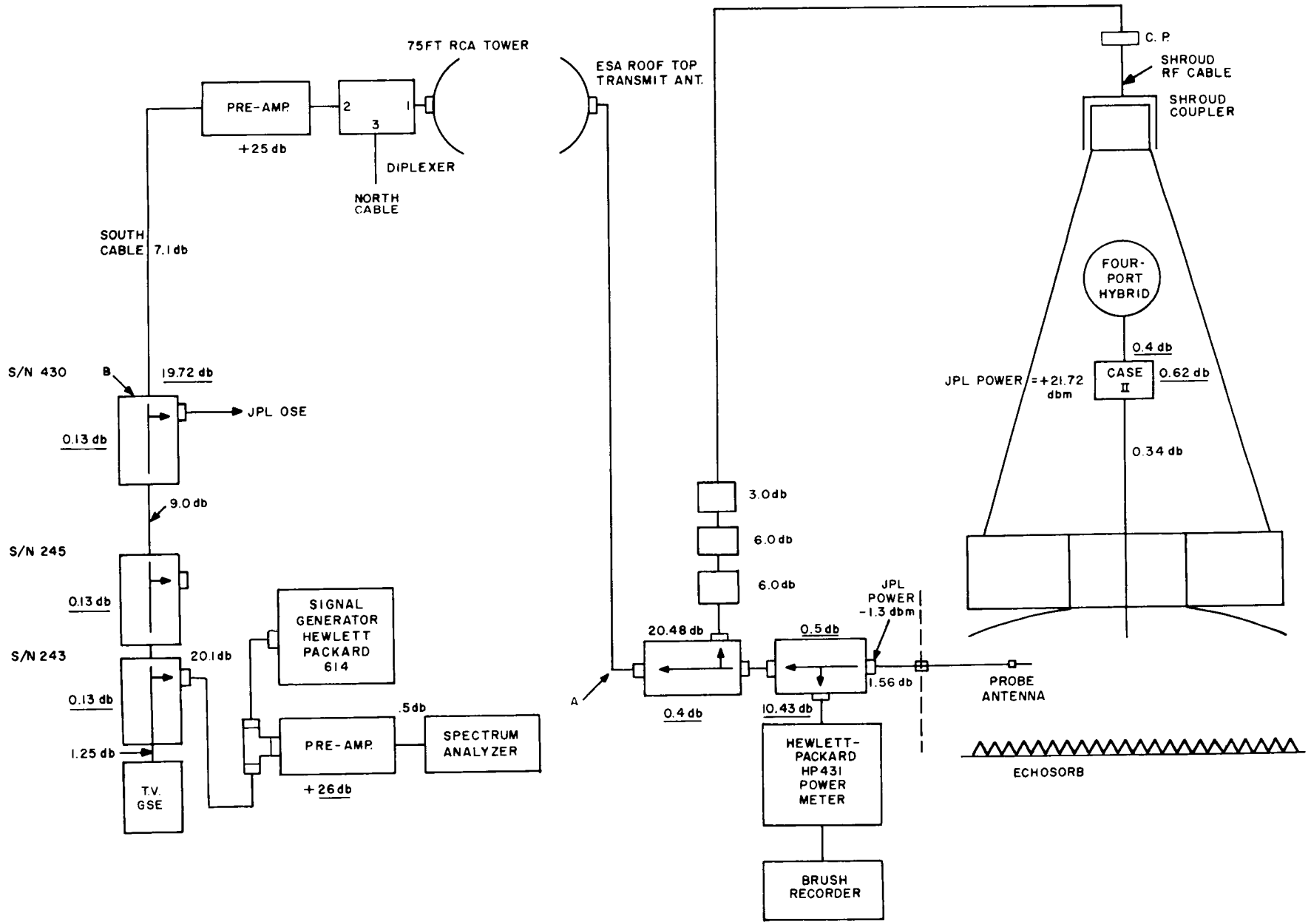

Figure B-20. Test configuration for ESA Television Reduced Power test

The TV communications equipment was turned off at T + 95 minutes 30 seconds.

c. Power Performance

The profile of the input voltage and current to the HCVR is given in Table B-19.

TABLE B-19
BATTERY PROFILE FOR SPECIAL RFI TEST

Elapsed Time (minutes)	Input to F-Channel HCVR		Input to P-Channel HCVR	
	Voltage (volts)	Current (amperes)	Voltage (volts)	Current (amperes)
T + 90'	35.12	0	34.78	.15
T + 91'	33.60	7.49	33.25	9.37
T + 93'	33.75	9.24	33.40	11.95
T + 94' 30"	33.04	8.97	32.95	10.85
T + 95' 30"	33.29	0	33.04	0
T + 96'	34.72	0	34.69	0

The battery drain during this test was 1.12 ampere-hours for F-Battery, Serial No. 85, and 1.38 ampere-hours for P-Battery, Serial No. 76.

d. Conclusions

It was determined that the interference would be present whenever the TV Subsystem was subjected to reduced power under the Agena shroud, that the interference was repeatable and thus could be anticipated, and that the interference was reduced with a stronger TV communication r-f signal.

The Spacecraft was taken to the launch pad in preparation for the Precountdown Test.

I. Precountdown Dummy Run (JPL Procedure 3R304.04)

This test was performed on July 6, 1964, with the Spacecraft mated for the first time to the Atlas-Agena vehicles and in place on the launch pad.

1. Purpose of Test

The objectives of the precountdown dummy run were to:

- Verify that the Spacecraft operates properly when controlled by the Launch Checkout Equipment;
- Verify by a series of checks that the spacecraft is ready for the countdown; and
- Check out the procedures that are to be used during the final launch operations.

2. Description of Test

a. Spacecraft Configuration

The TV Subsystem was in full flight configuration at this time with the following exceptions:

- Non-flight batteries were used;
- The bottom mylar shield and camera aperture mylar shield were non-flight items;
- Final potting and tie-down had not been performed; and
- The thermal shrouds were protected with strip-coat.

The Spacecraft was mated to the Atlas-Agena vehicles, which were in place on the launch pad, Complex 12. The Spacecraft was controlled by the Launch Checkout Equipment in the blockhouse by means of the umbilical connectors. Reduced-power jumper wires in the Umbilical Tower J-Box prevented TV Subsystem operation in full power. A radio link between the umbilical tower and a tower at the Ranger area transferred the TV signal picked up by a probe in the Agena to the OSE equipment in the hanger for

display. The monitor and test direction functions were performed at the hanger facility. Telemetry information was provided at the hanger by either a hardline signal from Spacecraft, or by an r-f signal sent by radio link from the launch pad antennas to the Deep Space Instrumentation Facility trailer and then by hardline to the hanger area. The cameras were illuminated by lights in the Agena Shroud.

b. Test Procedure

The test was performed using the sequence of events given in Table B-20. The gantry tower remains in place during the entire Precountdown Test.

TABLE B-20

SEQUENCE OF EVENTS DURING PRECOUNTDOWN DUMMY RUN

Elapsed Time (minutes and seconds)	Operation
T + 84'	The Cruise On Test switch on the blockhouse panel was depressed twice. This resets the Clock, turns on cruise-mode telemetry, and removes the external arming of the gates.
T + 88'	RTC-7 command. The TV Subsystem is not turned on since the gates are not armed. This is a special check to verify that the SCR gates are properly disabled through the arming system in the Spacecraft prior to launch.
T + 89'	The Cruise On Test switch is depressed once to permit Subsystem turn-on upon receipt of the next RTC-7 command.
T + 90'	An RTC-7 command puts both channels in Reduced-Power Warmup.
T + 90' 10"	The Cruise On Test switch is depressed once (normal position).
T + 91' 20"	Both channels are put in reduced power by the TV Sequencer Command (CC and S).
T + 95'	An RTC-5 command turns off both channels.
T + 96'	The Cruise Off switch in the blockhouse panel is depressed to turn off Channel-8 cruise-mode telemetry.

3. Test Evaluation

a. Video Performance

The evaluation of camera performance when the Spacecraft is on the launch pad is difficult because of the limitations of shroud-light illumination. Therefore, the best judgment of the video output at this time was that all cameras saw the lights and were in a "go" condition. As expected, rfi type noise, similar to that reported in the ESA Low Power Tests, was observed in the video output for the P3-, F_a-, and F_b-Cameras and is shown in Figure B-21. The video output from the P3 and F_a-Cameras had an appreciable amount of noise throughout the test run. The noise on the F_b-Camera video output was appreciable at the beginning of the run, but diminished appreciably before turn-off. There was no significant amount of rfi on video outputs of the P1-, P2-, and P4-Cameras. This rfi noise was found to be due to the non-flight configuration of the Spacecraft enclosed within the Agena structure and, therfore, not a major concern for launch. Further investigations during the Combined RFI Test and the Joint Flight Acceptance Composite (J-Fact) Test led to the conclusion that this condition was caused by the signal from the omni-antenna reflecting within the metal-lined Agena shroud and interacting with the video signals.

b. Communications Performance

The TV Subsystem was operated on the launch pad in reduced power only. The r-f test configuration for the Precountdown Dummy Run is shown in Figure B-22. No r-f power measurements were obtained for this test. When the TV Subsystem is in reduced-power mode, the beacon signal, if radiated from the same high-gain antenna, exceeds the video signal by about 10 db, and the video OSE receiver locks on the beacon, preventing proper detection of the video. To preclude this possibility, the beacon signal was radiated from the omni-antenna during the entire turn-on portion of the Precountdown Dummy Run. With the 26-db pad installed between the slot coupler and gantry antenna, adequate reduction of the beacon signal (about 15 db below the video signal) was assured. However, in this mode of operation, the rfi noise caused by the signal radiated from the omni-antenna reflecting within the Agena Shroud occurred on the video.

In reduced-power operation, F-Channel was slower than P-Channel in coming up to normal signal strength. As a result, the F-Camera video signals were noiser at the beginning of the test run.

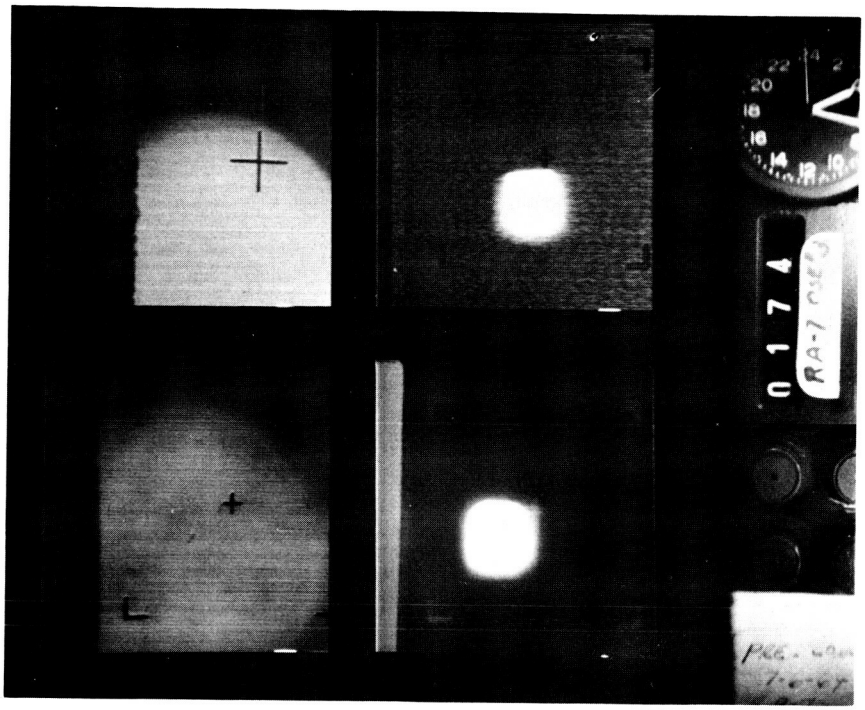

a. P3-Camera video

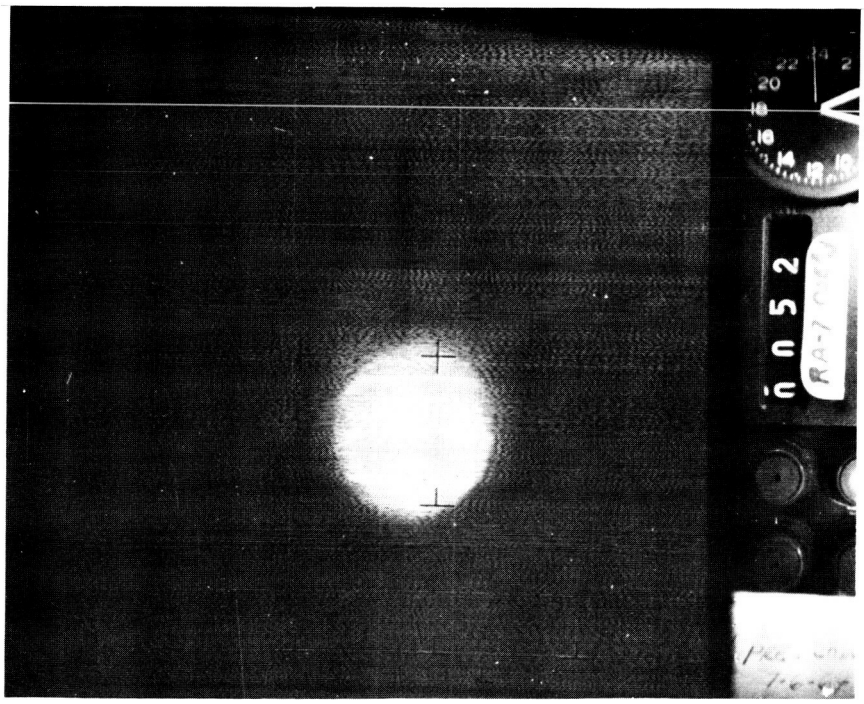

b. F_a-Camera video

Figure B-21. Video Interference during Precountdown Dummy Run

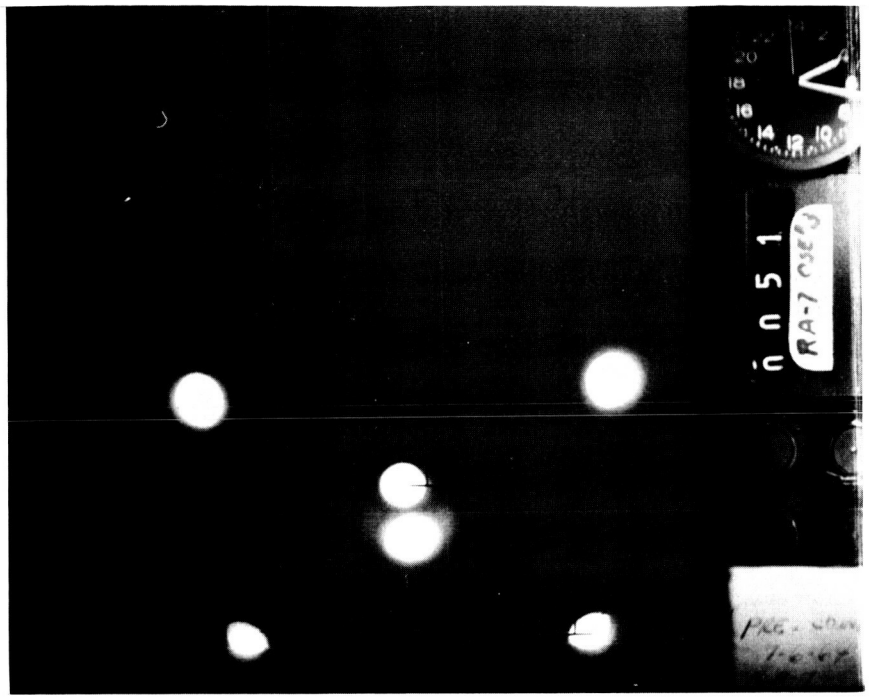

c. F_b-Camera video

Figure B-21. Video interference during Precountdown Dummy Run (Continued)

c. Power Performance

The TV Subsystem was powered by F-Battery, Serial No. 85, and P-Battery, Serial No. 76, during this Precountdown Dummy Test. These batteries were the same batteries that were used during testing at the ESA. The battery voltages were monitored at the blockhouse panel with digital voltmeters. Assuming a 1.5-volt drop across the SCR and associated wiring, the approximate inputs to the Transmitter Power Supplies were derived and are shown in Table B-21. The battery performance was normal. The total battery discharge for this test was 1.12 amperes for F-Battery and 1.36 amperes for P-Battery.

d. Telemetry Performance

The telemetry performance was normal.

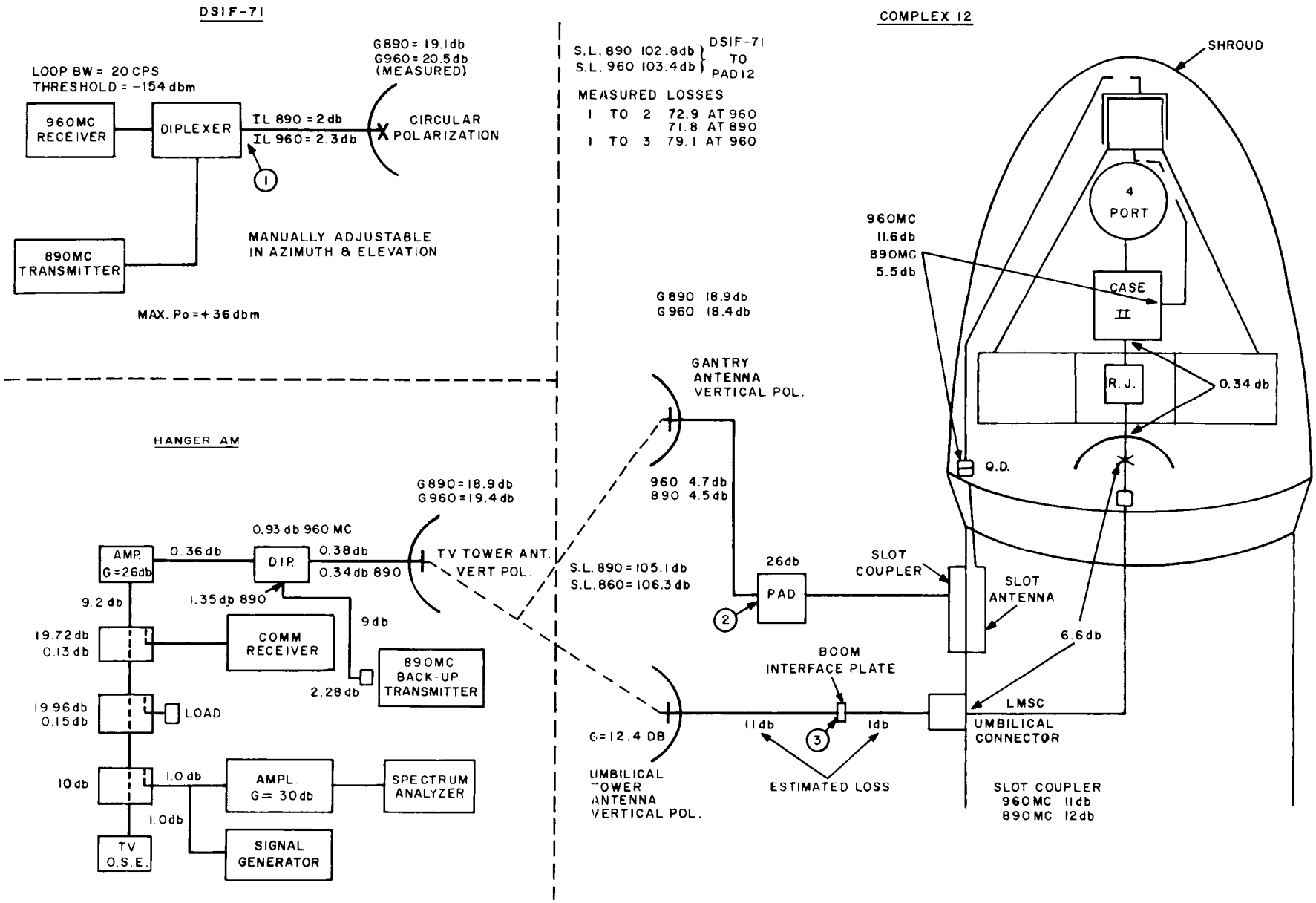

Figure B-22. RF Test configuration for Precountdown Dummy Run

TABLE B-21 INPUT VOLTAGE PROFILE DURING PRECOUNTDOWN DUMMY RUN					
Time (minutes and seconds)	Measured Input to HCVR		Computed Input to Transmitters		Operating Mode
	F-Battery (volts)	P-Battery (volts)	F-Channel (volts)	P-Channel (volts)	
-	35.12	35.89	-	-	TV System Off
-	35.49	35.25	-	-	Cruise On
T + 90'	34.22	33.69	32.7	32.2	RTC-7 Warmup
T + 91'	33.67	33.44	32.1	32.0	RTC-7 Warmup
T + 91' 20"	33.44	33.23	32.0	31.7	Reduced Power
T + 92'	33.35	33.15	31.8	31.7	Reduced Power
T + 93'	32.29	33.07	31.8	31.6	Reduced Power
T + 94'	33.25	33.00	31.8	31.5	Reduced Power
T + 95'	33.19	32.95	31.7	31.5	Reduced Power
T + 96'	34.49	34.39	-	-	RTC-5 Off
-	34.70	34.60	-	-	Cruise Off

4. *Conclusions*

The TV Subsystem gave adequate evidence of its compatibility with the launch facility interfaces and of its readiness to continue into the subsequent testing sequences.

J. ETR Combined Radiation Test (JPL Procedure 3R310.02)

1. *Purpose of Test*

The objectives of the ETR Combined Radiation Test, performed on July 7, 1964, at Complex 12, were:

- To verify, by exposure of the Spacecraft to all Atlas, Agena, and ETR offboard radiation sources with the gantry tower removed, that no r-f incompatibilities exist, and

- To observe the r-f signal strengths between the Deep Space Instrumentation Facility trailer and Ranger Spacecraft with the gantry tower in place and with the tower removed.

2. Description of Test

a. Spacecraft Configuration

The Spacecraft configuration for the Combined Radiation Tests was the same as that for the Precountdown Dummy Run Test.

b. Test Procedure

The test was performed in two parts. Part I ran from T-130 minutes to T-60 minutes. During this time, the TV Subsystem was not operated and r-f signal strengths were measured with the gantry tower in position. Part II began at T-60 while the gantry tower was being moved. All Atlas and Agena r-f sources were on at the start of this second part. By T-55, the gantry had been removed from the pad. The test sequence is given in Table B-22.

TABLE B-22
SEQUENCE OF EVENTS DURING THE COMBINED RADIATION TEST

Elapsed Time (minutes and seconds)	Operation Function
T - 39'	Beacon signal was transferred to the directional antenna.
T - 39'	The Cruise On Test switch on the blockhouse panel was depressed. This turns on cruise-mode telemetry, resets the clock, and arms the SCR gate circuits.
T - 37' 20"	RTC-7 command. Both channels placed in Reduced Power Warmup.
T - 36'	Both channels placed in reduced power by the Sequencer command.
T - 35' 30"	The beacon signal was transferred from the directional antenna to the omni-antenna.
T - 31'	RTC-5 command. Both channels turned off.
T - 30'	The Cruise On Test switch was depressed (normal position). The Cruise Off switch was actuated to turn off Channel-8 cruise-mode telemetry.

3. Test Evaluation

a. Video Performance

A variation in the test procedure was initiated to determine the contribution of the JPL beacon signal to the video rfi noise problem that had been observed during the previous reduced-power tests. This variation consisted of switching the beacon signal from the high-gain antenna to the omni-antenna shortly after the TV Subsystem came on in reduced power to obtain minimum beacon power during the transition period.

When radiated from the high-gain antenna, the beacon signal was approximately 7 db above the F-Channel power and 5 db above the P-Channel power. This resulted in extremely noisy video output on both channels, particularly on F-Channel video, which could not be satisfactorily detected.

After antenna switchover, as the beacon level to the high-gain antenna dropped off, but before the signal from the omni-antenna could build up, the video signal was observed to clear up for a short interval. Almost no rfi type noise was discernible on either the F- or P-Channel video outputs during this null period. As the signal from the omni-antenna began to build up in intensity, the video output became noisier and exhibited rfi noise characteristics similar to those observed during previous tests. This operation satisfactorily unmasked the clutter introduced into the video signal by beacon signal, interaction and provided clear evidence (all cameras saw the shroud lights) of satisfactory camera performance. Figures B-23 through B-25 are representative frames of video taken during this test procedure.

b. Communications Evaluation

The TV Subsystem was operated in reduced power with the r-f test configuration shown in Figure B-22. This configuration is similar to that used during the Precountdown Dummy Test with the exception that the gantry tower was removed during TV operation for the Combined RFI Test. Lacking the gantry antenna and associated feed lines, the Agena Shroud hat coupler radiated the signal from the omni-antenna directly to the hanger without benefit of additional padding to control the signal strength ratio between beacon and video signals. Under this condition, measurements with a spectrum analyzer indicated that the beacon signal strength was approximately 8 db below that of P-Channel and 3 db below F-Channel.

The Subsystem r-f power received at the hanger facility was too weak to be measured with the power meter. All power observations, therefore, were made at the spectrum analyzer, which provided information that r-f reduced power was normal for this test.

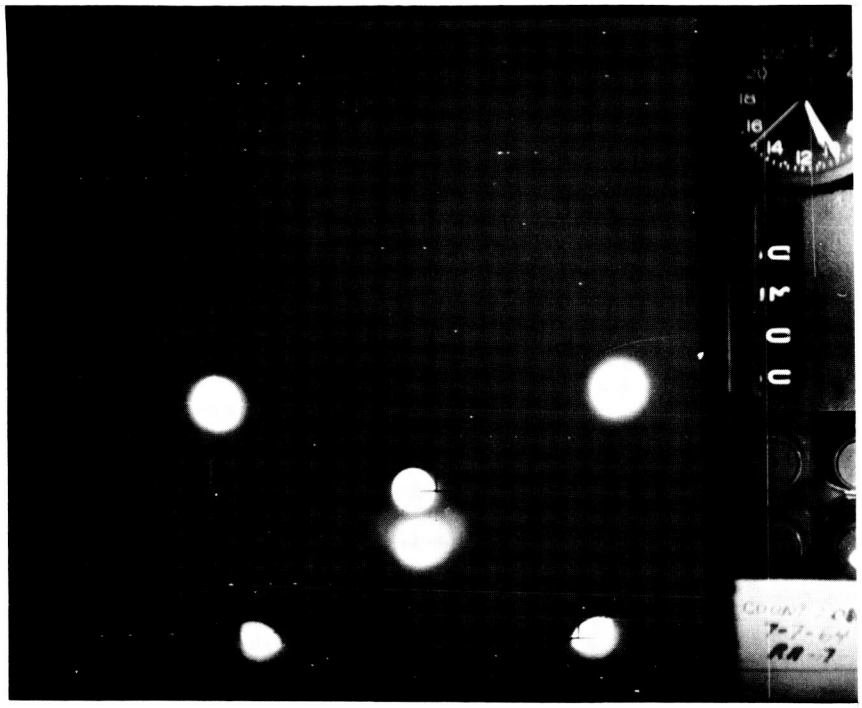

a. F_a-Camera

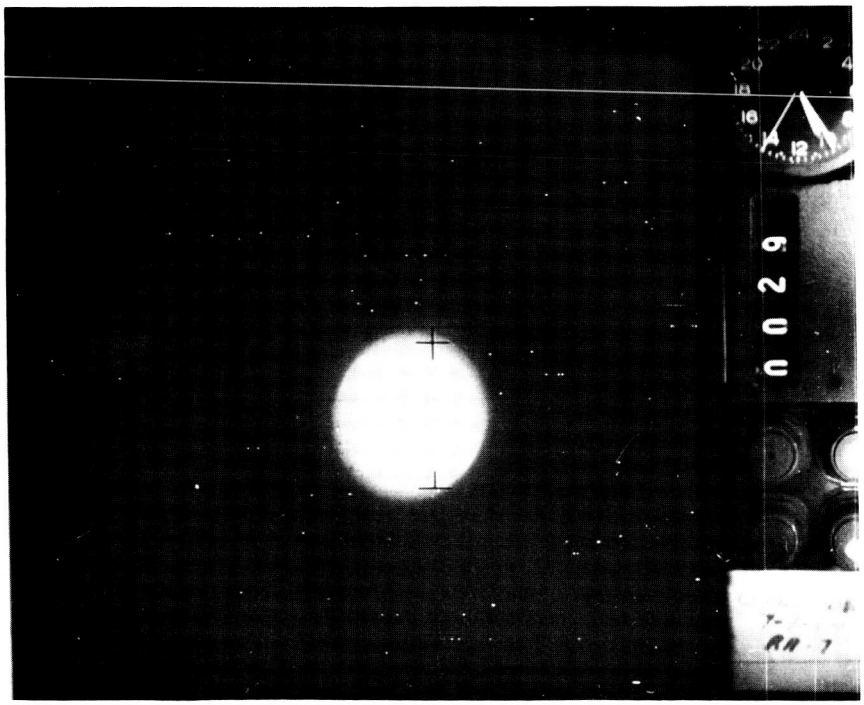

b. F_b-Camera

Figure B-23. Video signal near antenna null during Combined Radiation Test

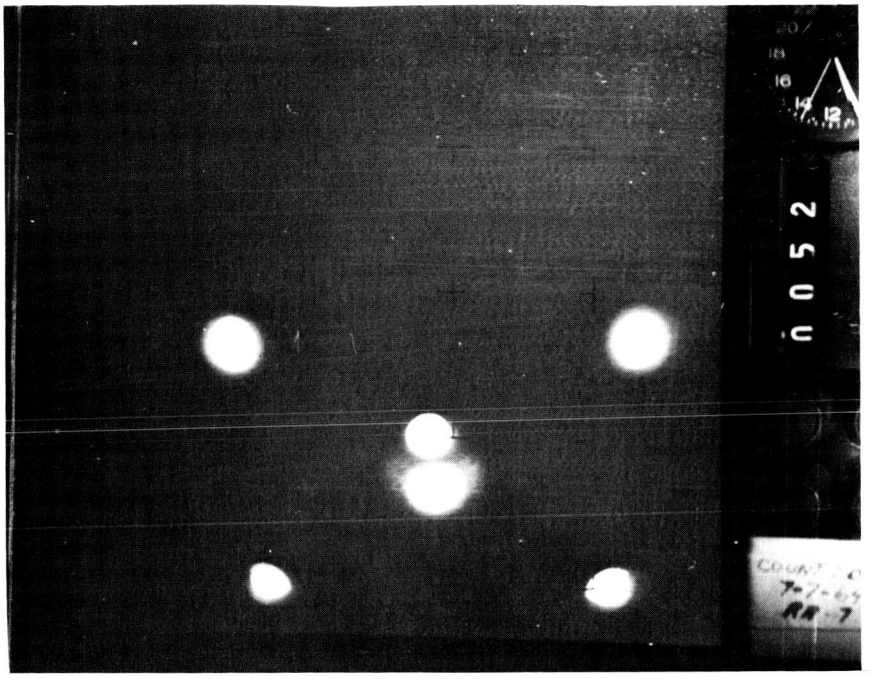

a. F_a-Camera

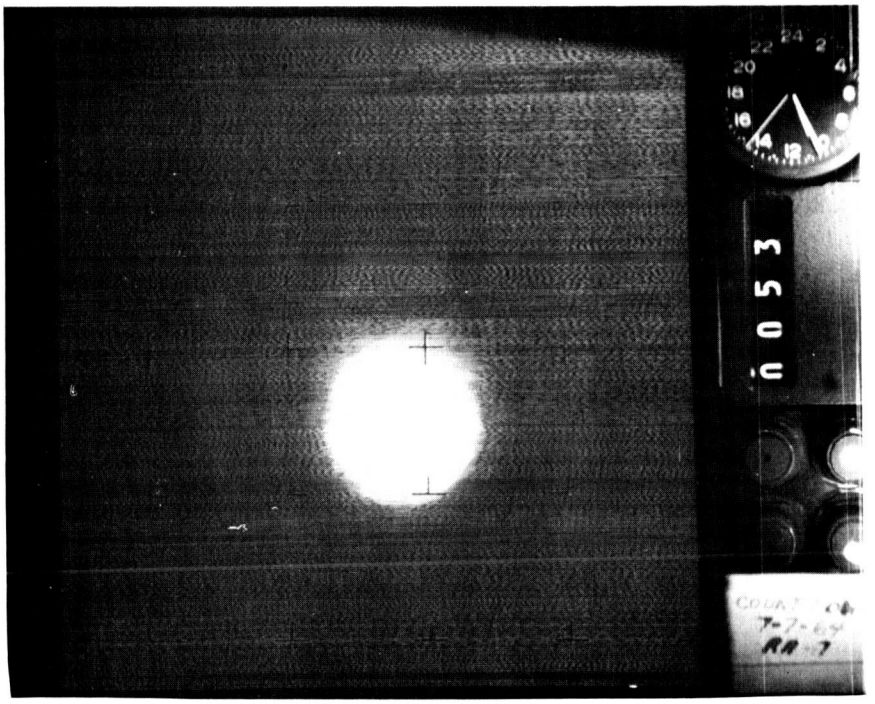

b. F_b-Camera

Figure B-24. Video signal after null during Combined Radiation Test

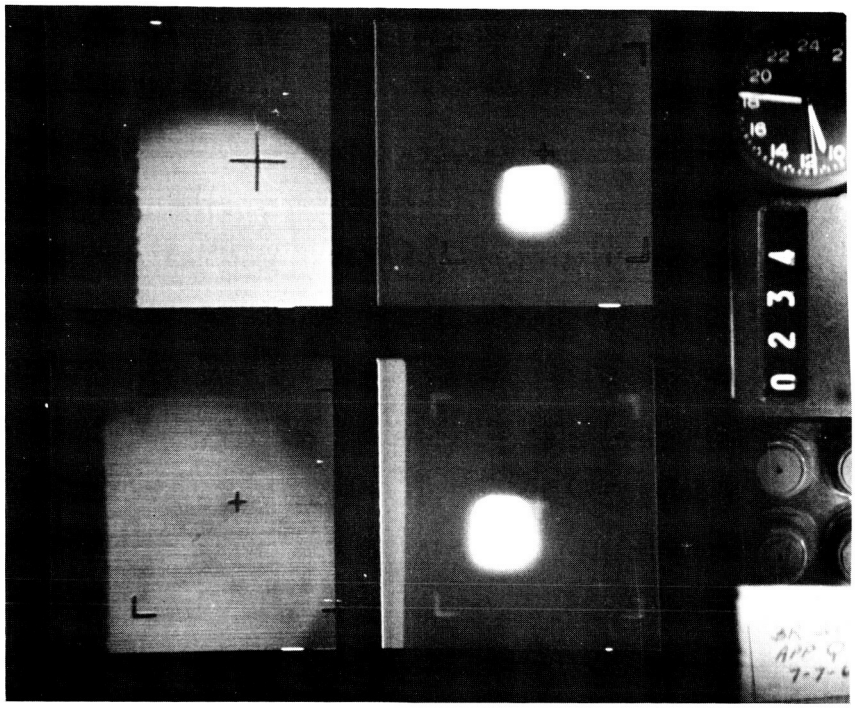

a. Signal near null

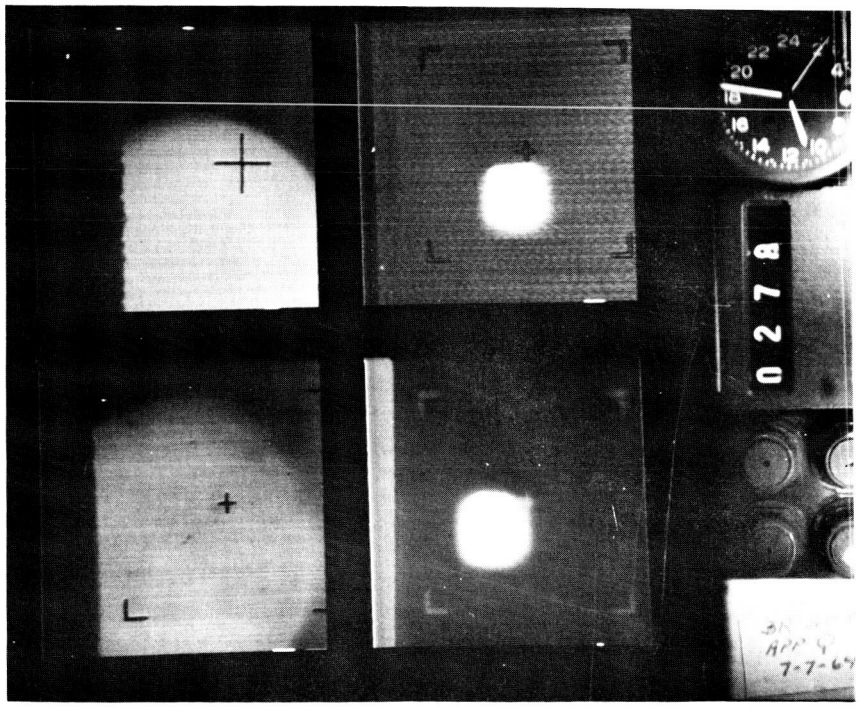

b. Signal after null

Figure B-25. P-Camera video during Combined Radiation Test

c. Power Performance

The TV Subsystem was powered by the F-Battery, Serial No. 85, and the P-Battery, Serial No. 76. Battery voltages and corresponding computed Transmitter Power Supply inputs are shown in Table B-23. Battery performance was normal. The total battery discharge for this test was 1.12 amperes for F-Battery and 1.36 amperes for P-Battery.

d. Telemetry Performance

The telemetry performance was normal.

TABLE B-23
INPUT PROFILE DURING THE COMBINED RADIATION TEST

Time (minutes)	Measured Input to HCVR		Computed Input to Transmitters		Operating Mode
	F-Battery (volts)	P-Battery (volts)	F-Channel (volts)	P-Channel (volts)	
T - 100	35.07	35.00	-	-	TV System Off
T - 39	35.45	35.23	-	-	Cruise On
T - 37	34.09	33.89	32.6	32.4	RTC-7 Warmup
T - 36	33.90	33.53	32.4	32.0	Warmup
T - 35	33.60	33.43	32.1	31.9	Reduced Power
T - 34	33.55	33.33	32.1	31.8	Reduced Power
T - 33	33.49	33.29	32.0	31.8	Reduced Power
T - 32	33.44	33.24	31.9	31.7	Reduced Power
T - 31	33.40	33.21	31.9	31.7	Reduced Power
T - 30	34.50	34.41	-	-	System Off
T - 0	34.95	34.88	-	-	System Off

4. Conclusions

By transferring the beacon signal from directional antenna to omni-antenna during TV Subsystem operation, sufficient reduction of interference was obtained to permit a more effective evaluation of camera performance. The rfi null period was of brief duration during this run since the transfer operation was begun before the r-f power levels were near optimum.

This same technique was employed for all future reduced-power tests on RA-7, but the transfer started later to produce a broad-null period. This test provided clear indication that the rfi type noise observed on the video signals was caused by beacon signal interference. However, the location for this interaction, the Spacecraft or ground receiver, could not be conclusively isolated.

K. Joint Flight Acceptance Composite Test (J-Fact) (JPL Procedures 3R309.05 and 3R307.02)

Following the ETR Combined Radiation Test, a Countdown Dummy Run was executed only on the Spacecraft on July 8, 1964, using JPL Procedure 3R309.05. The Countdown sequence of events was followed, but actual operations were not performed and the TV Subsystem was not turned on.

The Joint Flight Acceptance Composite Test (J-Fact) test was performed on July 10, 1964. This test is similar to the Countdown Dummy Run. However, all launch facilities were employed according to a Master J-Fact Countdown, and the TV Subsystem was operated.

1. Purpose of Test

The objectives of the J-Fact test are:

- To demonstrate that no incompatibilities exist between the Spacecraft and the Atlas and Agena vehicles;
- To verify that the procedures that are to be used during the launch operations are compatible; and
- To verify proper Spacecraft operation while the Spacecraft is assembled to the Atlas and Agena vehicles with the umbilical plug removed and in plus time (after simulated launch).

2. Description of Test

a. Spacecraft Configuration

The configuration of the Spacecraft for the J-Fact Test is unchanged from previous launch pad tests.

b. Test Procedure

The test was performed using the sequence of events given in Table B-24.

TABLE B-24
SEQUENCE OF EVENTS DURING J-FACT TEST

Elapsed Time (minutes and seconds)	Operation Function
T - 116	The Cruise On Test switch on the blockhouse panel was actuated. This operation turns on cruise-mode telemetry, resets the Clock, and arms the SCR gate circuits.
TV = 0	RTC-7 command. Both F- and P-Channels placed in Reduced-Power Warmup.
TV + 30"	The Cruise On Test switch was depressed (normal position).
TV + 1' 20"	Both channels placed in reduced-power operation by the Sequencer command.
TV + 2' 20"	The beacon signal was transferred from directional antenna to omni-antenna.
TV + 6' 20"	RTC-5 command. Both channels turned off.
TV + 7	The Cruise Off switch was actuated to turn off Channel-8 cruise-mode telemetry.
TV - 15	The Cruise On Test switch was depressed twice. This turns on cruise mode, resets the Clock. It does not enable the SCR turn-on circuitry.
T = 0	Simulated launch. The umbilical plug was removed.
T + 23	Umbilical plug was re-inserted.
after T + 23	The Cruise Off switch was actuated to turn off Channel-8 cruise-mode telemetry.

3. Test Evaluation

a. Video Performance

At the beginning of reduced-power operation, noise appeared on F- and P-Camera video signals. The noise was severe on the F-Channel video output. This noise cleared up during the beacon signal strength minimum that occurred after switchover. As the power from the omni-antenna increased, the video noise increased and exhibited the characteristics of r-f interference.

To further investigate the source of this video noise, a special operation, not a normal part of the J-Fact test, was performed in which the gantry antenna was disconnected from the coupler for the omni-antenna by removing the 25-db pad inserted in the line between the gantry antenna and the slot coupler and by terminating the coaxial cable from the slot coupler. These modifications caused the beacon signal level as received at the ground station to decrease by a maximum of 8 db (source signal was still received due to stray radiation from the slot antenna) without causing any significant change in the rfi type noise observed on the video signals. This operation was performed at approximately TV + 3:40 (well after the signal strength from the omni-antenna had increased to its normal value). About 1 minute later, the slot and gantry antennas were reconnected, but without inserting the original 26-db pad. The resultant high beacon signal strength caused the loss of F-Channel video and caused high noise on P-Channel video as observed at TV OSE. Selected frames of F- and P-Camera video outputs are presented in Figures B-26 to B-30.

These photographs, particularly those taken during the beacon null, indicate that all cameras were operating in a normal manner.

b. Communications Evaluation

The r-f test configuration was the same as that for the previous launch pad test except for the period that the gantry antenna was disconnected from the slot coupler. The gantry tower remained in position at the pad throughout the test. The r-f power received at the hangar was monitored with a spectrum analyzer and compared with the beacon signal strength. The relative amplitudes of F-Channel signal and beacon signal are shown in Figure B-31. Note that before the antenna switchover of the beacon signal to the omni-antenna, the beacon strength on directional antenna is greater than the F- and P-Channel signal strengths causing severe noise on both these channels and preventing satisfactory detection of the F-Camera video signal. When the beacon signal was transmitted from the omni-antenna, but without the +26-db pad between gantry antenna and slot coupler, the beacon signal was stronger than the video signals and prevented F-Channel video detection at the ground receiver. During the time the coaxial line to the gantry antenna was disconnected, the beacon signal

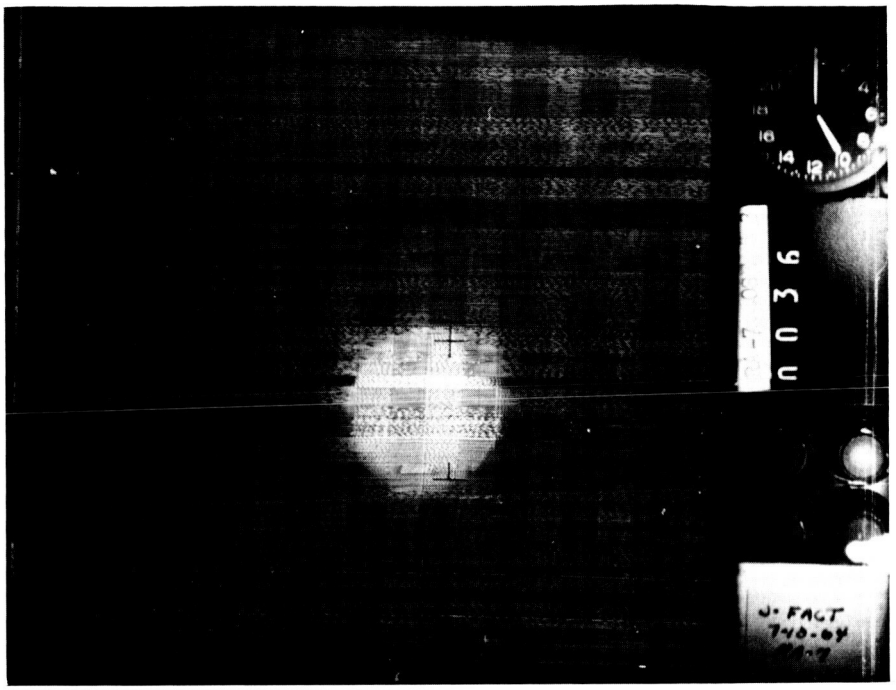

a. F_a-Camera

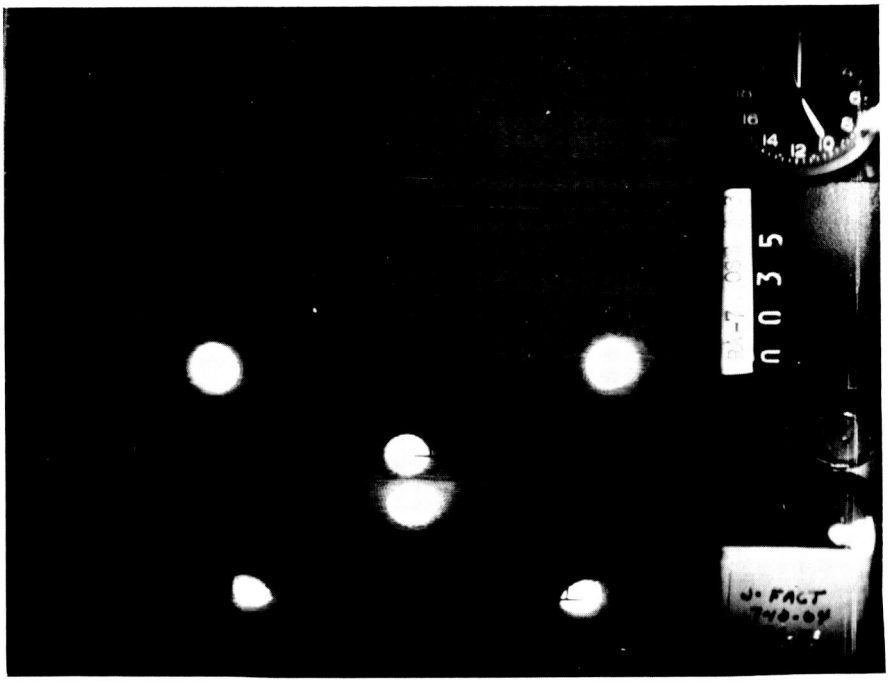

b. F_b-Camera

Figure B-26. Video signals before the gantry antenna is disconnected during J-Fact Test

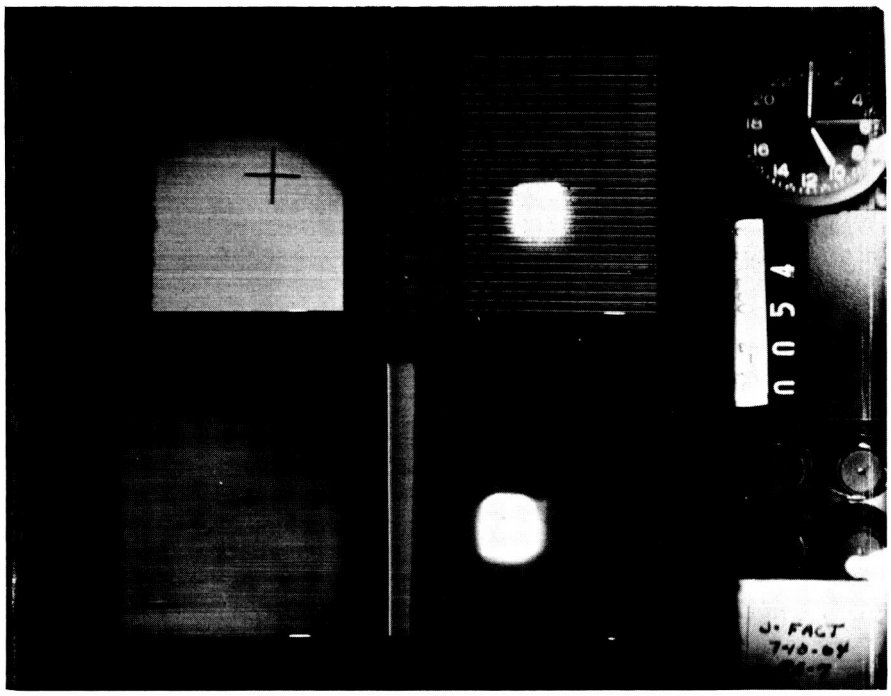

a. F_a-Camera

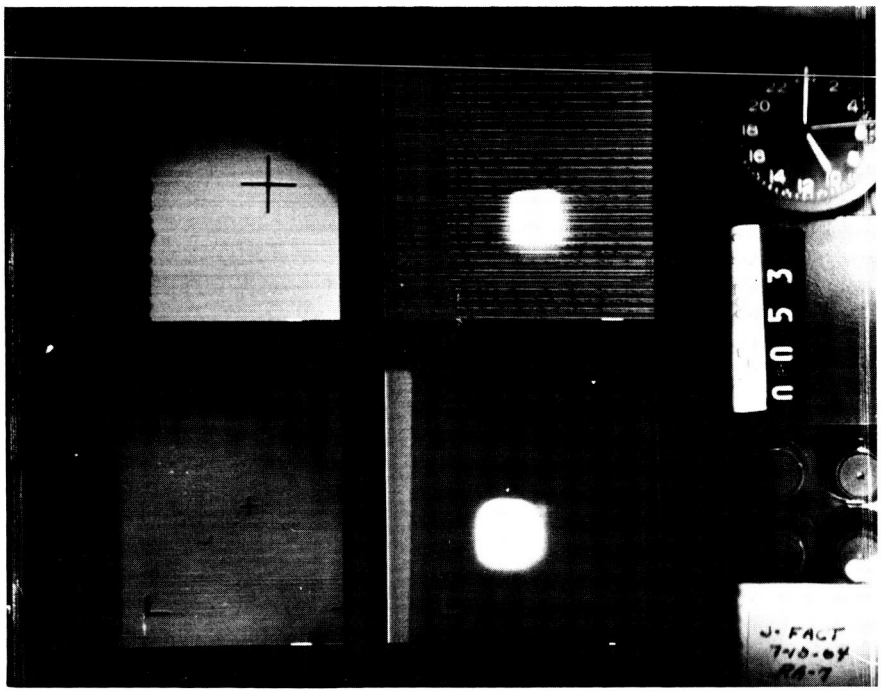

b. F_a-Camera

Figure B-27. Video signal after the gantry antenna is disconnected during J-Fact Test

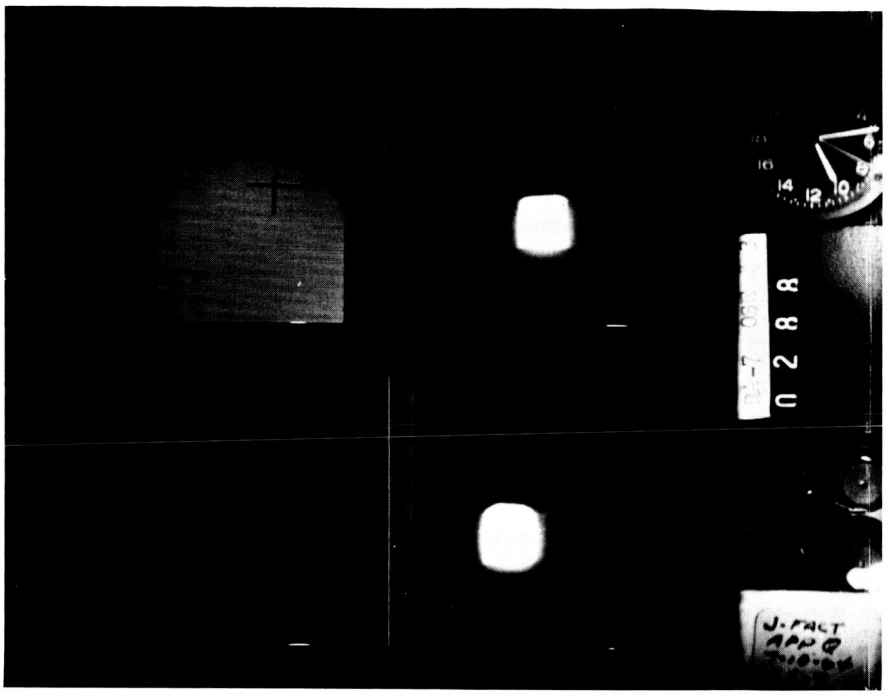

Figure B-28. P-Camera video at beacon minimum during J-Fact Test

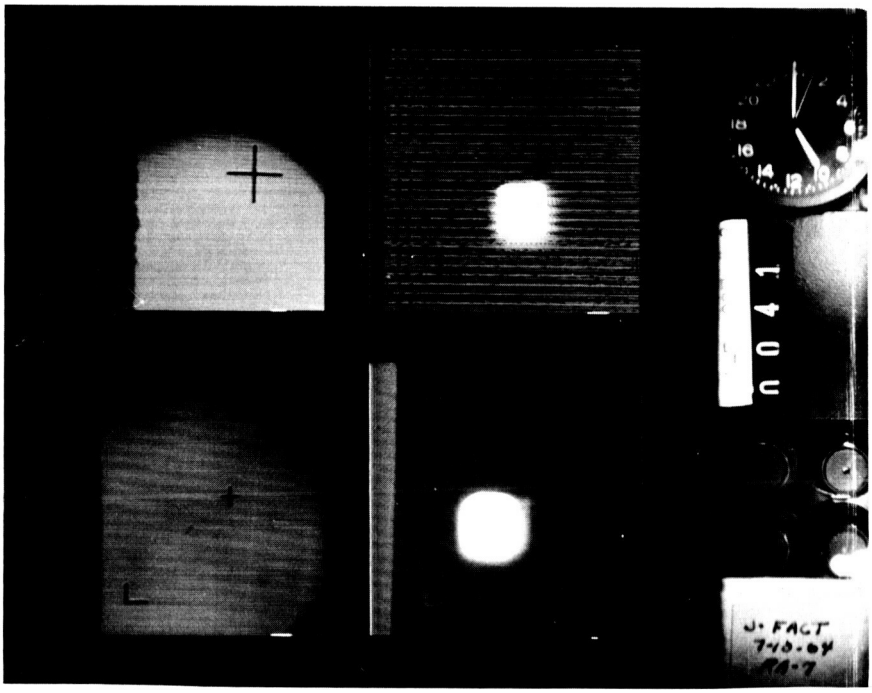

Figure B-29. P-Camera video before the gantry antenna is disconnected during J-Fact Test

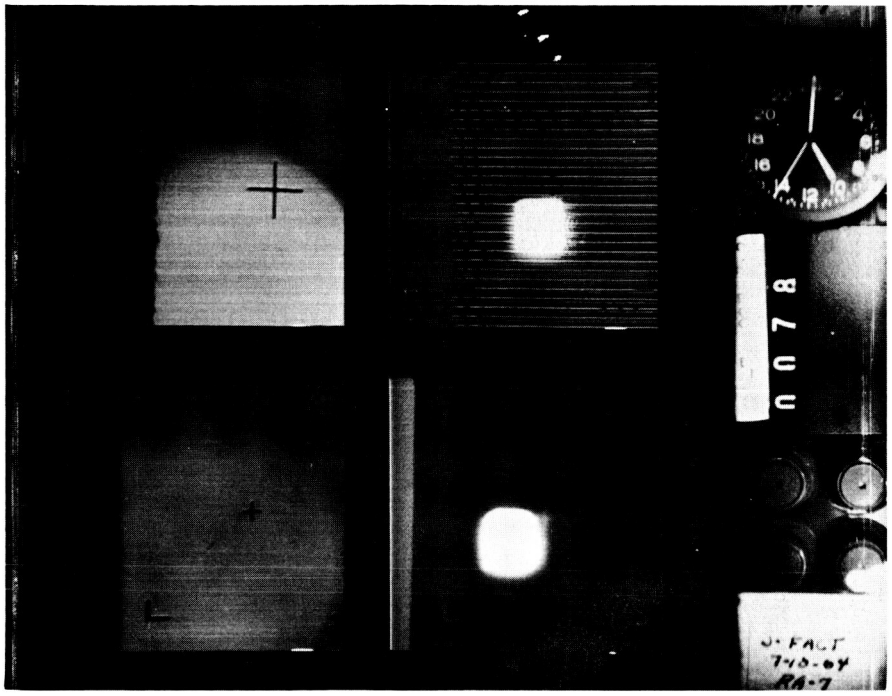

Figure B-30. P-Camera video after the gantry antenna is disconnected during J-Fact Test

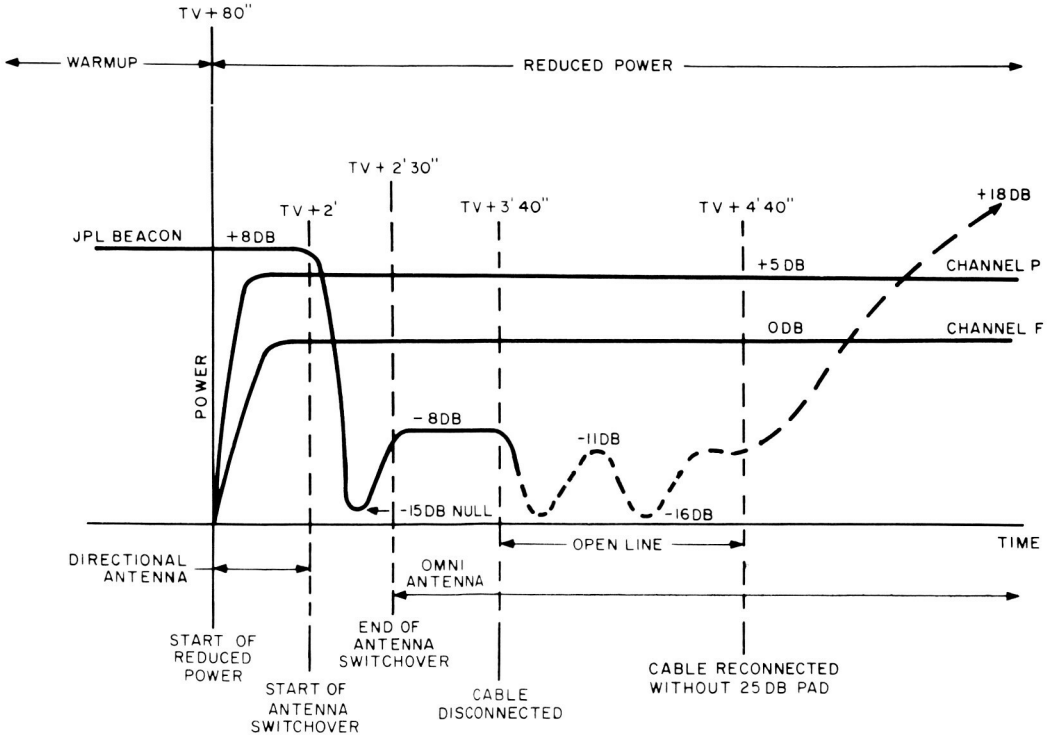

Figure B-31. J-Fact power profiles as measured with Spectrum Analyzer at OSE

monitored at the hangar on the spectrum analyzer appeared to be varying within the limits of -11db and -16db as referred to the F-Channel signal.

TABLE B-25

INPUT VOLTAGE PROFILE DURING THE JOINT FLIGHT ACCEPTANCE COMPOSITE TEST

Time (minutes)	Measured Input to HCVR		Computed Input to Transmitters		Operating Mode
	F-Battery (volts)	P-Battery (volts)	F-Channel (volts)	P-Channel (volts)	
-	35.09	35.04	-	-	System Off
T + 116	35.45	35.25	-	-	Cruise On
TV + 1	33.73	33.45	32.2	32.0	RTC-7 Warmup
TV + 2	33.39	33.19	31.9	31.7	Reduced Power
TV + 3	33.31	33.09	31.8	31.6	Reduced Power
TV + 4	33.20	32.95	31.7	31.5	Reduced Power
TV + 5	33.19	32.89	31.7	31.4	Reduced Power
TV + 6	33.09	32.87	31.6	31.4	Reduced Power
TV + 7	34.44	34.42	-	-	System Off

c. Power Performance

The TV Subsystem was powered by the F-Battery, Serial No. 85, and the P-Battery, Serial No. 76. Battery voltages and corresponding computed Transmitter Power Supply inputs are shown in Table B-25. Battery performance was normal. The total battery discharge for this test was 1.12 amperes for F-Battery and 1.46 amperes for P-Battery.

This test was the last test run on these batteries. The accumulated battery discharge for all tests in the ESA area and on the launch pad was 12.17 amperes for F-Battery and 15.95 amperes for P-Battery.

d. Telemetry Performance

All telemetry values were normal. The F-Channel cruise-mode telemetry was noisy during the first 30 to 40 seconds after reduced-power turn-on because of the higher beacon signal strength.

4. Conclusions

The noise on the video signal at the beginning of reduced-power operation and with the beacon signal on directional antenna is caused by the ground station receiver. The receiver locks on the stronger beacon signal and results in interference. The F-Channel signal, which is 3 to 5db below P-Channel power, is particularly susceptible to this interference.

The beacon signal null was broader during this test than it had been during the previous Combined Radiation Test. This was at least partly due to the additional delay before the start of antenna switchover to allow the reduced power to build up towards its maximum. Almost 30 seconds of clean video information was obtained during this test.

After the cable between the gantry antenna and slot coupler was opened, the beacon-signal strength received at the hangar on the common link with the video signals was appreciably reduced. Since no significant change in rfi noise on video was observed, it was concluded that the interference mechanism occurred within the Spacecraft. All indications, including the results of special rfi test performed on the spare TV Subsystem at ETR, led to the conclusion that this rfi was caused principally by the signal from the omni-antenna reflecting within the Agena shroud. The reflected r-f energy entered the camera units where it is interacted with the video signals, particularly at the low-level stages. Since the Agena shroud is discarded shortly after launch, this environment for rfi would not be present during an actual mission at time of TV turn-on. Consequently, the rfi noise need not be a consideration in determining the launch status of the Subsystem.

Based on the results of the J-Fact test, Subsystem performance was considered satisfactory. The Spacecraft was subsequently removed from the launch pad and returned to the hangar for final preflight preparations.

L. Camera Calibration (JPL Procedure 3R220.02)

Camera Calibration was performed on the TV Subsystem on July 11 and July 12, 1964. The Subsystem was separated from the Bus, and the shrouds and batteries were removed.

1. Purpose of Test

The purpose of this test is to measure the camera parameters to allow for the possible enhancement of the pictures received during the RA-7 mission. The information attained during this test could be used to compensate for the characteristics of each camera. The camera parameters measured during this test were:

- Linearity;
- Noise;
- Transfer Characteristics;
- Erase; and
- Shading.

2. Description of Test

The test was performed using a special collimator from JPL. The calibration of the collimator was verified before and after each test run. The TV Subsystem was operated without the shrouds and a fan was used to prevent the communication equipment and the camera equipment from overheating. Power for the test was supplied from the ground power supplies. Sixteen runs of approximately one-half-hour duration each were performed to obtain the necessary information for camera calibration.

3. Camera Calibration Sequence

a. Run No. 1. F_b-Camera Calibration (Only F-Channel on)

The collimator bracket used for this test did not require a mirror. The F_b-Camera could view the collimated light source directly. The system was in warmup for this test. Because of the unloaded condition of the F-Channel Transmitter Power Supply in warmup, chopper spikes from this supply could be seen in the "A" scope presentation of the F_b-Camera video output, although they were not seen on the recorded film.

b. Run No. 2. F_b-Camera Calibration (Only F-Channel on)

This run was performed with F-Channel in warmup only.

c. Run No. 3. F_a-Camera Calibration (Only F-Channel on)

This run was performed with F-Channel in full power. This eliminated any questions about waveform differences between warmup and full-power operation and reduced the amplitude of the communication power supply converter spikes. This amplitude was reduced by a factor of 5 from that observed during warmup.

During this test the Power Amplifier (PA) heat sink telemetry points in the terminal-mode telemetry were observed. It was found that point No. 75 was the P-Channel PA heat sink and point No. 80 was the F-Channel PA heat sink, which was the opposite to that called out in the documentation. However, the data indicated that the sensors functioned properly. All documentation was changed to agree with the equipment. The temperatures obtained are given in Table B-26.

TABLE B-26
90-POINT TELEMETRY RESULTS OF RUN NO. 3 ON POINTS NOS. 75 AND 80

Elapsed Time (minutes)	P-Channel PA Heat Sink Point 75 (°F)	F-Channel PA Heat Sink Point 80 (°F)
T + 2	76	76.5
T + 7	76	79
T + 12	78	85.7

d. Run No. 4. F_a-Camera Calibration (Only F-Channel on)

This test was performed with the TV Subsystem in full power. To verify the reversal in the PA heat sink telemetry information, points Nos. 75 and 80 on the 90-point telemetry were reviewed again. The results are given in Table B-27.

TABLE B-27 RESULTS OF CAMERA CALIBRATION RUN NO. 4 ON TELEMETRY POINTS NOS. 75 AND 80		
Elapsed Time (minutes)	P-Channel PA Heat Sink Point 75 (^{o}F)	F-Channel PA Heat Sink Point 80 (^{o}F)
T + 5	78	79
T + 14	80	92
T + 19	80	95

e. Run No. 5. F-Camera Calibration (Only F-Channel on)

This test was performed in full power to check F_a-Camera linearity.

f. Run No. 6. F_a-Camera Calibration (Only F-Channel on)

This test run performed in full power to check F_a-Camera shading.

g. Run No. 7. F_b-Camera Calibration (Only F-Channel on)

This test was performed in full power to check F_b-Camera shading. Because of tape erasures during these runs, three more runs were required to record the data on tape. The F_a- and F_b-Camera Calibration was then completed.

h. Runs No. 8 through 13. P-Camera Calibration (TV Subsystem)

These six runs were on P-Channel only to calibrate cameras P1, P2, P3, and P4. In all runs, the communications equipment was in full power. A fan was used in the vicinity of the P-Channel equipment to prevent overheating. During the camera calibration test, the voltages measured at the test connector on the camera electronics are given in Table B-28.

TABLE B-28 CAMERA CALIBRATION TEST RESULTS						
Test Jack	Camera and Camera Electronics Voltages					
	P1 31/28	P2 36/34	P3 21/39	P4 37/40	F_a 41/38	F_b 35/35
+27.5V	26.08	26.75	25.50	26.14	27.50	27.39
-6.3V	6.29	6.28	6.24	6.26	6.35	6.28
Focus Current (volts)	1.94	1.925	1.937	1.945	1.890	1.912
G1 (volts)	45.6/0	46.9/0	40.8	39.7	41.3/ 0.6	58.9/ 8.7
+40V	34.67	35.19	33.28	33.67	35.70	36.10
Vidicon Filament Current (volts)	0.12	0.125	0.110	0.125	0.116	-0.116
+6.3V	6.23	6.23	6.26	6.24	6.28	6.18
High Volt Series Regulator (volts)	3.42	2.97	3.98	3.63	2.30/ 2.50	2.29/ 2.44
1000/4V	211.5	211.0	207.6	213.8	210.0	212.4
Target V	29.8	34.40	33.42	28.25	30.56	29.38
-27.5V	27.3	27.3	27.30	27.30	27.10	27.10
G2 (volts)	301/288	294/273	284/263	285/264	301/263	295/282

4. Conclusions

The data obtained during this test was sent to JPL for analysis. After camera calibration, the following TV Subsystem preflight preparations were performed.

- Final cable potting was completed;
- Final harness tie down was performed;

- Flight batteries were installed (A10 F-Channel, Serial No. 94 and A11 P-Channel, Serial No. 93);
- Reflectometer readings were made on shrouds with results as predicted;
- Pressure vessels were checked and proper pressurization was verified; (The "dummy load" had a leaky valve stem, which was replaced and verified at this time as satisfactory.)
- Flight shrouds, with protective strip coat still on, were installed;
- Collimators and counter balance were mounted;
- Bottom, flight mylar shield, was installed;
- Subsystem was mated with the bus in preparation for System Test No. 11.

M. Pre-flight System Test No. 11 (JPL Procedure 3R300.13)

As modified by System Test (JPL Procedure 3R300.03 Supplement), this test was performed on July 15, 1964. For the first part of the test, power was supplied externally. For the second part, batteries were used for primary power.

1. *Purpose of Test*

The first part of the test is an accelerated mission simulation to verify that all Spacecraft equipment operates in a proper manner. The second is to verify the operation of the TV Subsystem with a short full-power test using battery power.

2. *Description of Test*

The first part of this test was performed in a manner similar to that for System Test No. 10 (June 27, 1964). Following this portion of the test a 3.5-minute terminal mode test was run using battery power. The sequence of events for this portion of the test is given in Table B-29.

TABLE B-29 SEQUENCE OF EVENTS FOR THE 3.5-MINUTE TERMINAL MODE TEST	
Elapsed Time (minutes and seconds)	Operation
	Cruise mode on. Gates circuits enabled for SCR turn-on.
T + 0	RTC-7 Command. F- and P-Channels in warmup.
T + 1' 20"	F- and P-Channels in full power.
T + 3' 30"	RTC-5 Command. Both channels off.
T + 4'	Cruise mode off.

3. *Test Evaluation*

a. Video Performance

The partial-scan video outputs obtained during the first and second parts of this system test were similar. Noise spikes appeared in the P1-Camera video output in less than 10 percent of the recorded frames. The Subsystem was operated in a horizontal position for this test. Fewer noise spikes appeared in the P1-Camera video output when tested in this position than when the Subsystem was operated in the vertical position. The video output from the P2-, P3-, and P4-Cameras was normal in both parts of the test.

A comparison of the video outputs for the full-scan cameras using external power input and internal power input shows no apparent difference as shown in Figures B-32 and B-33. The F_a-Camera video output was normal in both parts of the test.

In the F_b-Camera video output, the peak white level was approximately 375 millivolts at the GSE monitor. This level, which is approximately 200 mv low, was due to the collimator illuminance and position, since the camera gain was normal during camera calibration.

b. Communications Performance

The test configuration for both parts of the system test is shown in Figure B-34. The input voltage to the transmitter power supplies during the test was approximately 31.0 volts for F-Channel and 30.9 volts for P-Channel during the first part of test (on external power) and 32.7 volts for F-Channel and 31.6 volts for P-Channel during the second part of test (on battery power).

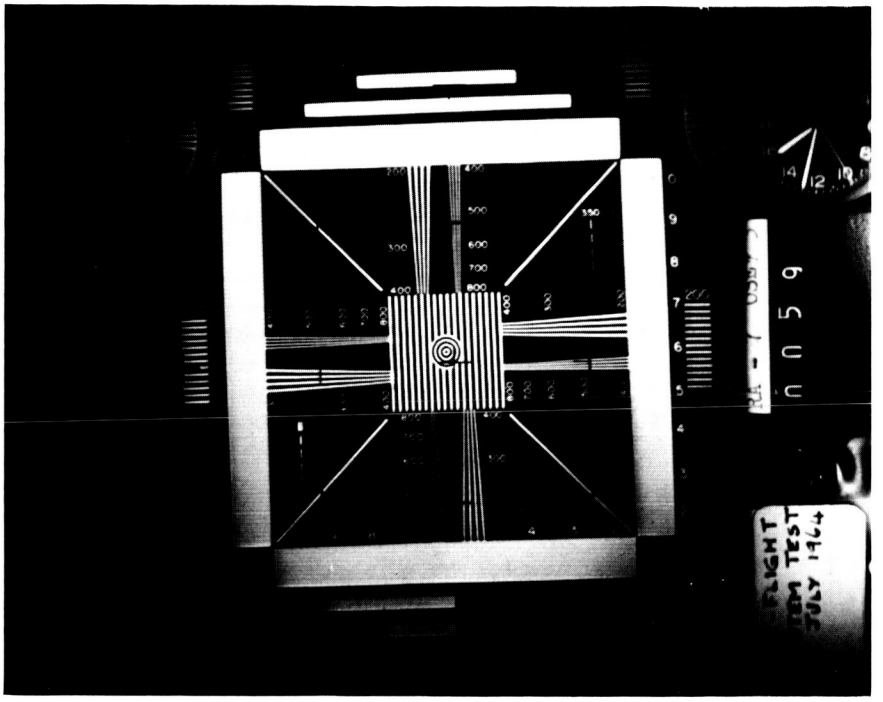

a. External power

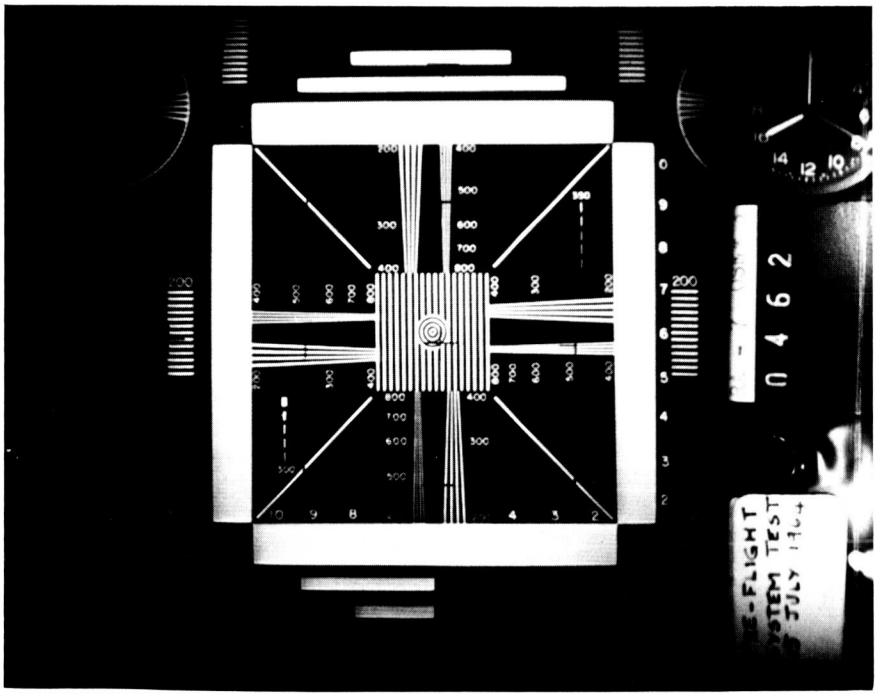

b. Battery power

Figure B-32. Comparison of F_a-Camera RETMA pattern during the Pre-Flight System Test

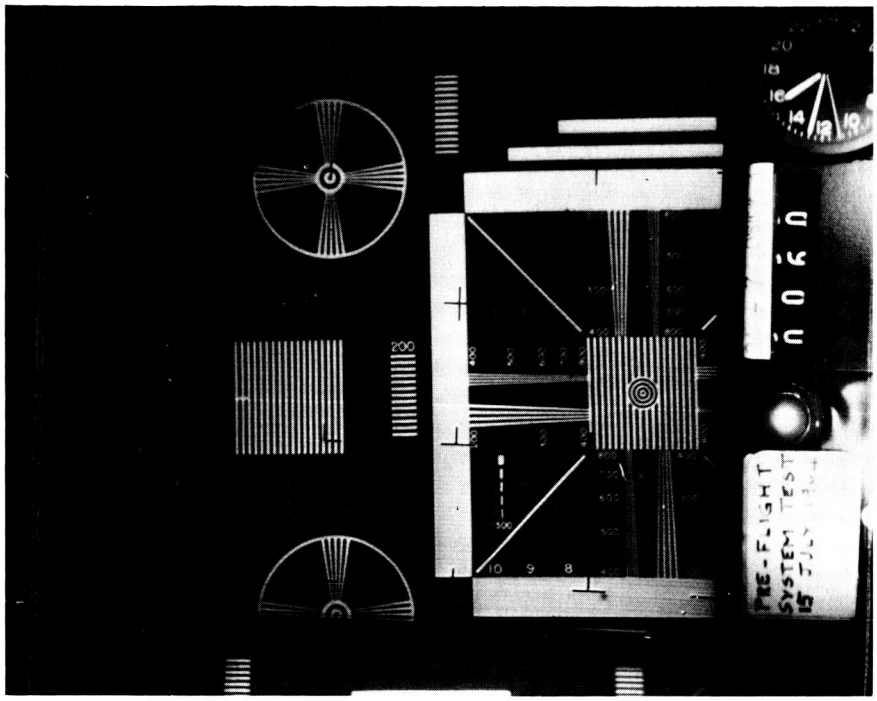

a. External power

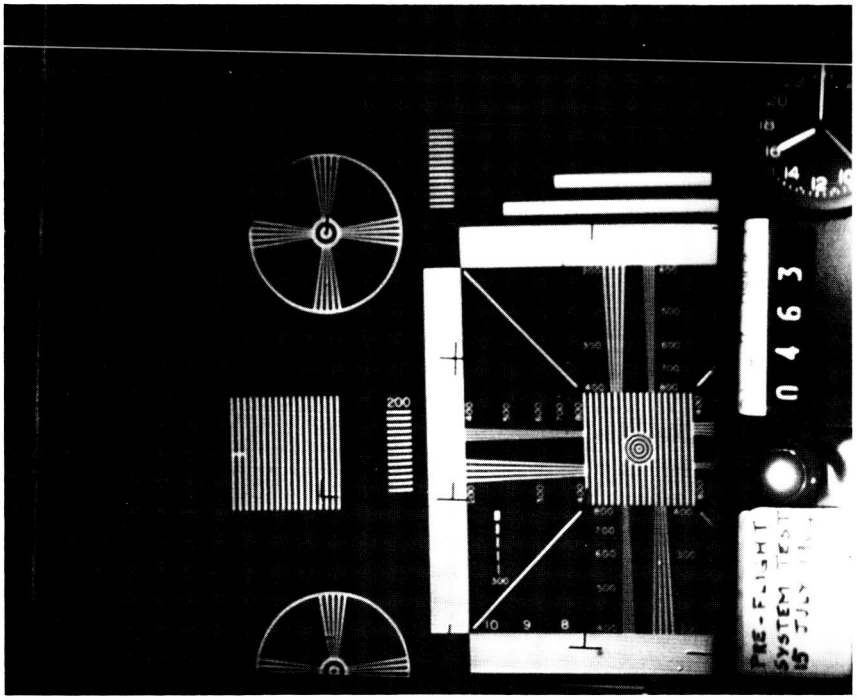

b. Battery power

Figure B-33. Comparison of F_b-Camera RETMA pattern during the Pre-Flight System Test

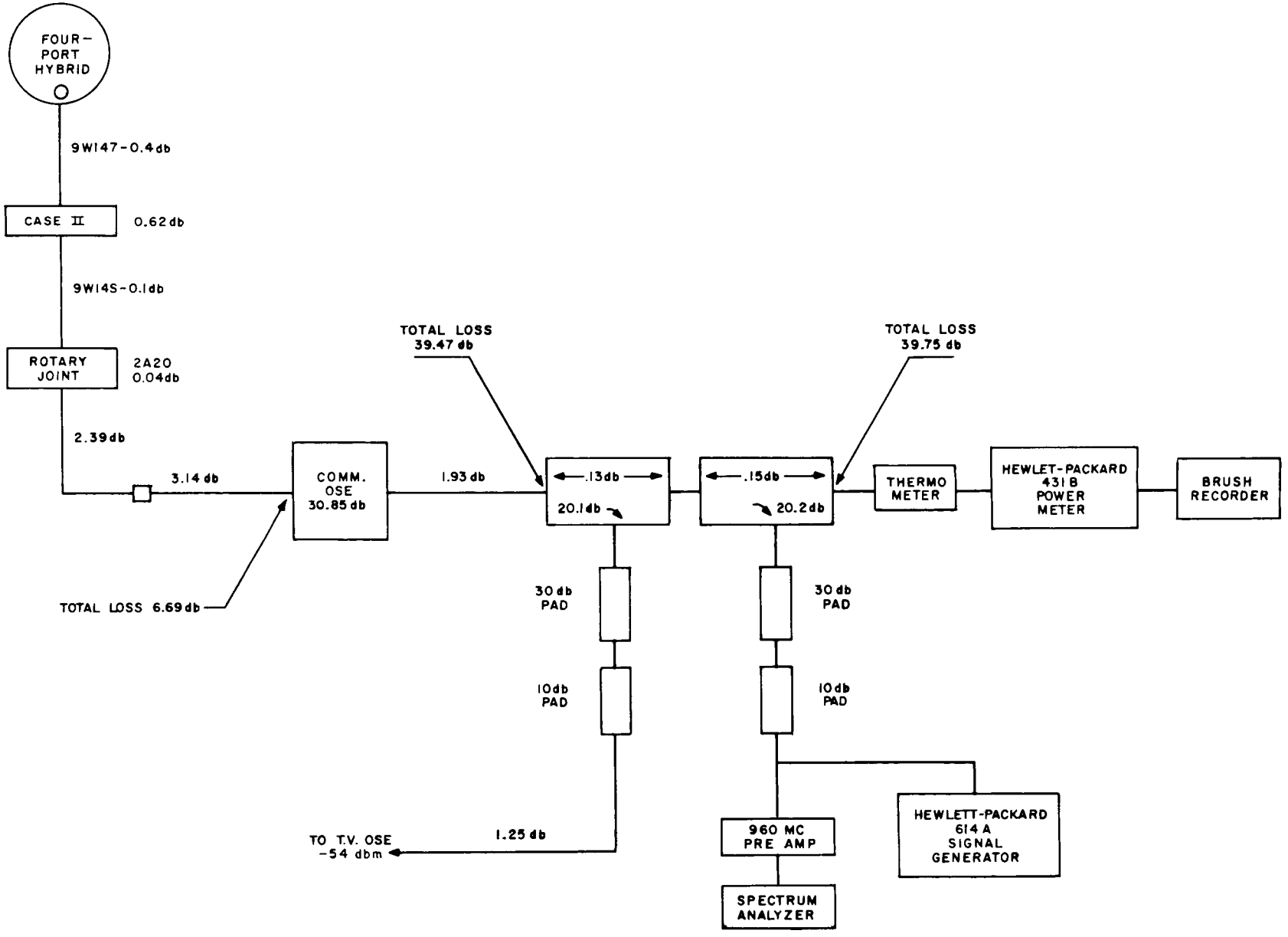

Figure B-34. Pre-Flight System Test RF Configuration

The power profile taken during the external power portion of the system test is given in Table B-30.

TABLE B-30 POWER PROFILE DURING PRE-FLIGHT SYSTEM TEST USING EXTERNAL POWER	
Elapsed Time (minutes and seconds)	Power Out at Four-Port Hybrid (watts)
C + 45' 30"	57
C + 46'	59.3
C + 47'	59.3
C + 48'	60
C + 49'	59
C + 50'	59
C + 51'	59
C + 52'	58
C + 53'	58
C + 54'	58
C + 55'	57.6

The power profile showed several 2- to 2.5-watt fluctuations at C + 48 minutes 30 seconds. These fluctuations were observed previously and were not considered serious.

The power profile taken during the second (battery operated) part of the system test is given in Table B-31.

TABLE B-31 POWER PROFILE TAKEN DURING PRE-FLIGHT SYSTEM TEST USING BATTERY POWER	
Elapsed Time (minutes and seconds)	Power Out Four-Port Hybrid (watts)
T + 1' 30"	60.8
T + 2'	60.3
T + 3'	59.9

Power was high at the start of the test because of two effects: (1) the battery voltage was higher than the external power supply voltage and (2) the transmitters were still warm from the previous test.

c. Power Performance

During the external power test, the power supplies were adjusted to provide the transmitter power supplies input voltages of 31.0 volts for F-channel and 30.9 volts for P-channel.

During the second part of the test, the battery discharge was 0.55 ampere hours for F-Battery, Serial No. 94, and 0.60 ampere hours for P-Battery, Serial No. 93.

The input to the HCVR and the Transmitter Power Supply during the internal power test is given in Table B-32. The cell voltages taken during this test are shown in Table B-33.

TABLE B-32

INPUT VOLTAGE PROFILE DURING TEST USING BATTERY POWER

Elapsed Time (minutes)	F-Channel		P-Channel	
	HCVR input (volts)	Transmitter Power Supply (volts)	HCVR input (volts)	Transmitter Power Supply (volts)
T - 5	40.92	——	40.85	——
T - 3	40.89	——	40.36	——
T - 1	40.90	——	40.35	——
T + 0	35.80	34.30	35.20	33.70
T + 1	35.54	34.04	34.80	33.30
T + 2	34.33	32.83	33.95	32.45
T + 3	34.03	32.53	33.75	32.25
T + 8	40.77	——	40.61	——

d. Telemetry Performance

The telemetry values were normal. However, when the r-f level was reduced to -130 dbm, approximately 400 mv of noise appeared on the telemetry data. This noise was not considered to be a problem.

TABLE B-33.

CELL VOLTAGES TAKEN DURING TEST USING BATTERY POWER

Cell	F-Channel					P-Channel				
	Off	Cruise Mode	Warmup	Full Power	Off +5 minutes	Off	Cruise Mode	Warmup	Full Power	Off +5 minutes
1	1.86	1.86	1.64	1.57	1.85	1.86	1.84	1.60	1.54	1.85
2	1.86	1.86	1.64	1.57	1.85	1.86	1.84	1.61	1.54	1.85
3	1.86	1.86	1.62	1.55	1.85	1.86	1.84	1.59	1.54	1.85
4	1.86	1.86	1.61	1.54	1.85	1.86	1.84	1.58	1.53	1.85
5	1.86	1.86	1.66	1.59	1.85	1.86	1.83	1.57	1.53	1.85
6	1.86	1.86	1.65	1.58	1.85	1.86	1.84	1.61	1.54	1.85
7	1.86	1.86	1.63	1.56	1.85	1.86	1.84	1.62	1.55	1.85
8	1.86	1.86	1.60	1.54	1.85	1.86	1.84	1.61	1.54	1.85
9	1.86	1.86	1.60	1.53	1.85	1.86	1.84	1.60	1.54	1.85
10	1.86	1.86	1.60	1.54	1.85	1.86	1.84	1.60	1.53	1.85
11	1.86	1.86	1.61	1.54	1.85	1.86	1.84	1.62	1.54	1.85
12	1.86	1.86	1.61	1.54	1.85	1.86	1.83	1.58	1.53	1.85
13	1.86	1.86	1.62	1.55	1.85	1.86	1.83	1.57	1.53	1.85
14	1.86	1.86	1.62	1.55	1.85	1.86	1.83	1.56	1.53	1.85
15	1.86	1.86	1.61	1.54	1.85	1.86	1.83	1.56	1.53	1.84
16	1.86	1.86	1.63	1.56	1.85	1.86	1.83	1.56	1.53	1.84
17	1.86	1.86	1.61	1.54	1.85	1.86	1.82	1.57	1.53	1.85
18	1.86	1.86	1.63	1.57	1.85	1.86	1.84	1.60	1.54	1.85
19	1.86	1.86	1.60	1.53	1.85	1.86	1.84	1.54	1.53	1.85
20	1.86	1.86	1.60	1.54	1.85	1.86	1.84	1.61	1.54	1.85
21	1.86	1.86	1.60	1.54	1.85	1.86	1.84	1.60	1.53	1.85
22	1.86	1.86	1.62	1.56	1.85	1.86	1.84	1.61	1.54	1.85
Total	40.91				40.77	40.84				40.61

Note: all readings correct to two significant places.

4. Conclusion

The test was completed satisfactorily. The TV Subsystem was considered ready for the final group of ESA tests prior to flight.

The TV Subsystem was removed from the bus, and the collimators and counter balance were removed from the Subsystem. Flight screws were installed on the shrouds. The strip coat on the shrouds was removed. Lenses were cleaned and capped. The TV Subsystem was taken to the ESA for its final checkout prior to launch pad check-out. The TV Subsystem was mated with the Bus in preparation for the ESA High-Power Test.

N. ESA High-Power Test (JPL Procedure 3R235.02)

This test was performed on the Spacecraft on July 20, 1964.

1. Purpose of the Test

This test was performed to verify that the final connection between the Four-Port Hybrid Ring on the TV Subsystem and Case II on the JPL Bus was made and that the remainder of the r-f link through to the high-gain antenna was intact.

2. Description of the Test

The test is similar to the previous ESA High-Power Test performed on June 30, 1964. A variation to that test was incorporated to establish more information on the rfi problem. The TV Subsystem went into full-power with the JPL beacon signal being radiated through the high-gain antenna. After approximately two minutes of full-power operation, the beacon signal was transferred to the omni-antenna. The test sequence is shown in Table B-34.

TABLE B-34
TEST SEQUENCE FOR THE ESA HIGH-POWER TEST

Elapsed Time (minutes and seconds)	Operation
T - 5'	Cruise On Test switch was depressed. Cruise mode on and the SCR gate control circuits enabled.
T + 0	RTC-7 Command. Both channels in warmup.
T + 1' 20"	Both channels in full power.
T + 3' 20"	Beacon signal transferred from the high-gain antenna to the omni-antenna.
T = 5' 30"	RTC-5 Command. Both channels off.
T + 6	Cruise Off. Cruise mode telemetry off.

3. Test Evaluation

a. Video Performance

The video observed on the P-Channel before switching the beacon signal to the omni-antenna is shown in Figure B-35. A comparison of these frames reveals very little change in the video performance. No rfi is seen in either case. The noise spikes previously seen in the video from the P1-Camera was present in approximately 30 percent of the recorded frames. The video from the P2-, P3-, and P4-Cameras was normal.

Prior to switching the JPL beacon signal to the omni-antenna, the video from the F_a-Camera did not have any rfi. Following the switchover, noise as shown in Figure B-36 was apparent. The noise may be due to r-f type of interference. It was determined after the test that the beacon signal radiating from the omni-antenna, with no Echo-sorb material to limit its radiation, was reflected from the steel walls of the ESA. The reflected beacon signal was probably the cause of the r-f noise observed in the F_a-Camera. The noise interference was of low enough amplitude to be considered of minimal importance. Again the rfi problem was considered not to be a flight problem, but only one of test methods.

There was no rfi observed in the video from the F_b-camera either before or after beacon signal switchover as shown in Figure B-37. The video was normal throughout the test.

b. Communications Performance

The performance of the communications system during this test was normal. The test setup is shown in Figure B-38. The input voltage to the Transmitter Power Supply was -31.7 volts for the F-Channel and -31.4 volts for the P-Channel. The power profile is recorded in Table B-35.

TABLE B-35
POWER PROFILE FOR ESA HIGH-POWER TEST

Elapsed Time (minutes and seconds)	Power Output at Four-Port Hybrid (watts)
T + 1' 30"	58.5
T + 2'	58.5
T + 3'	59.2
T + 4'	60.0
T + 5' 30"	61.0

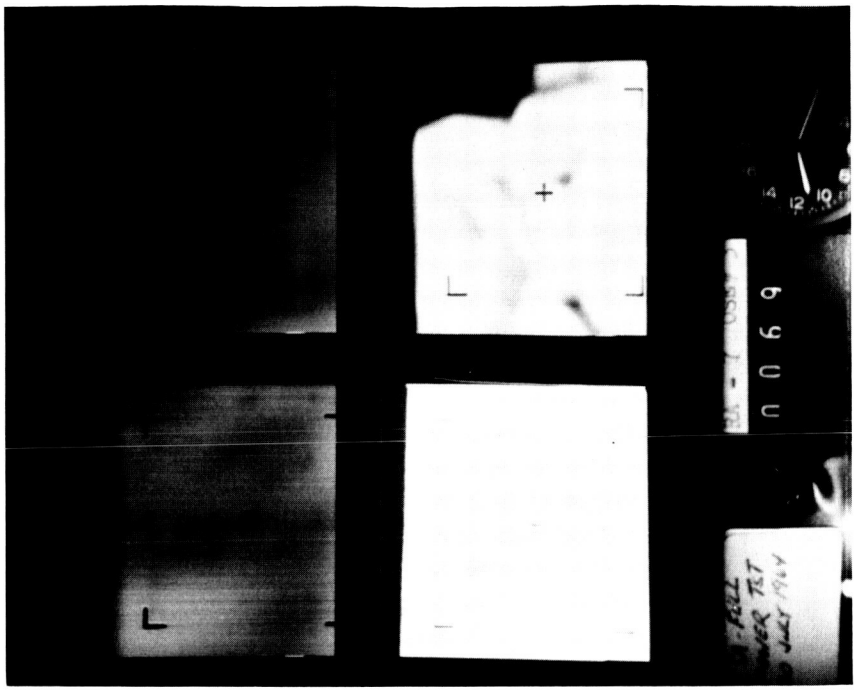

a. Before switchover

b. After switchover

Figure B-35. Comparison of P-Camera video before and after switchover of the JPL beacon during the ESA High-Power Test

a. Before switchover

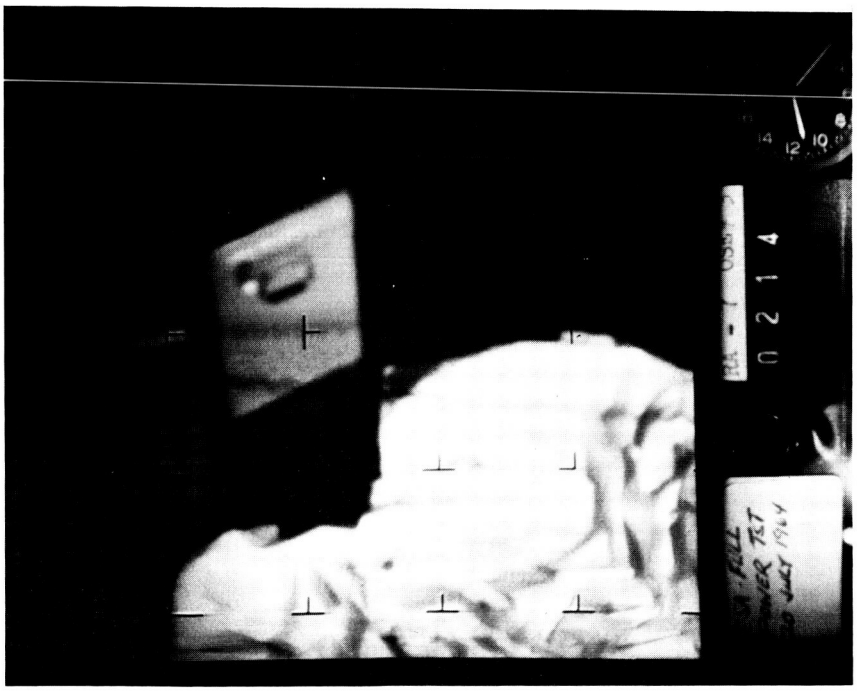

b. After switchover

Figure B-36. Comparison of F_a-Camera video before and after switchover of the JPL beacon during the ESA High-Power Test

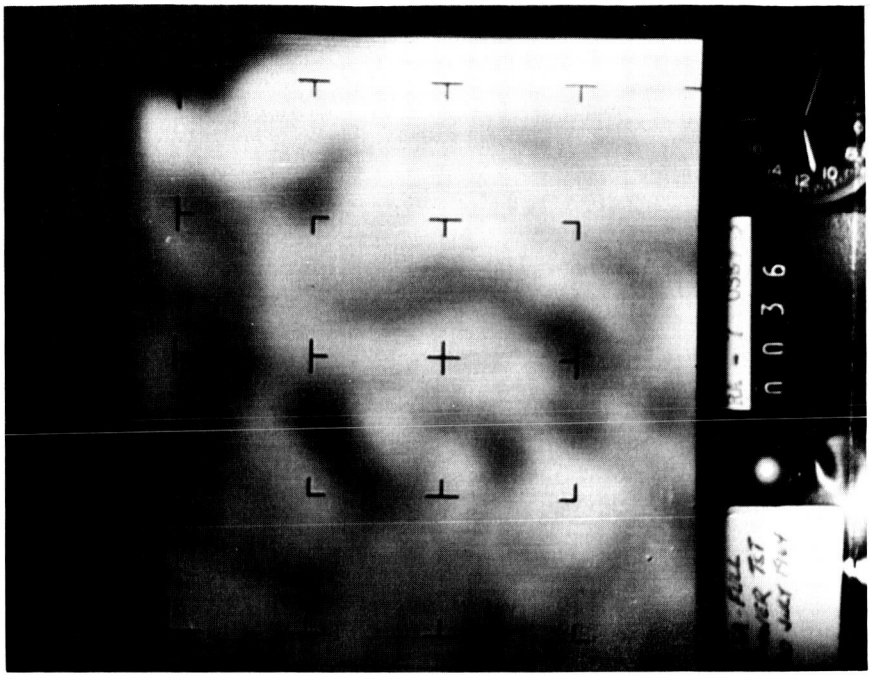

a. Before switchover

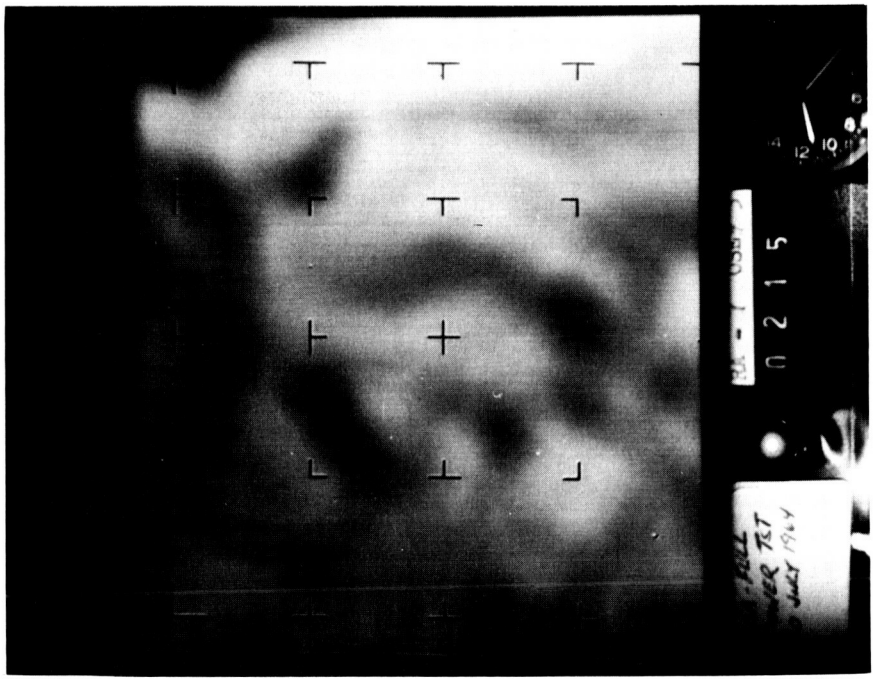

b. After switchover

Figure B-37. Comparison of F_b-Camera video before and after switchover of the JPL beacon during the ESA High-Power Test

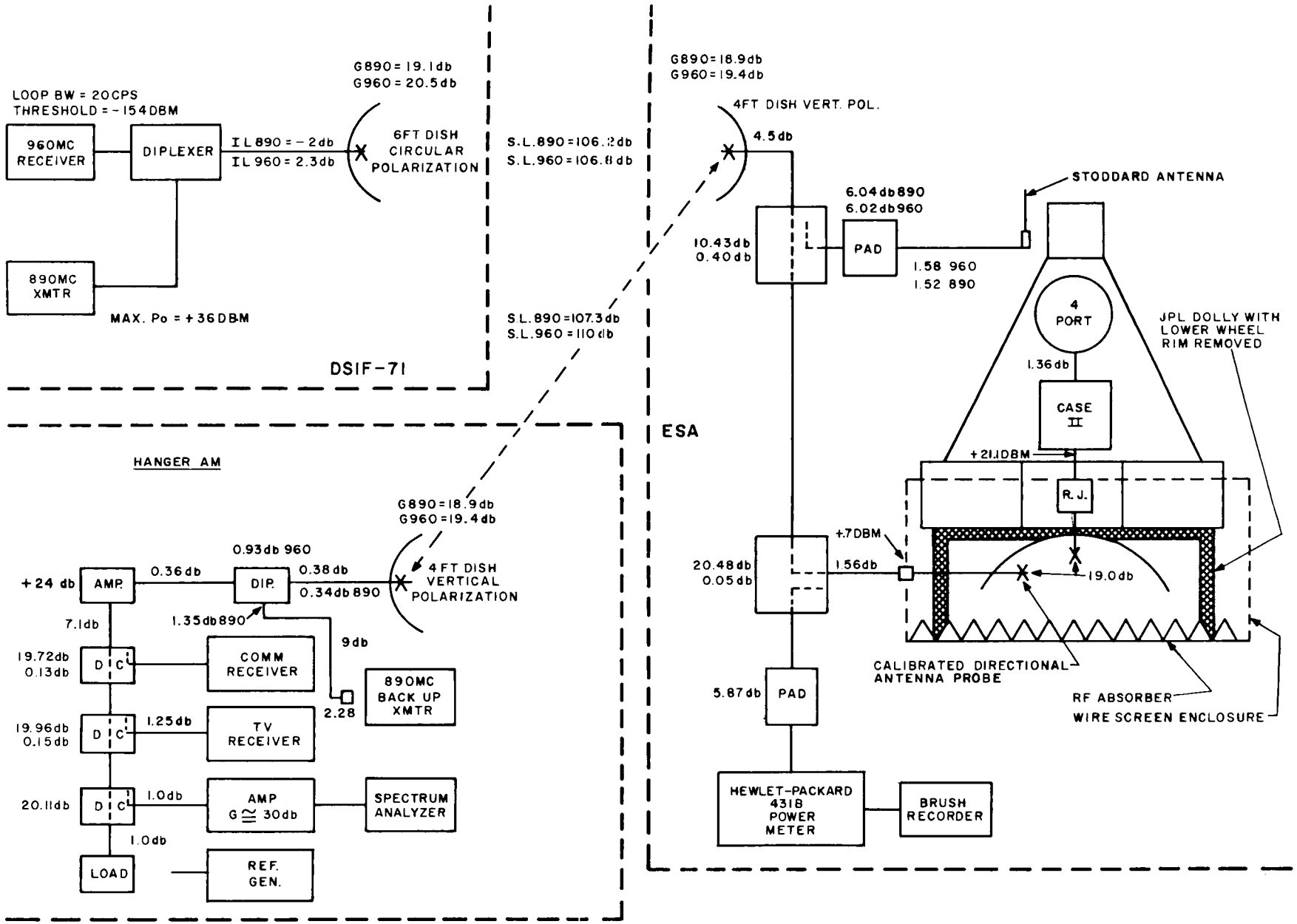

Figure B-38. ESA Full-power test r-f test configuration

c. Power Performance

This test was performed on battery power. The voltages recorded at the input to the HCVR and the input to the Transmitter Power Supply for this test are given in Table B-36. The power performance for this test was normal. The battery drain for this test is 1.5 ampere hours for F-Battery, Serial No. 94, and 1.8 ampere hours for P-Battery, Serial No. 93.

TABLE B-36

INPUT VOLTAGE PROFILE DURING ESA HIGH-POWER TEST

Elapsed Time (minutes)	F-Channel		P-Channel	
	Input to HCVR (volts)	Transmitter Input (volts)	HCVR Input (volts)	Transmitter Input (volts)
T + 0	40.89	——	39.72	——
T + 1	34.09	32.59	33.79	32.29
T + 2	33.35	31.85	33.09	31.59
T + 3	33.29	31.79	32.99	31.49
T + 4	33.29	31.79	32.95	31.45
T + 5	33.20	31.70	32.92	31.42
T + 6	36.20	——	36.04	——
T + 8	36.69	——	36.59	——
T + 15	39.52	——	39.04	——

d. Telemetry Performance

The telemetry for this test was normal.

4. Conclusion

The test was successfully completed, and the TV Subsystem performed properly in full power.

The TV Subsystem was then prepared for the last test to be performed at ESA. Final preparation included the mating of the Spacecraft with the Agena adapter ring and shroud.

O. ESA Low-Power Test (JPL Procedure 3R317.03)

1. Purpose of Test

The purpose of this test, performed at the Explosive Safe Area (ESA) on July 22, 1964, was to verify that the Spacecraft was ready for launch pad operation.

2. Description of Test

This test is the same as that described for the previous ESA Low-Power Test with the following exception: at T + 92 minutes 20 seconds the beacon signal was transferred from the high-gain antenna to the omni-antenna. This permited rfi free video during the switchover period.

3. Test Evaluation

a. Video Performance

The video signal received prior to switching the beacon signal and the video signal received during switchover was reasonably free of rfi as shown in Figure B-39. However, when the beacon power radiated from the omni-antenna reached its nominal level, the P-Camera video output became very noisy as shown in Figure B-39.

The P1-Camera video output exhibited noise spikes as previously observed. RFI type of marks showed up in the video after the beacon power was switched to the omni-antenna. This was anticipated, and therefore, was considered normal.

Noise transients were observed in the P2-Camera video output at the same point that they had occurred in the first ESA Low-Power Test of July 2, 1964. Again, they appeared in alternate frames. Predominant rfi appeared on the P3-Camera output after switchover. There was normal video on the P4-Camera throughout the test.

Prior to switchover, the signal level from F-Channel was too low to record any video signals. Video signals were recorded just after switchover; however, the radiated beacon power was low to the end of the test.

There was no rfi in the F_a-Camera video output prior to the beacon signal nominal power radiating from the omni-antenna. However, after the radiated power from the beacon had reached its nominal output, the rfi appeared in the F_a-Camera video output in the form of a checker-board pattern and high-frequency power fluctuations as shown in Figure B-40. However, this was anticipated and was considered normal.

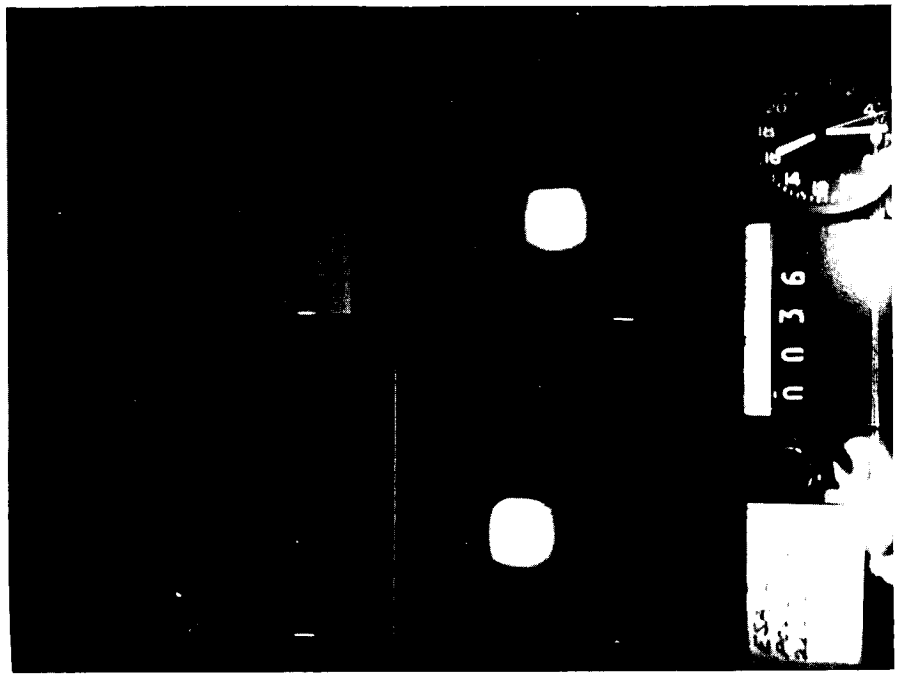

a. Before switchover

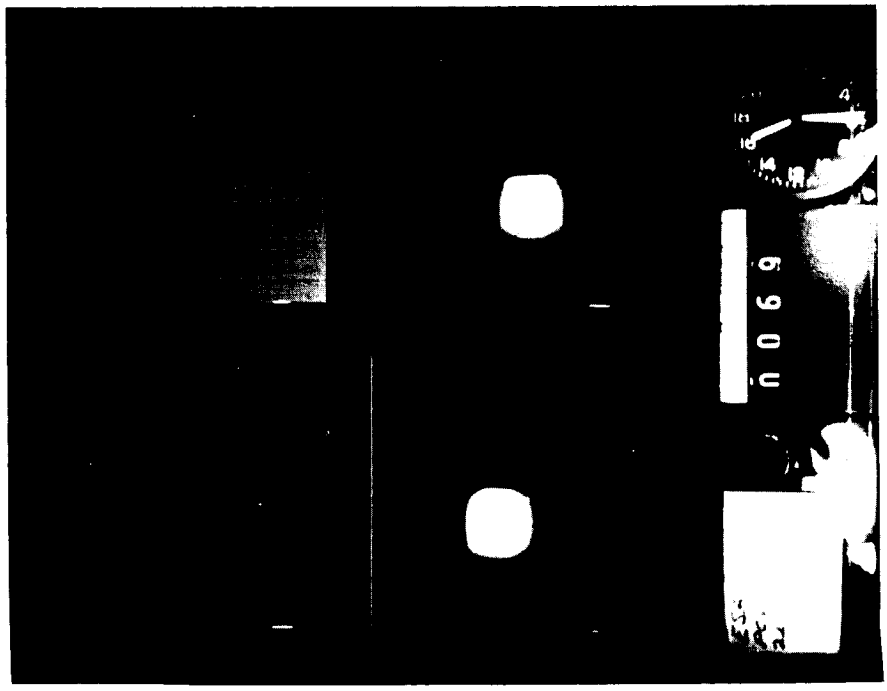

b. During switchover

Figure B-39. Comparison of P-Camera video before, during, and after switchover of the JPL beacon signal during the ESA Low-Power Test

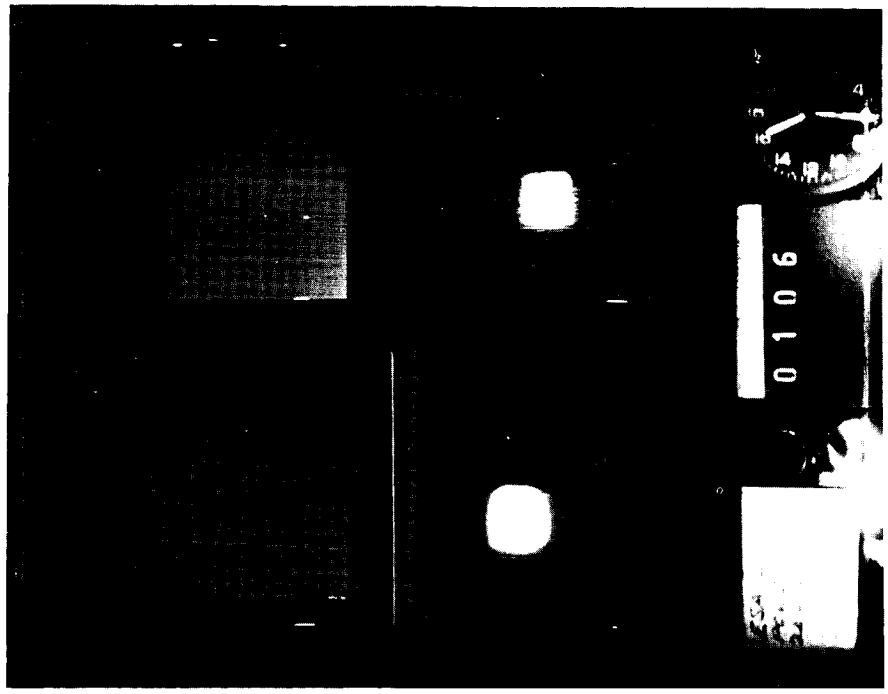

c. After switchover

Figure B-39. Comparison of P-Camera video before, during, and after switchover of the JPL beacon signal during the ESA Low-Power Test (Continued)

The F_b-Camera video output was normal during beacon switchover. After beacon signal reached nominal power output from the omni-antenna, rfi appeared in the F_b-Camera video output. This was anticipated and was considered normal. Figure B-41 shows the F_b-Camera video output during and after beacon switchover.

b. Communications Performance

The communication performance was normal for this test. The input voltage to the Transmitter Power Supplies was determined by subtracting the voltage drop through the SCR and associated wiring between the battery monitor point and the input to the Transmitter Power Supply. In reduced power, this drop was approximately 1.1 volts. The input voltage to the transmitter supplies was -32.4 volts for F-Channel and -32.30 volts for P-Channel. The power profile is given in Table B-37.

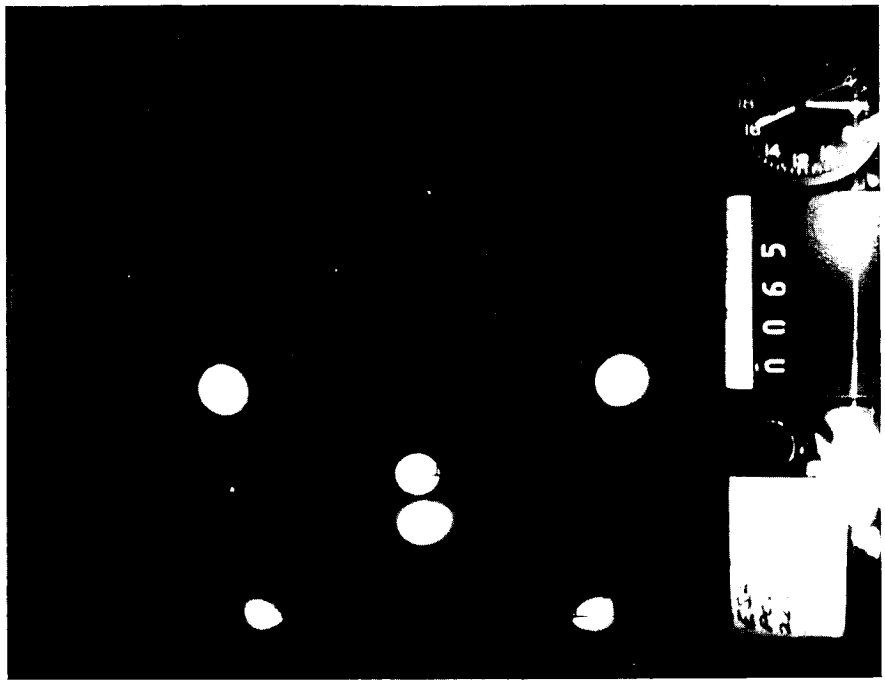

a. Before nominal output

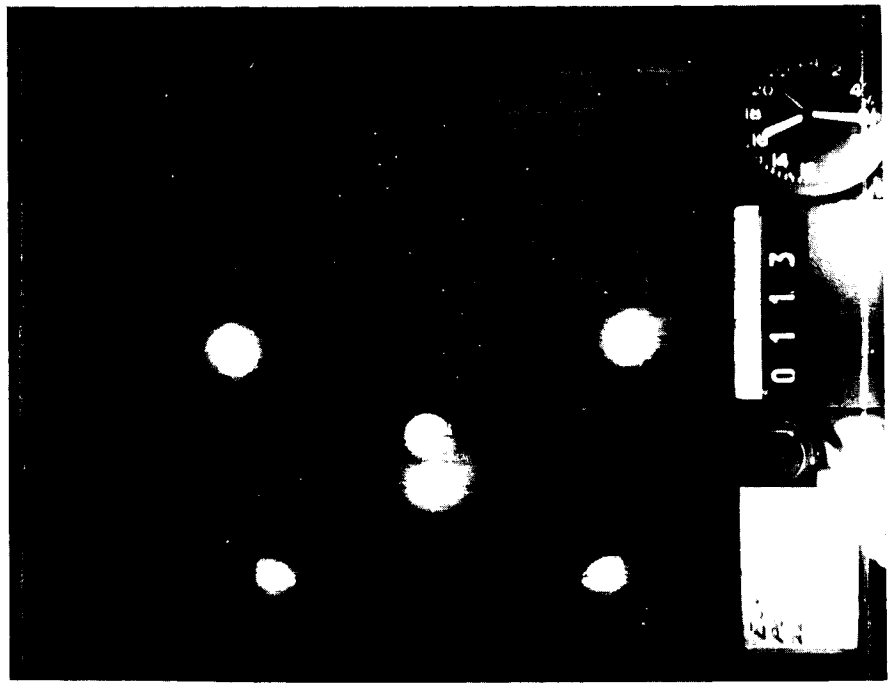

b. After nominal output

Figure B-40. Comparison of F_a-Camera video before and after beacon signal reached nominal power output during the ESA Low-Power Test

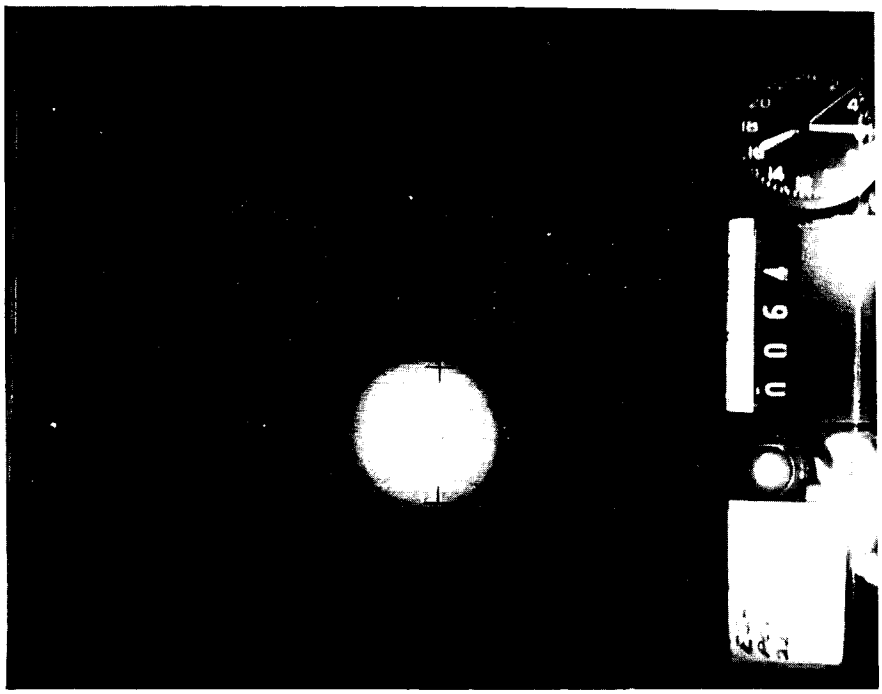

a. During switchover

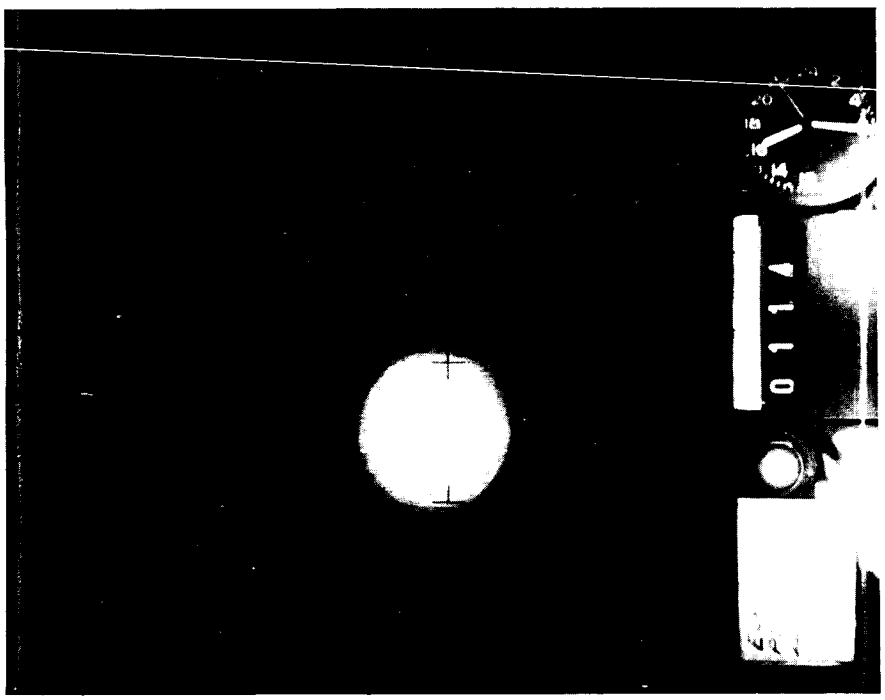

b. After switchover

Figure B-41. Comparison of F_b-Camera video during and after switchover of beacon signal during the ESA Low-Power Test

TABLE B-37 POWER PROFILE DURING ESA LOW-POWER TEST	
Elapsed Time (minutes and seconds)	Power Output at Four-Port Hybrid (milli watts)
T + 91' 30"	105.56
T + 92'	145.08
T + 93'	169.26
T + 93' 30"	169.26

c. Power Performance

The power performance was normal. Batteries were used for the entire test. The profile of the battery voltage taken at the input to the HCVR and the input to the Transmitter Power Supply is given in Table B-38. The power drain for this test was 0.64 ampere hour for F-Battery, Serial No. 94, and 0.8 ampere hour for P-Battery, Serial No. 93.

TABLE B-38 INPUT VOLTAGE PROFILE DURING ESA LOW-POWER TEST				
Elapsed Time (minutes)	F-Channel		P-Channel	
	Input to HCVR (volts)	Input to Transmitter Power Supply (volts)	Input to HCVR (volts)	Input to Transmitter Power Supply (volts)
T + 85	40.75	——	39.03	——
T + 88	40.75	——	39.03	——
T + 89	40.79	——	39.03	——
T + 90	33.89	32.79	33.58	32.48
T + 91	33.89	32.79	33.59	32.49
T + 92	33.70	32.60	33.40	32.30
T + 93	33.57	32.47	33.35	32.25
T + 94	33.51	32.41	33.27	32.17
T + 95	35.99	——	35.80	——
T + 96	36.19	——	35.99	——
T + 100	37.50	——	37.29	——

d. Telemetry Performance

The telemetry performance was normal for the entire test.

4. Conclusion

The test was a successfully completed and the Spacecraft was taken to the launch pad to commence launch procedures.

P. Precountdown Test (JPL Procedure 3R304.05)

The Ranger-7 Spacecraft was transported from the Explosive Safe Area and installed on the Atlas-Agena vehicles at the launch pad, complex 12, on July 23, 1964. The final Precountdown Test was initiated shortly after noon of the same day.

1. Purpose of Test

The Precountdown Test was performed to verify the compatibility of the Launch Checkout Equipment with the Spacecraft, and to provide a sequence of tests which checked the compatibility of all Spacecraft on-pad electrical interfaces, and which checked that all subsystems were in a ready condition for launch.

2. Description of Test

a. Spacecraft Configuration

The Spacecraft was in final flight configuration and was installed on the Atlas-Agena vehicles at the launch pad.

b. Test Procedure

The test was performed using the sequence of events given in Table B-39. The gantry tower remained in place during the entire Precountdown Test.

TABLE B-39

SEQUENCE OF EVENTS DURING PRECOUNTDOWN TEST

Elapsed Time (minutes and seconds)	Operation
T + 84'	The Cruise On Test switch was depressed twice. The first operation resets the clock, turned on cruise mode telemetry, and armed the SCR gate circuits. When the switch was depressed the second time, external arming of the gates was removed.
T + 88"	RTC-7 command. The TV Subsystem did not turn on because the gates were not armed. This was a special check to verify that the SCR gates are properly disabled through the arming system in the Spacecraft prior to launch.
T + 89'	Cruise On Test switch was depressed once to permit turn-on upon receipt of the next RTC-7 command.
T + 90'	RTC-7 command. F- and P-Channels placed in reduced power warmup.
T + 90' 10"	The Cruise On Test switch was depressed once. (normal position).
T + 91' 20"	Both channels placed in reduced power by the TV Sequencer command.
T + 92' 20"	The beacon signal was transferred from directional antenna to omni-antenna.
T + 96	RTC-5 command. Both channels were turned off.
T + 96	The Cruise Off switch in the blockhouse was depressed to turn off channel 8 cruise mode telemetry.

3. Test Evaluation

a. Video Performance

F-and P-Channel video signals were very noisy before antenna switchover. One film recorder would not sync on the F-Camera video signal during this time. The F- and P-channel video signals were free of noise during the beacon signal null that occurred just after switchover. After the beacon signal was switched to the omni-antenna, rfi noise was observed in the P3-, P4-, F_a-, and F_b-Camera video signals. Noise spikes were noticed in the P1-Camera pictures.

b. Communications Performance

The r-f test configuration was the same as that used for the previous launch pad dummy runs. The television r-f power received at the hangar was monitored with a spectrum analyzer and compared with the beacon signal strength. The gantry antenna remained connected to the omni-antenna slot coupler throughout the test run. The TV Subsystem performance in reduced power operation was normal.

c. Power Performance

The TV Subsystem was powered with flight batteries, Serial Nos. 94 (F-Channel) and 93 (P-Channel). The battery voltages were monitored during the test run at the blockhouse panel with digital voltmeters. The test data, presented in Table B-40 indicated normal battery performance. The total battery discharge for this test was 0.74 ampere hour for F-Battery, Serial No. 94, and 0.91 ampere hour for P-Battery, Serial No. 93.

d. Telemetry Performance

The telemetry performance was considered normal. Some noise on F-Channel telemetry prior to antenna switchover was anticipated.

4. Conclusion

The TV Subsystem gave adequate evidence of compatibility with the launch facility interfaces and of readiness to be committed to the Simulated Launch test.

TABLE B-40 PRECOUNTDOWN TEST BATTERY VOLTAGES			
Time	Measured Input to HCVR		Operating Mode
	F-Battery (volts)	P-Battery (volts)	
T + 84	40.65	40.54	System Off
T + 85	40.62	38.64	Cruise Mode (Pushbutton Reset)
T + 89	41.00	38.97	Cruise Mode (Pushbutton Set)
T + 90	33.79	33.49	Warmup
T + 91	33.79	33.50	Warmup
T + 92	33.40	33.29	Reduced Power
T + 93	33.50	33.19	Reduced Power
T + 94	33.45	33.15	Reduced Power
T + 95	33.45	33.10	Reduced Power
T + 96	35.70	35.56	System Off

Q. Simulated Launch Test (JPL Procedure 3R309.06)

1. Purpose of Test

The Simulated Launch Test was performed on July 25, 1964, using the standard countdown procedure, to verify that the Spacecraft and Atlas-Agena vehicles had no incompatibilities and that the vehicles and Spacecraft and all supporting agencies and equipment were ready for the actual countdown and launch.

2. Description of Test

a. Spacecraft Configuration

The Spacecraft was in final flight configuration on the launch pad.

b. Test Procedure

The operation for the Spacecraft was the same as that used for the countdown except that there was no actual launch. The umbilical plug remained connected after T = 0, and a shut down procedure for the Spacecraft was employed at the end of the test. The gantry tower was removed during this test. The sequence of events that effected the operation of the TV Subsystem during this simulated launch are given in Table B-41.

3. Test Evaluation

a. Video Performance

Camera performance was similar to that described for the Precountdown test. Good video outputs were obtained during the antenna switchover null as shown in Figure B-42.

b. Communications Evaluation

The r-f test configuration was similar to that for the Precountdown test except that the gantry tower was removed for this test. During omni-antenna operation, the beacon signal was received at the hangar as a result of pickup of radiation from the Agena slot antenna. The communications performance was normal.

c. Power Performance

Battery voltages during this test are given in Table B-42. Battery performance was normal. The total battery discharge for this test was 0.71 ampere hour for F-Battery, Serial No. 94, and 0.89 ampere hour for P-Battery, Serial No. 93.

d. Telemetry Performance

Telemetry performance was normal.

4. Conclusions

The TV Subsystem was ready for launch.

TABLE B-41

SEQUENCE OF EVENTS FOR TV SUBSYSTEM DURING SIMULATED LAUNCH

Elapsed Time (minutes and seconds)	Operation
T - 116'	The Cruise On Test switch on the blockhouse panel was depressed. This operation turned on cruise mode telemetry, reset the clock, and armed the SCR gate circuits.
TV = 0 (T-115)	RTC-7 Command. F- and P-channels in reduced power warmup.
TV + 30"	The Cruise On Test switch was depressed (normal position). This removed enable lines for the SCR gates.
TV + 1' 20"	Both channels in reduced power full-power operation.
TV + 2' 20"	The beacon signal was transferred from the directional antenna to the omni-antenna.
TV + 5'	RTC-5 Command. Both channels off.
TV + 6'	The Cruise Off switch was depressed. Channel 8 cruise mode telemetry was turned off.
T - 15'	The Cruise On Test switch was depressed twice.
T + 41'	The Cruise Off switch was depressed. Channel 8 cruise mode telemetry was turned off. All facilities were shut down.

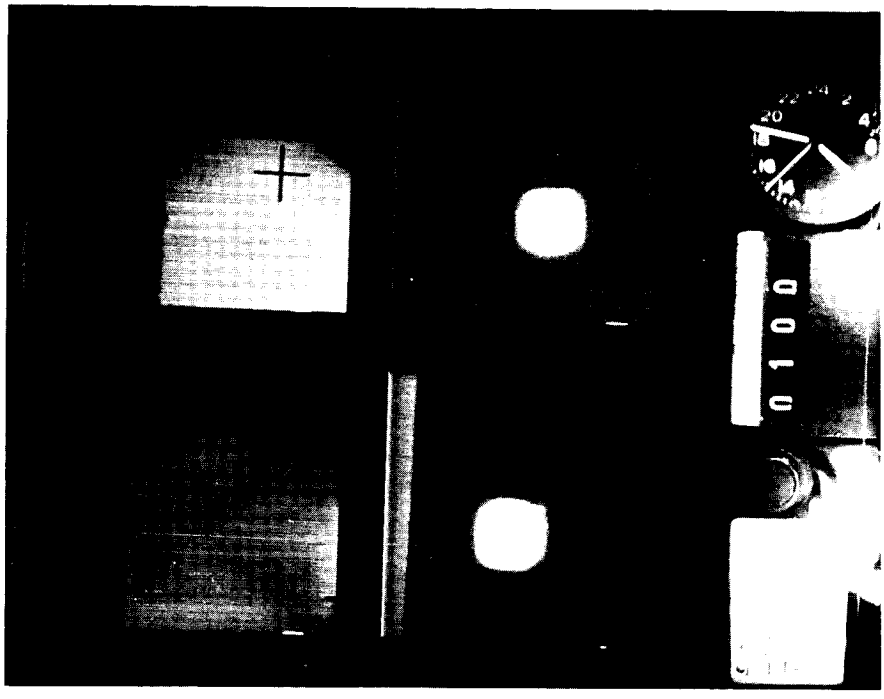

Figure B-42. P-Camera video at null during simulated launch

TABLE B-42

SIMULATED LAUNCH BATTERY VOLTAGES

Time (minutes)	Measured Input to HCVR		Operating Mode
	F-Battery (volts)	P-Battery (volts)	
T - 117	40.45	40.36	TV Subsystem Off
T - 116	40.80	38.09	Cruise Mode On
TV = 0	33.69	33.52	Warmup
TV + 1	33.69	33.39	Warmup
TV + 2	33.34	33.09	Reduced Power
TV + 3	33.35	33.05	Reduced Power
TV + 4	33.33	33.09	Reduced Power
TV + 5	35.59	35.29	RTC-5 Off
TV + 6	35.47	35.39	Cruise Mode Off
T - 16	39.77	39.67	System Off
T - 15	39.79	37.32	Cruise Mode On
T - 1	39.84	37.16	Cruise Mode On

R. Countdown on First Day (JPL Procedure 3R309.06)

The first day of the launch window was July 27, 1964. Launch countdown was started on schedule, but was cancelled at T-22 minutes because of a problem in the Atlas guidance system. The TV Subsystem checkout was performed prior to this time.

1. Purpose

The Countdown was performed to verify, by a series of checks and tests, that every aspect of the launch and mission equipment was operating properly before launch.

2. Description of Test

a. Spacecraft Configuration

The Spacecraft was in final flight configuration on the launch pad.

b. Test Procedure

The sequence of events up to T-22 were the same as those described for the Simulated Launch test and is given in Table B-41.

3. Test Evaluation

a. Video Performance

The video performance was similar to that observed during the Simulated Launch Test and, therefore, was considered normal. Figures B-43 and B-44 show camera performance during the beacon signal null that occurred after antenna switchover.

b. Communications Performance

The communications performance was similar to that observed during the Simulated Launch Test and, therefore, was considered normal.

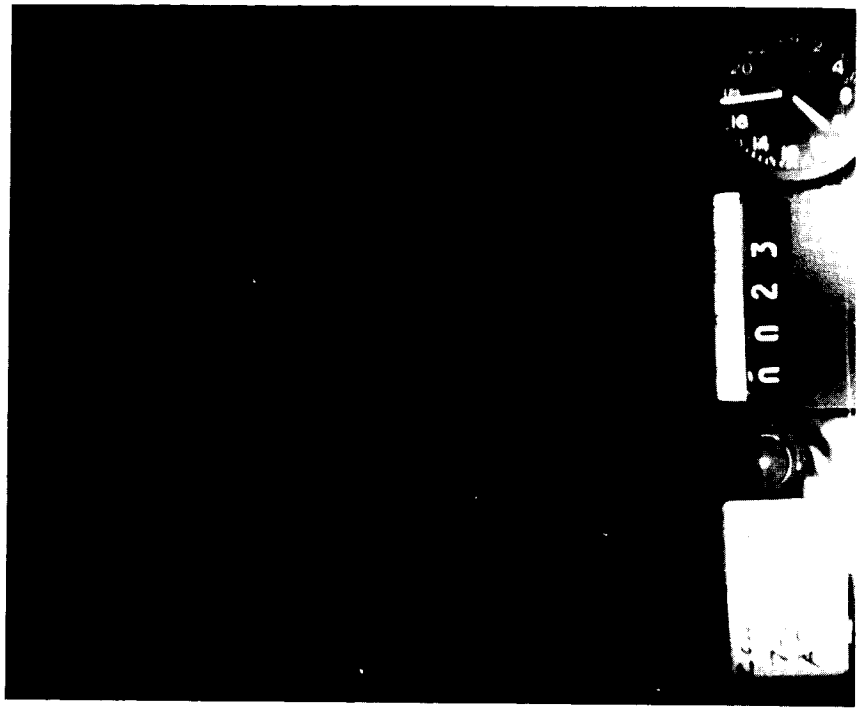

Figure B-43. P-Camera video at null during Countdown on First Day

c. Power Performance

Battery voltages during this test were normal and are given in Table B-43. The total battery discharge for this test was 0.71 ampere hour for F-Battery, Serial No. 94, and 0.87 ampere hour for P-Battery, Serial No. 93.

d. Telemetry Performance

Telemetry performance was normal.

4. Conclusion

The TV Subsystem was ready for launch.

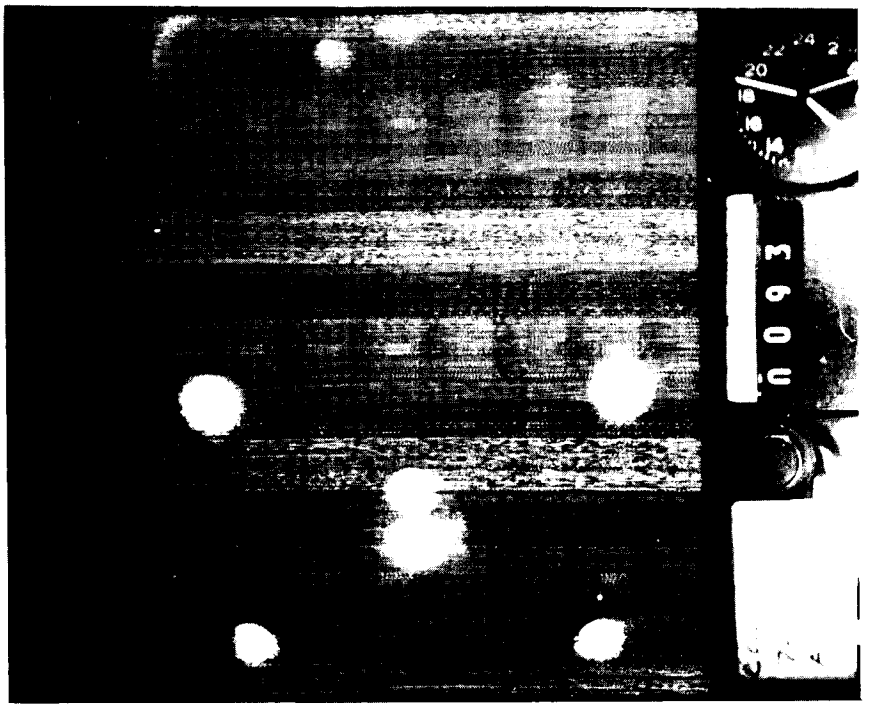

a. F_a-Camera

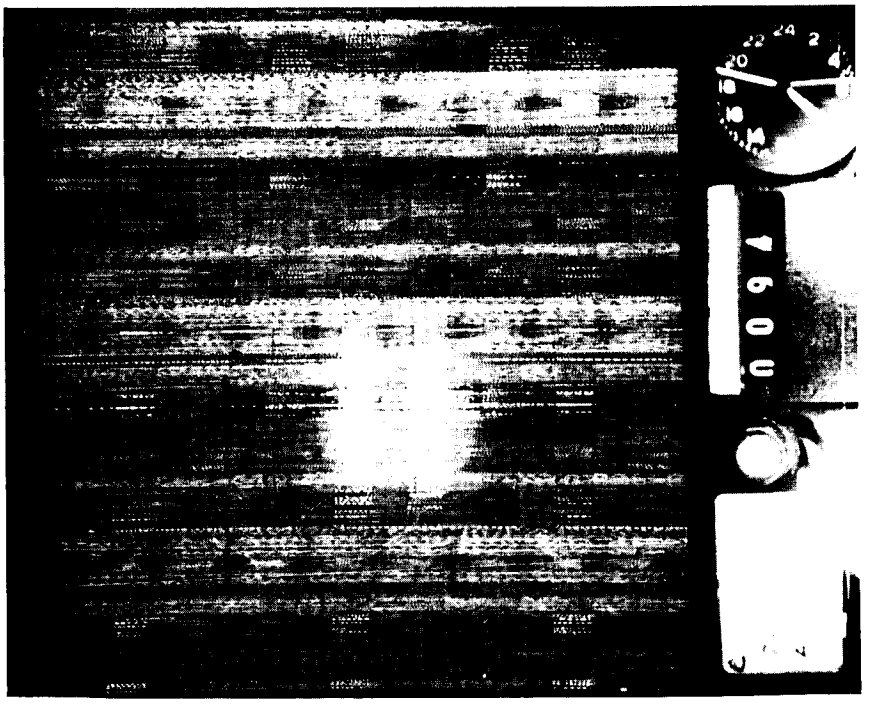

b. F_b-Camera

Figure B-44. F-Camera video at null during Countdown on First Day

TABLE B-43 BATTERY VOLTAGES OBTAINED DURING COUNTDOWN ON FIRST DAY			
Time (minutes)	Measured Input To HCVR		Operating Mode
	F Battery (volts)	P Battery (volts)	
T - 117	40.3	40.2	TV Subsystem Off
T - 116	40.6	37.4	Cruise mode on
TV = 0	33.8	33.5	Warmup
TV + 1	33.7	33.4	Warmup
TV + 2	33.4	33.1	Reduced Power
TV + 3	33.4	33.1	Reduced Power
TV + 4	33.3	33.0	Reduced Power
TV + 5	35.4	35.4	TV Subsystem OFF

S. Countdown on Second Day (JPL Procedure 3R309.06)

The second day of the launch window was July 28, 1964. Launch countdown was started on schedule and terminated at T = 0 with a successful launch of the Atlas-Agena vehicles. There were no unscheduled holds during this countdown.

1. Purpose

The Countdown was performed to verify, by a series of checks and tests, that every aspect of the launch and mission equipment was operating properly before launch.

2. Description of Test

a. Spacecraft Configuration

The Spacecraft was in final flight configuration on the launch pad.

b. Test Procedure

The sequence of events during Countdown on the second day is given in Table B-31 with the exception of the final event, which was launch.

3. Test Evaluation

a. Video Performance

Video performance was normal as verified during the beacon signal strength null that occurred after antenna switchover. Camera pictures taken during this time are shown in Figures B-45 and B-46. Some noise spikes were observed in the P1-Camera video, but the spike occurrence rate was low.

b. Communications Performance

Communications performance was normal.

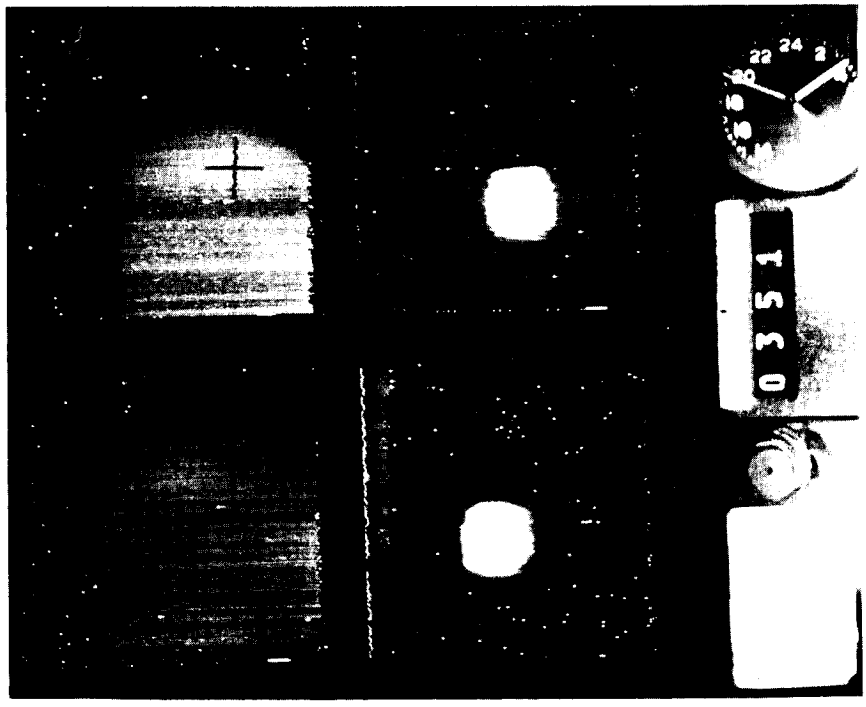

Figure B-45. P-Camera video at null during Countdown on Second Day

c. Power Performance

Battery voltages during the television operation were normal and are given in Table B-44. The total battery discharge for this test was 0.71 ampere hour for F-Battery, Serial No. 94, and 0.98 ampere hour for P-Battery, Serial No. 93. The total discharge for these final flight batteries since initial installation in the TV Subsystem was 5.58 ampere-hours for F-Battery and 6.87 ampere-hours for P-Battery.

d. Telemetry Performance

The 90-point commutator, which operated properly during TV Subsystem checkout, was turned off for the last time prior to launch while monitoring point 69 (F Sequencer Flip-Flop No. 1). Telemetry performance was normal.

4. Conclusions

The TV Subsystem was performing satisfactorily during Countdown. All systems were ready for launch, which occurred at 1650 hours GMT on July 28, 1964.

The Ranger-7 Spacecraft impacted on the moon at approximately 1325 hours, GMT, July 31, 1964. The TV Subsystem performance was normal.

TABLE B-44
LAUNCH BATTERY VOLTAGES

Time	Measured Input to HCVR		Operating Mode
	F-Battery (volts)	P-Battery (volts)	
T - 117	40.12	40.04	TV Subsystem Off
T - 116	40.40	36.86	Cruise Mode On
TV = 0	33.80	33.60	Warmup
TV + 1	33.70	33.40	Warmup
TV + 2	33.40	33.10	Reduced Power
TV + 3	33.30	33.00	Reduced Power
TV + 4	33.30	33.00	Reduced Power
TV + 5	35.30	35.20	RTC-5 Off
TV + 6	35.29	35.19	Cruise Mode Off
T - 16	38.65	38.36	TV Subsystem Off
T - 15	38.75	35.78	Cruise Mode On
T - 7	38.85	35.69	Beginning of Hold
T - 7	38.95	35.64	End of Hold
T - 1	39.05	35.62	Cruise Mode On
T = 0	0	0	Launch

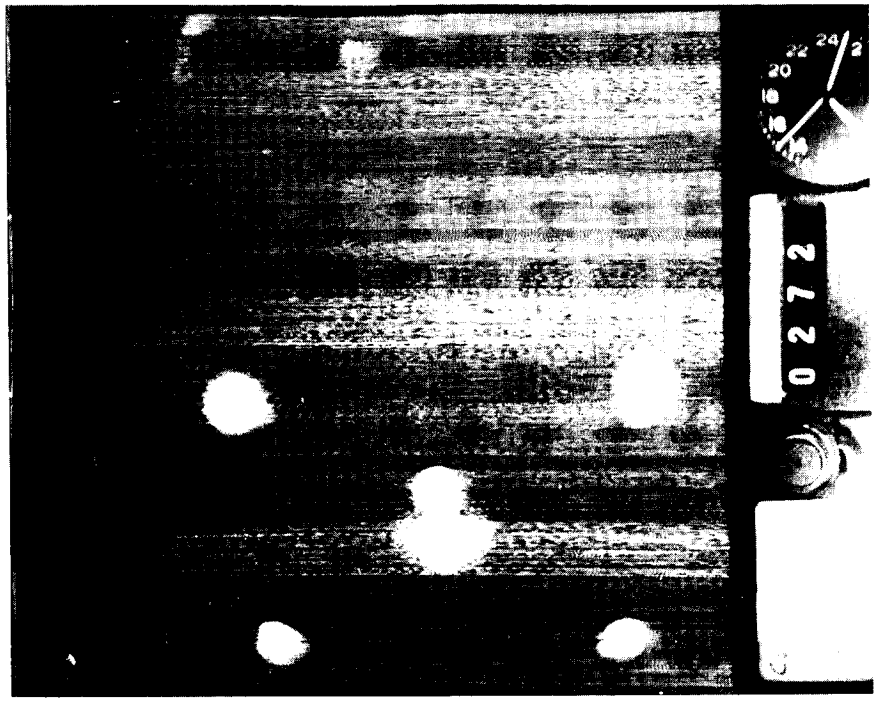

a. F_a -Camera

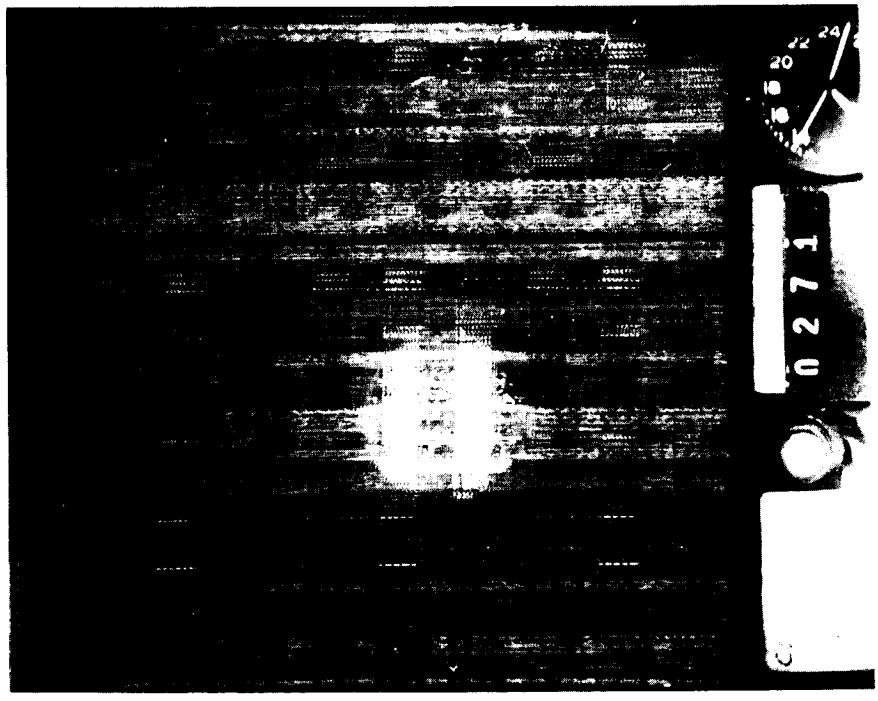

b. F_b -Camera

Figure B-46. F-Camera video output at null during Countdown on Second Day

Appendix C

Exposure Time Sequence for Partial-Scan Cameras

Appendix C

Exposure Time Sequence for Partial-Scan Cameras

The last two partial-scan pictures transmitted by RA-7 show the highest resolution of the moon's surface features. The time before impact of the last two exposures must be known before an accurate assessment of the size of the smallest visible features can be determined. Tests conducted at AED on a selection of partial-scan-style shutters show that exposure probably occurred 17 milliseconds after the initiation of the shutter drive pulses. Three different shutters with exposure times similar to the shutter on the P3 camera of Flight Model III-2 were tested to determine the time of actual exposure. The results are summarized in Table C-1. The time of exposure was measured for both the "in" and "out" strokes of the shutters. In addition, the occurence of exposure was checked at two different drive voltages.

TABLE C-1

EXPOSURE OCCURRANCE AFTER START OF DRIVE PULSE

Test Condition		Shutter Actuation Time (m sec)		
		Serial No. 3029	Serial No. 3041	Serial No. 3044
20.5 volts terminal voltage	IN stroke	14.8	16.3	15.5
	OUT stroke	15.3	16.1	16.4
19.0 volts terminal voltage	IN stroke	15.1	17.4	16.6
	OUT stroke	15.8	16.8	17.2

The exposure times for the three shutters, with 20.5 volts applied to the shutter terminals, (the nominal voltage for nominal flight battery voltage) is given in Table C-2.

TABLE C-2

SHUTTER SPEEDS

Shutter Serial Nos.	In Stroke (m sec)	Out Stroke (m sec)
3029	2.12	2.34
3041	2.25	2.34
3044	2.10	2.40

Table C-1 indicates that there is only a one millisecond delay in exposure for a reduction of 1.5 volts in battery voltage. Since two of the shutters tested indicate that exposure occurred approximately 17 milliseconds after the initiation of the drive pulse this value was used as the estimate of Flight Model camera operation.

The time of exposure can then be determined since the shutter drive pulse is initiated 86.7 milliseconds before the start of picture scan. With a line selecting oscelloscope the video from the secondary-on-line data (S.O.D.) magnetic tape was searched for the last line of video before impact. A polaroid picture of this line is shown in Figure C-1. Impact occurred at 404 microseconds of the 167th scan line of P3 camera (SN 21/39) video, one hundred and eleven milliseconds after the start of scan. Since it is estimated that exposure occurred 86 milliseconds before scan started, then the exposure occurred 187 milliseconds before impact.

The next to last picture was transmitted from the P1 (Serial No. 31/28) Camera. Exposure for P1 occurrs 200 milliseconds earlier than for the P3 Camera. Therefore, the last P1 exposure occurred 387 milliseconds before impact.

The area coverage of the last two pictures gives resolution of objects smaller than one meter. For a nominal terminal velocity of 2.65 km/sec, the last P3 Camera picture excluding the optical mask covered an area 42 meters wide by 28 meters high. (A complete frame would have been 49 meters high). There are 290 scan lines/picture height, however system bandwidth limitations restrict the resolution to approximately 200 TV lines (100 optical pairs), so the last picture resolved approximately 0.2 meter per TV line. The last P1 Camera covered an area 31 meters wide by 43 meters high giving approximately the same resolution. Table C-3 has been prepared to indicate the approximate coverage of each of the last 14 partial scan pictures. These numbers are calculated for a terminal velocity of 2.65 km/sec., and do not consider the angle between the velocity vector and camera optical axis. The area coverage is computed using the information taken from the performance of RTSP 1100A, Appendix H, "Camera Boresighting" for the modified Flight Model III-2. The coverage for each of the cameras is given in Table C-4.

The smallest recognizable crater in the last P3 picture is about one-fiftieth of the picture height or about 0.8 meter in mission requirements were satisfied. A similar timing sequence can be developed for the fuel-scan cameras. (See figure C-2) It can be determined that the last line of video from Camera F_a occurred after 345 microseconds of scan line 1074 or at 2.385 seconds from the start of scan. If the shuttered exposure in this case also occurs 70 milliseconds before the start of scan impact occurred 2.455 seconds after the F_a Camera exposure. The F_b Camera exposure then occurred 2.560 seconds earlier in time or 5.015 seconds before impact. A table similar to that for the partial scan cameras can be derived if desired.

TABLE C-3 FINAL PARTIAL SCAN CAMERA SEQUENCE				
Camera	Time Before Impact (seconds)	Altitude (kilometers)	Width (meters)	Height (meters)
P1	2.907	7.70	238	323
P3	2.707	7.17	667	720
P2	2.507	6.63	212	246
P4	2.307	6.10	583	598
P1	2.067	5.48	170	230
P3	1.867	4.95	460	498
P2	1.667	4.42	141	164
P4	1.467	3.88	371	380
P1	1.227	3.250	100	136
P3	1.027	2.720	252	273
P2	0.827	2.180	70	81
P4	0.629	1.650	157	162
P1	0.387	1.020	31	48
P3	0.187	0.488	42	28

TABLE C-4 PARTIAL-SCAN CAMERA ANGULAR COVERAGE		
Camera	Serial No.	Angular Coverage
P1	31/28	1.77^{o} X 2.40^{o}
P2	36/34	5.32^{o} X 5.77^{o}
P3	21/39	1.83^{o} X 2.13^{o}
P4	37/40	5.48^{o} X 5.62^{o}

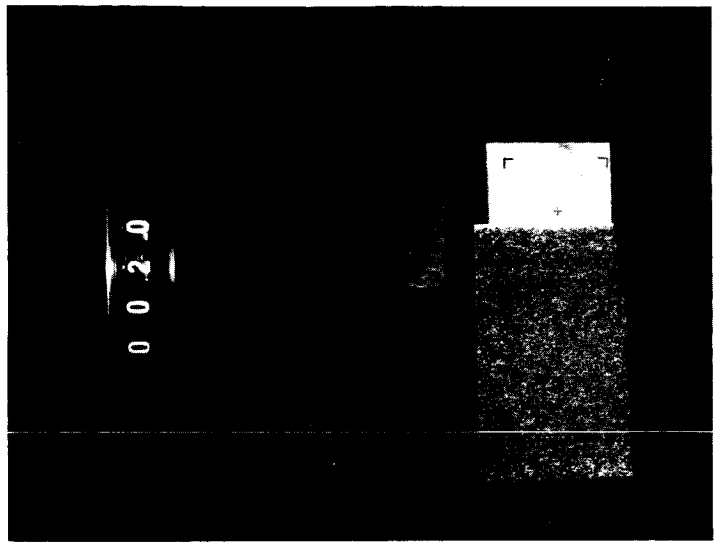

LAST PARTIAL SCAN PICTURE

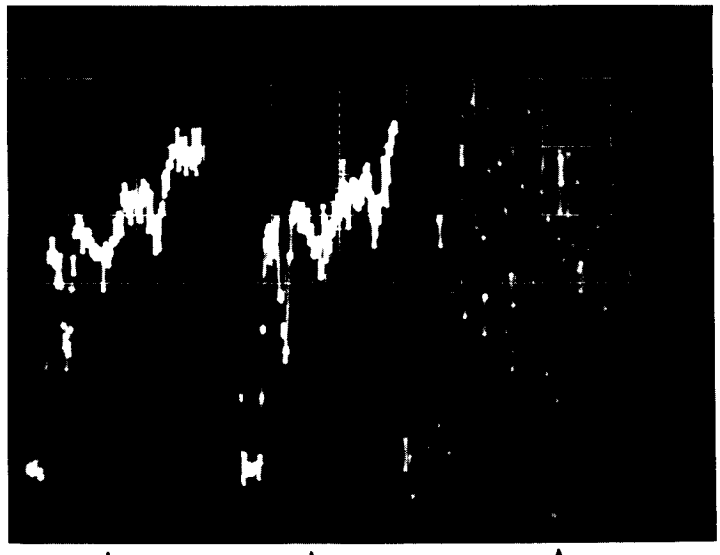

Figure C-1. Last Lines (166 and 167) of video P3 Camera

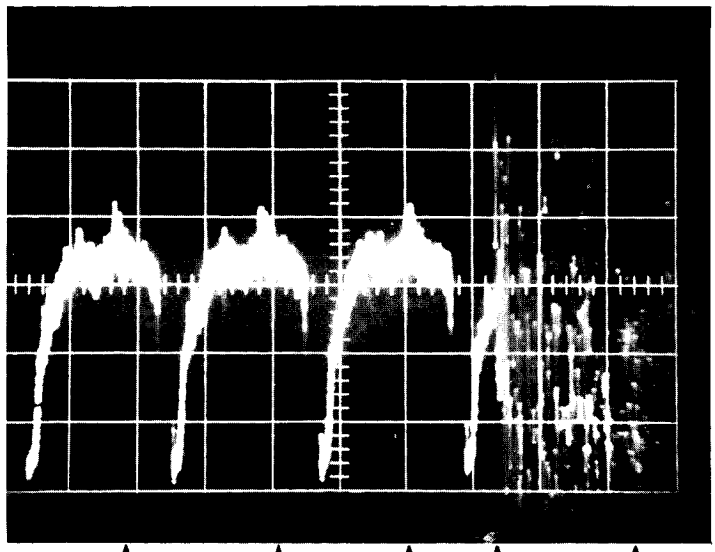

VIDEO SCANLINES 1071 1072 1073 1074 NOISE

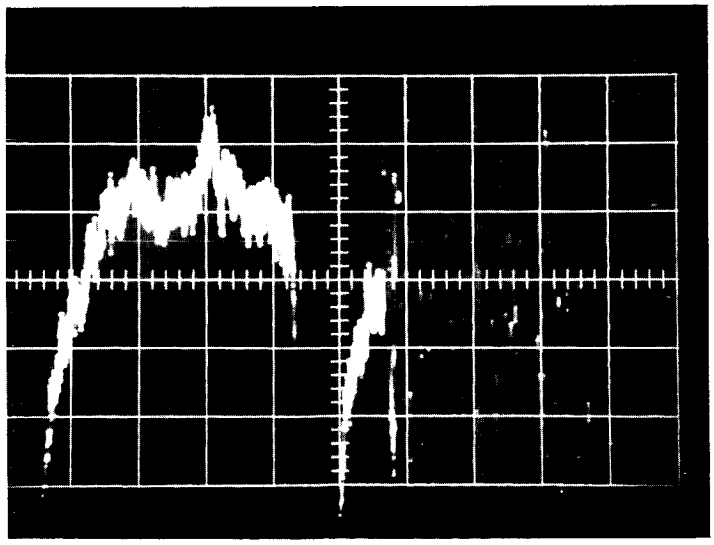

VIDEO SCANLINES 1073 1074 RECEIVER NOISE

Figure C-2. Line of Video from F_a Camera at Impact

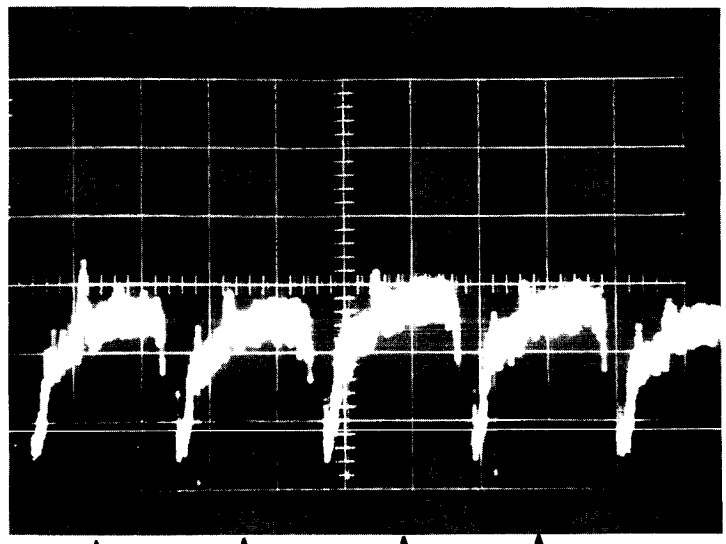

SCANLINE 1071 1072 1073 1074

3RD FROM LAST FRAME

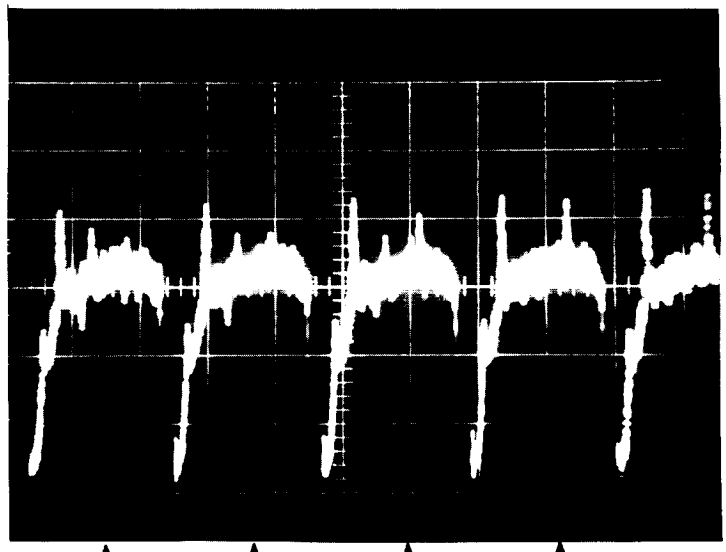

SCANLINES 1071 1072 1073 1074

2ND FROM LAST FRAME

Figure C-3. Line Video from Camera F_a Two frames Prior to Impact

Appendix D

Least Squares Fit of Spacecraft Temperatures

A. Introduction

It has been shown that the temperature T_k of a point in a spacecraft, k can be given by

$$\sigma T_k^4 = \sum_s C_{ks} I_s + \sum_{jm} b_{km} Q_{jm} \qquad \text{(D-1)}$$

where I_s are the equivalent radiation inputs, Q_{jm} are the electrical power sources of heat, and the other letters are constants characteristic of the spacecraft.* To obtain these constants from thermal-vacuum tests, the inputs can be varied, and the resulting temperatures recorded; a number of simultaneous equations result, which can then be solved for the desired constants.

If the number of tests is greater than the minimum required, a certain choice is available as to how the constants should be computed. The criterion chosen for handling this redundant data is to minimize the difference between the measured temperatures and the temperatures calculated by the fitted equation. If all tests are equally valid, this is a balanced method of getting the most information from these tests. On the other hand, the addition of a poorer test does not always improve the accuracy of the calculated constants.

B. Theory

The necessary equations will be derived, both for a specific example and in generalized matrix form. Concentration should be placed on the example, which will be the equation on the left, as this is usually easier to understand for the first reading.

The number of terms in the equation will depend on the specific spacecraft. For Relay or TIROS, four terms would be used with the electrical power inputs lumped into one term. For Ranger the equivalent radiation inputs will be considered negligible, and there will be five or six electrical power inputs, corresponding to the different fins. For the illustrative case, two electrical power inputs Q_A and Q_B will be considered

Q_A, Q_B	M, N = input number

*See the notes on Spacecraft Thermal Design by G. D. Gordon, p. IV-6 for the derivation.

The number of vacuum chamber tests run will, in general, be greater than the number of terms; otherwise, a least squares fit is neither necessary nor possible. For the example, three tests will be considered

$$j = 1,\ 2,\ 3 \qquad \Big| \qquad J = \text{test number}$$

The number of thermocouples is unlimited, and can be a single thermocouple. Each location is handled essentially separately, but for computations it is convenient to put them together in a matrix. For the example, a single thermocouple will be considered, so the number of thermocouples is:

$$\tau \qquad \Big| \qquad K = \text{thermocouple number}$$

With the above nomenclature, the spacecraft temperature can be written as

$$\tau_j' = a\,Q_{Aj} + b\,Q_{Bj} \qquad \Big| \qquad \tau' = Q_{JM}\,X_{MK}$$

A number of tests where τ is equal to σT^4 with various inputs Q_{JM} have been made, and the temperature has been determined; the coefficients $\underline{a}$ and $\underline{b}$ (or X_{MK}) are to be determined.

If the coefficients were known, it would be possible to calculate a fitted temperature τ_j', which would probably differ slightly from the test temperature τ_j' by a certain deviation given by

$$D_j = \tau_j - \tau_j' \qquad \Big| \qquad D_{JK} = \tau_{JK} - \tau_{JK}'$$

where there is a deviation for each test and for each thermocouple location. If these deviations are squared, they will all be positive, and summing over all the tests, it is desirable to have the sum a minimum. That is, the coefficients are to be chosen such that

$$\sum_j D_j = \text{minimum} \qquad \Big| \qquad \sum_J D_{JK}^{\,2} = \text{minimum}$$

By substituting the previous equations into the above, performing the indicated operations, differentiating the result with respect to each coefficient, and setting the result equal to zero, the following equations will evolve that must be satisfied by the coefficients*

$$a \sum_{j=1}^{3} Q_A^{\,2} + b \sum_{j=1}^{3} Q_A Q_B = \sum_{j=1}^{3} Q_A \tau$$

$$a \sum_{j=1}^{3} Q_A Q_B + b \sum_{j=1}^{3} Q_B = \sum_{j=1}^{3} Q_B \tau$$

$$P_{NJ}\,Q_{JM} X_{MK} = P_{NJ}\,\tau_{JK}$$

* More details of the least-square fit are presented in Paragraph D of this Appendix.

These can be solved for the coefficients and the result is

$$a = \frac{\sum_{j=1}^{3} Q_B^2 \sum_{j=1} Q_A \tau - \sum_{j=1}^{3} Q_A Q_B \sum_{j=1}^{3} Q_B \tau}{\left(\sum_{j=1}^{3} Q_A^2\right)\left(\sum_{j=1}^{3} Q_B^2\right) - \left(\sum_{j=1}^{3} Q_A Q_B\right)^2}$$

$$b = \frac{\sum_{j=1}^{3} Q_A^2 \sum_{j=1}^{3} Q_B \tau - \sum_{j=1}^{3} Q_A Q_B \sum_{j=1}^{3} Q_A \tau}{\left(\sum_{j=1}^{3} Q_A^2\right)\left(\sum_{j=1}^{3} Q_B^2\right) - \left(\sum_{j=1}^{3} Q_A Q_B\right)^2}$$

$$X_{MK} = (P_{NJ} Q_{JM})^{-1} P_{NJ} \tau_{JK}$$

C. Computer Solution

The inputs for the computer consist of the power inputs used and the temperatures read for each test. The Q_{JM} matrix is read so that each row represents another test. The temperature matrix T_{JK} is read so that column represents another thermocouple. The matrix inputs are therefore

	Fin A	Fin B	Fin C
Test 1	Q_{1A}	Q_{1B}	Q_{1C}
Test 2	Q_{2A}	Q_{2B}	Q_{2C}
Test 3	Q_{3A}	Q_{3B}	Q_{3C}
Test 4	Q_{4A}	Q_{4B}	Q_{4C}

	VID	SHR	BAT	HAT
Test 1	T_{11}	T_{12}	T_{13}	T_{14}
Test 2	T_{21}			
Test 3	T_{31}			

The temperatures are read as degrees Centigrade and then converted to watts per square inch.

In addition to the desired coefficients X_{MK}, several other quantities are printed out.

The matrix

$$C_{MJ} = (P_{NJ} Q_{JM})^{-1} P_{NJ} \qquad \text{(D-2)}$$

is printed out so that if the temperatures from another thermocouple are given, a single matrix multiplication (by hand) can be used to calculate the desired coefficients. Also, this matrix will show which tests predominate in determining the values for each coefficient.

The fitted temperatures T_{JK}' are also calculated, and these can be compared with the test temperatures. If these values are quite close, they indicate excellent internal agreement in the test data. If the set for one particular test shows a poor fit, then this may be a poor test (possibly the temperatures hadn't reached equilibrium and the inputs were not consequently the values assumed) or the spacecraft may be significantly different from those in the rest of the tests. The coefficients may be improved by discarding tests which show poor agreement with the rest of the data.

Another matrix being printed out is

$$Z_{JJ} = Q_{JM} \left(P_{NJ} Q_{JM}\right)^{-1} P_{NJ} , \qquad \text{(D-3)}$$

which constitutes an experiment since there has been little experience obtained with this matrix. When multiplied by the test temperatures, this matrix yields the fitted temperatures T_{JK}'. Similarity between two rows shows two tests that yield very similar data; conversely, a large (close to unity) diagonal term indicates a test that is very important in determining the coefficients. Note that the trace of this matrix, i.e., the sum of the terms on the major diagonal, is equal to Y times the number of terms in the original equation (M or N).

D. Application to Ranger

Some of the preliminary results obtained with the Ranger data are given to show how the program began, and to illustrate how it can be used. The first calculation of the coefficients was made by selecting five tests and using them to calculate five coefficients; there was no redundant data, and no least-squares fit was required. It turned out that due to the similarity of the tests, the experimental errors masked the true values of the coefficients. To overcome this difficulty, and obtain some information from the tests, some arbitrary constraints were placed on the coefficients. The following analysis is presented in order of increasing complexity.

A simple constraint that can be placed on the coefficients is that they are all equal. Thus the temperature would be given by

$$\sigma T^4 = aQ_A + aQ_B + aQ_C + aQ_D + aQ_{E,F} \qquad \text{(D-4)}$$

where a is the unknown coefficient. This is equivalent to stating that σT^4 is proportional to the total power input. A least-squares fit can be used, where the sum of the Q's are the single input. The result of such an analysis on nine Ranger tests is presented in the Column A of Table E-1 of Appendix E. The coefficient a is found to be equal to 1.05×10^{-3} in^{-2}, (its reciprocal is equal to 950 in^2, which is the product of surface area and average emittance).

The predicted temperatures based on the equation have been calculated and are also shown in the table. The fit is good, and the standard deviation is 2.3 degrees.

Another constraint that might be used is to assume that the coefficients are in arithmetical progression. This would recognize the fact that fins farther from the batteries may have a smaller effect on the temperature. The temperature equation would then be

$$\sigma T^4 = (a - 2b)Q_A + (a - b)Q_B + aQ_C + (a + b)Q_D + (a + 2b)Q_{E,F} \qquad \text{(D-5)}$$

where a and b are to be determined from the data. To use the least-squares fit, two auxiliary variables can be defined

$$x \equiv Q_A + Q_B + Q_C + Q_D + Q_{E,F}$$

$$y \equiv -2Q_A - Q_B + Q_D - 2Q_{E,F}$$

which would be used instead of the actual Q's. The temperature is then given by

$$\sigma T^4 = ax + by$$

and the coefficients a and b would be determined directly from the test data. When this was done for the battery, the results were that a is equal to 1.10×10^{-3} in^{-2} and b is equal to -0.12×10^{-3} in^{-2}. Substituting in Equation (D-5), the battery temperature is then given by

$$\sigma T^4 = \frac{1}{1000 \text{ in}^2}\left[1.34\, Q_A + 1.22\, Q_B + 1.10\, Q_C + 0.98\, Q_D + 0.86 Q_{E,F}\right]$$

The change in coefficients is in the direction expected, since the batteries are located in the vicinity of the A fin, and that coefficient is the highest. A similar analysis for the vidicon, which is located at the other end of the spacecraft produced coefficients that ran in the opposite direction. The fitted temperatures for the battery are presented in Table E-1, and the standard deviation is 1.4 degrees, which is a considerable reduction from the previous 2.3 degrees, therefore, the fit is much improved.

Another constraint, carrying the analysis one step further, is to have the coefficients related in a parabolic manner. The temperature equation would then be

$$\sigma T^4 = (a - 2b - 2c)\, Q_A + (a - b + c)\, Q_B + (a + 2c)\, Q_C + (a + b + c)\, Q_D + (a + 2b - 2c)Q_{E,F} \qquad \text{(D-6)}$$

where there are now three coefficients, a, b, and c, to be determined by the data. To use the least-squares fit, three auxiliary variables can be defined.

$$x \equiv Q_A + Q_B + Q_C + Q_D + Q_{E,F}$$

$$y \equiv -2Q_A - Q_B + Q_D + 2Q_{E,F}$$

$$z \equiv -2Q_A + Q_B + 2Q_C + Q_D - 2Q_{E,F}$$

and then the temperature is given simply by

$$\sigma T^4 = ax + by + cz$$

The results of the fit were that a equals 1.09×10^{-3} in^{-2}, b equals -0.09×10^{-3} in^{-2}, and c equals 0.03×10^{-3} in^{-2}. This represents a minor change from the previous calculations. In terms of the basic coefficients, the temperature is now given as

$$\sigma T^4 = \frac{1}{1000 \text{ in}^2}\left[1.21 Q_A + 1.21 Q_B + 1.15 Q_C + 1.03 Q_D + 0.85 Q_{E,F}\right],$$

which is the type of distribution that would be expected from the spacecraft geometry and an improvement over a strictly linear relation. The fitted temperatures are shown in Table D-1, and are not changed much from the previous case. The standard deviation is still about 1.4 degrees.

The process could be continued another step, where the coefficients would be related by a cubic equation, and there would be four unknowns. Finally, the five unknowns can be obtained directly by a least-squares fit. However, it is apparent from the analysis at this point that the point of diminishing returns has already been reached. The differences that remain between the fitted data and the original data are mostly due to random experimental errors, not to the constraint that was imposed.

E. Mathematical Derivation

The desired matrix equation is

$$\tau_{JK} = Q_{JM} X_{MK} \tag{D-7}$$

where the temperatures T_{JK} and the electrical power inputs Q_{JM} are known, and the coefficients X_{MK} are unknown. If Q_{JM} is a square matrix there are as many equations as unknowns, and by inverting this matrix the desired coefficients are obtained, that is,

$$X_{MK} = Q_{MJ}^{-1} T_{JK}. \tag{D-8}$$

If there is an excess of tests, it is not in general possible to choose coefficients to satisfy all the equations. A new set of temperatures T_{JK}' is then defined, and when the coefficients are chosen, the following equation is satisfied exactly:

$$T_{JK}' = Q_{JM} X_{MK}. \tag{D-9}$$

The difference between these fitted temperatures and the original test temperatures T_{JK} are therefore,

$$D_{JK} = \tau_{JK} - Q_{JM} X_{MK}; \tag{D-10}$$

this difference is to be minimized by suitable choice of the X_{MK} coefficients. The simplest way to eliminate the negative signs is to square all the differences, and the first step is to take the transposition of Equation (D-10), which is

$$D_{K'J} = \tilde{\tau}_{K'J} - X_{K'N} P_{NJ} \tag{D-11}$$

where dummy coefficients have been changed for clarity.

TABLE D-1

DIFFERENT CONSTRAINTS FOR LEAST-SQUARES FIT

					A		B		C	
			Battery Test Temp.		Constant Coefficients		Linear Relation		Parabolic Relation	
x_i	y_i	z_i	T_i	σT_i^4	ax	T_i'	$ax+by$	T_i'	$ax+by+cz$	T_i'
216	52	24	11.73	.241	.2272	7.56	.2319	9.00	.2318	8.97
217	52	26	9.79	.234	.2283	7.90	.2330	9.33	.2330	9.33
219	55	25	10.84	.238	.2304	8.54	.2348	9.88	.2351	9.97
226	54	34	13.48	.247	.2482	13.83	.2537	15.41	.2538	15.44
236	54	34	15.78	.255	.2482	13.83	.2537	15.41	.2538	15.44
238	34	54	16.62	.258	.2504	14.46	.2583	16.71	.2584	16.73
303	19	73	35.71	.333	.3187	32.34	.3318	35.43	.3314	35.34
237	55	21	13.48	.247	.2493	14.15	.2546	15.66	.2544	15.61
267	16	92	25.73	.292	.2809	22.85	.2924	25.83	.2929	25.96
Calculated Coefficients					$a = 1.0519 \times 10^{-3}$		$a = 1.1025 \times 10^{-3}$ $b = -.1208 \times 10^{-3}$		$a = 1.0923 \times 10^{-3}$ $b = .0925 \times 10^{-3}$ $c = .0295 \times 10^{-3}$	
Goodness of fit $\sigma = \sqrt{\frac{1}{N}\sum(T_i - T_i')^2} =$					± 2.47 deg.		± 1.39 deg.		± 1.39 deg.	

When Equation (E-11) is multiplied by Equation (E-10), the result is

$$D_{K'J}\, D_{JK} = (\tilde{\tau}_{K'J} - \tilde{X}_{K'N} P_{NJ})\,(\tau_{JK} - Q_{JM}\, X_{MK}) \tag{D-12}$$

Note that the matrix multiplication must be made in this order, so that the summation is over the values of J, that is, over all the different tests. The value of K remains fixed, and the coefficients for each thermocouple are determined independently from the other thermocouples.

Expanding Equation (E-12) the result is

$$D_{K'J}\, D_{JK} = \tilde{\tau}_{K'J}\tau_{JK} - \tilde{X}_{K'N} P_{NJ}\, \tau_{JK} - \tilde{\tau}_{K'J} Q_{JM} X_{MK} + \tilde{X}_{K'N} P_{NJ} Q_{JM} X_{MK} \tag{D-13}$$

Now a value of $\tilde{X}_{K'N}$ must be chosen such that this is minimized, hence we differentiate with respect to it, and set the result equal to zero. The variation of $\tilde{X}_{K'N}$ is obtained explicitly; to get the result of the variation of X_{MK}, note that the equation is not changed if we take the transpose. The effect of the X_{MK} variation is thus to double the explicit variation of the coefficient $\tilde{X}_{K'N}$. The result is

$$\frac{\partial}{\partial X'_{K'N}} D_{K'J}\, D_{JK} = 0 - P_{NJ}\, \tau_{JK} - P_{NJ}\, \tau_{JK} + 2\, P_{NJ}\, Q_{JM}\, X_{MK} \tag{D-14}$$

Setting this equal to zero the result is

$$P_{NJ}\, \tau_{JK} = P_{NJ}\, Q_{JM}\, X_{MK} \tag{D-15}$$

This equation apparently could have been obtained from Equation (D-7) simply by multiplying on the left by P_{NJ}; however, there is an important difference. For each thermocouple (i.e., each value of K) there were J number of tests, and only M coefficients to be fitted, in Equation (D-7). Now, in Equation (D-15) the number of equations has been reduced to N equations, which is equal to the number of coefficients. Thus, in this case, Equation (D-7) cannot be satisfied exactly, but Equation (D-15) can be satisfied.

To solve for the coefficients, the reciprocal of $P_{NJ}\, Q_{JM}$, which is a square matrix, is obtained, and used to multiply both sides of Equation (D-15). The result is

$$(P_{NJ}\, Q_{JM})^{-1}\, P_{NJ}\, \tau_{JK} = X_{MK} \tag{D-16}$$

which can be written as

$$X_{MK} = C_{MJ}\, \tau_{JK} \tag{D-17}$$

where

$$C_{MJ} = (P_{NJ}\, Q_{JM})^{-1}\, P_{NJ} \tag{D-18}$$

In the computer program, the C_{MJ} matrix is first obtained from the Q_{JM} matrix, after which the X_{MK} can be calculated.

Appendix E

Ranger Calculation—Flight Discrepancy

(Ratio Factors from RA-6)

Appendix E

Ranger Calculation—Flight Discrepancy (Ratio Factors from RA-6)

It is necessary to justify the calculated fin inputs (SA α) in order to account for the discrepancy between the calculated values and those actually encountered. This discrepancy was attributed to external energy inputs which would be expected to affect all parts of the vehicle in the same manner.

With the three telemetry temperatures, it is possible to calculate the three parameters x, y, z used in the least-square equations, derived in Appendix D.

$$x = Q_A + Q_B + Q_C + Q_D + Q_E + Q_F \tag{E-1}$$

$$y = -2Q_A - Q_B + Q_D + 2\,(Q_E + Q_F) \tag{E-2}$$

$$z = -2Q_A + Q_B + 2Q_C + Q_D - 2\,(Q_E + Q_F) \tag{E-3}$$

The values of the parameters calculated with flight temperatures are: x = 304 watts, y = 14.6 watts, z = 190 watts. The values used for the flight duplication test were: x = 302.7, y = 18.1, z = 71.3. These parameters give the temperatures in Table E-1.

TABLE E-1
TV SUBSYSTEM TEMPERATURES

	Hat	Vidicon	Shroud	Battery	Camera Electronics
Measured in Flight (RA-6)	40	-	36	37	-
Flight Duplication Temps.	38.5	27.5	38	36	35
Temperatures Calculated with x = 304; y = 14.6; z = 190	40	33.5	36	37	41

The temperatures indicate:

a) The power distribution during the duplication test was wrong, or

b) The z value calculated with the telemetry data is wrong.

The flight x, y, and z values differ from the duplication test values in that energy is less in the top and bottom sections and greater in the middle section. The duplication test was run with the fin inputs maintained in the usual ratio, where possible. Due to the assumed nature of the discrepancy, this distribution should be approximately correct.

No unique solutions for flight fin inputs were possible since there are three equations, (E-1), (E-2), and (E-3) for the five unknowns, Q_A, Q_B, Q_C, Q_D, and $Q_E + Q_F$.

In order to solve for the Q's, two constraints must be imposed. It was assumed for constraint conditions that the fins had flight inputs in the usual ratio. Different combinations of constraints gave Q's which varied widely.

Since it is not possible to account for the flight x, y, and z values with a reasonable energy distribution, it is best to base predictions on the duplication tests.

Every attempt to match flight temperatures verified the x value of about 303 watts and indicated less energy input to fins E and F than calculated. The following two methods were tried to get the actual flight inputs on the basis of the duplication test:

1. It is most reasonable to ratio all the fins by the same amount to produce x = 303.

$$Q_f = \psi Q_C$$

where: C indicates calculated value, $(SA\alpha)$

f indicates actual flight value.

$$\psi = \frac{x_f}{x_C} = \frac{303}{243} = 1.25$$

The parameters for this ψ value are x = 303, y = 66.5, and z = 24.5. Calculated temperatures with these parameters do not agree with measured duplication temperatures.

2. Another method is to group fins and use two factors.

$$Q_f = \psi\, Q_C \text{ for fins A, B, C, D}$$

$$A_f = \phi\, Q_C \text{ for fins E and F.}$$

$$\psi = \frac{(Q_A + Q_B + Q_C + Q_D)\ f}{(Q_A + Q_S + Q_C + Q_D)\ C} = 1.34$$

$$\phi = \frac{(Q_E + Q_F)\ f}{(Q_E + Q_F)\ C} = .93$$

The parameters (x = 303, y = 29.5, and z = 73.5) give temperatures which agree with the test.

Two factors which give even better agreement with the test are $\psi = 1.37$ and $\phi = 1.85$. These should be used for temperature prediction of Flight Model III-II based on the given assumption regarding the cause of the high temperatures in Flight Model III-I.